Università degli Studi di Ferrara

DOTTORATO DI RICERCA IN
SCIENZE CHIMICHE

CICLO XXIX

COORDINATORE Prof. Carlo Alberto Bignozzi

Simultaneous recovery of cellulose and other value-added compounds from orange waste

&

Synthesis of spiro and ureidic compounds for modulation studies of mptp protein

Settore Scientifico Disciplinare CHIM/06

Dottorando
Dott. Cristofaro Dario

_____
(Firma)

Tutore
Prof. Benetti Simonetta

_____
(Firma)

Co-tutore
Prof. Trapella Claudio

_____
(Firma)

Anni 2014/2016

Abstract

This thesis is divided in two separate sections, both conducted in the Department of Chemical and Pharmaceutical Sciences under the supervision of Prof. Dr. Simonetta Benetti and Prof. Dr. Claudio Trapella.

The first project aimed to demonstrate the opportunity of utilizing a new type of citrus waste, called decanter centrifuge orange waste (DCOW), to extract cellulose and other constituents of the matrix. These could be sold as either mixture or isolated compounds (or derivatives) thus avoiding environmental dangerous waste disposal. A sequence of extraction steps and pH-dependant treatments were studied in order to isolate five different products from DCOW. The choice of the solvents used for extraction was directed by economic issues as well as by the need to attain food-grade compounds. An acidic treatment was utilized in order to isolate a pectic fraction, while a basic treatment allowed purifying the cellulose fraction. α-Cellulose was successfully isolated (with a yield of 9.81% ± 0.25 on dry basis) and used to produce cellulose acetate, a well-known commercial product. The other isolated fractions were analytically characterized and consisted of polyphenols, carbohydrates and terpenes, which represent all high-value products whose further purification may results in appealing saleable products.

The second project was intended to synthesize potential inhibitors of mitochondrial permeability transition pore (mPTP) complex opening, which is known to be responsible for ischemic-reperfusion injury (IRI). Up to now, only few compounds are known to directly inhibit this complex. Of them, dicyclohexylcarbodiimide (DCC) and oligomycin A were elected as drug design starting points. Since DCC is slowly hydrated in human body to form dicyclohexylurea (DCU), the latter was chosen as the real starting reference substrate for the synthesis of the target compounds. Therefore, symmetric and asymmetric ureas and thioureas were produced. Besides, some aliphatic carbamate derivatives were synthesized to better understand the influence of the rings adjacent to the carbonyl group on biological activities. Studies were also conducted to synthesize new spiro compounds mimicking oligomycin A structural core. In this case, 1-phenyl-1, 3, 8-triaza-spiro[4,5]decan-4-one template was used to produce the corresponding *N*-8 substituted derivatives. Almost all these derivatives were produced in reasonably high yields, using inexpensive reagents and under rather mild reaction conditions. Noticeably, preliminary results from biological characterization showed that these derivatives have both inhibitor and activator potency against mPTP opening. While the identified inhibitors may be useful for IRI treatments, alternative use of the activators as antitumor compounds was hypothesized.

List of contents

List of tables

List of figures

Acknowledgments

Primarily, I would like to thank Prof. Dr. Simonetta Benetti for giving me the opportunity to carry out my PhD here in Ferrara.
I really want to thank Prof. Dr. Claudio "Trap" Trapella, because he showed me the enthusiasm and drive a group must possess and display in order to get the job done.
I would also like to thank In4tech Synthesis for the financial support and for giving me the chance to see a bigger reality, outside the University.

I would like even to express my eternal gratitude to Dr. Tatiana Bernardi who helped me in every possible way: I do not think I am exaggerating when I say I could not have done this work without you. I just hope I will always return the favour.
Sincerely, I really want to thank Dr. Carmela De Risi, which follow me closely for the last 12 months. Carmela, thank you for you encouragements and everyday discussions. I still do not know how you could bear my continuous rants. You were a very precious friend in a sad time. I do feel very lucky to have met you and have the opportunity to work with you in the near future.
Irene, you did a wonderful job on your thesis here, and I know you will keep learning a lot during your Ph.D. in England. You will get better and better.
Special thanks go to Gabriele Bertocchi. You know the reason.
Proper thanks go to Dr. Alberto Casolari and Dr. Paolo Formaglio for the NMR analysis.
Thanks to the staff of FreshPlaza© who allowed me to use photos from their archives.

I would like to thank my family who have been very supportive (especially financially…thanks Dad) along those years. Big thanks go to my mother: you have always offered me a kind word (or sometimes a scolding) and so much love.

Finally, yet importantly, I want to thank the beautiful woman who wakes up every morning near me and makes me the man I want to be. I really think I would be lost without you, Sara.
Whatever will comes our way, we will still be together.

Author's declaration

Some of the results presented herein were obtained by, or in collaboration with other co-workers. They are all fully acknowledged in the list below. All other results are the work of the author.

Piece of work	Chapter	Collaborator
Orange waste extract mass analysis	7	Dr. Tatiana Bernardi
Orange waste extract HPLC analysis		Dr. Tatiana Bernardi Dr. Valentina Donegà
Ureas synthesis	14	Dr. Viky Papathanassiou
Ureas mass analysis		Dr. Anna Fantinati
Spiro-derivatives synthesis		Dr. Irene Boz
Spiro-derivatives mass analysis		Dr. Irene Boz
Spiro-derivatives HPLC analysis		Prof. Claudio Trapella Dr. Erika Marzola
Ureas and spiro derivatives biological assays		Prof. Paolo Pinton Dr. Gianpaolo Morciano

If there's one thing I know
it's that I never really know enough.
Ben Cooper

In the middle of difficulty lies opportunity.
Albert Einstein

Simultaneous recovery of cellulose and other value-added compounds from orange waste

1. Introduction

The term “citrus” (“agrumi” in Italian, “citricos” in Spanish) is a generic designation for a large group of edible fruits. According to the current system of plant taxonomy, the genus “*Citrus*” belongs to the subfamily of *Aurantioideae*, family of *Rutaceae*. The genus comprises several varieties of fruits (and trees) known by their popular names: sweet oranges (*Citrus sinensis*), sour and bitter oranges (*C. aurantium*), mandarins (*C. reticulata*), grapefruits (*C. paradise*), pomelos (*C. grandis*), lemons (*C. limon*), limes (*C. latifolia* and *C. aurantifolia*), and a very large number of hybrids.[1]

Citrus fruits can grow almost in every country 30–35 degrees north and south of the Equator. For some varieties, less susceptible to frost damage, the zone of cultivation reaches 40 degrees on both hemispheres. Thus, citrus is the most widely produced fruit, as a group of several species, and it is grown in more than 80 countries.[2]

The contribution of the citrus industry to the world economy is vast (estimated at 10.68 billion US$ annually, including 3.82 billion US$ from citrus fruits production, 6.44 billion US$ from citrus juice manufacturing, and 420 million US$ for fresh citrus marketing) and it provides jobs to millions of people around the world in harvesting, handling, transportation, storage, and marketing operations. In addition to oranges, mandarins, limes, lemons, pomelos, and grapefruits, other citrus fruits such as kumquats, citrons and hassaku oranges also have a substantial commercial importance.[3]

Citrus fruits production has recently reached 121 million metric tons (Table 1). Approximately a third of the production resides in the Americas (North and South), and about 10–12% is in the Mediterranean region. Production trends indicate that oranges constitute about 57% of the total citrus output, followed by mandarins, clementines, satsumas, and tangerines, which comprise about 25% of the output. The group of lemons and limes constitute 11–12%, and grapefruit and pomelos comprise roughly 6-7%. China leads in citrus production, with more than 29.567 million metric tons of fruit produced during 2013–2014, followed by Brazil and United States. Chinese citrus production is mostly oriented toward fresh fruit market, while Brazilian citrus production is more oriented toward the processing. The U.S. citrus productions are focused toward both the processing and the fresh fruit market (Figure 1).[4]

Citrus production for 2013/2014 (thousand tonnes)					
Country	Total Citrus	Orange	Tangerine	Lemons and Lime	Grapefruit
World	121273	68925	31203	13172	7625
China	29567	7600	17850	400	3717
Brazil	18966	16850	998	1100	78
USA	9394	6783	726	832	1053
Mexico	7503	4400	430	2250	423
India	7400	5000	n.a.	2200	200
South Africa	2635	1715	195	312	413
Italy	3250	1935	760	545	10

Source: (FAO, 2016)

Table 1: Citrus production for 2013/14

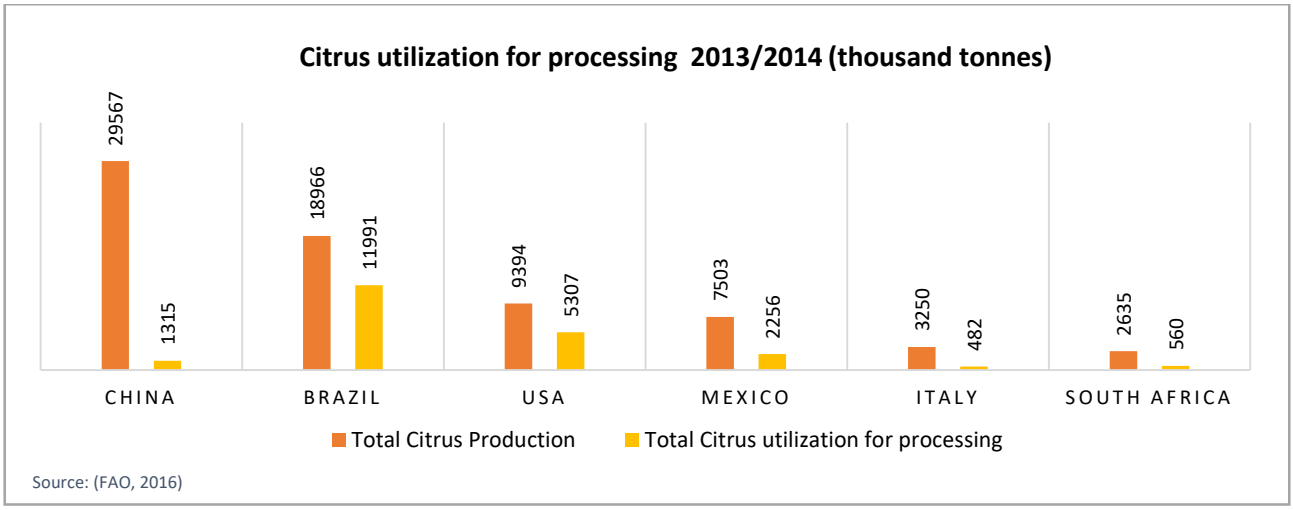

Figure 1: Citrus utilization for processing 2013/14 (originally in colour)

The role of citrus fruits in providing nutrients and medicinal value has been long recognized. Citrus fruits are well known for their characteristic flavour, thirst-quenching ability, and as one of the main sources of vitamin C. In addition to ascorbic acid, these fruits contain several phytochemicals, which play the role of nutraceuticals, such as carotenoids (lycopene and β-carotene), limonoids, flavanones (naringin and hesperidin), and vitamin-B complex and related nutrients (thiamine, riboflavin, nicotinic acid/niacin, pantothenic acid, folic acid, biotin, choline, and inositol).

Fresh citrus fruit consumption is important because the nutrients and the health-promoting factors (especially antioxidants) from these sources are immediately available to the body and the loss of nutrients is negligible compared with processed juices.[5]

Citrus fruits are covered with a peel, or rind, which protects the pulp of the fruit. On the outside, the rind is made up of a cuticle, thinly covering the epidermal layer. This epicarp, usually referred to flavedo (from Latin *flavus*, “yellow or blond”), contains numerous oil sacs, or glands, filled with essential oils. In addition to these oil sacs, the flavedo contains coloring molecules (chlorophylls, flavonoids and carotenoids), which concentrate heterogeneously throughout this layer.

The mesocarp, also called albedo (from Latin *albedo*, “whiteness”), is made of a white spongy portion of parenchymatous cells, loosely arranged with large intercellular spaces and irregular in shape (Figure 2). The albedo thickness varies widely among the different citrus varieties, from a few millimeters in mandarins to a few centimeters or more in grapefruits and pomelos.

The endocarp consists of a pulp with segments (locules), separated by a membrane of thin epidermal tissue and containing numerous spindle-shaped juice sacs (vesicles) and seeds. The juice sacs in each segment are attached to the segment wall and in contact with the peel by means of fine threads of varying length. Embedded within the cellular tissue in the central part of each juice vesicle are oil droplets.

The core of the fruit is composed of a white spongy tissue similar to that found in the albedo. The core and segment membranes are collectively called the "rag" of the extracted juice.

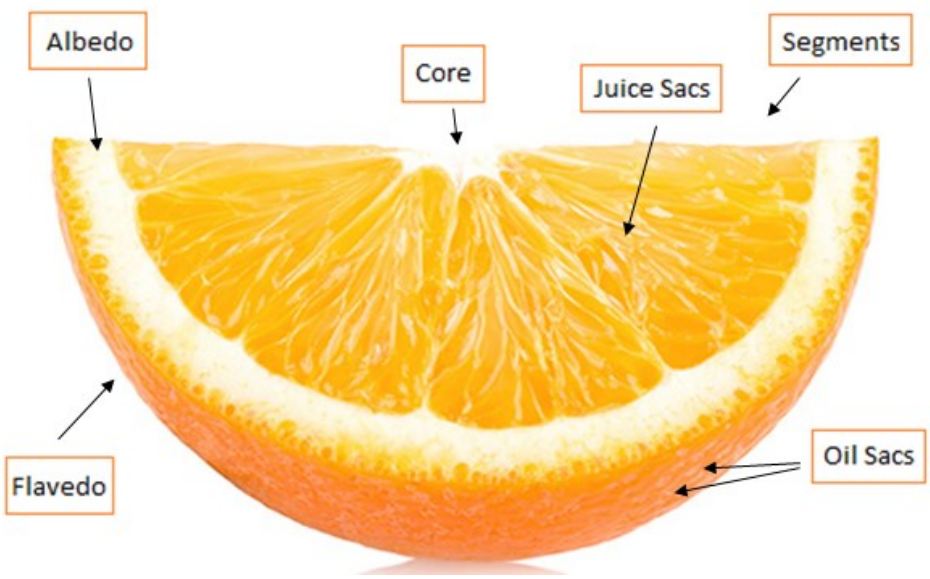

Figure 2: Segment of an orange (originally in colour)

1.1 Sweet Orange

Sweet orange (*Citrus sinensis* (L.) Osbeck) constitutes by far the most important class of commercial citrus grown in the world. More than a half of the citrus produced in the world falls into this category.

Sweet oranges are known by different names around the world, including *naranja* in Spain, *arancia* in Italy, *laranja* in Brazil and *malta* in India.

Sweet oranges can be classified into four classes with distinct characteristics: “common orange,” “acidless orange,” “pigmented orange,” and “navel orange”. Among the common oranges, Valencia, Pineapple, Hamlin, Parson Brown, Jaffa, and Shamouti are grown abundantly in several parts of the world. The Mediterranean region is a secondary center of diversity in the sweet orange species. Here, many new and improved sweet orange varieties have been developed through bud mutations and chance seedlings. These include the high-quality blood oranges (Sanguinelli of Spain) and the high-quality standard sweet orange varieties. The Spanish Sanguinelli, Moro, and Tarocco varieties have a distinct flavour and are more likely to show blood coloration than other blood orange varieties due to high presence of anthocyanins.[6]

About two-thirds of all sweet oranges fall into the common orange category. Common oranges are referred to as "white" or "blond" oranges. In Spain they are called *blanca* and in Italy *bionda*. The most predominant variety in this group is the Valencia orange, which constitutes about half of all the oranges grown in the United States, especially in Florida. Valencia oranges are also the most predominant commercial variety of any type of citrus. One reason for this is their long growing season (February/March to August/September, depending on the climate), their ability to adapt to a wide range of growing conditions and their resistance to freeze damage. Thus, they are grown in every major orange-producing country in the world.[7]

The origin of Valencia oranges is uncertain; most likely, they came from the Azores Islands and perhaps from Portugal and not (contrary to popular belief) from the well-known city of Valencia in Spain, which is also famous for its orange production.

All common round orange varieties are suitable for processing, but some are preferred to others. The Valencia is the most widely grown variety for processing. The early-maturing varieties tend to produce poorer juice colour, lower yields of soluble solids, and more after-processing bitterness (if harvested early) than most mid-season and late varieties. Navel oranges are primarily grown for fresh market because of their tendency to develop a bitter taste in processed products due to the presence of limonin derivatives in their juice.

1.2 Nutritive value of sweet orange

Since ancient times, man has known the importance of orange as a fruit with beneficial medicinal values. Orange provide adequate nutrition with respect to vitamin C; however, it also contains other nutrients such as mineral salts[8], carotenoids and flavonoids[9]. Nutrients from a fresh source are immediately available to the body, although in a small amount (Table 2). However, even a small amount of vitamins can prevent the appearance of sub-clinical signs of deficiencies.

Orange or orange juice can be an excellent source of health-promoting substances during the day. An ordinary glass of orange juice provides a good portion of the nutrients required by human body for one day. In citrus fruits and specifically in oranges, carotenoids are mainly associated with pulp and its particles extracted in the juice (Table 3). It is advisable to eat fruit rather than to drink its juice since many antioxidants present in the pulp or fibrous part are removed when juice is sieved.[10,11]

Nutritional properties of four orange varieties

	Alanya	Finike	W. Navel	Shamouti
Dry matter (g/100 ml)	11	12.82	12.48	12.2
Vitamin C (mg/100 ml)	51.51	46.26	38.69	34.27
Reducing sugar (g/100 ml)	4.02	6.12	5.78	6.09
Sucrose (g/100 ml)	4.16	4.24	4.47	3.33
Zn (mg/l)	1.70	3.16	2.34	1.72
Fe (mg/l)	0.86	1.4	0.72	0.70
Cu (mg/l)	0.54	2.77	0.56	1.37
K (mg/l)	1364	1107	1255	1011
Mg (mg/l)	102.4	99.1	96.6	84
Mn (mg/l)	0.02	0.11	0.05	0.05
Na (mg/l)	7.7	7.3	12.7	5.7
Ca (mg/l)	94.7	93.3	53.7	88.0
P (mg/l)	150.1	125.2	157.5	174.2

Source: (Topuz A.. et al.,2005)

Table 2: Nutritional properties of different varieties of orange

Vitamin C content decreases with fruit maturity in oranges, tangerines, and grapefruits. Fruits of early harvest or normal harvest are therefore more healthful than fruits of late season as far as this vitamin is concerned. Conversely, thiamin (vitamin B1) increases from about 0.5‑0.6 g to about 0.75‑0.8 g per gram of juice with maturity in oranges. Similarly, niacin content also increases.[12]

Carotenoid levels in fresh squeezed orange juice

Carotenoid	Quantity (mg/L)
Violaxanthin isomers	2.62
Luteoxanthin + (Z)-antheraxanthin	1.33
(9Z)-Violaxanthin + antheraxanthin	5.70
(Z)-Luteoxanthin	0.61
Mutatoxanthin	0.70
Lutein	0.57
Mutatoxanthin	1.29
Zeaxanthin	0.55
Antheraxanthin	1.18
Zeinoxanthin	0.31
β-Cryptoxanthin	1.69
α-Carotene	0.19
β-Carotene	0.17
Apigenin-d	11.11
Vicenin-2	32.61
Narirutin hexose	20.83
Neoeriocitrin	7.33
Narirutin	23.35
Hesperidin	355.92
Didymin	4.99

Source: (Stinco et al., 2013)

Table 3: Carotenoid levels in fresh squeezed orange juice

Oranges have very high content of potassium (130 mg in 100 ml of orange juice), while sodium content is relatively low (1 mg in 100 ml of orange juice). The ratio of K and Na inside the fruit plays an important role in maintaining electrolyte balance and maintaining cells osmotic balance. Regarding fruit consumption benefit, a glass of orange juice or few fresh oranges each day provide daily-required electrolytes. Potassium and sodium are also important constituents of fluids present within and outside human cells.

Orange also provides iron: a medium-sized orange (200 g) contains about 2 mg of iron. Thus, two oranges a day provide half of the amount of iron recommended (by the Dietary Reference Intake) for an average healthy 40-years man.[13] Furthermore, iron from oranges is more available than from other sources, since the simultaneous presence of ascorbic acid increases iron absorption.[14]

In orange, the presence of ascorbic acid allows folic acid, a compound prone to oxidation, to retain its reduced form.[15] Vitamin E has been reported to be present also in oranges.[16]

Orange juices also provide minerals that are part of the vital enzyme system of the human body. In addition, several compounds like flavonoids, pectin and cellulose, are present in orange fruit.

All citrus fruits contain carbohydrates in the form of sugars: sucrose, glucose, and fructose. Total soluble solids in juice consist mainly of those sugars. Fibrous rag (mainly formed by cellulose and pectin), usually removed in industrial juice manufacturing processes, are also eaten when fresh oranges are consumed. A 150-gram edible portion of orange provides 17 g of carbohydrates that can supply up to 73 kilocalories.[17] While commercial orange juice contains roughly 10 g of sugar every 100 ml. The sugar found in major quantity in commercial juice is usually sucrose.[18] However, oranges do not contain high doses of proteins compared to many other foods (most of which are animal-related), and thus, from a nutritional point of view, cannot substitute a protein source in the diet.

In fresh citrus fruit, albedo and internal membranes contain a good portion of fibre. Fibre is a generic term that includes those plant constituents that are resistant to digestion by secretions of the human gastrointestinal tract. Dietary fibre may be classified as water-soluble fibre and insoluble fibre. Gums, mucilages, some hemicelluloses, and pectins are part of the soluble fibre class. While celluloses, hemicelluloses, and lignins are insoluble fibres.

Pancreatic enzymes do not digest dietary fibres since human lacks the necessary enzyme to break down those polymers. Cellulose shares with starch the recurring structure of D-glucose chain, but their bonding differs: the starch comprises α-1,4 linkage, which is hydrolyzed by amylase in both human saliva and intestine. On the other hand, cellulose is formed by β-1,4 bonds, which can only be hydrolyzed by cellulase enzymes. Similarly, pectins and hemicellulose cannot be broken down in human intestine and are excreted through feces. However, intact fibre prevents gastrointestinal disorders by easing the motion and rapid passage through the intestine, and also minimizes the absorption of harmful compounds in the diet. Dietary fibre is reported to lower the incidence of ischemic heart diseases. Moreover, synthetic fibrous substances have been utilized to promote the lowering of blood cholesterol from the intestinal lumen. Orange pectin also reduced plaque formation on the surface of aortas and decreased the narrowing of coronary arteries. There is a 7.6% decrease in plasma cholesterol, a 10.8% decrease in low-density lipoprotein (cholesterolcarrying lipoprotein, or LDL), and a 9.8% decrease in ratio of low-density lipoprotein to HDL in human volunteers given a pectin diet.[19]

The presence of flavonoids, limonin and other phenolic compounds, also found in orange juice, seems to have an inhibitory effect on tumor growth. In two study conducted on rats, fed on orange juices, breast and colon tumors growth less and with minor proliferation compared to control groups.[20,21]

2. Orange juice manufacturing process

The Merriam-Webster dictionary defines juice as the extractable fluid contents of cells or tissues. Although many fruit juices are the obvious result of expressing the liquid from the whole or cut fruit, there are some fruits where the distinction is not so apparent. For example, squeezing peeled mango flesh yields little juice, until the flesh is comminuted and a dense puree is obtained. Adding water to mango puree decreases its consistency, but it cannot be considered juice anymore. In contrast, comminuted apples yield a readily expressible juice. The fluid expressed from lemons, limes and excessively acid fruits is certainly juice, but the liquid is too sour to be consume directly without dilution with sugar and water to produce commercial beverages like lemonade or limeade.[22]

Codex Alimentarius defines juice as "unfermented but fermentable juice, intended for direct consumption, obtained by the mechanical process from sound, ripe fruits, preserved exclusively by physical means. The juice may be turbid or clear. The juice may be at its original concentration ("not from concentrate" (NFC) juice), or it may has been concentrated and later reconstituted with water ("from concentrate" juice (FCJ)), in a proportion suitable for maintaining the essential composition and quality factors of the juice. The addition of sugars or acids can be permitted but must be endorsed in the individual standard".[23]

The citrus fruit processing industry is a multiproduct sector that utilizes the entire fruit. Canned orange juice was the first commercial citrus juice produced, in the early 20th century. In fact, among citrus fruits, oranges are the main variety utilized for processing (Figure 3).

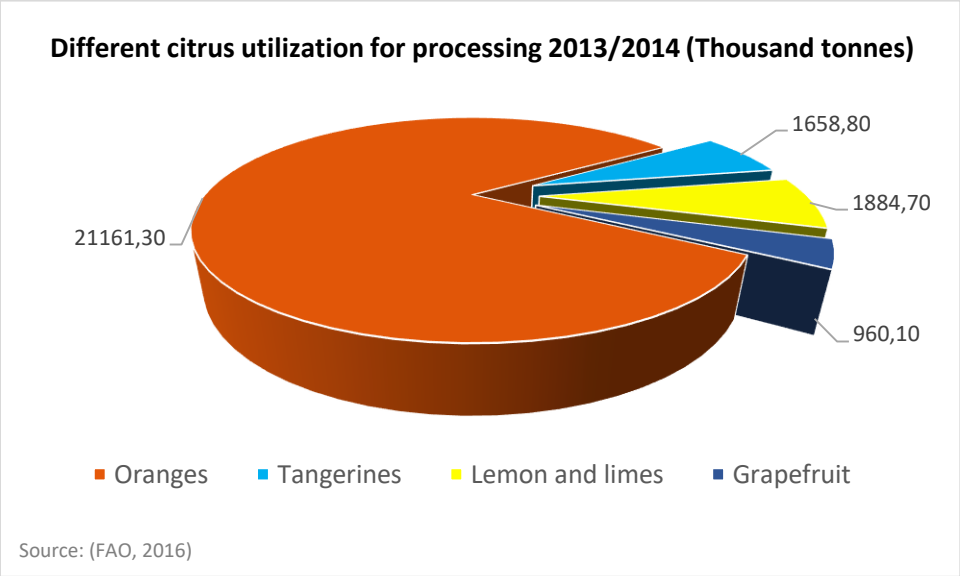

Figure 3: Different citrus utilization for processing 2013/14 (originally in colour)

After its extraction from the fruit, orange juice is either marketed at its original concentration or concentrated. "Single-strength juice," also known as 100% juice, is either NFC juice or juice

reconstituted from a concentrate by dilution with water to the natural single-strength Brix value. Both kinds of single-strength juice belong to the category of “ready to serve” (RTS) or “ready to drink” (RTD) juices. NFC juice is fresh juice extracted from the fruit without being concentrated or diluted. It is usually judged of higher quality than juice from concentrate and is slightly more expensive. NFC juice is, at present, the closest match to freshly squeezed juice. It meets with outstanding consumer acceptance for its flavour, convenience, and it resembles the image of a healthy food product.

Fresh, “raw,” or “freshly squeezed” unpasteurized NFC is in small but increasing demand by the nature-oriented consumers, even if it has a very short shelf life.[24] Although, it possesses some risk of contamination with pathogenic microorganisms like Escherichia Coli,[25] even if it is possible to reduce it to some extent immerging the fruit in hot water before the squeezing of the juice.[26]

The unique nature of citrus fruit lends itself to specific processing methods. Orange processing consists mainly of receiving and storage of fruit, fruit washing and grading, juice extraction, juice finishing or screening, heat treatment, packaging, and storing. Blending of previously prepared or purchased juices is very common, along with the manufacture of byproducts such as pulp wash juices, oils, aromas, animal feeds, pectins, flavours, fuels, phyto products and many more.

2.1 Gathering and washing

The methods of collection and transport of the fruit differ among countries and depend on the scale of the processing plant. Fruit arrives at the juice plant from either the orange grove or, in rare cases, from a packing house. Usually, the orchard is divided into blocks, where representative samples are taken from to determine the maturity index (degrees Brix and titrable acidity). When the index meets the standard set by the processing industry, the block is harvested. Generally, the majority of the fruit is harvested by hand. Mechanical harvesting has been recently introduced but is still not widely practiced for economic reasons. The pickers collect the detached fruit in bags that they empty afterwards into pallet bins and then into a truck (Figure 4). Otherwise, the use of a special vehicle (called “the goat”) allows automatically lifting of the bins to the tub of the truck. When the tub is full, the goat moves near the final transport vehicle, which can be a dump truck or a tractor-driven trailer. Thus, the fruit travels to the factory in bulk, in a truck or in a trailer. The proportion of fruit badly damaged in transport depends on the distance, the quality of the road, the weather, and the degree of maturity: the nearer the juice plant to the orange grove the better the conditions of the received fruit.

Figure 4: Workers gathering oranges in Sicily (originally in colour) (Courtesy: Fresh Plaza)

At the factory, the trucks are weighed and subsequently emptied on a conveyor or into a pit by gravity. Fruit from the field usually contains leaves and stems that can affect conveying equipment. Such fruit can be passed over a trash or leaf eliminator. A common trash eliminator is the spread roller conveyer, which consists of roll bars with sufficient separations between them to allow trash to fall (Figure 5a).

Here, the fruit is given a first inspection for the removal of badly damaged fruit. It is important to remove the rotten and wounded fruit before storage to avoid contamination.

Figure 5a: First inspection on a trash eliminator (originally in colour) (Courtesy: Fresh Plaza)

Fruit coming from a packing house, on the other hand, has already been graded and has the trash removed (Figure 5b). The fruit most likely has been waxed, since packing houses do not like to grade their fruit until it has been waxed. Thus, no grading during unloading is necessary.

Figure 5b: A packing house working with different citrus fruits (originally in colour) (Courtesy: Fresh Plaza)

In most plants, the fruit is elevated and distributed into surge bins. The bins are equipped with inclined baffles, which ease the descent of the fruit, avoid crushing by excessive pressure at the bottom and distribute the fruit evenly. At the bottom of the bin, an adjustable discharge gate regulates the exit rate. At the exit from the surge bin, a withdrawal belt takes the fruit to an elevator, which delivers it to the washer.

Fruit coming from a packing house is usually clean and leafless and may not need washing at all. However, moist fruit is more easily conveyed. Also, as stated before, the packing house tends to put waxes on their fruit to prevent water loss and thus retarding rotting and spoilage. Washing helps

remove some of this wax and allows the fruit to be moved more efficiently. Rotating brushes under a water spray are commonly used to wash oranges just prior to processing (Figure 7). Water can also be chlorinated (using 100–200 ppm free chlorine) to improve the sanitation effect. Detergents approved for use on foods can be sometimes applied. In the manufacture of juice products that do not undergo any heat treatment, careful fruit washing becomes imperative to remove excessive microbiological contamination. Fruit washers also often eliminate much of the trash and damaged fruit that has not been previously removed.[26]

The best fruit-washing system consists of a gridded roller that pours solid trash into one or more screw conveyers running under the washer that allows to separate the solid and liquid debris that falls through the roller. Else, after the washing step, the oranges are discharged on a roller-grader that allows workers to remove manually foreign objects and fruit not suitable for juice extraction. The rejected material is either dropped into discharge chutes or placed on a discharge conveyor.

Figure 6: Orange washer (originally in colour) (Courtesy: Fresh Plaza)

From the roller-grader the fruit is conveyed to the juice extraction area. In most plant layouts the juice extraction area is an indoor area, usually on an upper floor of the plant in which case a feeding transport system is required. The reason for such a layout is sanitation and ease of conveying the extraction products and by-products for further processing by simply gravitation. Most juice extraction systems require presizing of the fruit, which is usually allocated before the extractors.[27]

2.2 Juice extraction and pasteurization

The process of juice extraction from orange is commonly regulated through two specific extraction procedures: the Brown extraction system, which was the first utilized for the production of orange juice, and the widely utilized FMC extraction method. Even though there are other juice extractors that differ somewhat, the FMC cup extractors and the Brown reamers set the standard in juice extraction equipment. Both extractors are widely used and are known to produce high-quality citrus juices.

In both methods, the juice is obtained from the fruit by pressing or by reaming. The main difference regards the extraction of the oil. In the Brown extraction system, the oranges, after being washed and graded, are sent to the “Brown oil extractor” (BOE), which consists of rotating rolls with sharp stainless-steel points on their surface. The axis of the rollers is perpendicular to the direction of the citrus flow, so the oranges are spun while advancing through the rollers. The sharp points puncture the entire surface of the fruit, rupturing the oil glands and liberating the oil. The oil released is washed away by water sprays and sent to a centrifuge where the two phases can be separated. Prior to juice extraction, fruit needs to be dried to remove the oil and water clinging to the surface. The advantage of this system is that the rasping of the peel is made without producing much debris, easing the separation of the oil in the next phases. From the dryer, fruits are arranged by size and fed, one by one, into a conveying chain bearing opposing half cups. Each orange, enclosed between two half cups, is automatically cut into two halves. The fruit halves are pressed against rotating reamers: the juice is collected while the peels are discharged.

In the FMC system, the peel oil is obtained simultaneously with the juice extraction. The oranges are sorted and then pressed, without halving (Figure 7).

Figure 7: FMC extraction system (originally in colour) (Courtesy: Fresh Plaza)

During the squeezing, the orange is enclosed and supported by a pair of cups with intermeshing fingers, thus preventing bursting or disintegration of the peel because of the pressure.

When the fruit is placed inside the lower cup, the upper cup comes down and squeezes the fruit. The upper and lower cups have holes in the center of the cup with a sharp edge that cuts about a l-inch-diameter hole in the bottom of the fruit, and all of the inside portion of the fruit is forced down into the hole into a perforated pipe. This orifice tube has a delimited diameter at the bottom that creates a backpressure on the incoming fruit material. The core material ejected out the bottom of the orifice tube is usually discarded out the bottom of the extractor with the peel. The juice is squeezed through the openings in the strainer tube and conveyed through the rear of the machine to juice-processing equipment. The outer peel slides through openings in the upper cup and falls out the back and bottom of the machine into a screw conveyer and out of the plant. As the outer peel slides out of the upper cup, it is bent backward, bursting the juice oil sacs in the flavedo. This bending/scraping motion releases the oil in the oil sacs. A water spray washes the peel to form a slurry consisting of water and peel oil. This emulsion washes down the front of the machine into a small screw conveyer and is transported to the oil recovery equipment.[28] Therefore, the juice and essential oil are recovered separately and simultaneously. According to JBT FoodTech, 75% of the world's citrus juice production in over 35 different countries is based on this technology.[29]

The great advantage of the FMC system is that the peel and the juice are completely separated, due to the design of the extractor machine, avoiding contamination between them. Although, the squeezing may affect the oil glands during the extraction, contaminating the juice in the process.

Brown extraction system allows a cleaner recovery of the oil, but pieces of the peel may linger on the extraction machines and fall into the juice line.

In any case, the raw juice exiting the extractors is collected in a surge tank and chilled to 7-9°C to avoid microbial and enzymatic deterioration. Rapid chilling is. accomplished by pumping the juice through a heat exchanger with refrigerated water as the cooling liquid. The chilled raw juice is sent directly to the next phase or kept in cold tanks until further use.

Next, the juice passes through a phase of screening, filtration and centrifugation to remove suspended solid in excess (even if some of them are kept to give the juice the "freshly-squeezed" appearance).

Stabilization of orange juices by pasteurization has two simultaneous purposes: inactivation of pectinolytic enzymes and destruction of pathogenic microorganisms. Inactivation of pectin methylesterase (PME) is essential for the stability of the uniform cloudiness of the juice and for preventing gelation in concentrates.[30] Destruction of the microorganisms is of paramount importance for food safety and for the prevention of spoilage. Although, due to the low pH of orange juice (pH < 4), growth of pathogenic microorganisms is suppressed.

Orange juices need about 82.5°C for two seconds or 93°C for one second to pasteurize and deactivate pectinase enzymes.[31] According to Rebeck, [32] citrus juice is flash-pasteurized at 85–93°C with a holding time of 30 s. The commonly established industrial practice consists in heating the juice to 92–98°C for about 30 s immediately after extraction and screening.

During thermal pasteurization, destruction of microorganisms and inactivation of enzymes are not the only outcome. Other effects of the heat treatment include destruction of vitamins, undesirable colour changes and change in flavour.[33,34] Each of these heat-induced chemical degradations possess its own kinetic. The activation energy of the chemical reaction is lower than that of the thermal inactivation of enzymes, which, in its turn, is lower than that of the thermal killing of microorganisms. Therefore, for a giving stabilization effect, heat treatment at a higher temperature for a shorter time results in less thermal damage to quality than heat treatment at lower temperature for longer time. Hence, orange juices are rapidly heated in appropriate heat exchangers, for the specified time necessary for stabilization, and then cooled as rapidly as possible. The promptness of the cooling step often determines the degree of the thermal damages. Often water, flavour and colour additive (like flavonoids) are added to the juice after pasteurization to replenish the original juice concentration as well as the flavour.

The inactivation kinetic of PME was also evaluated taking advantage of microwave heating[35] on laboratory and pilot scale. Recently, pulsed electric field (PEF) was also investigated.[36,37]

Low pulp Valencia orange juice was also sterilized using high-pressure homogenization (HPH). Juices pre-homogenized at 20 MPa, partially depulped by centrifugation and finally homogenized at 150 MPa gave a resultant product with fresh taste, colour, cloudiness and aroma composition close to those of the original fresh juice. These quality properties were preserved for 15 days under refrigerated storage.[38]

Experiments with ultraviolet light was also performed on orange juice with a wavelength of 254 nm, inactivating most of the microorganisms, extending shelf life, but without deactivating PME.[39]

2.3 Evaporation and packaging

Another process employed in orange juice finishing is evaporation. Orange juice contains 85-90% water. Thus, evaporation process aims to remove a considerable amount of this water, to concentrate the juice. Evaporation gives several advantages to an orange juice industry: it reduces the mass and the volume of the juice, allowing storage space and transportation costs reduction. Concurrently, it helps pasteurizing the juice, deactivating pectinase enzymes and preventing spoilage. Like pasteurization, the disadvantages are that the heat treatment reduces the oxidative shelf life of the product and removes delicate flavour components. Although, improper storage (which regards both the package and the temperature storage conditions) can have a greater impact on decreasing the oxidative shelf life of orange concentrates than heat treatment during evaporation or pasteurization.[40]

In order to avoid evaporation of volatile compounds, it is possible to operate at low temperature under reduced pressure or vacuum. However, lowering the temperature increases the viscosity exponentially, which complicates heat transfer and fluid flow.

There are several ways to restore original aroma. As stated before, the first one is with the addition of artificial aroma, bought outside the plant. It is also possible to use the same aroma, which have been evaporated, employing a fractional distillation, recovering the more volatile compounds. Lastly, but more widely diffused, aroma is restored blending the concentrated orange juice with untreated orange juice.

Evaporation generally involves two types of evaporators. The most common and one of the most efficient is the thermally accelerated short time evaporator (TASTE) (Figure 8). A common TASTE evaporator is based on the "descending turbulent mist" principle: a series of tubular heat exchangers using condensate from one another as the heat source. The first exchangers uses steam from a boiler as the heat source. The product mist falls freely down the tubes, absorbing heat and evaporating water. As it does so, it accelerates until, near the bottom of the tube, it reaches near sonic velocities, resulting in a pressure drop as the product falls. With plate heat exchangers, a vacuum vessel is used to evaporate the water from the heated juice, with a similar effect.[28]

Figure 8: A TASTE evaporator (originally in colour) (Courtesy: Fresh Plaza)

Orange juices are normally concentrated to 62–65 °Brix, then diluted with four volumes of water to produce five volumes of juice at 12 °Brix. Hence, they are designated as “five to one” concentrates. The traditional frozen concentrated orange juice made by the cutback process for the retail market is a four to one concentrate. Further concentration up to 72 °Brix (six to one concentrate) would be highly desirable.[41]

The viscosity of the concentrate limits the practical maximum concentration attained. Evaporation of juice to concentration levels above 65 °Brix in commercial TASTE evaporators would result in longer residence time and excessive caramelization of the concentrate.

Orange juice concentrates are marketed in small units for home use or in bulk for reprocessing. Concentrates in small units are retail marketed as frozen, in 6, 12, or 24 oz. easy-open metal cans or 350 g plastic cups. Both four to one and five to one strengths are available. If the cold chain temperature of ‑18°C, normally observed with frozen foods, is maintained, a shelf life superior to 1 year is guaranteed. Concentrates destined to reprocessing (or reconstitution) are aseptically stored in refrigerated stainless-steel tank farms, or aseptically filled into a 200 L plastic lined or coated steel drums and stored under refrigeration. The temperature of bulk concentrate should not allow exceeding 2°.[42]

2.4 Pulp wash

The pulp expelled from juice centrifugation machines retains 75-80% of juice, which can be recovered by washing and refinishing it several times. The resulting juice is commonly referred to as pulp wash or water-extracted soluble orange solids (WESOS). During the first wash, about 50% of the available juice from the expelled pulp can be recovered. If two stages are used, 60% of the available juice can be obtained, and if three stages are used, the recovery of 75% of the available juice in the pulp can be achieved. A four-stage system can recover up to 80% of the available juice from the pulp.

The most efficient multistage pulp wash system is a countercurrent flow where fresh water is used in the last stage and backwards until the first stage: this reduces the time needed for the juice in the pulp and the washing solution to equilibrate. The efficiency of a pulp wash system depends on a balance of parameters, including the water-to-pulp ratio and the number of stages. The ideal water-to-pulp ratio is between 1.5 and 2.0; more than three or four stages contribute little to the percent recovery of juice from the pulp.[28] A pulp wash system can increase the juice yield by 2.5 to 3.5 kilograms of soluble solids per ton of fruit. This increase in yield due to pulp washing can represent a significant increase in juice yield, especially when juice is in high demand. Pulp wash juice is generally considered inferior to extracted juice in both colour and flavour. Flavonoids and carotenoids content in pulp wash juices constitutes the major defect in pulp wash in comparison with conventional orange juices.[10] Recently, it was found that dimethylproline may be used as a marker to discern between orange juice and pulp wash.[11]

However, pulp wash juice contains a greater amount of high-molecular weight compounds, such as pectin and hemicellulose that add viscosity to resulting concentrates. This added viscosity can pose problems in transportation during evaporation and chilling. For this reason, enzymes, like pectinase and cellulase, are added during the first stage of pulp washing that help break down these high-molecular weight compounds.[43,44]

Without enzyme treatment, concentration levels of over 40 °Brix can be difficult to achieve.

An alternative enzyme treatment consists of adding enzymes to the final pulp wash and holding the juice for about an hour at 46 °C. If necessary, the pulp wash can even be pasteurized and/or centrifuged before evaporation.

Pulp wash recovered and concentrated separately can be used in fruit drinks or in other food products but not in 100% orange juices. Pulp wash may also be used as a carbohydrate source in drink bases and as a clouding agent.[45]

Lastly, the exhausted pulp can be dried and sold as a source of fibre or it can join the peels in the production of animal feed.[46,47]

3. Orange waste

Citrus fruit (orange in particular) offers a great potential for the production of commercial products other than the juice. In fact, even if orange processing industry treats the largest quantity of industrial fruits, it also produces the biggest amount of by-products. The production of the juice generates nearly half of the weight of the fruit as a waste. For the industries is essential to transform these by-products into marketable compounds.

Because of their quantity and perishable nature, orange peels constitute a problematic waste. They contain about 75-85% moisture, rot rapidly, release liquids, attract flies and create mycotoxins. Clearly, this waste must be removed from the plant as rapidly as possible. Thus, it is necessary to refine the peel waste management more than attempting to increase profits.

As previously stated, the recovery of essential oils is an integrated part of the orange processing activity during (or before) the squeezing of the fruit. On the other hand, the peel of the fruit, recovered by both Brown and FMC extraction systems, previous proper treatments, may be employed as cattle feed (Figure 9). In some countries, this waste material is still disposed by spreading the solid waste on adjacent fields and flushing the liquid wastes into streams or sewers,[48] thus generating a heavy toll on the environment.

Figure 9: Orange dried peel (originally in colour) (Courtesy: Fresh Plaza)

Economically, the most profitable solution for the orange processor is to sell the peels without any further treatment to nearby farmers, for direct feeding of ruminants. Cattle-breeders located near orange canneries early recognized the value of cannery waste. In fact, the high water content and perishable nature of the waste would not allow transporting it economically for feeding purposes.[49]

In the last two decades, industries have searched for other food-grade by-products by recycling orange waste materials like pectin, jellies, jams, fruit sections, juice drinks, and purees. Peel extracts

are also commonly used as beverage bases in many parts of the world, mainly as the result of improved debittering techniques. As previously stated, it is also possible to employ cloudy peel extracts as stable clouding agents in the drink industry while shaved peel may also be utilized to make potpourris or candied peel.[50]

The different types of waste encountered in an orange processing may be classified as solid wastes and liquid wastes. Solid wastes include cannery waste (consisting of peel, rag and seed), screenings from orange pulp, sludge from essential oil distillation, residues from plants producing pectins. Liquid wastes include cannery effluents, pulp drying plant effluents, distillery effluents, effluents from pectin plants.[51]

The peel, pulp, rag and seed are usually mixed together and dried in rotary driers, bagged or stored in bulk and sold as orange pulp. Some orange processing plants use a multiple effect steam evaporators to concentrate the liquor pressed from the peel into 72 °Brix orange molasses for sale as feedstuff.

The process of preparing orange pulp and orange molasses from peel, rag and seed is often planned before the construction of the orange juice extraction plant and it comprises several passages.
After extracting the juice from the orange, peel is dropped into a conveyer to be carried to the feed mill. Pulp, rag and seed are removed from the extracted juice finishing operation. The pulp will be combined with the peel and will be stored in a peel bin, usually located outside the feed mill building. If water is not added in the extractor room, the moisture content will be about 76-78%. If oil peel still need to be extracted, then water has to be added for the extraction. This will result in an increase of the moisture content of the peel. From the peel bin, the wet peel are conveyed to a liming station where lime (which is a mix of calcium hydroxide and calcium oxide) is spread on them. The addition of lime presents various advantages such as neutralizing the organic acids, forming calcium pectate with the existing pectin (which reduce the viscosity) and remove some water. Evidently, the addition of lime results in higher percentage of calcium (1.6-2%) in the dried orange pulp.

Then, the peel is dropped into shredders where it is chopped into small pieces that are subsequently pressed to reduce the moisture of the peel to 70-75% (Figure 10). The press cake is dropped into the dryer feed screw conveyer and the press liquor is screened and pumped to the evaporator feed tank.

Figure 10: Orange peel shredder and press (originally in colour) (Courtesy: Fresh Plaza)

The resulting cake is usually dried with an oil-furnace dryer and pelleted, after being cooled down. The moisture content of the final product is near 10%.

The press liquor obtained in the pressing stage can be mixed to the initial wet peel to produce a sellable product called orange pulp. Otherwise, the liquor can be fed to an evaporator and concentrated to 72 °Brix. As stated before, this product is called orange molasses and it is also sold as feedstock.

The disposal of liquid waste from juice processing plants is of particular concern for the orange juice industry. This waste or effluent generally consists of fruit-washing wastewater, peeling and hand-grading table wastewater, and water dripping from waste bins. In several countries, water purification does not reach a satisfactory level and wastewater are emptied into lakes or discharged into rivers, generating water contamination. To improve the environmental sanitation and reduce pollution wastewater must be processed and recycled. In an orange processing plant, the processing of effluent water is mostly based on the use of conventional shaker screens to remove coarse particles. It also possible to employ small amounts of lime and polyelectrolytes (like ferrous sulphate, sodium aluminate, ferric chloride, or combinations of these chemicals) to induce coagulation and flocculation. In conjunction with air flotation, this process will result in a clear effluent and a reduction of the chemical oxygen demand (COD) of the liquid by 10-20%. It will also give a dewatered float concentrate of 5-10% (by weight) dry organic solids. Consequently, the

sludge formed may be passed for drying in a specific by-product plant or added to the processing of the pulp.

Biological treatment methods have been recognized as a reasonable option to treat wastewaters with a high organic content[52] such as those coming from orange juice processing industries.

However, the presence of bio-recalcitrant compounds frequently makes impossible to achieve an efficient treatment of these wastewaters. Possibly, this situation can be overpassed through the combination of biological and chemical processes. Biological treatment mineralizes the large biodegradable portion, reducing effectively the COD of the wastewater. The fruit juice wastewater could be efficiently treated by the combination of an aerobic biological treatment with a coagulation/ flocculation process (using ferric chloride), allowing the direct discharge into watercourses.[53]

In order to reduce costs, bio-gasification (or anaerobic digestion) of orange waste (both wastewater and peel waste) was also taken into consideration. Bio-gasification would produce a fuel in form of methane and at the same time eliminate or mitigate disposal issues. According to Koppar & Pullammanappallil,[54] it is possible to convert orange peels to biogas in a thermophilic leach-bed digester, while using wastewater as substrate for anaerobic digestion. Based on the experimental methane potential, it was estimated that the biogas produced through anaerobic digestion of both orange waste feedstocks can be used as a fuel to generate more electricity than that consumed by the processing facility, hence producing an income.

Recently, it was studied the possibility to produce biologically activated carbon (BAC) from orange dried peel. Biological activated carbon (BAC) has great advantages in low concentration and refractory organic wastewater degradation. Since most of the orange peels retain a porous structure, BAC possesses a hydrophilic surface group and can act as a cheap adsorbent. The adsorption can be enhanced by carbonization and activation. The as-prepared active carbon with loose pore structure, large specific surface area and massive surface functional groups exhibits enhanced reactivity due to small crystallite size and crystallite thickness, and may be used to treat wastewater which contains organic materials, like the ones produced by juice plants.[55]

Albeit those recent researches, a large fraction of orange waste is still deposited every year. This deposition is not beneficial due to both economic and environmental arguments such as high transportation costs, lack of disposal sites, and the land-filling material having high organic content.[56]

3.1 Orange waste composition

The opportunity to utilize citrus wastes at full potential necessitates a deep knowledge of their chemical composition. Apropos of this, it should be noted that, as for all vegetal products, the exact chemical composition varies between species and is affected by natural factors such as growing conditions, climate and maturity.

Unprocessed orange waste may include a vast variety of products like peel, seeds, rags and core (Figure 11).[57]

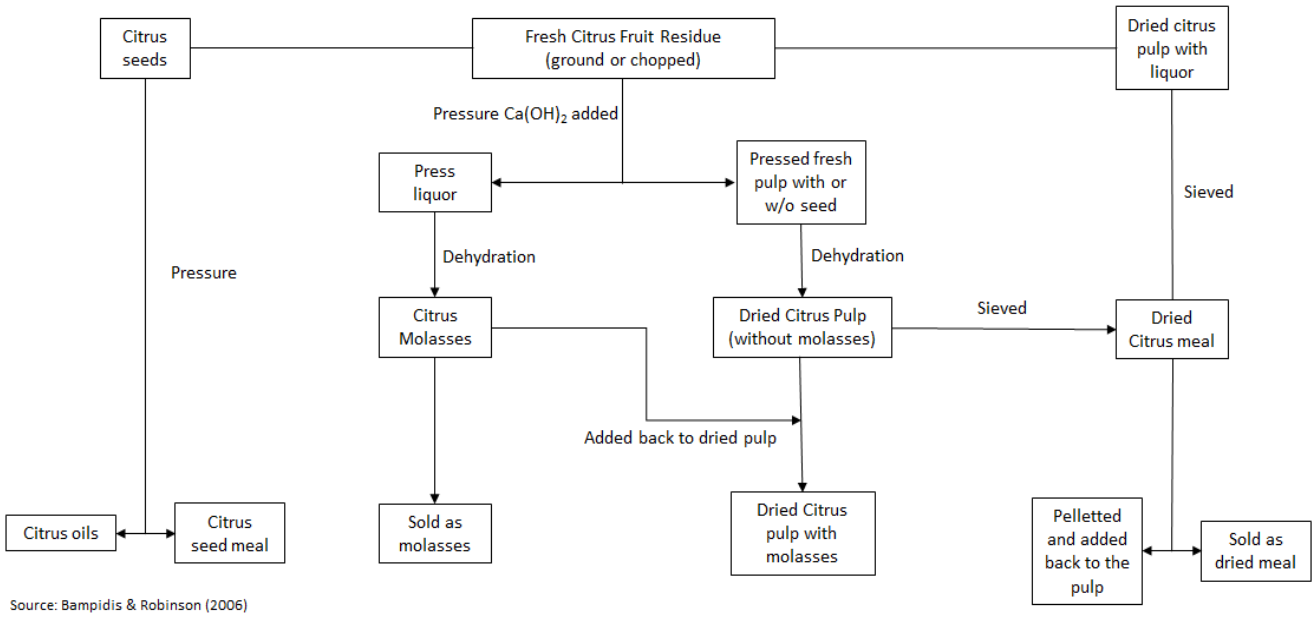

Figure 11: Schematic presentation of citrus by-product production

As previously specified, orange juice industry tends to mix those wastes, dry them mechanically (or chemically), before sending them to cattle-farms.[58] Furthermore, problems with product definition may arise due to homonymy between the pulp of the orange (which is the solid residue present in the juice and collected by centrifugation) and the orange pulp (which is the mixture of the pulp of the orange with the other wastes of the juice process). For these reasons, standardization of citrus waste composition is challenging and a separate discussion for each waste is recommended.

Orange seeds composition is usually explored by either pressing or solvent-extraction methods.[59–61] Sweet orange seeds contains lipids (especially fatty acids[59], limonoids[60] and steroids[62]), carbohydrates and amino acids.[63] Most of the fatty acid content is due to linoleic acid presence (40%).[64]

Aside for specific industry, seeds are no longer collected by orange juice factory and are mixed (and crushed) during orange waste drying process.[57]

Rivas et al.[65] analysed Valencia orange peel recovered from a citrus processing plant through several extractions (mostly done in water and ethanol) and treatments (Table 4). Pectins account for half of peel weight, whose presence is found in both flavedo and albedo. Similar quantities of pectins, cellulose and hemicelluloses in Valencia orange dried peel were also found in a previous study.[66]

Orange Peel Composition (Percent on Dry Basis)	
Compound	%
Soluble sugars	16.9
Fibre	
Cellulose	9.21
Hemicelluloses	10.5
Lignin	0.84
Pectins	42.5
Ashes	3.5
Fats	1.95
Protein	6.5
Other compounds	4.35

Source: (Rivas et al., 2008)

Table 4: Orange peel composition

Marín et al. [67] examined in depth the chemical composition of both orange peel and orange pulp obtained from a citrus industry (Table 5). Orange pulp seems to possess the highest quantity of fibre (especially pectins), and higher quantity of fats and protein, while orange peel seems to have a higher concentration of flavonoids.

Chemical Composition (Percent on Dry Basis)		
Compound	% (Peel)	% (Pulp)
Soluble sugars	6.04	9.57
Fibre		
Cellulose	24.52	37.08
Hemicelluloses	7.57	11.04
Lignin	7.51	7.52
Pectins	12.07	23.02
Ashes	2.55	2.56
Fats	1.52	4.00
Protein	6.55	9.06
Flavonoids	11.00	4.5

Source: (Marín et al., 2007)

Table 5: Chemical composition of orange peel and pulp

Regarding this two research works, it is possible to highlight the difference in the fibre content: in the first work pectins account for nearly 42% of the peel weight, in the latter, pectins content is

around 12%. This variance may be caused by orange peel and pulp washing process. As stated in chapter 2.5, industry is likely to use pectinolytic enzymes to break down pectin chains and reduce the viscosity of the matrix, simplifying convey operations. Treatment with enzyme mixtures obviously reduces the exhausted wastes pectic content and increases cellulose, hemicelluloses and lignin percentage composition. Additionally, operational extrusion processing values (e.g. screw speed, barrel temperature, feed moisture) possess a noticeable effect on percentage composition of both insoluble and soluble dietary fibre of orange pulp.[68]

Ashes, which are usually analyzed through AOAC method,[69] are due to traces of elements (mostly potassium and calcium).[70,71]

Protein content is calculated by multiplying the elemental N content (calculated through elemental analysis) by the universal factor of 6.25. Amino acids[63,72] and citrusin[73] are the main source of azote in orange waste.

As previously highlighted, fatty acids account for the fat content in seeds. On the contrary, in peel fats are due to terpenes presence. Several terpenes has been already identified in orange peel waste: α-pinene, β-phellandrene, β-myrcene, D-limonene, β-pinene, sabinene, δ-3-carene, α-terpinene, α-cubebene, β-cubebene, caralene, *trans*-caryophyllene, valencene and δ-cadinene. However, D-limonene is the main terpene found in orange peel waste.[74,75]

Other compounds frequently found in orange waste are phenolic compounds (e.g. flavonoids).[76] Phenolic compounds are a class of products which the fruit plant synthesize from aromatic amino acids (phenylalanine and tyrosine) through the phenylpropanoid metabolic pathway.[77] Similarly as described for the fibre content, orange juice extraction and orange peel and pulp washing may alter the presence of flavonoids and carotenoids in orange waste.

Besides flavonoids and terpenes, a main component of orange waste is the dietary fibrous residue (which is composed by pectin, cellulose and hemicellulose): a schematic representation of the main components of orange waste is given in Figure 12

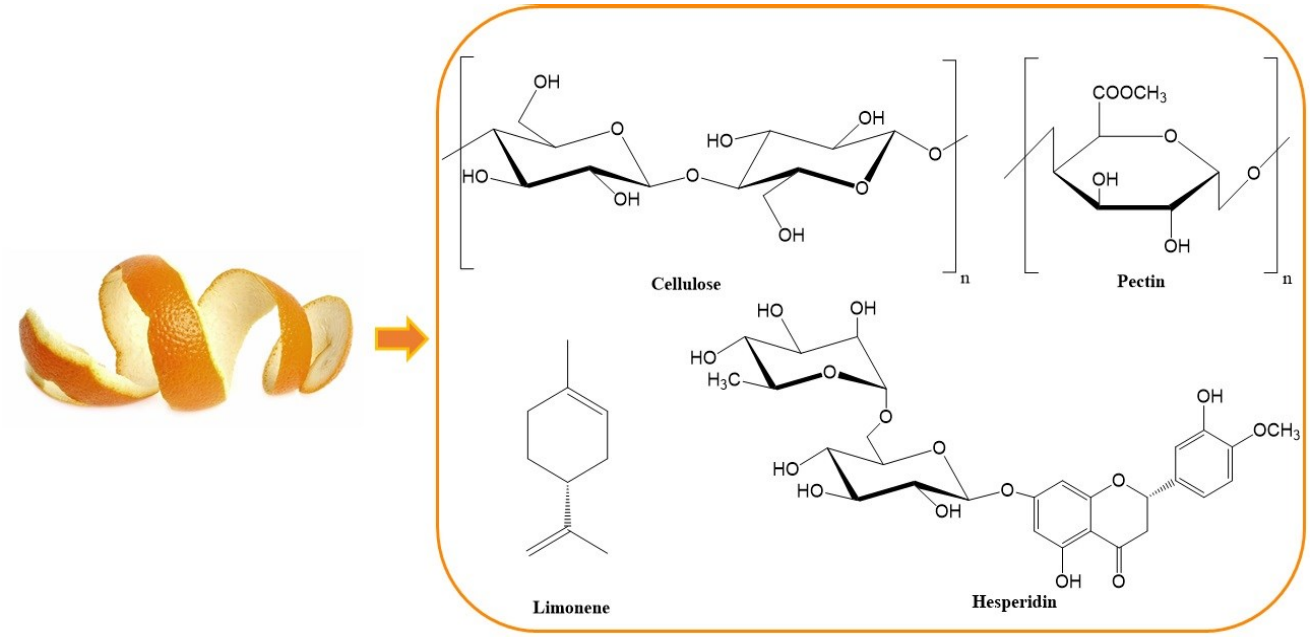

Figure 12: Schematic representation of main components of orange waste (originally in colour)

3.2 Direct valorisation of orange waste

To reduce process costs, researches regarding application of orange juice by-products have always aimed to direct utilization, the so-called 1st generation waste valorisation. This category takes account of all methods employing orange waste without component differentiation and with minimal transformation. Main products of this kind of process are biogas, biofuel, ethanol, and enzymes (Figure 13).

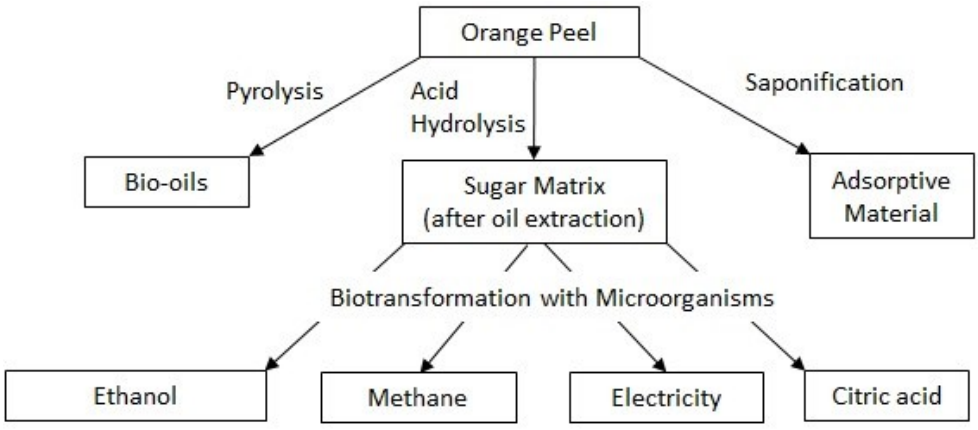

Figure 13: Schematic presentation of orange peel direct application

Ethanol synthesis is related to a biorefinery approach: a culture of microorganisms (often yeast) is fed with a sugar matrix (e.g. orange peel) in an incubator to obtain bioethanol. Precautions must be taken in advance to remove limonene from the matrix due to inhibition effect on the microorganisms' growth.[78] However, it is possible to encapsulate microorganisms during fermentation to protect them from D-limonene.[79]

Microorganisms can also be used to produce bioelectricity using orange peel waste as a renewable carbon source in a dual chamber mediator-less microbial fuel cell (MFC).[80]

Orange waste, especially peel, can be pyrolysed to produce bio-oil[81] and solid biofuels.[82] A high yield of renewable methane and an organic amendment can be obtained through the thermophilic biomethanisation of waste orange peel, following the removal of valuable essential oils from the peel. It is also possible to co-composte waste orange peel with the organic fraction of municipal solid waste at different proportions (17–83%).[83,84]

Fungus *Aspergillus Niger* can be employed with orange peel sugar matrix (obtainable after auto-hydrolysis) to produce citric acid in bot sub-merged[65] and solid-state fermentation.[85]

Finally, the high value of carbon in orange waste can also be exploited to produce adsorptive material to remove Violet B dye,[86] heavy metals (e.g. ions of lead, cuprum and iron),[87,88] and chromium.[89]

4. From waste to resource: single component extraction

As stated above, orange waste contains numerous high-value biological products. To obtain the maximum advantages of them, it is necessary to understand how it is possible to analyse, quantify and extract every single components.

Ideally, the best way to proceed would be based on consecutive extractions followed by treatments based on different pH to separate the target substances without modifying the other products left inside the matrix (Figure 14).

The process proposed in this thesis allows a new orange waste recycling, obtaining five different products, saleable as crude mixtures, purified compounds or derivatives.

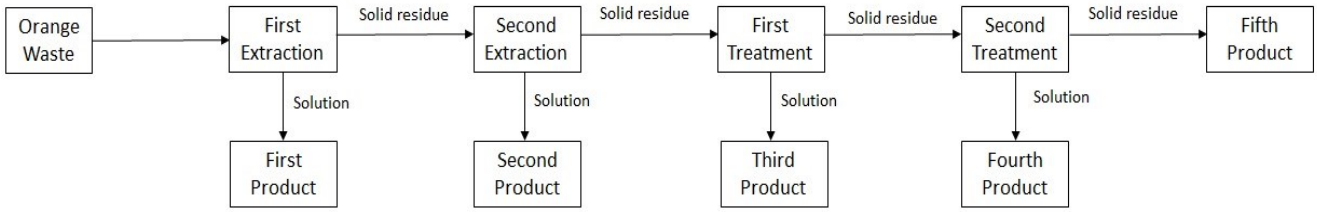

Figure 14: Schematic representation of a possible process for the total recycle of orange waste

4.1 Essential oils

Orange fruit contains essential oils inside little sacs or glands (also called “oil glands”), whose diameter ranges from 0.4 to 0.6 mm. Oil glands are located in the flavedo, at irregular depths.
Orange peel typically contains more than 5 kg of oils per 1000 kg of oranges and approximately 90% of these is D-limonene,[90] a cyclic terpene (Figure 15).

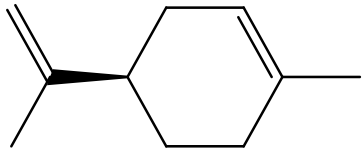

Figure 15: Chemical structure of D-limonene

The production of essential oils from orange peel is economically viable, since this by-product has a high added value (Figure 16). However, these oils are usually not used in their raw form, but purified by a process called “folding” or “deterpenation” that removes large parts of undesirable terpenes, leaving a purified D-limonene fraction.

Figure 16: Citrus essential oil as saleable products (originally in colour) (Courtesy: Fresh Plaza)

Orange essential oils have also a main role in natural cleaning product for the germicidal properties of some of its components. Indeed, small amounts of D-limonene can have an important effect on wastewater as germicide.[91]
D-Limonene is famously known as a flavour in food and beverages as well as in the production of medicines and cosmetics. At room temperature, D-Limonene appears as a colourless liquid with an extremely strong orange aroma. However, orange essential oils often appear coloured. This is due to the presence of a non-volatile fraction formed by steroids, carotenoid and polymethoxyflavones,[92] which is not removed by common deterpenation processes. Moreover, traces of organophosphorus pesticides, used during fruit growth, can also be present.[93]

In spite of their potential significance, there exist few studies dealing with the extraction of essential oils from orange peel, but there are many researches on the deterpenation of these oils.[94,95] This is probably due to two main reasons: (i) the traditional procedures are very rapid and low cost, although they do not allow selective extraction; (ii) as described in chapter 2.2, FMC system allows the simultaneous extraction of both orange oil and juice.

If essential oils are not removed in the squeezing process, they can be recovered from the peel by cold pressing, steam distillation or solvent extraction, usually with an apolar solvent like hexane or cyclohexane. The maximum extraction yield for citrus oils is 0.4 g 100 g^{-1}, i.e. for every ton of fruit processed 4 kg of oil are produced.[96]

As stated before, the limitations of the conventional deterpenation processes have given rise to extensive research on alternatives for orange oil deterpenation, especially with supercritical carbon dioxide. Such surveys have covered all aspects from fundamentals to practical process design, and employed different approaches from experimental to mathematical modelling and optimization.[74,97]

An interesting end-product resulting from the bio-conversion of limonene, is the monoterpene alcohol α-terpineol (Figure 17), whose annual consumption in flavours has been estimated at over 13 000 kg. Major uses are in various flavour compositions, such as lemon, lime, orange, ginger, and peace.[98]

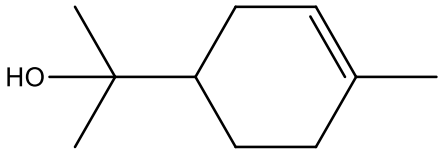

Figure 17: Chemical structure of α-terpineol

Although α-terpineol is found in natural essential oils, it is usually synthesize through pinene hydration by aqueous mineral acid to the cis-terpin hydrate, followed by partial dehydration.[99]

However, more and more "natural" flavours are produced *via* biotransformation or bioconversion, applying to the consumers' demand for natural products.[100] D-Limonene biotransformation to α-terpineol has been long researched using various fungus like *Penicillium digitatum*[99,100] and *Penicillium sp*.[101]

The solid residues remaining after the essential oil extraction could be reutilized to obtain flavonoids or the pectic and cellulolytic fibres.

4.2 Flavonoids

Flavonoids comprise a vast group of naturally occurring, low molecular weight, and polyphenolic compounds broadly distributed in the flora kingdom. They represent one of the most important classes of biologically active compounds and occur both in glycoside and aglycone form.

From a structural point of view, flavonoids are based upon a fifteen-carbon skeleton consisting of two benzene rings (A and B, Figure 18) linked via a heterocyclic pyrane ring (C).

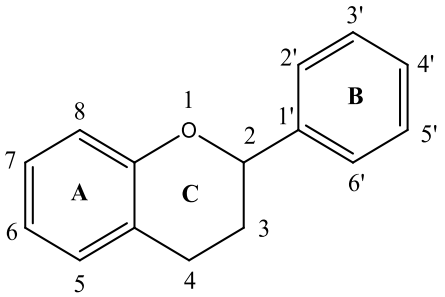

Figure 18: Chemical base structure of flavonoids

Up to now, more than 8000 different flavonoids have been identified.[102] The various classes differ in the level of oxidation and substitution pattern of the C ring, while individual compounds within a class differ in the pattern of substitution of the A and B rings. According to their molecular structures, flavonoids are divided into six classes: flavonols, flavanones, flavanonols, flavones, flavanols and anthocyanidins (Figure 19).[77]

The different flavonoids have diverse biological functions, including protection against ultraviolet (UV) radiation and phytopathogens, signaling during nodulation, male fertility, auxin transport, as well as the coloration of flowers as a visual signal that attracts pollinators.[103]

Flavonoids are the most common and widely distributed group of plant phenolic compounds, occurring virtually in all plant parts, particularly the photosynthesising plant cells. They are a major coloring component of flowering plants.[104]

Preparation and processing of food may decrease flavonoid contents depending on the methods used. For example, commercial orange juices were found to contain less flavanones than the pulp,[10] which suggest that the flavanones may be partly removed during processing.[105]

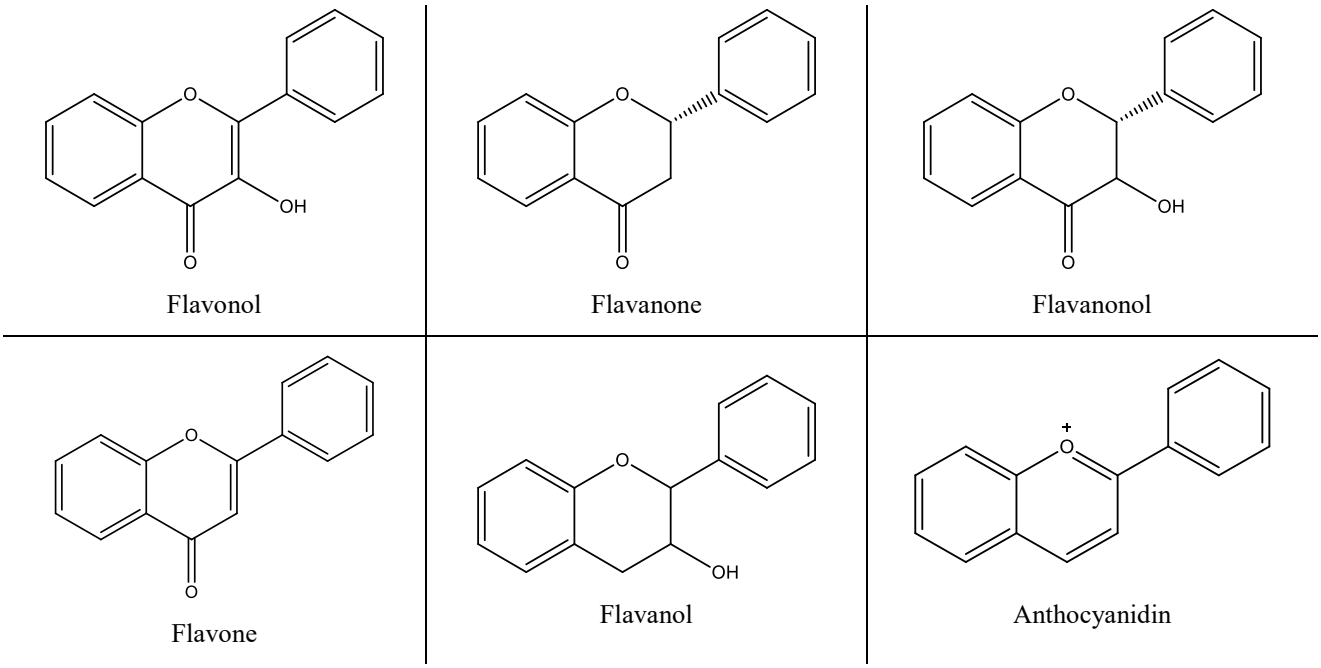

Figure 19: Chemical base structure of the six class of flavonoids

Flavonoids in sweet orange peel are comprised primarily of flavanone glycosides (narirutin 4'-*O*-glucoside, eriocitrin, narirutin, hesperidin, isosakuranetin rutinoside) and polymethoxyflavones (sinensetin, nobiletin, 3,5,6,7,8,3',4'-heptamethoxyflavone, tetra-*O*-methylscutellarein, tangeretin and 5-hydroxy-3,7,8,3',4'-pentamethoxyflavone).

Hesperidin (Figure 20) is the most abundant flavonoid in orange and it is found in the albedo (which has the major concentration of this flavanone), the flavedo and the juice. It is also found in the seeds, although its value decreases when the fruit matures. In young immature oranges, hesperidin can account for up to 14% of the fresh weight of the fruit.[106]

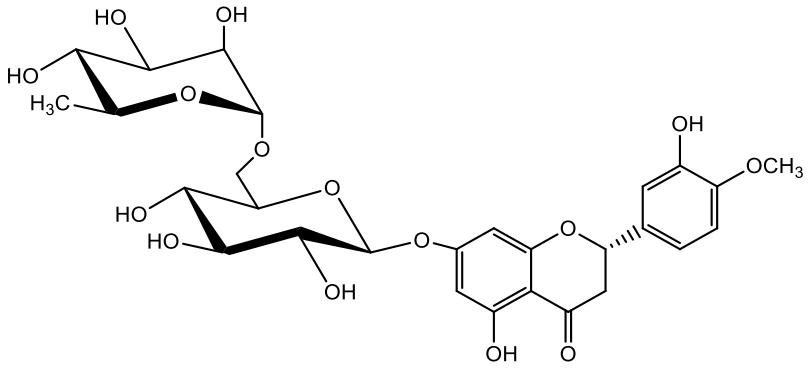

Figure 20: Hesperidin

Hesperidin is a flavanone glycoside, comprising of an aglycone, hesperetin and an attached disaccharide, rutinose (O-α-L-rhamnosyl-(1→6)glucose). Pure hesperidin occurs as pale yellow needles. It is slightly soluble in methanol, hot glacial acetic acid and almost insoluble in water. However, it is easily soluble in dilute alkali due to ring-opening elimination reaction.
Hesperetin, the aglycone of hesperidin, was found to actively inhibits the replication of herpes simplex, polio and parainfluenza type viruses.[107]

Polymethoxyflavones (PMFs) (Figure 21), a group of phenolic compounds unique for *Citrus* species, are mostly accumulated in the flavedo[108] and their profile in citrus fruit is characteristic of each species.[109] Polymethoxylated flavones are most abundant in tangerines, while in oranges they comprise 0.l-0.5% of the peel on a dry weight basis. Commercial orange peel oils contain nobiletin and 3,5,6,7,8,3',4'-heptamethoxyflavone as the most abundant methoxylated flavones. The total flavone content in orange oil ranges from 0.2 to 0.4%.[110]

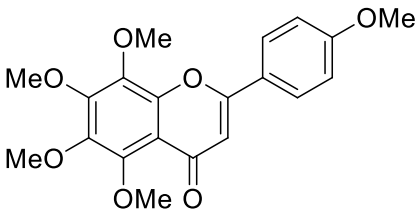

Tangeretin

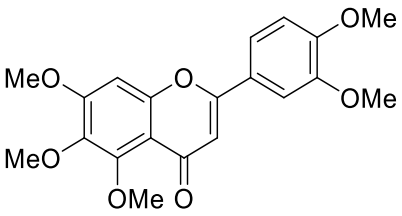

Sinensetin

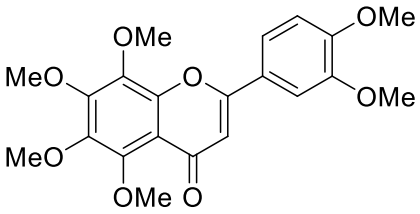

Nobiletin

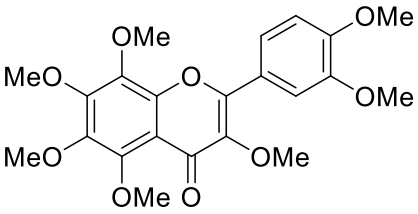

3,5,6,7,8,3',4'-Heptamethoxyflavone

Figure 21: Common PMFs found in sweet orange peel

PMFs demonstrated greater anti-adhesive effects on red blood cells and platelets than flavanone glycosides. Moreover, PMFs have demonstrated a more stronger anti-inflammatory activity than hesperidin, naringenin and hesperetin.[107]

The study of flavonoids requires a deep knowledge of separative techniques: both analytical and preparative.

Historically, thin-layer chromatography (TLC) was the major separation technique for flavonoids. Nowadays it is still employed for qualitative analysis of phenolics compounds in plant and fruit extracts. However, the majority of published work now refers to qualitative and quantitative applications of high-performance liquid chromatography (HPLC).

Flavonoids can be separated, quantified, and identified in one operation by coupling HPLC to ultraviolet (UV), mass, or nuclear magnetic resonance (NMR) detectors.

Recently, capillary electrophoresis (CE) has also been gaining attention for flavonoids analysis.[111]

A number of techniques have been used for the separation of flavonoids on a preparative scale. These include HPLC, Diaion, Amberlite XAD-2 and XAD-7, and Fractogel TSK/Toyopearl HW-40 resins, gel filtration on Sephadex, and centrifugal partition chromatography (CPC).[112]

Regarding extraction, the solvent is chosen depending on the type of flavonoid present, considering polarity of the compound as the main parameter. Flavanones and methylated flavones are usually extracted with chloroform, diethyl ether or ethyl acetate, while flavonoid glycosides and more polar aglycones are extracted with alcohols or aqueous alcoholic solutions.

Orange peel can be extracted in a Soxhlet apparatus, first with hexane, for example, to remove the terpenes fraction, and then with ethyl acetate or ethanol to obtain flavonoids. Extraction is generally performed with magnetic stirring or shaking but other methods have recently been introduced to increase the efficiency and speed of the extraction procedure.

Microwave-assisted extraction (MAE) has been described for the extraction of various compounds, including flavonoids,[113] from different matrices This simple technique can allow separation in a few minutes. During MAE, microwave energy is applied to the sample, which is suspended in the extraction solvent. Since a certain degree of heating is involved, heat-sensitive compounds should be removed before the extraction in order to avoid involuntary degradation.

There is no single isolation strategy for the separation of flavonoids and one or many steps may be necessary for their isolation.

Once a suitably polar plant extract is obtained, a preliminary cleanup is advantageous, since low concentrations of flavonoids (PMFs in particular) are present in orange peel. Therefore, the purification step may help to separate flavonoids from the rest of the matrix. Extraction with a cold alcohol solution may be a solid choice since it produces a solution and a solid fraction (also called alcohol insoluble solid, AIS),[72] which contains the fibrous part of the orange peel and hesperidin (which is poorly soluble in cold neutral alcohol). Hesperidin can be recovered by submitting orange peels to an alkaline treatment with $Ca(OH)_2$ (alone or mixed with CaO) which isomerizes

flavanones and solubilizes the derived calchones; a successive acidification of the filtered liquid provokes the inverse reaction and the separation of insoluble flavonoids. Unfortunately, $Ca(OH)_2$ also induces the insolubilization of pectin, as calcium pectate, which could hamper flavonoids crystallization and alter pectin final form.[114] However, it is possible to recover both substances using hot water, to solubilize most of the hesperidin present, simultaneously obtaining two raw fraction: a solid residue formed by cellulose and pectins, and a solution containing hesperidin and other flavonoids. The solution is sequentially treated with $Ca(OH)_2$ and an acid, to separate hesperidin from impurities. While the fibre fraction is subjected to pectin extraction procedure.[48]

Purification of hesperidin may be also achieved by using a styrene-divinylbenzene resin, which can absorb dilute extract of the flavanone, allowing better separation from the other flavonoids present in the orange matrix.[115]

Recently, the use of pressed electric field allowed to improve the extraction of naringin and hesperidin from orange peel, using distilled water as the extraction solvent.[116]

Separation and purification of PMFs is challenging because of the complexity of orange waste matrix.

PMFs were reported to be extracted using different methods such as solvent extraction in a Soxhlet apparatus, extraction with a supercritical fluid and microwave assisted extraction. Among these extraction methodologies, Soxhlet allows to obtain the major quantities of PMFs, while MAE reduces extraction time from hours to minutes. Several strategies have been reported for separation of these compounds using various methodologies.[117–119] Usually, combination of column chromatography and preparative-high performance liquid chromatography (Prep- HPLC) is used.[120]

PMFs are rather extracted from orange oil extract[92,121–123] than from peel, since the separation tends to be less complex due to the absence of glycosides flavanones, which are not present in the oil.[124]

It is rather common that PMFs are extracted as a mixture of compounds, rather than as single extracts. For example, the ethyl acetate fraction of Navel orange peel consists of significant antioxidant compounds (with radical scavenging activity) and can be used as a food additive of natural origin or a pharmaceutical supplement.[125–127]

Analysis of purified flavonoids is usually done with HPLC, MS or HPLC-MS, since flavonoids have typical UV-adsorption and MS fragmentation.[128]

4.3 Pectin

In 1825, the French scientist Henry Braconnot coined the term pectin for the gel-forming substance discovered in tamarind fruit by Vauquelin in 1790.[129]

Pectin is widely used in the food industry for jelly and jam making and in drug and cosmetic industries, as a stabilizer.

Pectin is a structurally complex polymer primarily made up of D-galacturonic acid units joined by α-(1→4) glycosidic linkages (Figure 22). Moreover, some carboxylic acid moieties can be methyl-esterified whereas C-2 and C-3 hydroxyl groups can be acetylated or, less commonly, ferouylated.

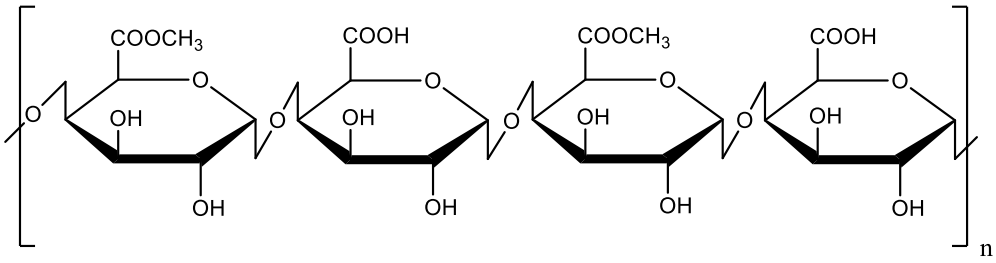

Figure 22: Pectin chain

In addition, several side chains containing sugars, such as xylose, arabinose, glucose, fucose, mannose or galactose, have been found to be linked to the main backbone structure.[130] In rhamnogalacturonan, the galacturonic acid residues are partly substituted by α-1,2 linked rhamnose residues (Figure 23).

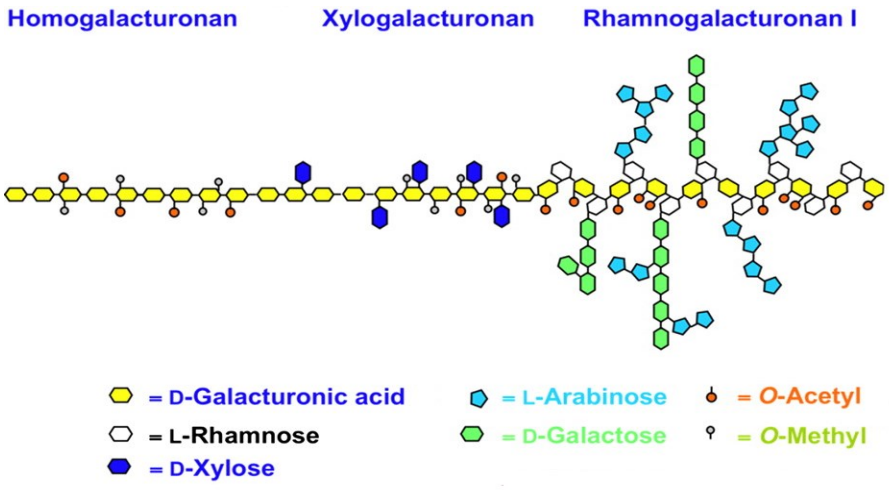

Figure 23: Schematic structure of pectin (originally in colour) (Adapted from Harholt et al., 2008)

Commonly, a pectin extraction process involves three fundamental steps: a pre-treatment of the sample, the solvent extraction from the starting material and the isolation of the purified pectin from the solvent. Different analytical methods were developed, in time, to identify the properties and characteristics of the pectin extracted.

Orange peel requires first to be washed, to remove seeds and soluble solids (monosaccharides and disaccharides), then it is shredded and dried.[131] If preliminary treatment is skipped, it is also recommended to remove essential oils with an organic solvent and to heat the peels to 97°C to inactivate pectic enzymes.[132] Enzymes can also be inactivated using ethanol, which partially dehydrates and extracts soluble substances from the orange waste.[133] A 10 minutes pre-treatment in a microwave field with a power above 0.63 kW can also lead to the complete suppression of the pectolitic activity in orange peels.[134]

The protopectin, the water-insoluble matrix formed by cellulose, hemicellulose and pectin, requires an extraction step with a suitable solvent in order to solubilize specifically the pectin fraction. Usually this is accomplished in a Soxhlet apparatus with a mineral acid within a pH range of 1.3-3. Commonly used acids are sulphuric [135] and nitric acid,[136,137] even if the most wide used in orange peel extraction is hydrochloric acid.[131,132,134,138] Recently, to reduce economic costs, lower environmental impact and improve safety work conditions, citric acid has also been employed.[139,140]
Low pH value is needed since large hydrogen ion concentrations repress the repulsive charge of the carboxylate groups of pectin. This loss of charge can help pectin to form gel, increasing the amount of the precipitate.[141]
Alkaline conditions tend to be avoided since they can cause instability in the backbone of galacturonic acid leading to decomposition of pectin molecules, thereby lowering the yield of the extraction step.[142]
Neutral conditions can be attained using ethanol with EDTA as chelating agent, to help the release of pectin from cell wall of orange peel. Though yields are lower compared to acid extraction, the amount of pectin extracted using distilled water is still double.[143]
However, it should be noted that extraction at pH=7, can be achieved only if the starting material is washed several times, since orange waste contains traces of citric acid.

It is also possible to employ a microwave oven (the so-called microwave assisted extraction, MAE) to enhance the penetration of the extracting solvent into orange tissues.[135,143,144]

Ultra-high pressure (UHP) technology was applied successfully for pectin extraction from navel orange peel, resulting in an improved intrinsic viscosity and viscosity-average molecular weight of pectin compared to traditional heating technique.[145]

Recently, an experimental system based on an induced electric field with an O-core transformer structure was established and used to extract pectin from orange peel. The acidic solvent acts as the secondary coil connected to a purpose-made glass chamber, which forms a closed loop.[146]

Comparing different extraction methods presents some challenges because various variables must be taken into account. The yield of the extraction step using an acid solvent in a Soxhlet apparatus is rather better (more than 20%) than other methods, but requires high temperature (90-110°C), and could take up as far as 8 hours,[138] even if good results can already be attained after 1-1.5 hours.[132,145]

On the contrary, microwave technology speeds up the process to 15 minutes and allows to obtain the greatest amount of material per unit time.[143] Ultra-high pressure-holding extraction times can vary from 5 to 25 minutes, even if, due to the instantaneous transfer of the pressure in this process, the extraction could already finish successfully after 10 minutes. Regarding solvent to orange peel ratio, traditional heating extraction range from 20:1 to 30:1 w/w on dry basis,[136,137] while microwave assisted extraction requires 12.5:1 w/w on dry basis.[134,141] Ultra-high pressure system can be economically unfavourable requiring 50:1 w/w on dry basis.[145]

The chemical structure of pectin is widely heterogeneous, depending on the origin of the orange plant, the fraction of the fruit extracted, and extraction method. For these reasons, there is no official method for the determination of the whole molecule of pectin. However, food scientists have developed several parameters to determine its quality and to quantify concentration of its components. Characteristics, functionality and applications of pectin relate to degree of esterification (DE), degree of acetylation, concentration of anhydrogalacturonic acid and ash content. While, molecular mass distribution relates to the fine chemical structure of pectin.

Anhydrogalacturonic acid (AGA) is the fundamental unit of pectin molecule and its quantification is a primary method used to determine the pectin content in a sample. AGA can be determined, once pectin has been hydrolysed chemically or enzymatically, by a colorimetric test and quantified with a spectrophotometer and a calibration curve. Common reagents employed are carbazole,[143] *m*-hydroxydiphenyl[145,147] or *p*-hydroxydiphenyl.[132] However, the colorimetric tests require the removal of any traces of neutral carbohydrates due to uncontrollable reactions of the reactive with other non-uronide sugars present in the sample.[143]

The degree of esterification (DE) is a key factor to determine conformation and rheological properties of pectins. DE may be measured directly by titration, via gas chromatography (GC) or by diffuse reflectance Fourier transform infrared spectroscopy (DRIFTS).[132,148]

According to the number of carboxyl groups esterified with methanol, types of pectins are divided into high-esterified pectins with a methoxyl content >7% and degree of esterification >50%

(typically 55–75%); and low-esterified pectins with a methoxyl content <7% and degree of esterification <50% (typically 20–45%).

The quantification of acetyl groups in pectin is significant because their presence inhibits gel formation of both high and low methoxyl pectins by steric hindrance of chain association. Hydroxylamine at room temperature can hydrolyse ester groups of pectin, producing pectin hydroxamic acid and acetohydroxamic acid. The latter forms with ferric ions a soluble red iron complex that can be quantified with a spectrophotometer.[149]

Ash content affects the ability of pectin to gel and it is a criterion of its purity. The ash content can be determined by incinerating the pectin in a muffle furnace over 600°C.

One of the most important characteristic of pectin solutions is their viscosity. Gelling properties are related to viscosity of pectin solutions. Moreover, the intrinsic viscosity relates to the molecular weight of pectin molecules. Higher concentrations inevitably cause higher viscosities, but the extent to which the viscosity increases depends on the molecular weight or length of the pectin molecules in solution. The degradation of pectin typically involves long pectin molecules being split up into shorter ones. Hence the measurement of intrinsic viscosity is a measure of quality.[143]

4.4 Cellulose

Cellulose is an isotactic biopolymer with repeating unit of D-glucose linked via a β-1,4 glycosidic bond (Figure 24). The actual base unit, the cellobiose, consists of two molecules of D-glucose. Cellulose is the most abundant organic polymer on earth, and fulfils an important role in cell wall of plants, providing the backbone structure of plant materials.

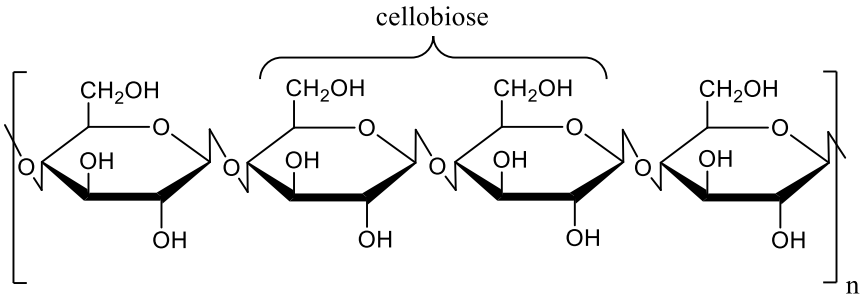

Figure 24: Cellulose chain

Naturally occurring cellulose has polymerization degrees of over 10 000, which correspond to a molecular weight of about 2 000 000 g mol^{-1}. Depending on the method of isolation and the source of extraction, cellulose has an average degree of polymerization of 300-3000, and thus has average molecular weights of 50 000-500 000 g mol^{-1}.

The possibilities by which cellulose can be modified with physical and chemical methods are vast (Figure 25).

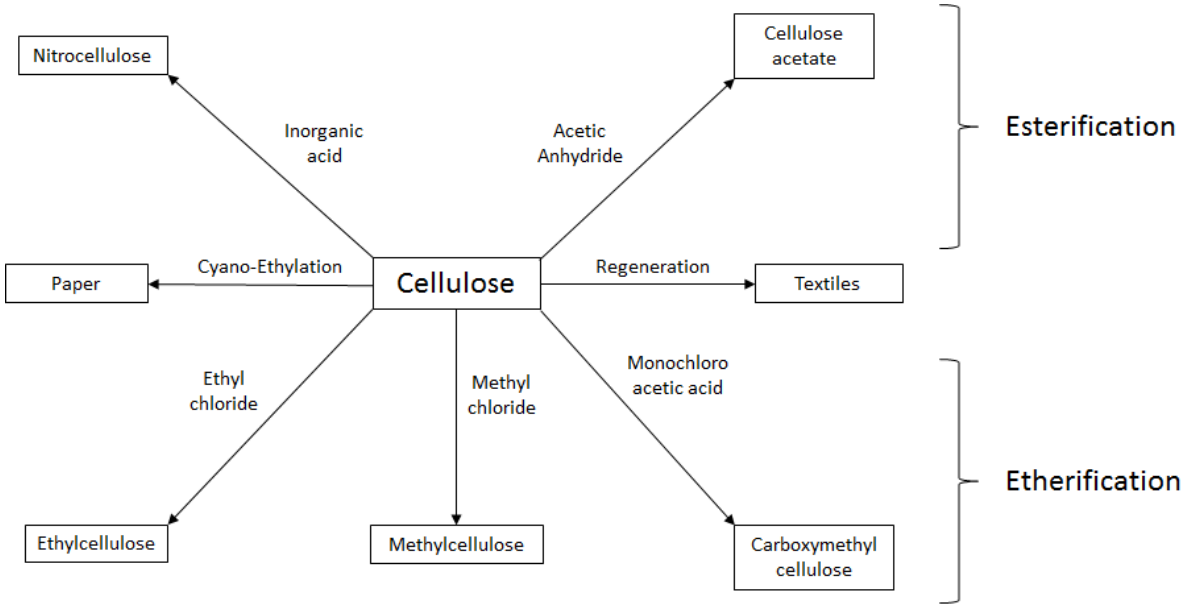

Figure 25: Possible cellulose derivatives

Purified cellulose can be converted into a broad range of different products by suitable elaborations of its native hydroxyl groups. Cellulose as raw material is processed in the paper industry. In the textile and clothing industry, cellulose is used as regenerated cellulosic fibre (called "viscose").[150]

In sweet oranges, cellulose constitutes 10-20% of the peel[65,67,80,151] and 15-25% of the pulp.[67,152]
As a naturally occurring polymer, cellulose can contain other constituents (or other polymers) in addition to glucose molecules. Especially in plants, lignin and hemicellulose tends to be built into or onto the cellulose polymer chains during biosynthesis.[153] Thus, removal of such species is dictated in order to obtain a pure cellulose sample from a natural source.
Cellulose, hemicellulose and lignin are insoluble in water and in most organic solvents; accordingly, chemical modifications are required to enhance solubility.
In cellulose extraction from wood chips, ether bonds between lignin and cellulose can be cleaved using salt of sulphurous acid (producing lignosulphonates by-products), as employed in the sulphite process, or otherwise using sodium sulphide and sodium hydroxide, in the so-called Kraft process.[154] It is possible to exploit these methods even with orange pulp, provided that other existent impurities have already been removed.[151,155] For these reasons, methods to isolate pure cellulose from orange waste rely on sequential extractions of cellulose accompanying substances, like pectin, flavonoids and hemicellulose. Pectin, which can be chemically bonded with cellulose or trapped inside a matrix formation,[156] must be removed without using mineral acid, in pursuance to prevent chain hydrolysis. Therefore, nitric acid may be used to extract the pectic fractions, simultaneously recovering a fibre fraction containing cellulose, hemicellulose and uronic acids. Successively, it is possible to recover cellulose using a sodium hydroxide solution. This procedure was successfully applied on the peels of Valencia oranges by Aravantinos-Zafris et al.,[66] allowing recovery of 94% of the total cellulose. However, the composition of neutral sugars in the extracted cellulose highlights only 91.8% of glucose, due to incomplete dissolution of pectin and hemicellulose fractions. Nevertheless, the fibre fraction isolated shows high water/oil absorption capacity (WAC/OAC) compared to literature data.

Flavonoids, especially hesperidin, deeply contribute to the yellowing of the isolated product as the time goes on, and need to be removed beforehand. Consequently, it is necessary to use an adequate solvent or a solution composed of more extractive solvents. The azeotrope water/ethanol/toluene (21/55/24, w/w/w, b.p. 74°C) proved to be very efficient for the simultaneous extraction of the water soluble pectin fraction and flavonoids, while the azeotrope trichloromethane-hexane (72/28, w/w, b.p. 69°C) allows the removal of the liposoluble fraction.[151,155]
Alkaline solutions lead to significant swelling of cellulose, simultaneously allowing to dissolve existent hemicelluloses. For this reason, the characterization and fractionation of the polysaccharide components in a cellulose matrix, like in orange peel and pulp, can be carried out with the help of concentrated sodium hydroxide solution. While polyoses (β- and γ-fraction), also called hemicellulose, are soluble in an aqueous sodium hydroxide solution (17.5% concentration), α-

cellulose is insoluble. It is also possible to recover the β-component from the γ-fraction by neutralization: the β-fraction precipitates, while the γ-component remains into solution.[153] However, this process usually increases ash content in the final product, which compromises its degree of purity and limits its uses. Therefore, it is recommended the adoption of a chelating agent, e.g. EDTA, during sodium hydroxide treatment to lower the ash content of the final product.[151]

Analyses of cellulose are rather complex due to its insolubility in typical analytical solvents. Thus, the main characterization of isolated cellulose is made with Fourier transform infrared (FTIR) spectroscopy.[86,88,155]

It is also possible to completely hydrolyse cellulose chain, using a strong acid solution like sulphuric acid or hydrochloric acid and, consequently, analysing the carbohydrate fraction by HPLC.[66,157]

Another important parameter studied for cellulose isolated samples is crystallinity. This is analyzed by X-ray diffractometry,[151,158] which yields informations on the lattice structure, polymorphic composition, and accessibility of the cellulose fibres.

After isolation and purification from orange peel, cellulose can be utilized for numerous applications (e.g. adsorptive material for heavy metals in water solution[159] or as paper pulp supplements[160]).

If the final application requires a certain degree of whiteness, residual traces of pigments need to be removed. Usually, this is accomplished via a bleaching step, using a peroxide reagent.[158]

Of the three classes of cellulose, α-cellulose has the highest degree of polymerization and therefore, fulfils many roles in different applications in polymer industries. The acetylation of α-cellulose obtained from orange mesocarp requires acetic acid and acetic anhydride, in presence of a suitable catalyst.[161] Acetylation of cellulose (whose degree is measured through titration or NMR) can lead to two different products, cellulose triacetate, which can be used to create fibres or film base, and cellulose diacetate, which is used for cigarette filters and eyeglass frame.

α-Cellulose may also be further processed to produce microcrystalline cellulose (MCC).[158] MCC is widely used in pharmaceuticals as a binder in oral tablet and capsule formulations, and in food industries as fat replacer and bulking agent. Orange peel cellulose can also be converted to carboxymethyl cellulose (CMC). CMC is produced by etherification reaction of α-cellulose with sodium chloroacetate in alkali medium. CMC is widely used as a thickener, water binder, extrusion aid and film former in pharmacy, cosmetics and the food industry in order to improve the consistency and flow properties.[162]

4.4.1 Cellulose Acetate

In 1865, Schützenberger was the first to discover that heating cellulose in a sealed glass tube with acetic anhydride produced cellulose acetate (CA) (Figure 26). Fifteen years later, Franchimont found that cellulose acetate could be produced at room temperature using sulphuric acid as catalyst, but failed to recognize the economic potential of this discovery. The commercial breakthrough came in the early 1900s, with the discovery of cellulose diacetate, a product that is soluble in acetone and with mechanical properties close to collodion.[163]

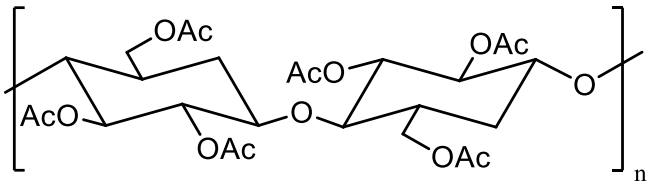

Figure 26: Acetylated cellulose chain

As stated before, the presence of hydroxyl groups make it possible to prepare cellulose esters from various organic acids. The esterification reaction of the primary and secondary hydroxyl groups of cellulose does not differ from that of other alcohols. However, in cellulose the splitting of the molecule chain competes with the catalysed esterification, and need to be well controlled under the appropriate conditions. The speed and completeness of the reaction is dependent on the quality of the cellulose, whereas the different reactivity of the primary and secondary hydroxyl groups has little influence on industrial processes. Free acids, acid chlorides, and acid anhydrides are possible esterification reagents for the three hydroxyl groups in each glucose unit.

Esterification with free acids requires high temperatures and high catalyst concentrations, but only low molecular mass products are obtained.

Acyl chlorides in pyridine were suggested for use in the production of esters from higher fatty acids (lauric acid, stearic acid and palmitic acid), without ever having attained any industrial significance.[164]

All industrial processes are currently based on acetic acid anhydride as a reactant, whereby theoretically three moles of anhydride per unit of glucose are used and three moles of acetic acid are formed.[165]

Attempts to use ketene, which could be directly accumulated without incurring acetic acid, which must again be processed, did not lead to any results.[166]

Numerous catalysts were suggested to accelerate the reaction but only sulphuric acid and perchloric acid are of any practical importance. The catalytic effect of sulphuric acid lies primarily in the rapid and quantitative formation of acidic cellulose–sulphuric acid esters, which are substituted by acetyl groups as the reaction progresses and the temperature rises.[167]

The cellulose bases generally consist of highly purified cotton linters with an α-cellulose content of over 99% or refined wood pulp with an α-cellulose content between 95 and 97%. Special care should be taken during drying, since over-drying of cellulose (whose water content should lie between 3 and 8%) impairs its reactivity considerably.

For a long time, cellulose from wood pulp could only be used for the manufacture of lower-quality cellulose esters because of the 90-95% α-cellulose content. Celluloses with an α-cellulose content of 96% have been available for about 20 years, due to special processing techniques, which produce cellulose esters comparable to those produced from linters as tensile strength, colour, clarity of the solutions, and light stability.

The accessibility of cellulose is very important, because cellulose acetylation is a heterogeneous reaction. High accessibility eases the diffusion of the reactants into the interior of the cellulose. Therefore, adequate shredding of the cellulose sheet and adequate swelling are necessary operations prior to the acetylation. The basic principle behind pretreatment is that the penetrating medium, which always contains some water, disrupts the hydrogen bonding in the bundles of cellulose chains causing swelling and enhancing diffusion of reactants.[168]

Due to the topochemical character of the reaction, cellulose monoacetate and diacetate can be obtained only by hydrolysis of the triacetate. Attempts to stop the acetylation to diacetate formation would only resulted in a product composed of cellulose triacetate and unreacted cellulose. For these reasons, cellulose esters with lower acetic acid content are produced by subsequent hydrolysis in a homogenous system by adding water or dilute acetic acid (under controlled conditions of temperature, water content, and time) to destroy the excess anhydride, and remove a certain number of acetyl groups (Figure 27).

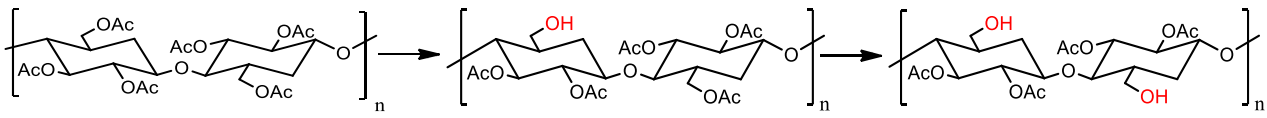

Figure 27: Schematic progressive deacetylation of cellulose triacetate (originally in colour)

The symbol n represents the average degree of polymerization (DP) while the extent to which the hydroxyl groups are substituted is called the degree of substitution (DS). For cellulose acetate, also called secondary cellulose acetate or cellulose diacetate, the DS is between 2.2 and 2.6, which means that less than one acetyl group per anhydroglucose unit is hydrolyzed

Cellulose diacetate, called cellulose acetate from now on, is the most important cellulose ester. It is primarily used for textile yarn and cigarette filter tow. The global consumption of cellulose acetate is projected to exceed 951 thousand metric tons by 2020.[169]

Cellulose acetate synthesis consists of four different step: pretreatment, acetylation, partial hydrolysis and precipitation (Figure 28).

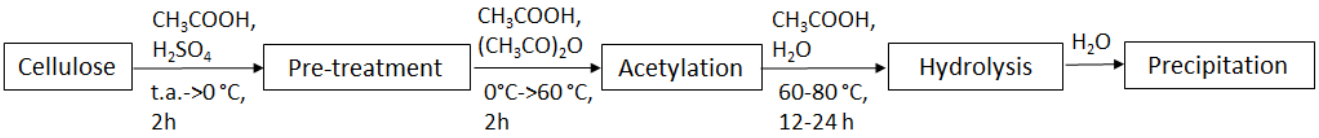

Figure 28: Schematic representation of the four step of cellulose acetate synthesis

In the pretreatment, shredded cellulose is mixed with one third of its weight of acetic acid and a very necessary amount of water, about 6% of its weight. As stated before, if cellulose is too dry at the time of use, more water must be added to the acetic acid. In this phase, a small amount of sulfuric acid may be used to assist cellulose swelling and to make the solid more accessible to the esterifying mixture.[170]

The acetylation mixture consists of a solution of 60% acetic acid and 40% acetic anhydride to which has been added 10–14% sulfuric acid based on the weight of cellulose used. The reaction is highly exothermic and requires that the heat be dissipated to avoid cellulose degradation and browning. In preparing for acetylation, the liquid reactants are cooled to a point (0 °C) where the acetic acid crystallizes.

Is it also possible to use methylene chloride instead of acetic acid as the solvent medium. In this case, it is possible to exploit the evaporative cooling effect of methylene chloride during the acetylation step, thus avoiding the use of a cooler.

The acetylation process takes place in heterogeneous fashion until the end of reaction where the whole reaction mass becomes a viscous liquid. This allows, by direct or indirect viscosity measurement, adjustment of the degree of polymerization at the stopping point. Acetylation is normally stopped by adding water or diluted acetic acid, which destroys the excess anhydride. Sulfuric acid is not usually neutralized since it is also the catalyst for the subsequent hydrolysis.[171]

In the standard process, hydrolysis is controlled by the concentration of water (5 to 15%), usually added in the stopping step after acetylation, the reaction time (3 to 10 hours) and the temperature (between 60 and 80 °C). Again, chain degradation has to be taken into account. The faster, high-temperature hydrolysis at 140 to 150 ◦C with neutralized catalyst is another option.[172]

Finally, often after a concentration process in which a certain amount of acetic acid is removed, the resulting cellulose acetate is precipitated in water in the form of flakes or powder, washed and dried.

The cellulose acetate is usually dissolved in a suitable organic solvent and spun by dry spinning. The viscosity and the filterability of the spinning solution (spinning dope) are particularly important in the production of cellulose acetate fibres. The spinning dope has a high viscosity, which depends on the degree of polymerization. The strength and stretch properties of the fibres also depend on the concentration and the degree of polymerization as well as on the distribution of the acetate groups along the cellulose chain.

The fibres are formed by evaporating the solvent with a counter current of air at 80-100 °C. Then they are stretched while still plastic to increase their strength. By blending and twisting of cellulose acetate or triacetate fibres with nylon or polyester, a combination of properties is achieved that make them suitable for different end uses in linings.[173]

5. Research Project: Aim, problems and objectives

Italy's orange production is estimated at 2.05 million metric tons, with 344 thousand tons directed to processing (Figure 29).[174] Since half of the weight of the orange is discarded during the squeezing procedure, around 172 thousand tons of orange waste is generated. The preferred alternative for disposal is usually cattle breeding which offer little economic value. Thus, orange juice industries welcome the opportunity of finding new products (and new markets) from these waste.

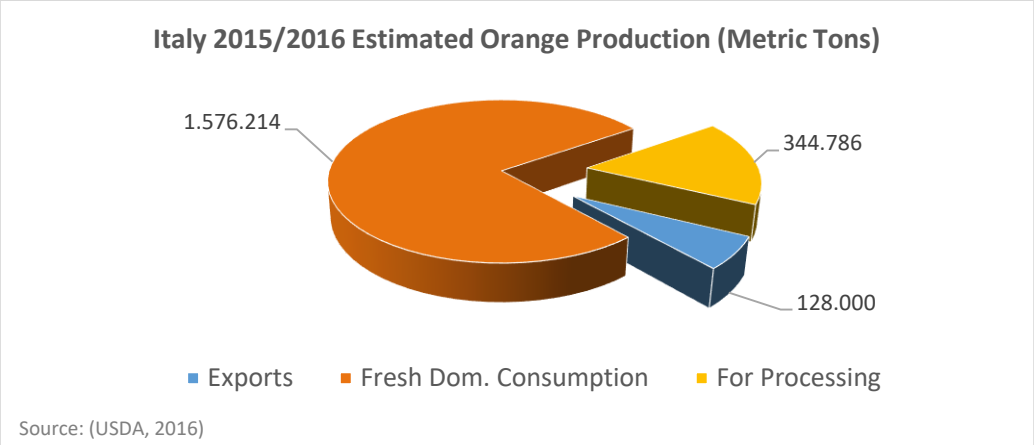

Figure 29: Estimated orange production in Italy for 2015/2016 (originally in colour)

In4tech Synthesis s.r.l., a chemical research company located in Ferrara (Italy), requested our research group to investigate the possibility of extracting cellulose from decanter centrifuge orange wastes (DCOW). This type of waste is generated shredding the peels and then mixing them together with pulps and rags. After a pasteurization step, the waste is centrifuged to recover a clear orange liquid and an orange/yellow solid waste that is collected and discarded.

Figure 30: Decanter centrifuge orange waste (originally in colour)

At first, the aim of this project was to develop a reliable method to extract cellulose from the DCOW. The client's request was to determine α-cellulose content and to study the possibility of acetylating extracted α-cellulose.

In the firsts few months it has been found that cellulose accounts for only 3% of the entire DCOW residue. However, once the residue is dried, cellulose accounts for half of the weight of the solid residue. In comparison with standard dried peel and pulp, this waste is enriched in cellulose fraction and was recognized as a good starting point for investigating acetylation procedures.

Nonetheless, from a commercial point of view, cellulose extracted from orange waste would have a much higher price compared to the one obtained from wood or cotton, and would not be competitive on the market. Thus, our client strongly sought to identify most of the by-products derived from the cellulose extraction procedure of the DCOW.

For these reasons, our group developed a sequence of different extractions, based on the polarity of employed solvents, followed by an acidic and alkali treatment (Figure 31).

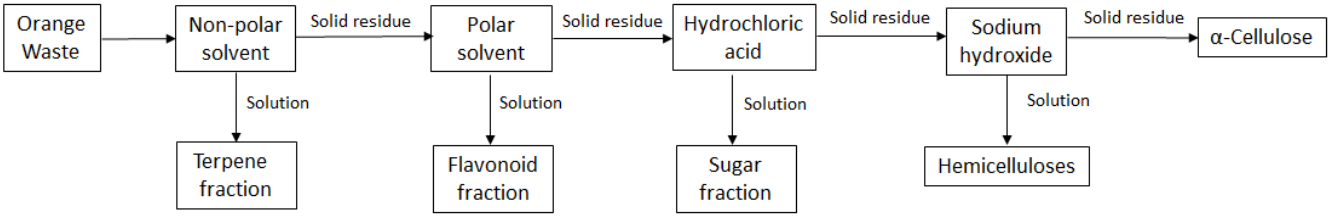

Figure 31: Schematic representation of the proposed procedure for products isolation

The first two extractions aimed to remove and collect two different fractions containing terpenes and flavonoids. The analysis of these fractions were accomplished through mass spectrometry measurements, RF-HPLC and NMR.

The acidic treatment, done with a diluted hydrochloric solution, was required to remove pectic residue from the waste. Unfortunately, pectin is not removed completely during the enzymatic treatment in the industry and need to be eliminated before the acetylation of the final cellulose.

The final sodium hydroxide treatment removes β- and γ-cellulose that can hinder further derivatization.

The crystallinity of α-cellulose extracted from orange waste is usually lower than the one extracted from orange wood,[155] thus sulphuric acid required for the catalysis was also lower.

Overall, the extraction procedure developed allows obtaining and characterizing all but the pectin fraction, which was impossible to isolate with commonly employed methods. However, this could be achieved avoiding the use of pectinase prior to the centrifugation process.

6. Materials and equipment

6.1 Materials & reagents

Orange waste

Experiments were conducted using decanter centrifuge orange wastes (DCOWs) (Figure 30) of Valencia variety (*Citrus x Sinensis*) obtained from a FMC-based orange juice plant, in Sicily.
DCOWs are produced mixing together shredded peels with pulps and rags. After an enzymatic treatment at 50°C that removes most of the pectin (in order to reduce the viscosity during conveyance), the waste is pasteurized at 85-90°C and then centrifuged to recover a sellable liquid and a solid waste.
Upon deliverance to our University, DCOWs were frozen immediately at -10 °C. Before use, they were defrosted at -4 °C for 12 hours, then at room temperature in a desiccator for 2 hours.

Commercial samples and standards

All the chemicals were brought from Sigma Aldrich and used as received. All purity percentages are given as a weight percentage.
A sample of Hesperidin (≥80°C), and a sample of α-cellulose were purchased for comparison purposes.
A sample of cellulose acetate (DS 2.6) was kindly provided by the juice factory.
Deuterated chloroform (99.8% atom D) and deuterated DMSO (≥99.9%) were used as such for NMR analysis. Both were purchased from Sigma Aldrich.

Cleaning procedure for laboratory equipment

Dedicated glassware was used during the five different process.
Particular attention was required during the extraction of the flavonoids fraction, which contains small traces of carotenoids that stain glassware, spatulas and NMR-tubes.
Large pieces of glassware (e.g. 0.6 L and 1.5 L glass Büchner funnels) were thoroughly washed with soap, hot water and lastly with ethanol to avoid any bacterial contamination from DCOWs presence between experiments.
Round-bottom flasks used during cellulose extraction and acetylation needed to be washed with sulfuric acid solution (49%) after use, to remove traces of cellulose.

6.2 Equipment

NMR

1H-NMR and 13C-NMR were registered with Varian spectrometers at 300 MHz and 400 MHz at room temperature. Chemical shifts (δ) are reported with respect to trimethylsilane in the following manner: chemical shift (multiplicity; coupling constants; proton integration).
Signal multiplicity are shortened in the following manner: s for singlet; d for doublet; t for triplet; q for quartet; br for broad signal; m for multiplet; dd for double doublet. The program used to elaborate the spectra was MestReNova 6.0.2.

Mass-Spectrometer

Direct Infusion mass spectrometry was performed in ESI mode (both positive and negative) with a Finningan LCQ Duo Ion Trap (Capillary Temp: 160 °C, Capillary Voltage: 10.32 V Infusion flow rate: 18 mL/min, Sheath gas flow rate: 20 AU) (Figure 32).

Figure 32: Mass-Spectrometer Finningan LCQ Duo Ion Trap (originally in colour)

Infrared-Spectrometer

IR-Spectra were recorded with FT-IR Spectrometer Perkin Elmer Spectrum 100 (Figure 33). Spectra were analysed with Spectrum 6 Software.

Figure 33: FT-IR Perkin Elmer Spectrum 100 (originally in colour)

High-performance Liquid Chromatography

The chromatographic analyses were carried out using 1525 Binary HPLC pump (Waters), equipped with a temperature control model and 2998 photodiode array detector (DAD) (Waters) (Figure 34). The program used was Waters Breeze™ 2.0 HPLC system. Analyses were carried out at room temperature using a reversed-phase system. The chromatographic column used in the analyses was Sunfire C18 (4.6 x 250mm, 5µm). Elution was accomplished by a two-solvent gradient system adapting the procedure reported by Manthey and Grohmann (1996).[124] The initial solvent was 80% 0.02 M phosphoric acid in 20% methanol (v/v). The final solvent was 100% methanol. The linear gradient was run over 60 min at 1.0 mL min-1. The column was operated at 30°C. Flavonoids were detected at 285 and 330 nm.

Figure 34: HPLC system (Left: Binary pump and column oven; Right: Detectors) (originally in colour)

Centrifuge

Liquid-solid separation was carried out using a L-530 Benchtop Lab Centrifuge. It was set at 5000 rpm for 30 minutes at room temperature.

Oven

The moisture content of DCOW was determined following oven drying in a Binder ED Drying Oven. Samples were dried at a maximum temperature of 70 °C until constant weight was reached. Samples were allowed to reach room temperature inside a desiccator before weighting.

Rotary evaporator

Solvent removal was carried out using a Heidolph Laborota 4000 Rotary Evaporator with HB Digital Bath and a Laboport Vacuum Pump.

7. Experimental Section

7.1 Extraction with cyclohexane

100 grams of wet DCOW were mixed with 200 mL of cyclohexane in a 600 mL beaker at 30°C for 2 hours. The mixing was achieved by automatic stirring with an anchor stirrer. Magnetic stirrer with stir bar was abandoned after a few tries because the polar nature of the waste makes the mixing rather difficult. Even the anchor stirrer tend to daub the compound on beaker's walls due to centrifugal force and inertia. In laboratory experiments, it was possible to resolve this problem by continuous adjustment of the beaker position or using a spatula to scrub the remains. In a hypothetical industrial plant, this problem can be partially solved using a counter-current screw extractor.

The mixture was then filtered through a 1.5 L glass Büchner funnels 120 mm (40-100 μm) under vacuum for 30 minutes. 1.5 L glass Büchner funnels 120 mm (16-40 μm) under vacuum was employed for the first experiments, but it clogged few minutes after the start of the filtration.

The residue was collected (Figure 35) and extracted a second time with the same procedure.

The final residue was dried at room temperature in a vacuum desiccator (CR).

Figure 35: DCOW residues after cyclohexane extraction (originally in colour)

The filtrate was collected (CF) and the volume was measured before concentration under pressure. The evaporation of the solvent was interrupted at 20 mL, to avoid the formation of a sticky product, probably due to the presence (even minimal) of carbohydrate substances (Figure 36).

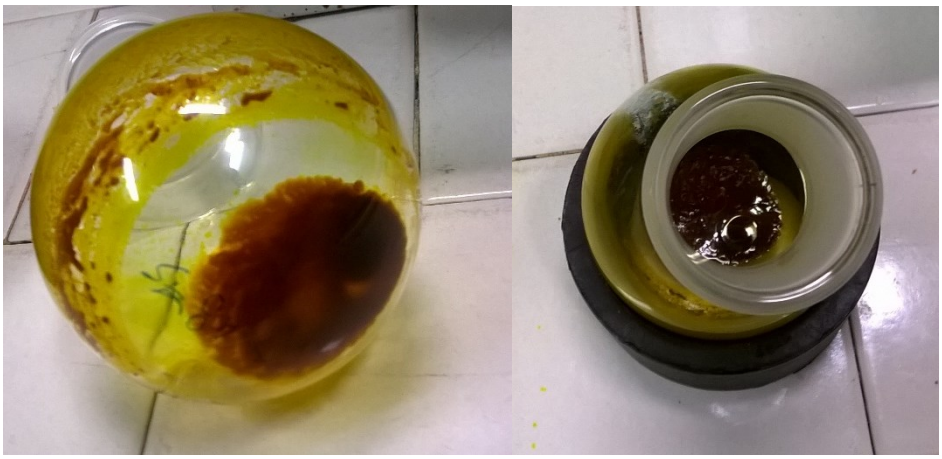

Figure 36: Product derived for excessive evaporation of the precipitate (originally in colour)

CF was then centrifuged and filtrate again, using a 30 mL glass Büchner funnels 30 mm (10-20 μm). The residue was discarded, while the filtrate was concentrated, weighed and redissolved in methanol for further analysis (CFM).

The ^{1}H NMR of the crude product (Figure 37) shows the strong presence of terpenes (alkene proton at δ = 5.4 ppm) and flavonoids (methoxyl group around δ = 4 ppm and low aromatic signals near 7)

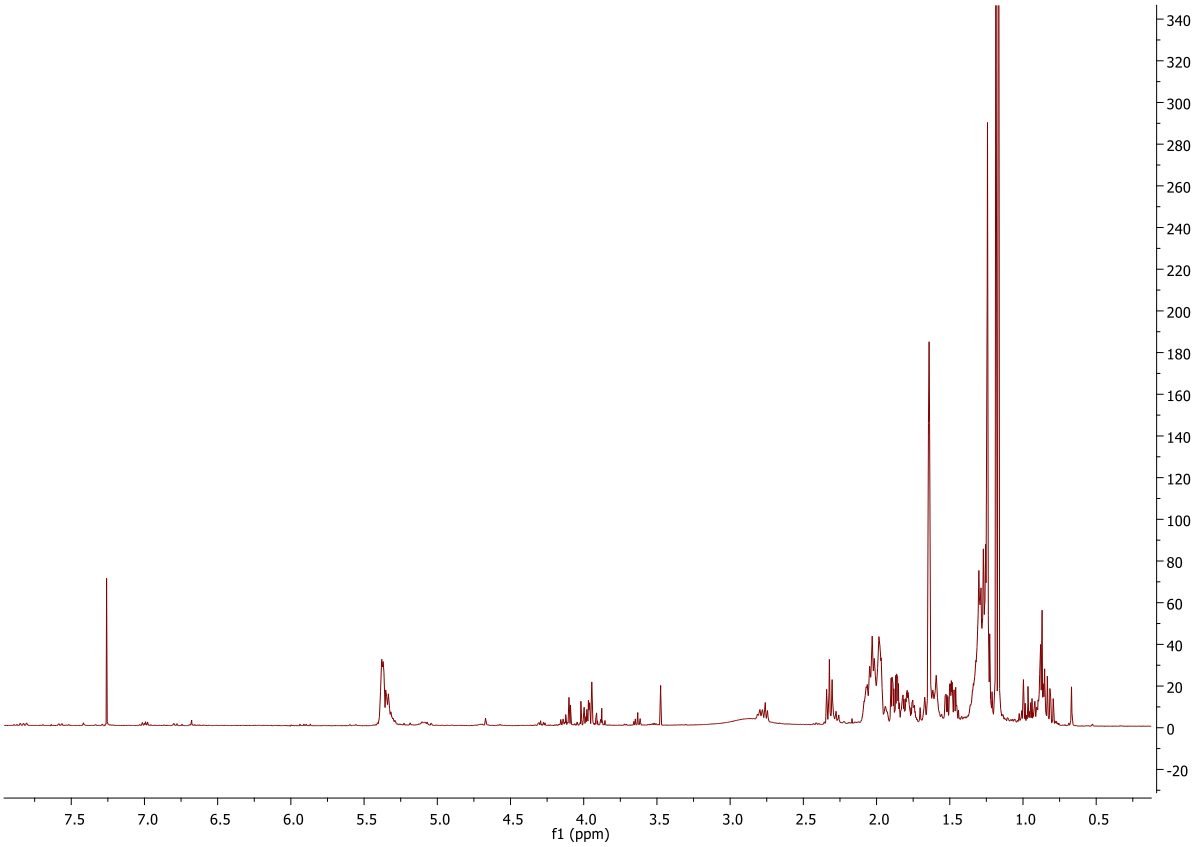

Figure 37: ^{1}H NMR of CFM ($CDCl_3$)

The mass (Figure 38) and the HPLC (Figure 39) analysis confirmed the previous hypothesis.

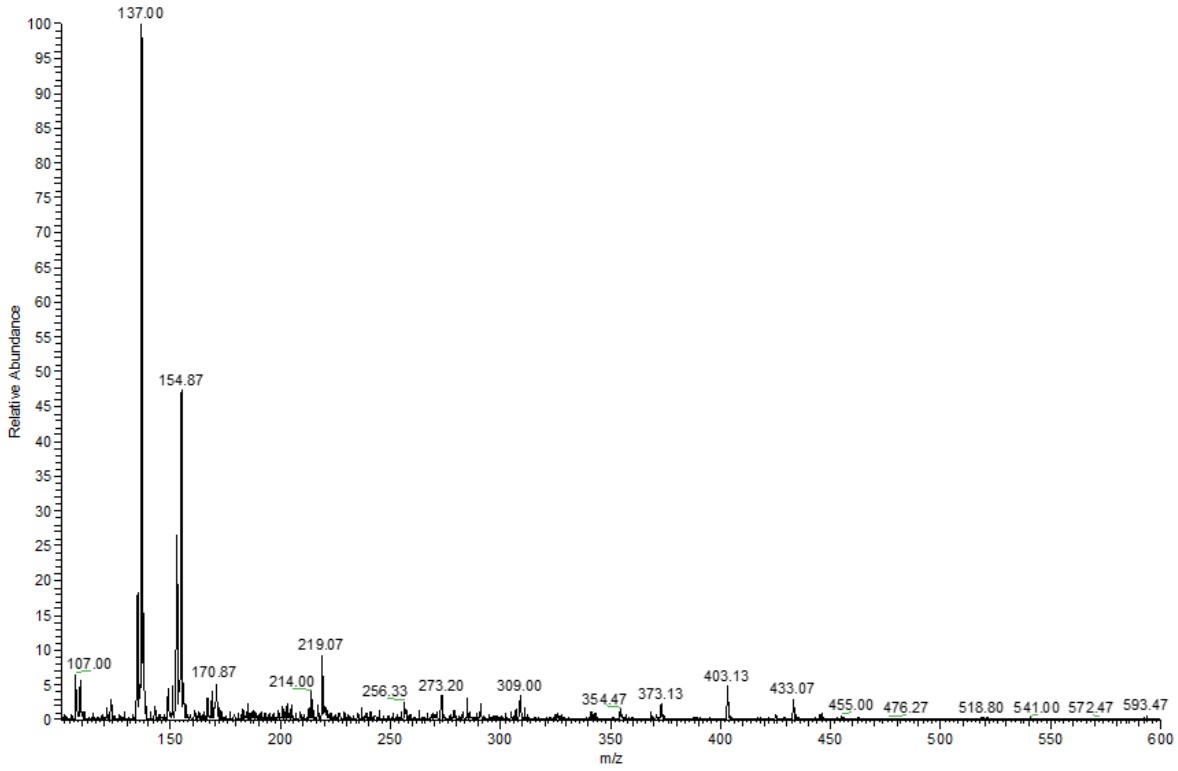

Figure 38: MS-ESI (positive) of CFM

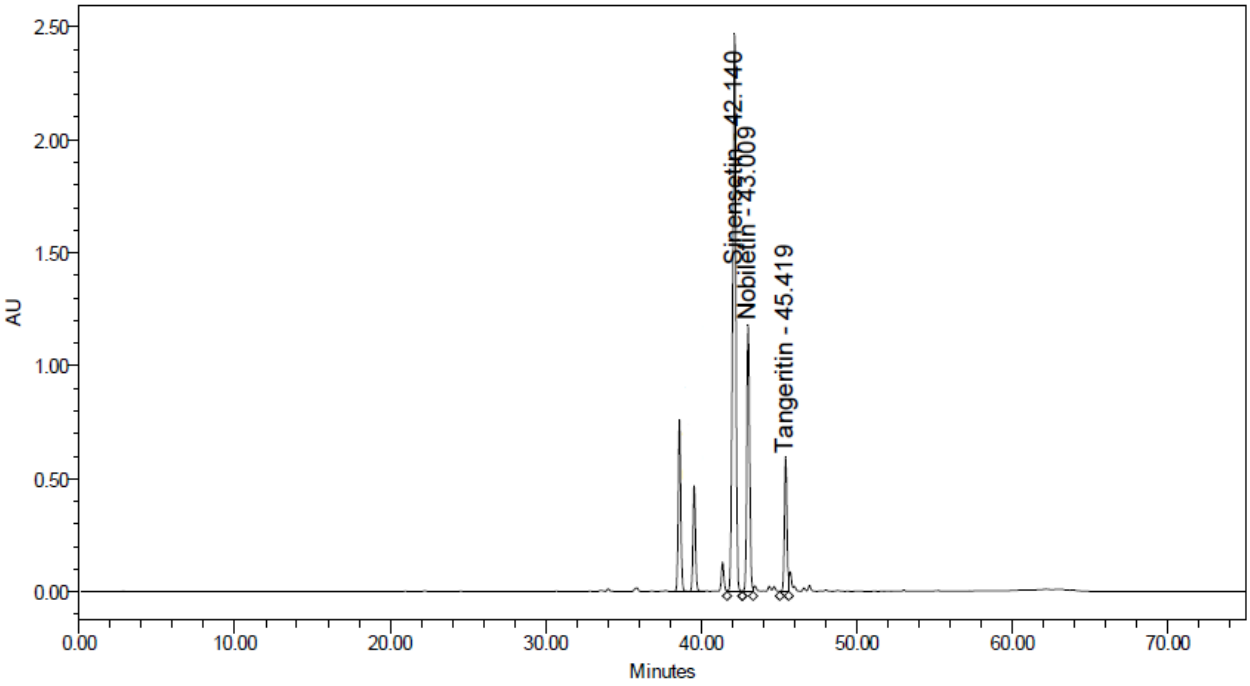

Figure 39: HPLC chromatogram of CFM at 330 nm

7.2 Extraction with ethyl acetate

The same extraction procedure of chapter 7.1 was applied for the extraction using ethyl acetate, obtaining a residue (ER) (Figure 40) and a filtrate (EF). EF was concentrated at 20 mL, centrifuged and filtered: the residue was discarded while the filtrate was concentrated, weighed and redissolved in methanol for further analysis (EFM).

Figure 40: DCOW residues after ethyl acetate extraction (originally in colour)

From ^{1}H NMR analysis (Figure 41), it seems ethyl acetate extracts more polymethoxyflavones that the cyclohexane. This difference is better appreciated by MS (Figure 42) and HPLC analysis (Figure 43).

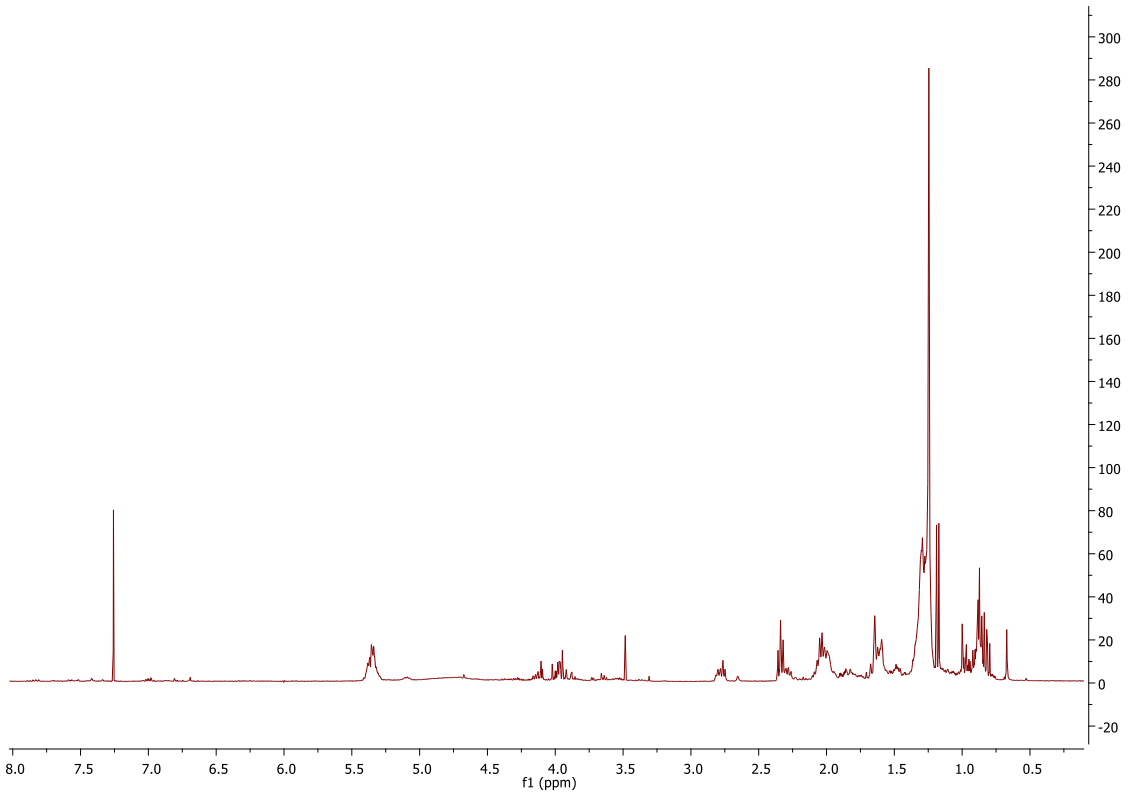

Figure 41: ^{1}H NMR of EFM ($CDCl_3$)

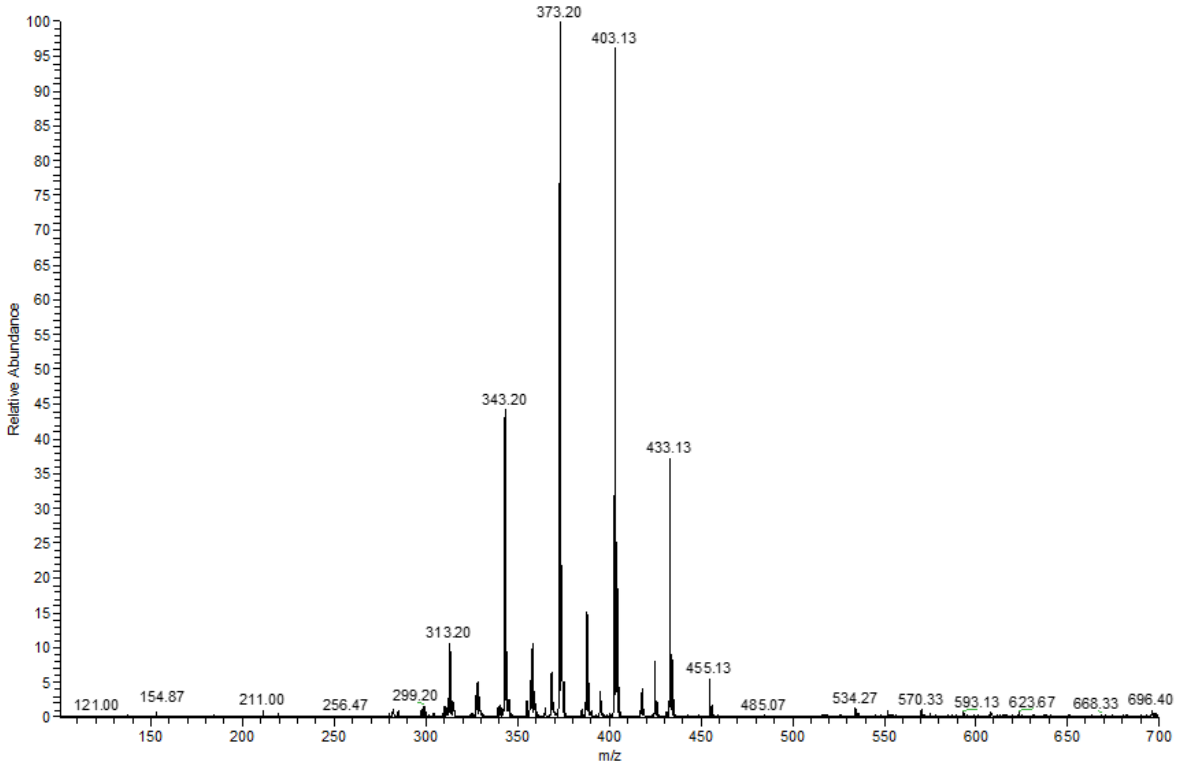

Figure 42: MS-ESI (positive) of EFM

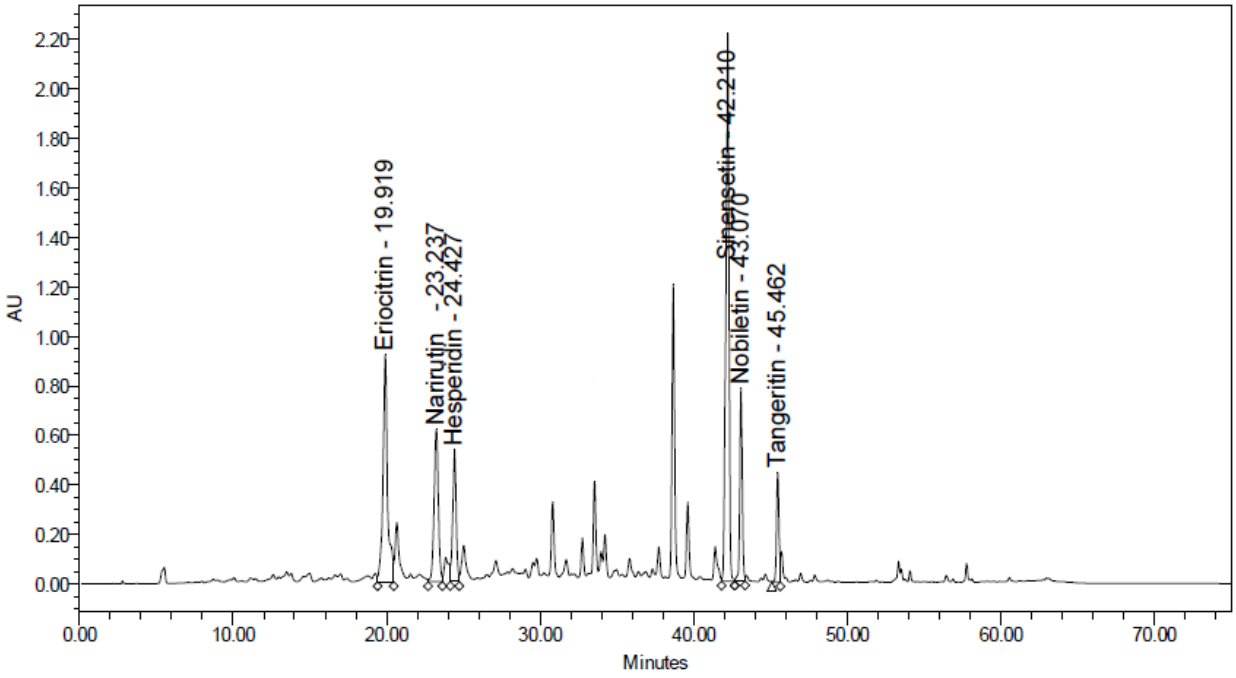

Figure 43: HPLC chromatogram of EFM at 285 nm

7.3 Extraction with acetone

The same extraction procedure of chapter 7.1 was employed for extraction with acetone, obtaining a residue (AR) (Figure 44) and a filtrate (AF). AF was concentrated at 60 mL, centrifuged and filtered: the residue was discarded while the filtrate was concentrated, weighed and redissolved in methanol for further analysis (AFM). The addition of methanol precipitate a pale yellow solid which was filtered and collected (AFMP).

Figure 44: DCOW residues after acetone extraction (originally in colour)

As seen in Figure 45, acetone extract both polymethoxyflavones (methoxyl group around δ = 4 ppm) and flavanones (The peak of hydroxyl group in the 5 position of flavonoids falls around δ = 12 ppm due to deshielding by the adjacent carbonyl group while the peak of hydroxyl group in the 4' position falls around δ = 9 ppm).

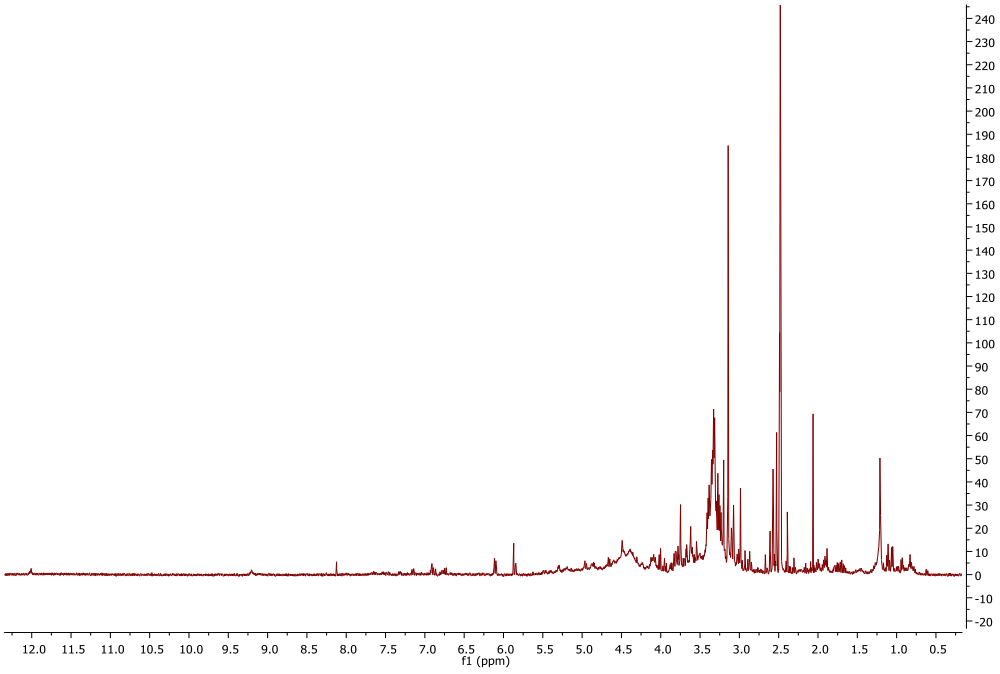

Figure 45: ^{1}H NMR (DMSO-d) of AFM

The mass spectrum, both positive (Figure 46) and negative (Figure 47) confirmed the presence of polymethoxyflavones and glycoside flavanone (positive peak at 611, negative at 609). The negative peaks at 191 and 383 are due to citric acid presence (citrate and citrate dimer).

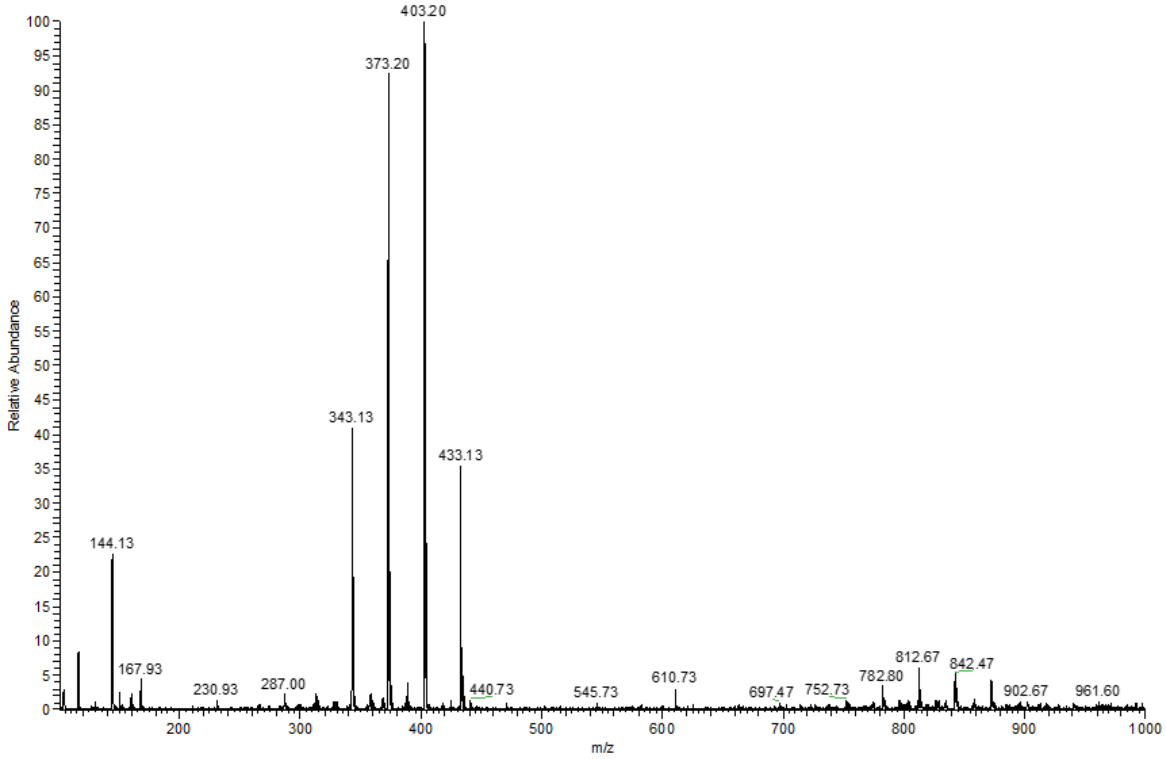

Figure 46: MS-ESI (positive) of AFM

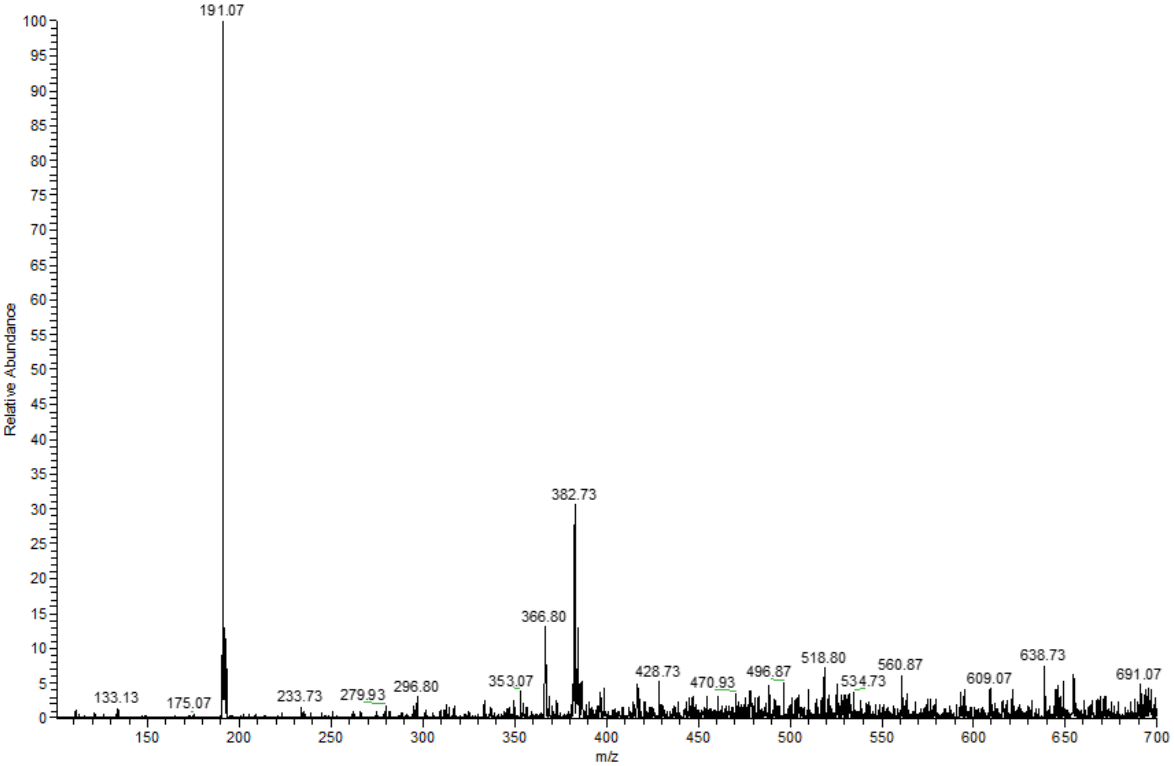

Figure 47: MS-ESI (negative) of AFM

Figure 48 shows the presence of both polymethoxyflavones and glycoside flavanones.

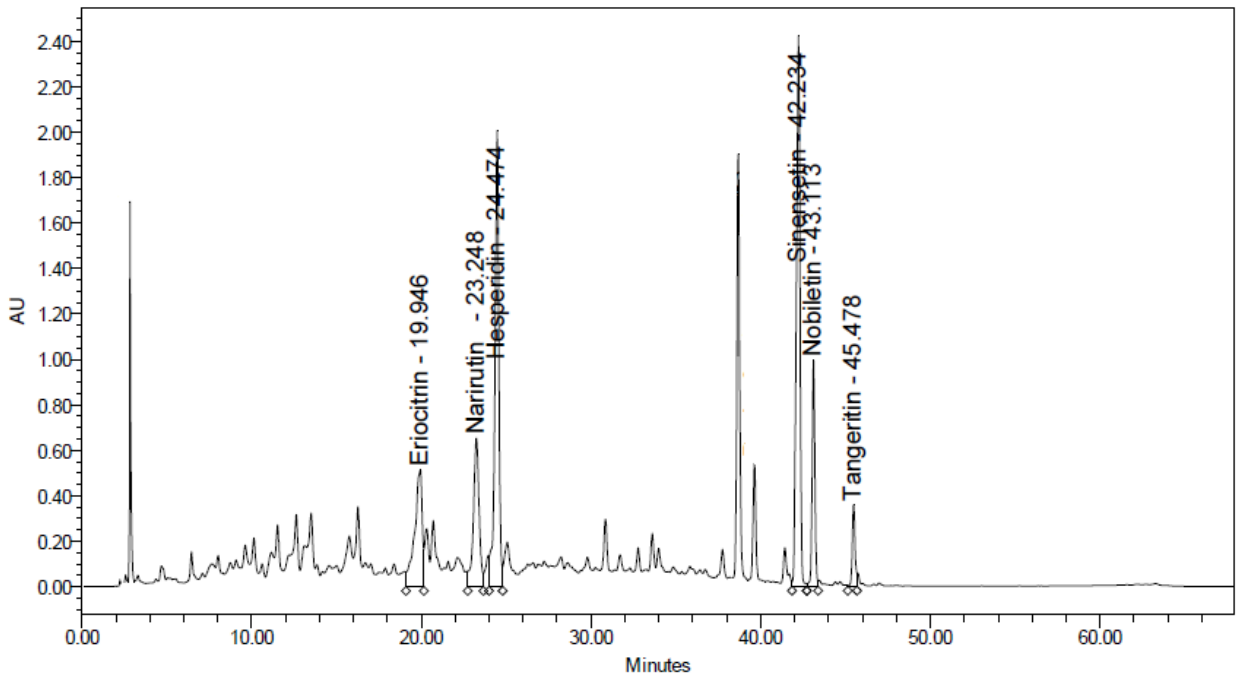

Figure 48: HPLC chromatogram of AFM at 330 nm

AFPM, which is insoluble in all but alkali and acid solutions, was washed and filtered one time with methanol and then two times with acetone. The filtrate was concentrated and analysed by NMR (Figure 49, Figure 50), while the solid was analysed by infrared spectroscopy (Figure 51).
The filtrate is mainly composed by hesperidin, while the solid seems a pectic substance.

^{1}H NMR (400 MHz, DMSO-d_6) δ 12.01 (s, 1H), 9.10 (s, 1H), 6.99–6.82 (m, 3H), 6.11 (d, J = 7.1 Hz, 2H), 5.48 (d, J = 12.3 Hz, 1H), 5.40 (d, J = 4.7 Hz, 1H), 5.18 (t, J = 5.1 Hz, 2H), 4.97 (t, J = 6.7 Hz, 1H), 4.76–4.54 (m, J = 5.1 Hz, 2H), 4.49 (s, 3H), 3.78 (s, 1H), 3.75 (s, 3H), 3.66-3.36 (m, 5H), 3.28 – 3.03 (m, 5H), 2.74 (d, J = 15.5 Hz, 1H), 1.06 (d, J = 5.9 Hz, 3H).

^{13}C NMR (101 MHz, DMSO-d_6) δ 197.50, 165.53, 163.46, 162.96, 148.36, 146.84, 131.36, 118.39, 114.56, 112.38, 103.71, 101.03, 99.80, 96.77, 95.98, 78.81, 76.67, 75.90, 73.39, 72.47, 71.10, 70.68, 69.98, 68.75, 66.44, 56.07, 42.48, 18.29.

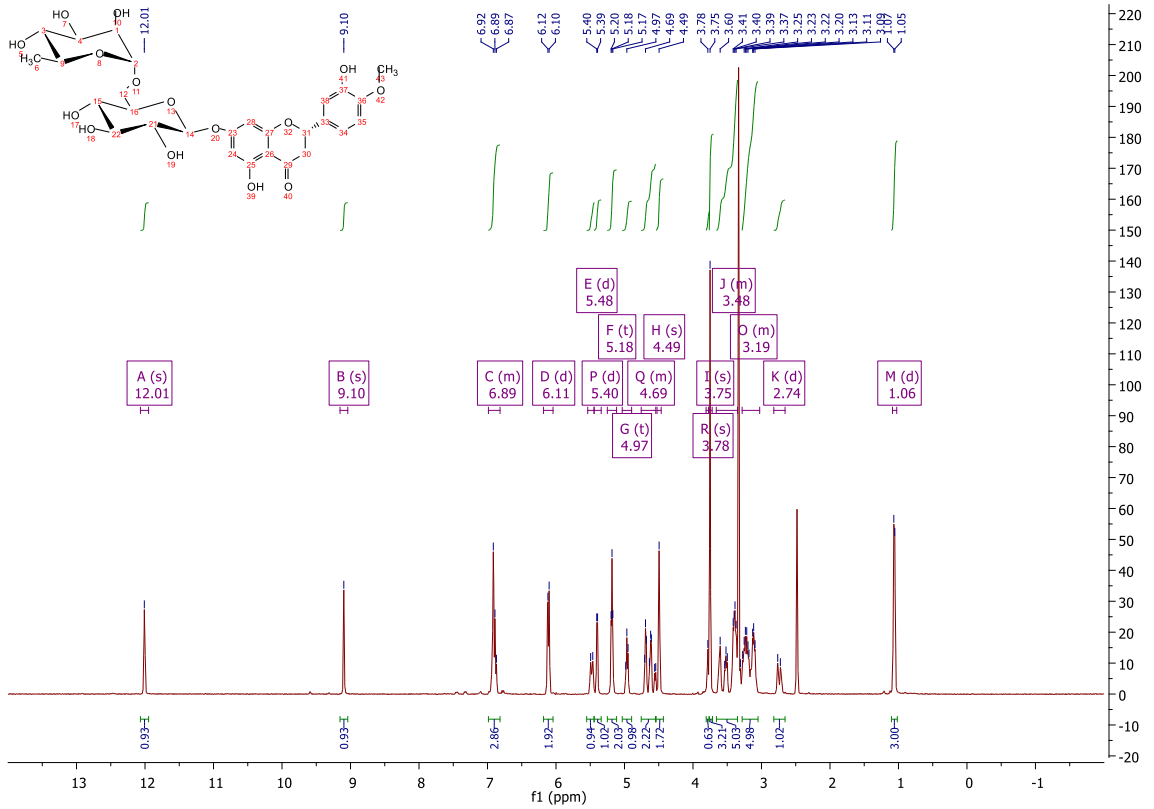

Figure 49: ^{1}H NMR (DMSO-d) of extracted hesperidin (originally in colour)

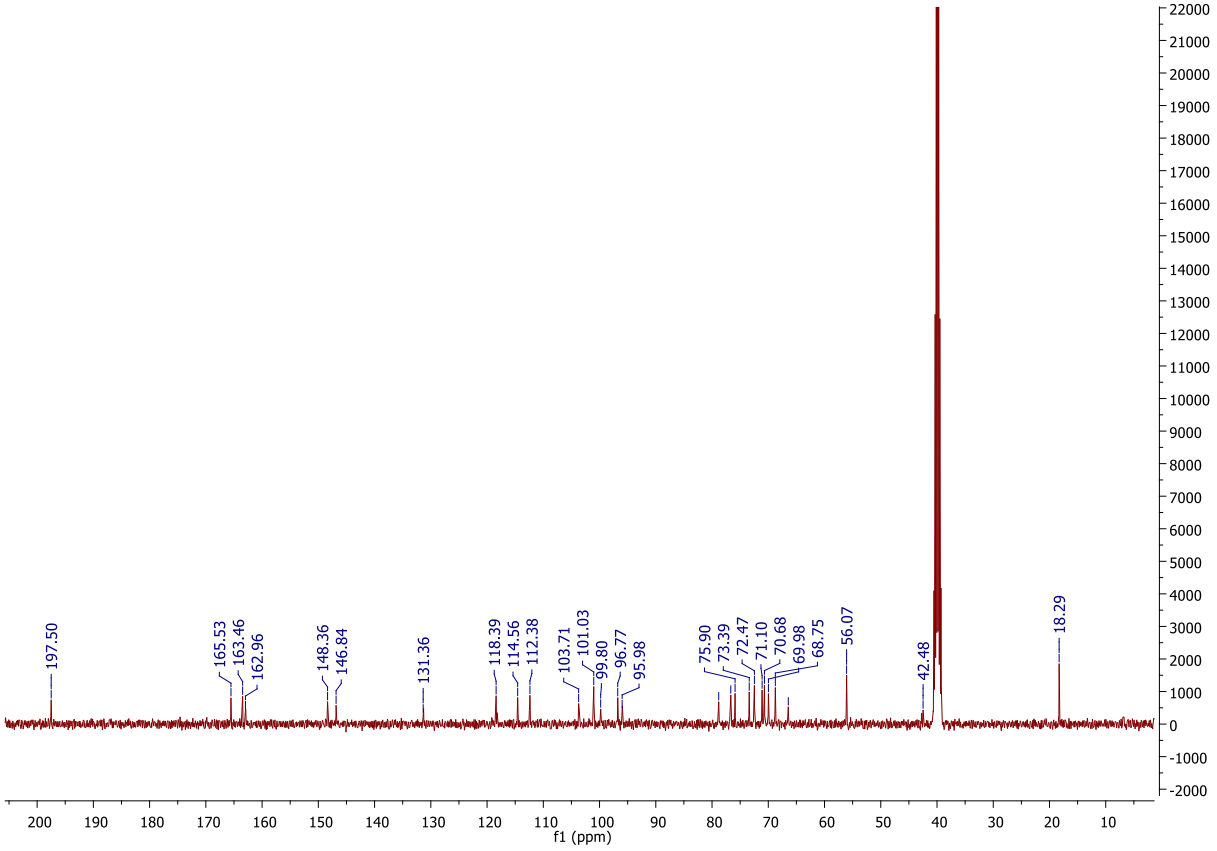

Figure 50: ^{13}C NMR (DMSO-d) of extracted hesperidin (originally in colour)

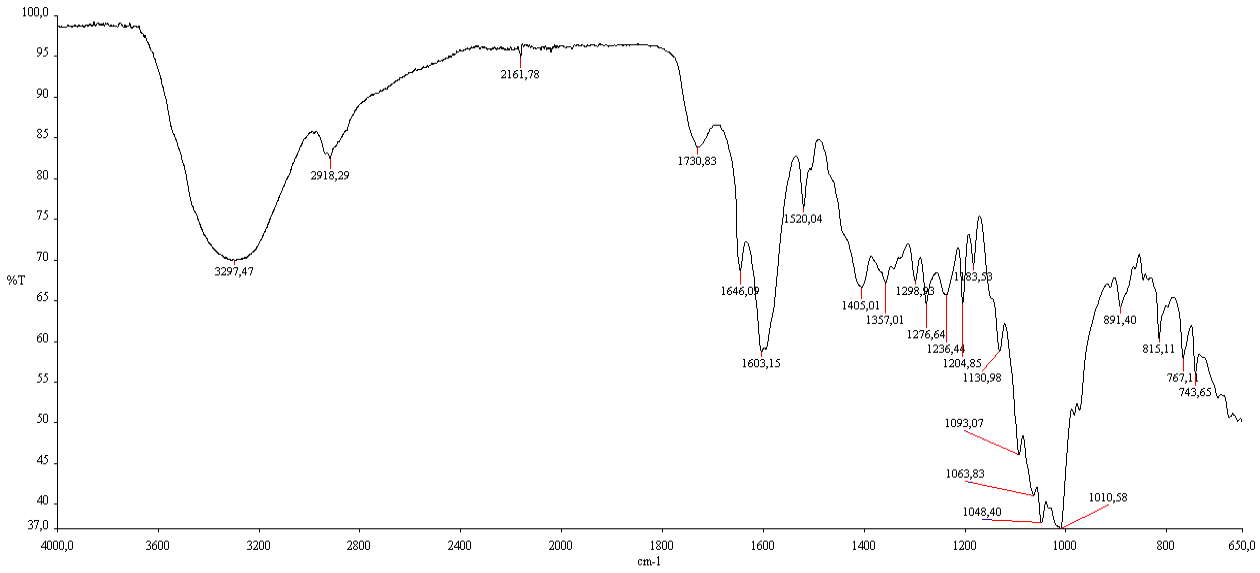

Figure 51: FT-IR of AFPM after hesperidin extraction

7.4 Extraction with ethanol

The same extraction procedure of chapter 7.1 was employed for extraction with ethanol (≥99.9%), obtaining a residue (EtR) (Figure 52) and a filtrate (EtF).

Figure 52: DCOW residues after extraction with ethanol (originally in colour)

EtF was concentrated at 60 mL, centrifuged and filtered: the residue was discarded while the filtrate was concentrated, weighed and redissolved in methanol (EtFM) for NMR (Figure 53), MS (Figure 54) and HPLC analysis (Figure 55). Similarly to what previously described in the extraction with acetone, the addition of methanol precipitate a pale yellow solid which was filtered and collected (EtFMP). The composition of this precipitate is identical to the one obtained in the extraction with acetone.

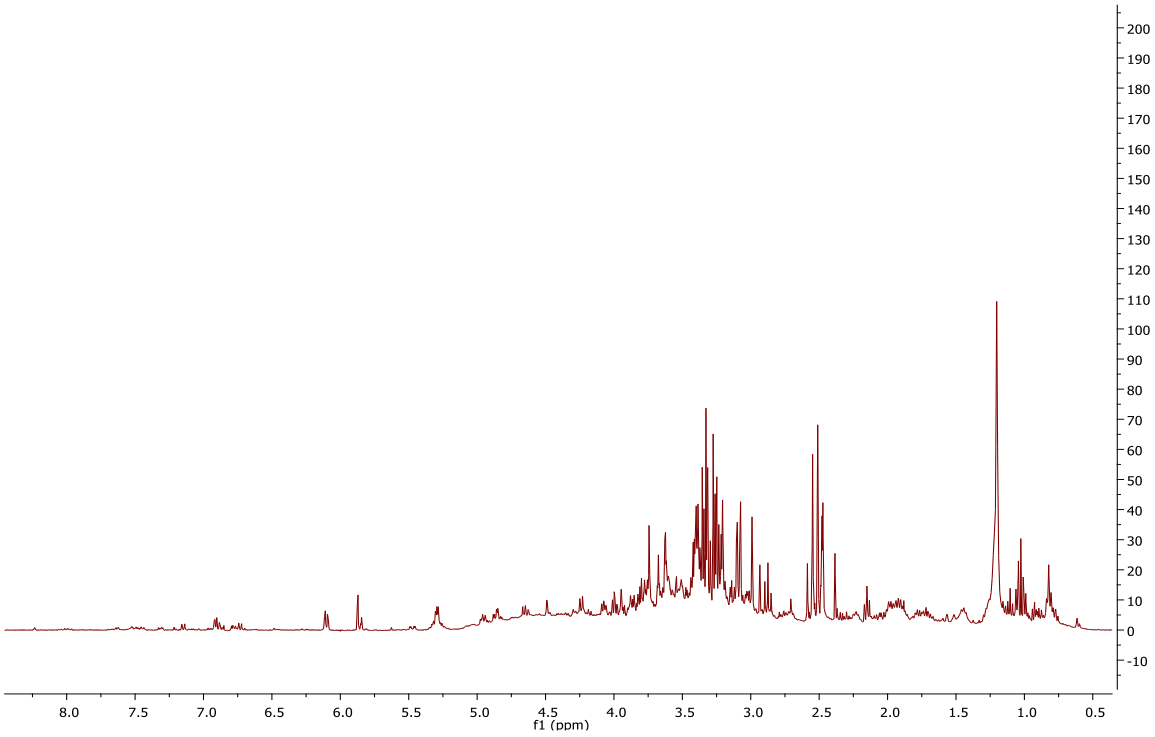

Figure 53: ^{1}H NMR (DMSO-d) of EtFM

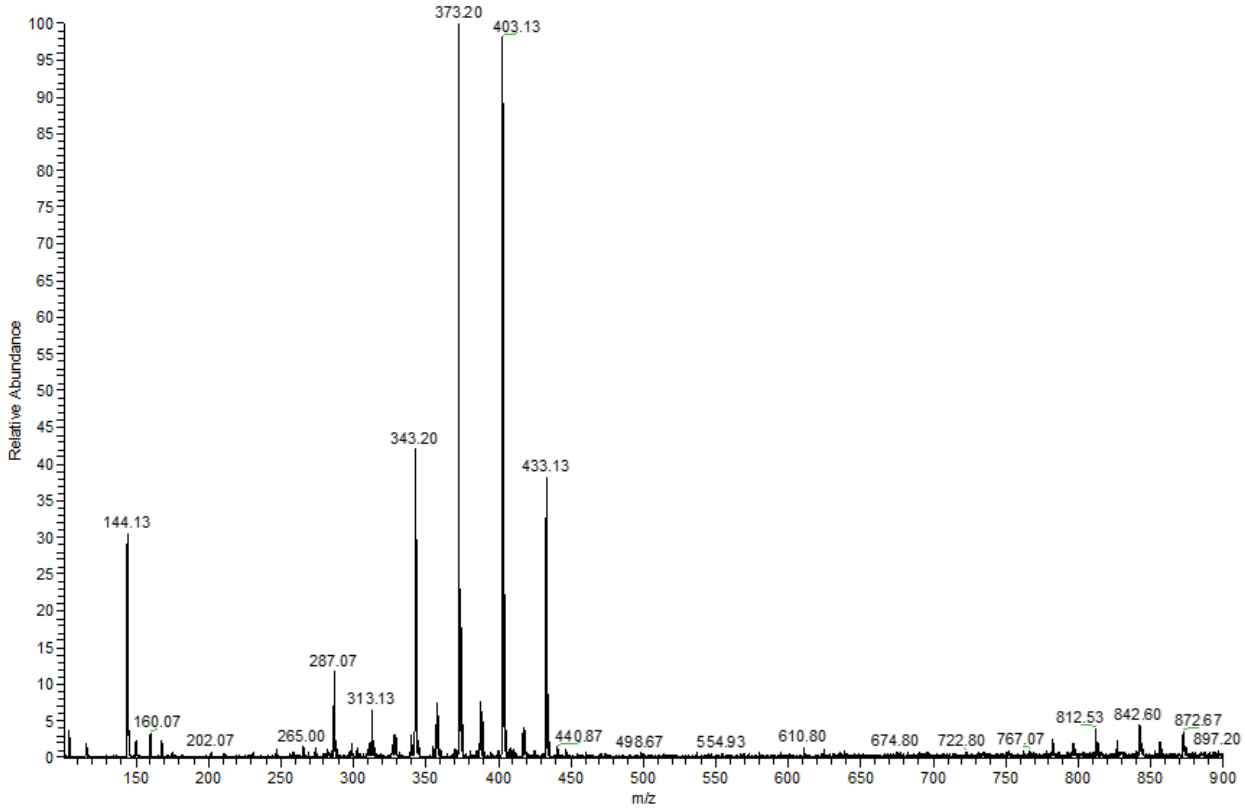

Figure 54: MS-ESI (positive) of EtFM

Ethanol seems to extract better polymethoxyflavones than glycoside flavanones. The peaks at the far right of the mass spectrum are due to dimer between different polymethoxyflavones with sodium and potassium ions.

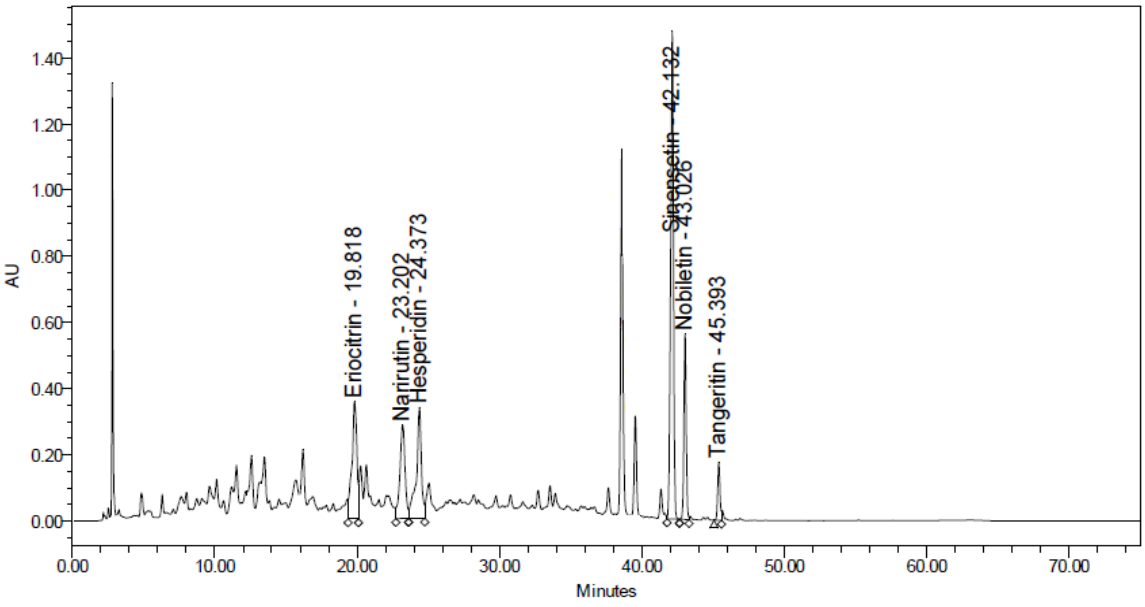

Figure 55: HPLC chromatogram of EtFM at 330 nm

7.5 Pectin extraction

10 grams of the fibrous residue resulted from continuous extractions with cyclohexane and acetone (CR+AR) (Figure 56), were treated with 300 mL of acidified water (pH = 1.5) at 80°C for 90 minutes.

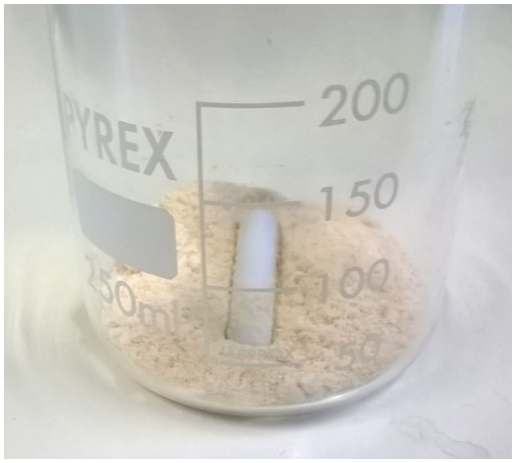

Figure 56: Solid residue after exhaustive cyclohexane and acetone extractions (originally in colour)

After cooling, the solution was filtered and the residue was collected, washed two times with methanol, dried and weighed (Figure 57). The solution was poured into pure ethanol and stored at -4°C over night to induce precipitation. Neverthless, even if the solution appeared cloudy and pearly, it was not possible to achieve any substantial filtration. Soxhlet extraction was tried twice, but it was unsatisfactory.

Figure 57: Solid residue after pectin extractions (originally in colour)

7.6 α-Cellulose extraction

5 grams of the fibre fraction obtained from pectin extraction were treated with 100 mL of NaOH (17,5%) at 30°C for 2 hours, to dissolve hemicellulose.

The solution was then filtered through a 30 mL glass Büchner funnels 30 mm (10-20 µm), recovery 0.9 grams of α-cellulose and a solution containing β-cellulose and γ-cellulose. The solution was neutralized with HCl 0.1 M to precipitate the β-cellulose.

α-cellulose was analyzed by infrared spectroscopy (Figure 58) and compared to the commercial standard (Figure 59).

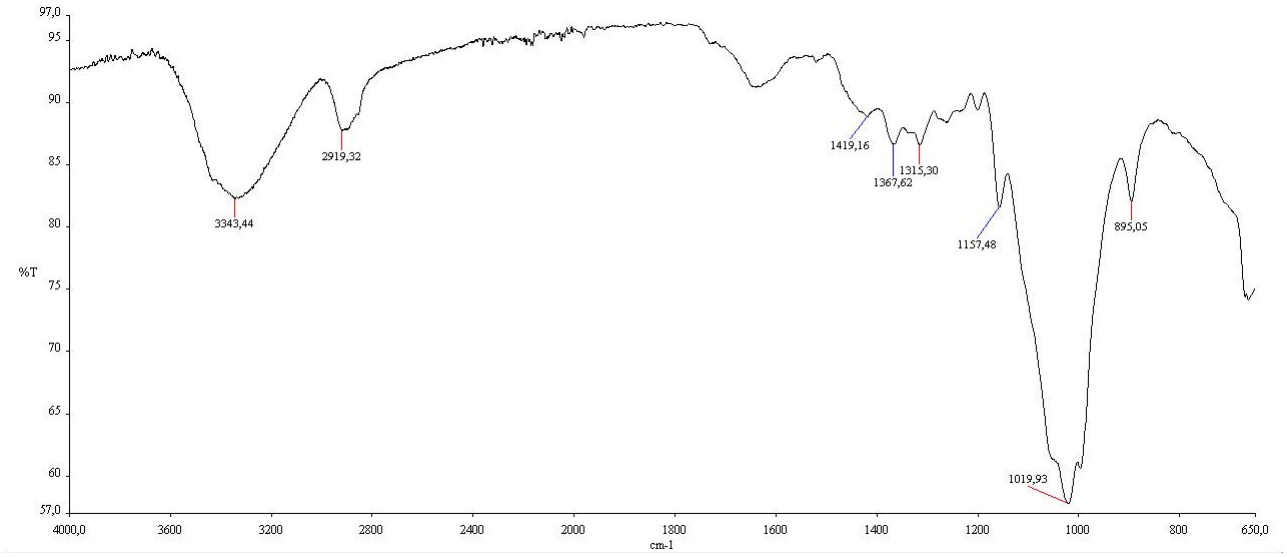

Figure 58: FT-IR of α-cellulose extracted from DCOW

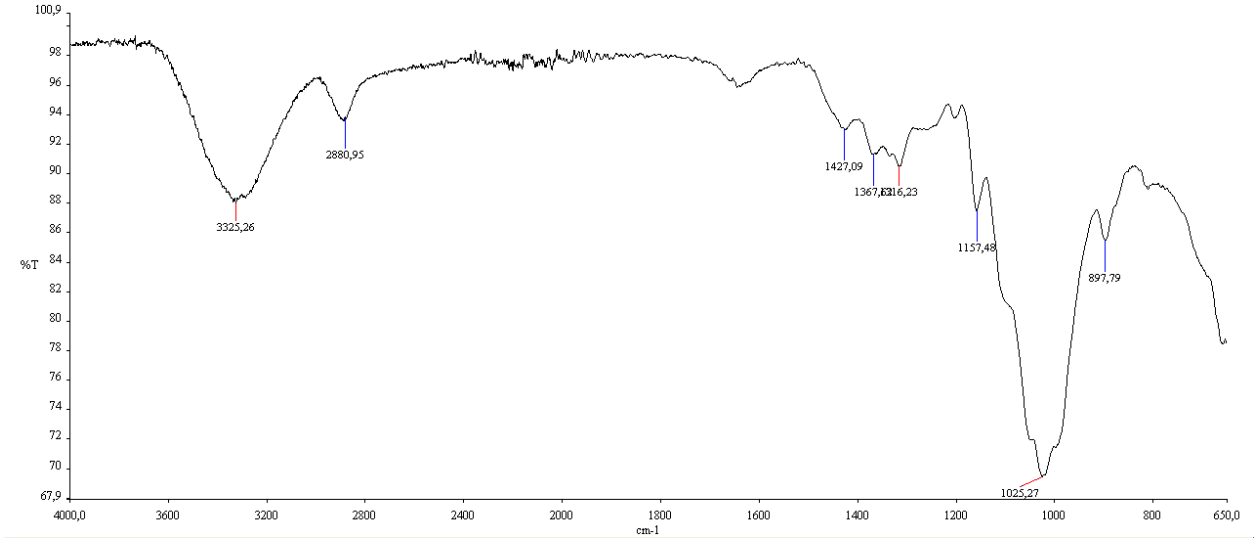

Figure 59: FT-IR of commercial α-cellulose

7.7 Cellulose Acetate Synthesis

5 grams of isolated α-cellulose were pre-treated with 20 mL of acetic acid (95%) for 2 hours at room temperature to swell the cellulose. The solution were suspended in 40 mL of glacial acetic acid (≥99%) and 0.02 mL of sulphuric acid (98.0%) and stirred at 50°C for 60 minutes. Then, the temperature of the solution was slowly cooled down with an ice bath.

15 mL of acetic anhydride (≥99%) and 10 mL of glacial acetic acid were added dropwise with a dropping funnel in 30 minutes. The temperature of the cellulose solution was monitored for the entire reaction, to prevent temperature from rising abruptly and damage the final product. After the addition was over, the solution was returned slowly to room temperature.

The temperature was then raised again to 50°C and the solution was left stirring for 2 hours, during which it became transparent and complete dissolution of cellulose acetate was achieved.

15 mL of acetic acid (60%) were added dropwise to avoid precipitation of cellulose acetate and left stirring for 24-30 hours to attain the partial hydrolysis of the cellulose triacetate into cellulose diacetate.

The reaction mixture was then precipitated with a solution with cold water (200 mL) and sodium acetate (5g), which help neutralizing the residual sulphuric acid. Cellulose acetate was then filtered and washed with methanol to facilitate air-drying. The final product was weighted (4.2 grams) and analyzed with infrared spectroscopy (Figure 60) for comparison with the commercial sample (Figure 61).

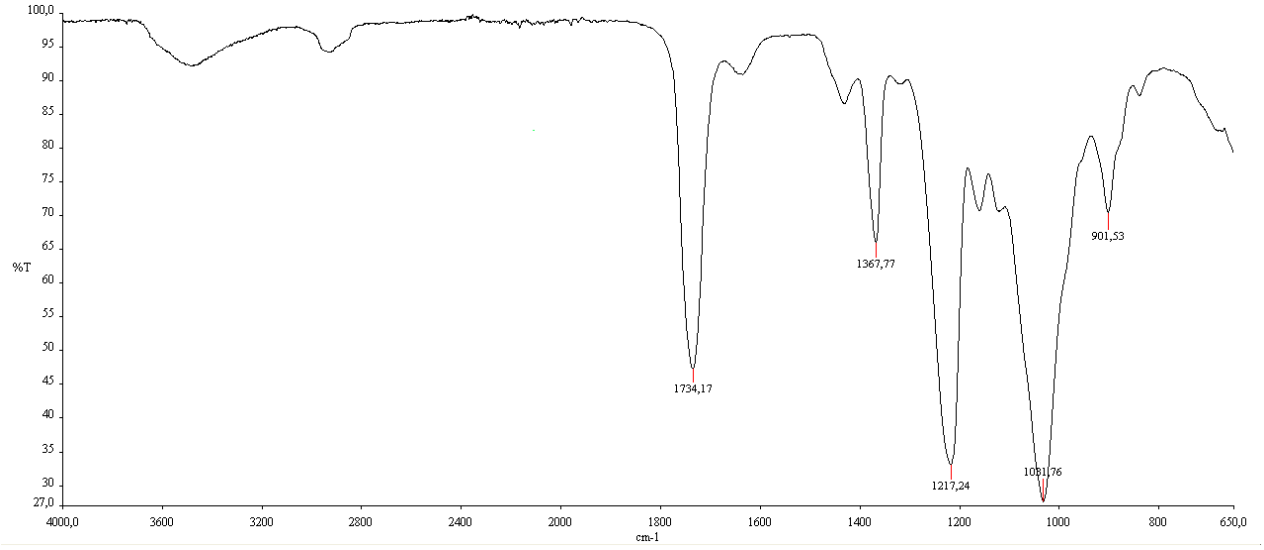

Figure 60: FT-IR of cellulose acetate from DCOW

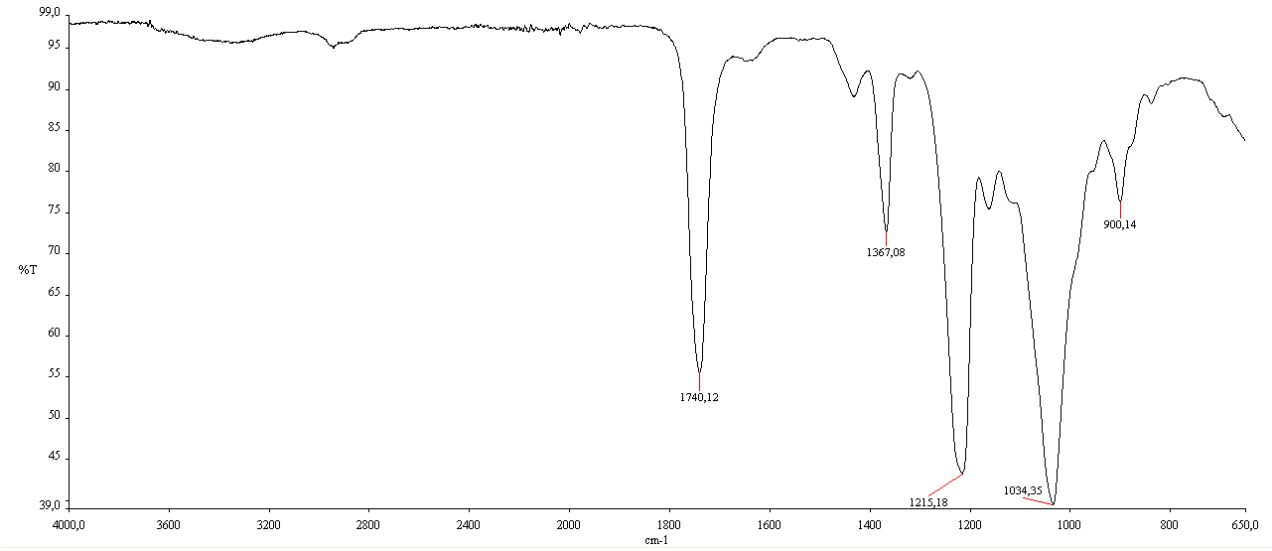

Figure 61: FT-IR of commercial α-cellulose

The degree of acetylation of both samples was measured by titration. To 2.0 g of cellulose acetate in a 500 mL conical flask were added 100 mL of acetone and 10 mL of distilled water and stirred until dissolution. Then, 30.0 mL of NaOH 1 M were added and the solution was stirred for 30 minutes. 100 mL of distilled water at 80 °C were poured and the reaction was left cooling to room temperature. The solution was titrated with sulphuric acid 0.5 M, using phenolphthalein as indicator.

8. Discussion and conclusions

In this initial project, a suitable method for the extraction and isolation of α-cellulose from decanter centrifuge orange waste has been demonstrated.

The isolation was achieved by progressive extraction with solvents of increasing polarity and two sequential treatments with hydrochloric acid (to remove pectin) and sodium hydroxide (to remove hemicelluloses), respectively.

Continuous liquid-solid extraction was carried out at 30°C for 2 hours, avoiding Soxhlet equipment due to the ooze-like nature of the product. Oven drying of the matrix was also not performed, under client's request and to avoid loss of volatile compounds. Nevertheless, oven drying was used to estimate the initial moisture content of the orange waste (82.65% ±1.23).

In the case of maceration (i.e. the preparation of an extract by solvent extraction), drying of the solid residue was achieved at room temperature (2 days) or under pressure (1 hour). This was possible as a result of solvent exchange inside the waste. However, remarkable difficulties were observed during extraction with non-polar solvents, probably due to the hydrophilic nature of the biological matrix, which repels non-polar solvents and forms conglomerates. On the other hand, polar solvents penetrate the macromolecular structure and carry the water away. The measurements of the final volume of the filtrate at each extraction are reported in Table 6 and partially confirm this hypothesis.

Decanter centrifuge orange waste extraction

Solvent used (200 ml)	Precipitate volume (ml)	Residue Dried Weight (g)
Cyclohexane	141,5 ± 2,3	10,46 ± 0,44
Ethyl acetate	151,1 ± 1.7	10,28 ± 0,37
Acetone	209,9 ± 0,6	9,56 ± 0,30
Ethanol	217,5 ± 1,2	9,85 ± 0,49

Table 6: Results of DCOW extraction with different solvents

It seems that not only cyclohexane and ethyl acetate fail to drag water away, but also a fraction of them remains stuck inside the matrix. On the contrary, polar solvents help the filtration, partially modifying the structure of the waste, which shifts from a sludge to a powder (Figure 62). This effect is even more accentuated when acetone is used, and it is probably caused by disruption of hydrogen bonds.

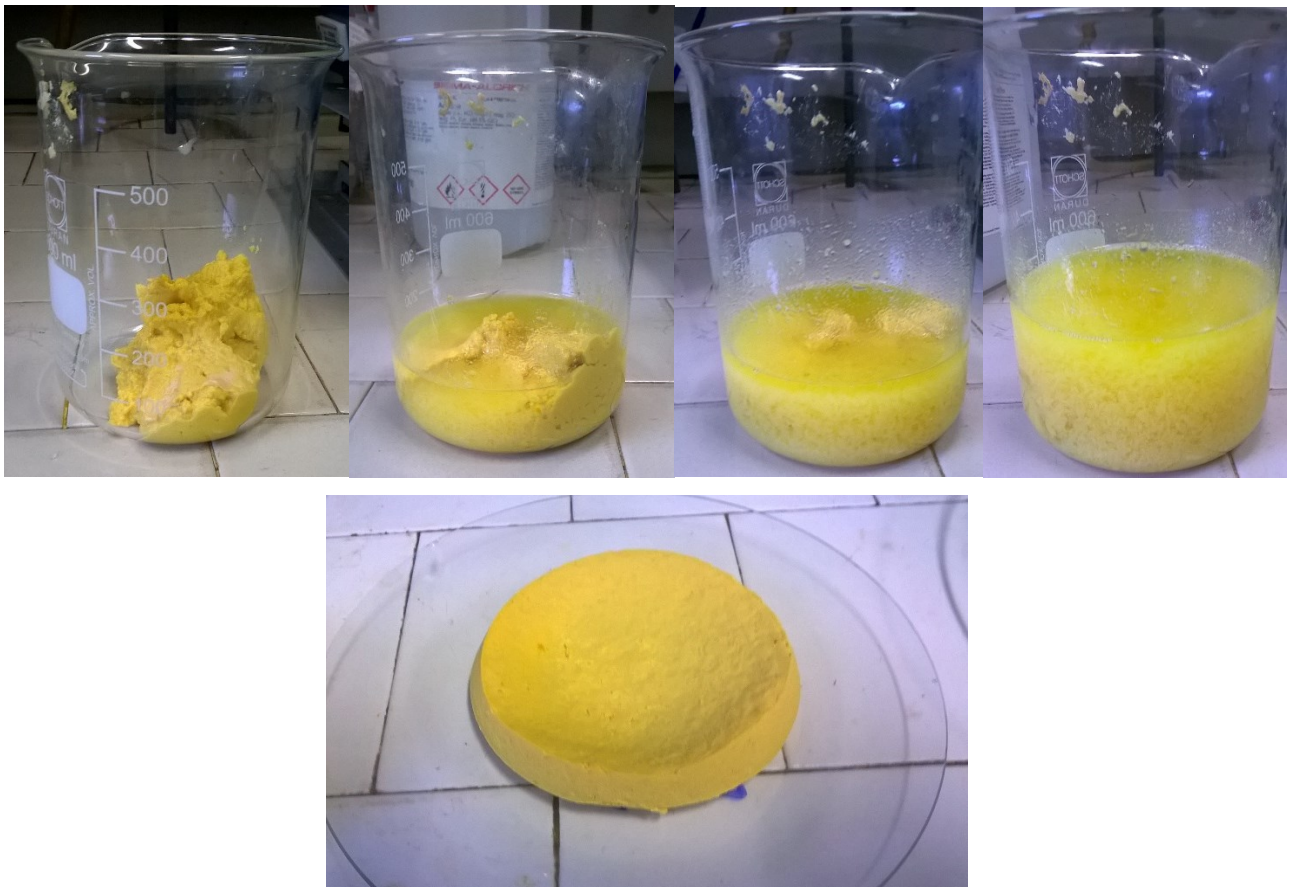

Figure 62: Transition of DCOW from sludge to powder (originally in colour)

Cyclohexane was used in these experiments instead of *n*-hexane to assure the safety conditions which could be hypothetically required in an industrial plant. The main product extracted by cyclohexane was a mixture of terpenes, with α-terpineol as the major component. This is unusual however, because α-terpineol is present only in traces in orange peel.[93] As stated before, orange waste coming from the orange juice extractor plant is subjected to both an enzymatic treatment and a pasteurization before centrifugation. It is known that pasteurization may promote the oxidation of D-limonene to α-terpineol,[6] so it is very likely that the latter is formed by this side-reaction occuring in orange waste.

Ethyl acetate allows the extraction of a fraction rich in polymethoxyflavones and their 5-hydroxy derivatives, as indicated by MS analysis. This shows three different series of ion masses: common polymethoxyflavones found in citrus compose the main sequence 313, 343, 373, 403, and 433 $[M+H]^+$ (Figure 63 and Figure 64), the second sequence (328, 358, 388 and 418) is originated by the small presence of 5-hydroxy derivatives, [175,176] while the last sequence is due to ion peaks $[M+Na]^+$.

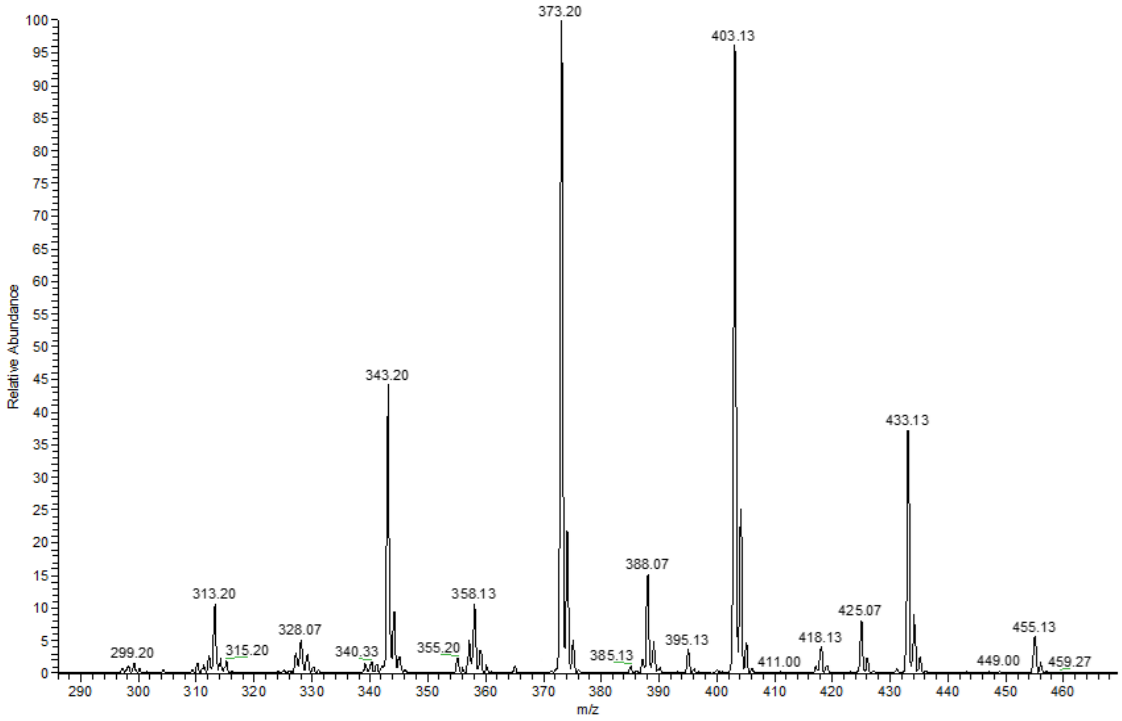

Figure 63: MS-ESI (positive) of ethyl acetate fraction (zoom)

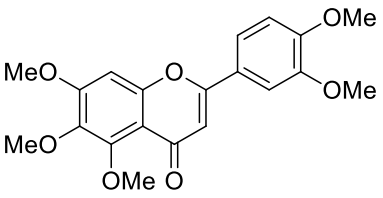

Sinensetin

372.37 g/mol

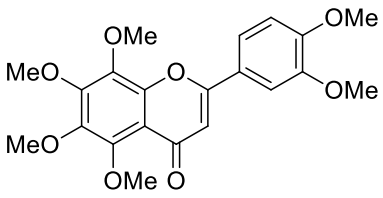

Nobiletin

402.39 g/mol

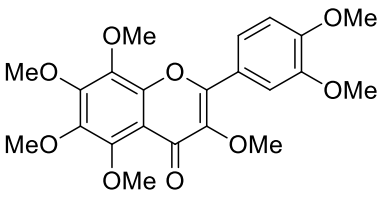

3,5,6,7,8,3'-4'-Heptamethoxyflavone

432.42 g/mol

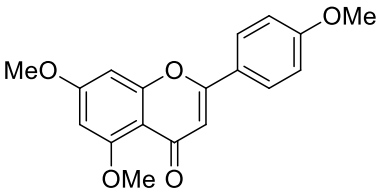

5,7,4'-Trimethoxyflavone

312.32 g/mol

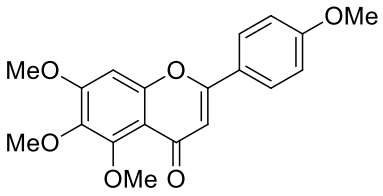

Tetramethyl-o-scutellarein

342.34 g/mol

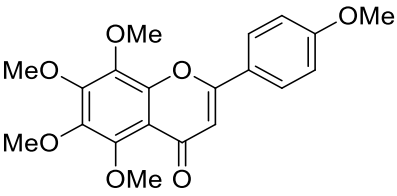

Tangeretin

372.37 g/mol

Figure 64: Formulas of common polymethoxyflavones found in orange by-products (with their molecular weight)

Though the crude solution has well-established biological properties, namely anti radical activity,[125,126] future works will aim to separate these different compounds.

Both acetone and ethanol extracted larger quantities of polymethoxyflavones and glycoside flavanones (see Chapter 7.3 and Chapter 7.4) compared to non-polar solvents. In particular, acetone is one of the few solvents that solubilizes hesperidin thereby allowing better extraction yields.

After extraction with acetone, it was possible to use an alcohol to precipitate both pectin and hesperidin, thus separating them from the mixture of polymethoxyflavones.
Different combinations of solvents may also be used to achieve the isolation of two or more compounds. In particular, European law tolerates the use of ethyl acetate, along with acetone and ethanol, for extraction procedures in food processing, in compliance with good manufacturing practice.[177]
From a costs reduction point of view, the preferable procedure would require an exhaustive and continuous acetone extraction with a counter-current screw extractor. The extraction plant should be built as close as possible to the orange juice extraction factory in order to minimize transportation costs.

To obtain a pure cellulose fraction, it was necessary to extract pectin which may hamper further derivatization. Figure 65 shows the IR spectrum of a sample of isolated α-cellulose contaminated by pectin: a strong band at 1600 cm^{-1} is due to pectin carboxylate group.[178]

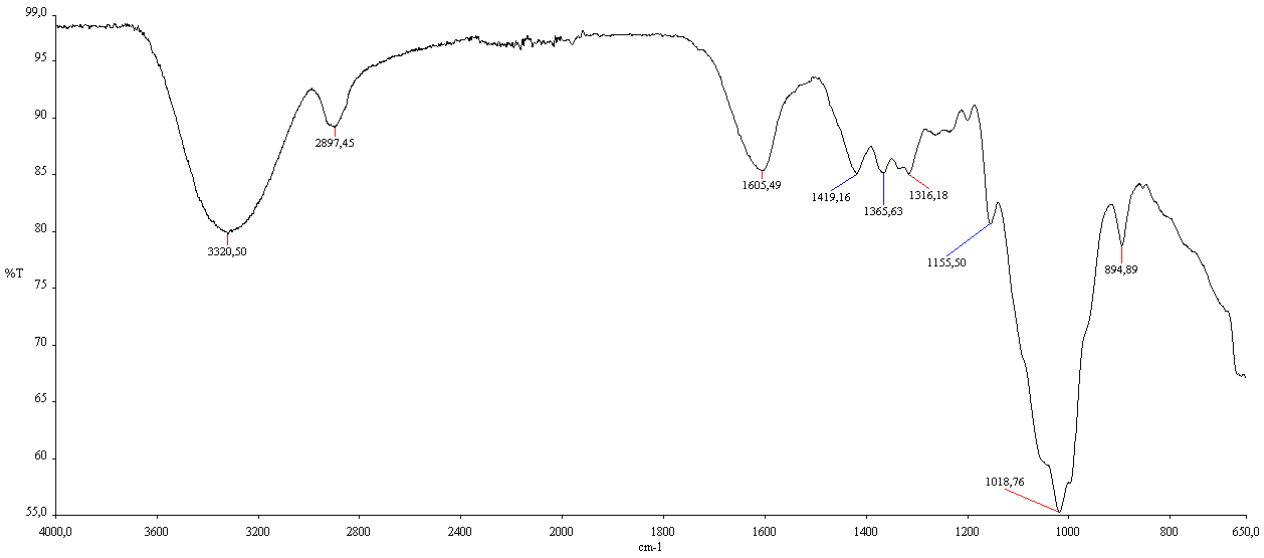

Figure 65: α-cellulose from DCOW with traces of pectate

Even if it was not possible to precipitate pectin, it still accounted for half of the weight of the fibre fraction. The resulting solution of galacturonic acid can be recover and reutilized.[179] Alternatively, if pectinase enzymes are not employed during pre-treatment of DCOW, pectin could be recovered and purified.

α-Cellulose was isolated from the final cellulose fraction with a yield of 9.81% ± 0.25 on dry basis. Next, α-cellulose was acetylated with acetic anhydride and sulphuric acid to obtain cellulose acetate. However, the yield of the acetylation reaction performed on α-cellulose deriving from DCOW was lower (32.7% ± 2.7) compared to the one performed on commercial α-cellulose (87.2% ± 0.8). This result may be due to the crystallinity of orange waste α-cellulose: sulphuric acid catalysis may likely accentuate the competition between the chain hydrolysis and the acetylation process. Nonetheless, DCOW-derived cellulose acetate showed comparable features with commercial samples including the full solubility in acetone. Importantly, evaporation of acetone solutions provided transparent films as expected (Figure 66).

Figure 66: Cellulose acetate from DCOW after evaporation (originally in colour)

It is worth noting that the degree of acetylation in DCOW-derived cellulose acetate samples was 2.4. This result represents an improvement in comparison to reported studies.[161,180]

Future studies will be addressed to develop a suitable separation technique to recover polymethoxyflavones from acetone, ethanol and ethyl acetate solutions, and α-terpineol from cyclohexane solution. This would likely address economic issues of the extractive process allowing for the production of different saleable compounds.

Moreover, X-ray and viscosity analysis should be performed to study crystallinity and average molecule weight of recovered cellulose, enabling fully characterization of the final product.

Synthesis of spiro and ureidic compounds for modulation studies of mptp protein

9. Introduction

9.1 Mitochondria

Mitochondria are organelles that can be found in variable number in different types of cell. They have been identified for the first time by Altmann in 1890.[181] At first they were called "bioblasts", as they were considered autonomous elementary organisms responsible for metabolic and genetic functions, with a specific DNA (mitochondrial DNA) and the ability to synthetize their own proteins. However, only after 1950 electron microscope made it possible to clarify their structure.[182,183]

Mitochondria have a typical double membrane structure that gives rise to four functional compartments (Figure 67): the outer mitochondrial membrane (OMM), the inter-membrane space (IMS), the inner mitochondrial membrane (IMM) and the matrix.

The OMM is permeable to small molecules ($M_r < 6500$) and to ions, which freely move through porins (a crossing-membrane proteins family). Instead, the IMM is impermeable to small size molecules and to the most part of ions, including H^+. However, it is permeable to oxygen, carbon dioxide and water. IMM consists of cristae that increase the area housing complexes of electron transport chain (ETC) and ATP synthase, allowing an increase in energy production. Through these complexes, mitochondria control the basic rates of cellular metabolism, by the oxidative phosphorylation mechanism. The matrix includes a vast number of enzymes that facilitates biological reactions (except glycolysis), such as pyruvate dehydrogenase (PDH), citrate synthase, carbamoyl phosphate synthetase, pyruvate carboxylase acyl-CoA dehydrogenase and transaminases.

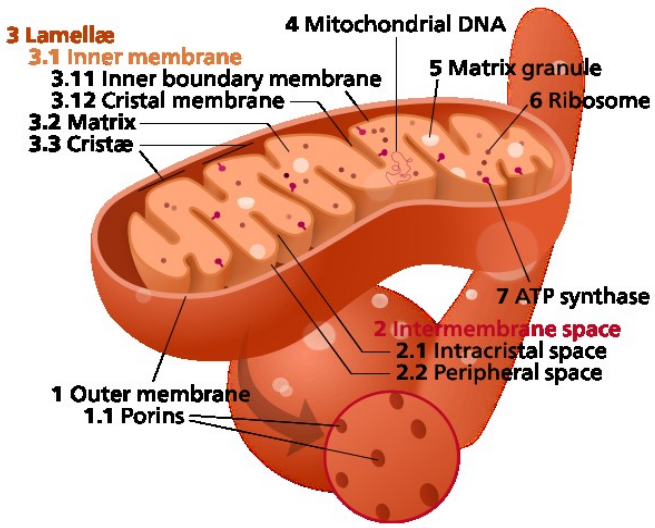

Figure 67: Mitochondrial Structure (CC) (originally in colour)

9.2 Oxidative phosphorylation mechanism and ATPase.

As mentioned before, a key role of mitochondria is the oxidative phosphorylation mechanism, which consists in the storage, as ATP molecules, of the energy produced by catabolic pathways and temporary preserved by electron transport chain reactions. The amount of energy-released permit a better understanding of the vital role played by the oxidative phosphorylation compared to anaerobic fermentation. Glycolysis produces 2 ATP molecules and 2 NADH molecules per unite of glucose, while 30 to 36 ATPs are produced by the oxidative phosphorylation of the 10 NADH and 2 succinate molecules made by converting one molecule of glucose to carbon dioxide and water.[184]

NADH and reduced flavin adenine dinucleotide ($FADH_2$), generated by fatty acid oxidation, glycolysis and the citric acid cycle, are subsequently oxidized within the mitochondria. Energy from these oxidation steps is transferred along a series of electron-transport protein complexes that form an electron-transport chain embedded in the IMM (Figure 68).[185]

In the last passage, electrons transferred by ETC reduce molecular oxygen into water. A small percentage of electrons do not complete the whole series and instead directly leak to oxygen, resulting in the formation of reactive oxygen species.

The energy developed in every oxidation is used to pump protons out of the matrix, utilizing three different membrane protein complexes and generating a large electrochemical gradient across the membranes. This gradient exerts a proton-motive force, which tends to drive H^+ back into the matrix through the ATP synthase, which use this potential energy to convert ADP and phosphate into ATP.

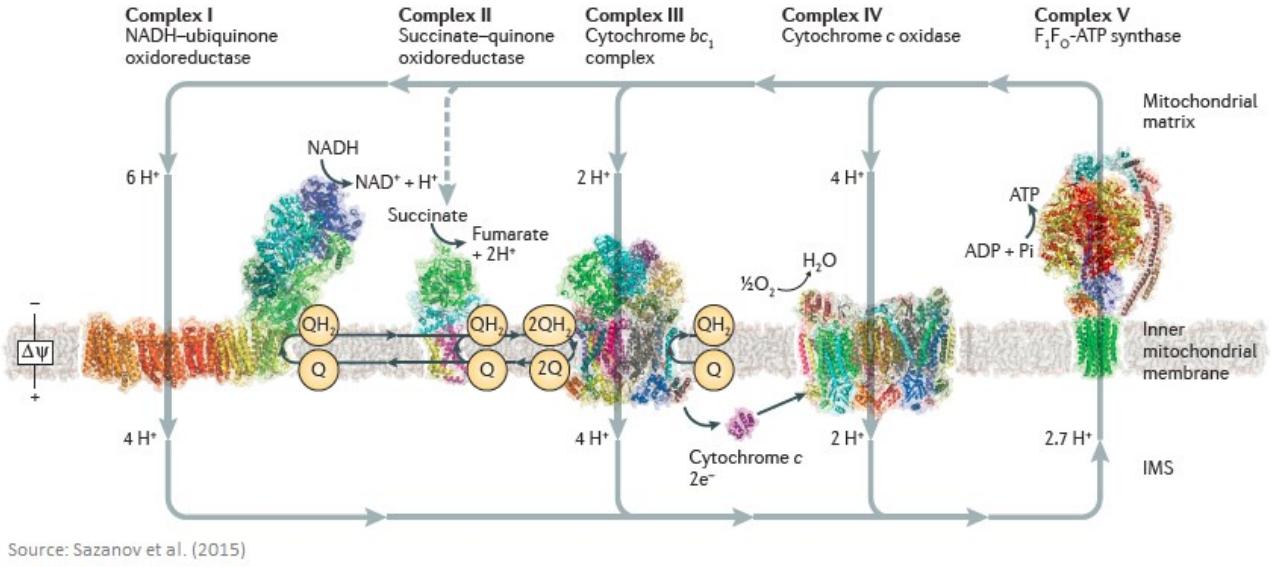

Figure 68: Electron Chain Transfer (originally in colour)

In the first step of ETC, two electrons and two protons pass to ubiquinone (Q) synthesizing ubiquinol (QH_2). This step may be due to three main different transporters: nicotinamide adenine dinucleotide (NAD), succinate or flavin-adenine dinucleotide (FAD). In Complex I, two electrons are removed from NADH and transferred to ubiquinone. The reduced product, ubiquinol, freely diffuses within the membrane, while Complex I translocates four protons (H^+) across the membrane.

Complex I is one of the main sites at which premature electron leakage to oxygen occurs. In fact, ubiquinone is able to accept two electrons, passing through a radical form. Thus, during the first and the second step there may be the direct transfer of one electron from radical ubiquinone to oxygen, generating superoxide anions and hydroxyl radicals.

Complex II provides for an additional entering point for electrons into the chains, transferring electrons originating from succinate (oxidized to fumarate) to Q. Other electron donors (e.g., fatty acids and glycerol 3-phosphate) also direct electrons into Q (via FAD). Complex II is a parallel electron transport pathway to complex I, but unlike complex I, no protons are transported to the inter-membrane space in this pathway.

Then, electrons pass from ubiquinones to Cytochrome C thanks to Complex III, generating a flux of four protons to the inter-membrane space. Every ubiquinone can oxidize two different cytochromes C, as it is a single-electron transporter.

Finally, Complex IV, the cytochrome oxidase, catalyzes the reduction of molecular oxygen into water, hence, the flux of two protons through the IMM.

To summarize, a total gradient of 10 protons is generated through the IMM during the complete transfer of electrons from a NADH transporter to a molecule of oxygen.

Thanks to the proton electrochemical gradient in the IMM, an IMM transmembrane potential is generated, called proton motive force. This is used in order to accumulate energy into ATP molecules. An exergonic proton influx is produced by ATP synthase, which is hence able to catalyze the reaction of ADP and Phosphate to produce ATP. This is called chemiosmotic model, because of the contemporaneous occurrence of a transfer process and a chemical reaction in two different ATPase domains, F_O and F_1 (Figure 69).[186,187]

Before illustrating this chemiosmotic model, it should be considered that one of the most interesting features of ATPase is the parallelism between structure and activity that have been deeply investigated after F_1 crystallization.[188]

F_O, which is located inside the IMM, is also called C-ring, because it is formed by 10 hydrophobic C subunits organized to form an oligomeric ring that makes up the F_O rotor.

The F_1 domain is composed by five different subunits located in the mitochondrial matrix. Three α and three β subunits are alternative placed to form a ring out of a central linear γ subunit. Its main role is the catalysis of the reaction between ADP and phosphate to form ATP. This is due to a rotational catalysis mechanism in three steps, based on a constantly alternate affinity of each one of the three β subunit to ADP and Phosphate, to ATP and to none of them. In this way, firstly a β subunit binds ADP and Phosphate. Secondly it acquire a major affinity to ATP and, hence, it catalyzes the formation of ATP itself. Finally, it loses its affinity to ATP and it releases it into the matrix.

F_O and F_1 domains links together with a lateral bridge, consisting of δ, α and β subunits and thanks to ε one, which connects γ subunit with the c ring. Because of this ATPase structure, proton influx and ATP synthesis are deeply connected.[189]

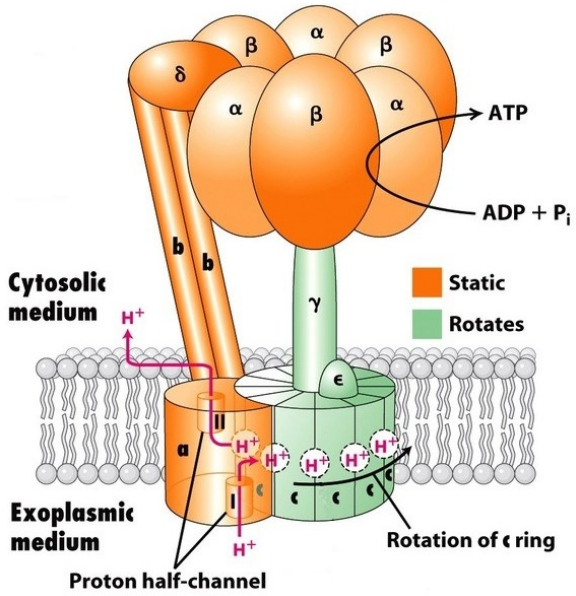

Figure 69: ATP synthase structure (Adapted from Lodish et al., 2004) (originally in colour)

Moreover, it has been demonstrated that ATP synthesis is repressed by the inhibition of the electron flux and even that the electron flux is inhibited by the repression of ATP synthesis. In fact the use of oligomycin, known for its binding the F_O subunit, inhibits both the ATP synthesis and the electron flux. To illustrate this mechanism, it should be considered that three conditions are required to synthetize ATP: a substrate able to be oxidized, such as NADH or succinate, an ADP molecule and phosphate. Clearly, if the oxidation reaction is inhibited, even the electron and, hence, the proton fluxes are repressed. Thus, ATPase receive no stimulation by the proton motive force to the production of ATP. However, more noticeably, even the ATP synthesis inhibition represses the electron flux.

Oligomycin A binds the C ring, physically inhibiting the passage of protons through ATPase channel.[190]

If the proton gradient is not dissipated by the return of protons into the mithocondrial matrix, eventually the outside of the mitochondrion develops such a large positive charge that the electron-transport chain can no longer pump protons against the gradient, inhibiting the oxidation reactions. Even if there is an exception, called “proton leak”, where protons enter the matrix without passing through the ATP synthase complex.[191]

Besides, the ATPase activity is mainly related to ADP rate, which determines oxygen consumption. For this reason, the cell energy status could be measured either by the ADP concentration or by the ATP-ADP system mass-action ratio, which is ATP/(ADPxP_i). As naturally adenosine is completely phosphorylated, this ratio is usually high. However, when a cell process requires high levels of energy, ATP is demolished to ADP and the ratio decreases. As explained before, ADP is an ATP synthase activator, hence, in this condition ATP synthesis induction leads to a mass-action ratio increasing. In this way, ATP production and energy storage is perfectly balanced and related to energy consumption.[192]

Finally, ATPase can promote either ATP synthesis or ATP hydrolysis. In the latter, ATPase actively transport H^+ ions through the IMM against their gradient. The energy required for this pumping process is given by ATP hydrolysis. For instance, when cells are in a hypoxic state, oxidative phosphorylation mechanism is interrupted, as there can not be an electron transfer to oxygen molecules. However, this activity is promptly inhibited by IF_1 protein, which is activated when pH decrease under 6.5. During hypoxia, anaerobic glycolysis is active and both cytosolic and mitochondrial matrix pH dramatically decreases. Therefore, IF_1 inhibit ATPase activity, inducing its dimerization (Figure 70).[193] When oxygen returns available, pH increases, IF_1 becomes unstable and ATPase activity is restored. However, while the inhibited ETC is re-exposed to oxygen, reactive oxygen species may be generated.

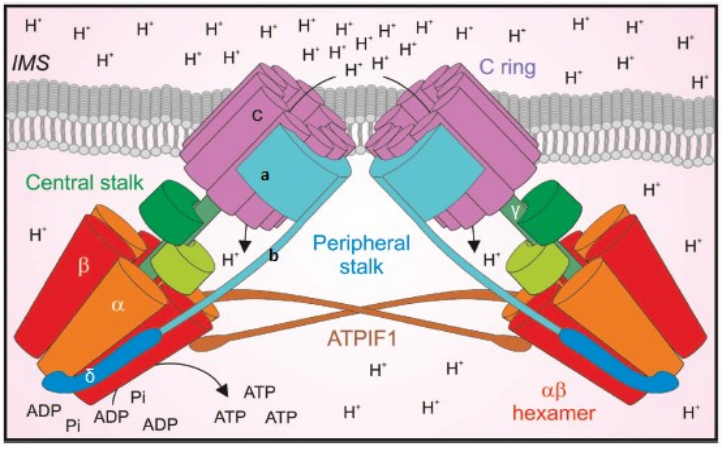

Figure 70: ATPase dimer stabilized by IF1 (Source: Bonora et al., 2014) (originally in colour)

9.3 Ca^{2+} homeostasis and mitochondria

The control of cellular Ca^{2+} is of critical importance, as the range of Ca^{2+} - regulated functions covers a large number of processes that are essential to cell life, such as gene transcription, enzyme phosphorylation and dephosphorylation and programmed cell death.[194]

In physiological conditions, calcium is mainly stored in endoplasmatic or sarcoplasmatic reticulum (ER/SR) and in the Golgi apparatus, where it respectively reaches a concentration of 300-600 µM and 200-500 µM. It is even present at lower concentration in the cytosol, which has normally Ca^{2+} of 100nM.

In recent years, several plasma membrane Ca^{2+} channels and their distinctive function have been identified (Figure 71). The channels have been historically divided in three major groups: the voltage-gated channels (VOCs), the receptor-operated channels (ROCs), and the store-operated Ca^{2+} entry channels (SOCEs). The endo/sarcoplasmic reticulum (ER/SR) and more recently, the Golgi apparatus (GA), are recognized as the main intracellular Ca^{2+} stores. Two types of Ca^{2+} receptors/channels essentially operate Ca^{2+} mobilization from them, the ubiquitous inositol 1,4,5-trisphosphate receptors (InsP3R) and the ryanodine receptor (RyR), which is not present in all cell types.[195]

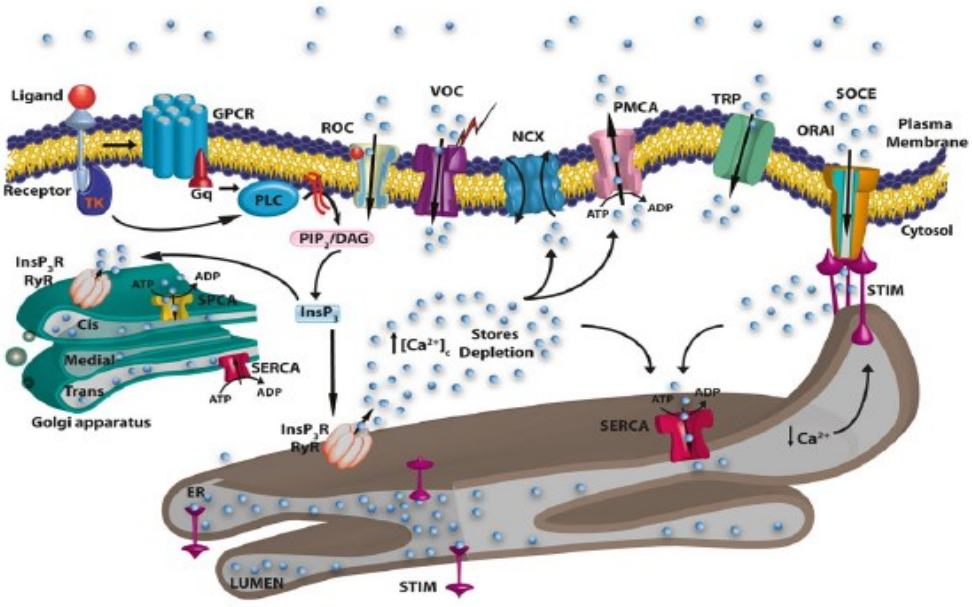

Figure 71: Cell Ca2+ homeostasis (Source: Brini et al., 2013) (originally in colour)

Ca^{2+} can also be found into mitochondria (Figure 72) in resting condition of 100nM concentration. Mitochondrial Ca^{2+} transport has unique characteristics. The uptake does not need ATP hydrolysis for Ca^{2+} entry, but utilizes a uniporter (MCU) and the membrane potential maintained across the inner membrane by the respiratory chain as the driving force. For Ca^{2+} efflux, mitochondrial exchangers use the concentration gradient of Na^{+} across the inner membrane to cause the release of Ca^{2+} back into the cytosol.

The cycle is then completed thanks to the efflux of Na^{+} via the Na^{+}/H^{+} exchanger (NHE) (Figure 72). The rates of Ca^{2+} influx and efflux are generally slow, ensuring the maintenance of a low matrix Ca^{2+} concentration during resting conditions.

When cytoplasmic Ca^{2+} increases above a given threshold (>10 μM) a rapid Ca^{2+} accumulation by mitochondria is initiated and matrix Ca^{2+} increases dramatically. Eventually, excess Ca^{2+} accumulation by mitochondria may result in the opening of a large non-selective channel in the inner mitochondrial membrane, the mitochondrial permeability transition pore (mPTP) that collapses the membrane potential, induces swelling of the inner membrane. Therefore, inner membrane may breaks the outer one, releasing proteins of the intermembrane space (IMS) into the cytoplasm.

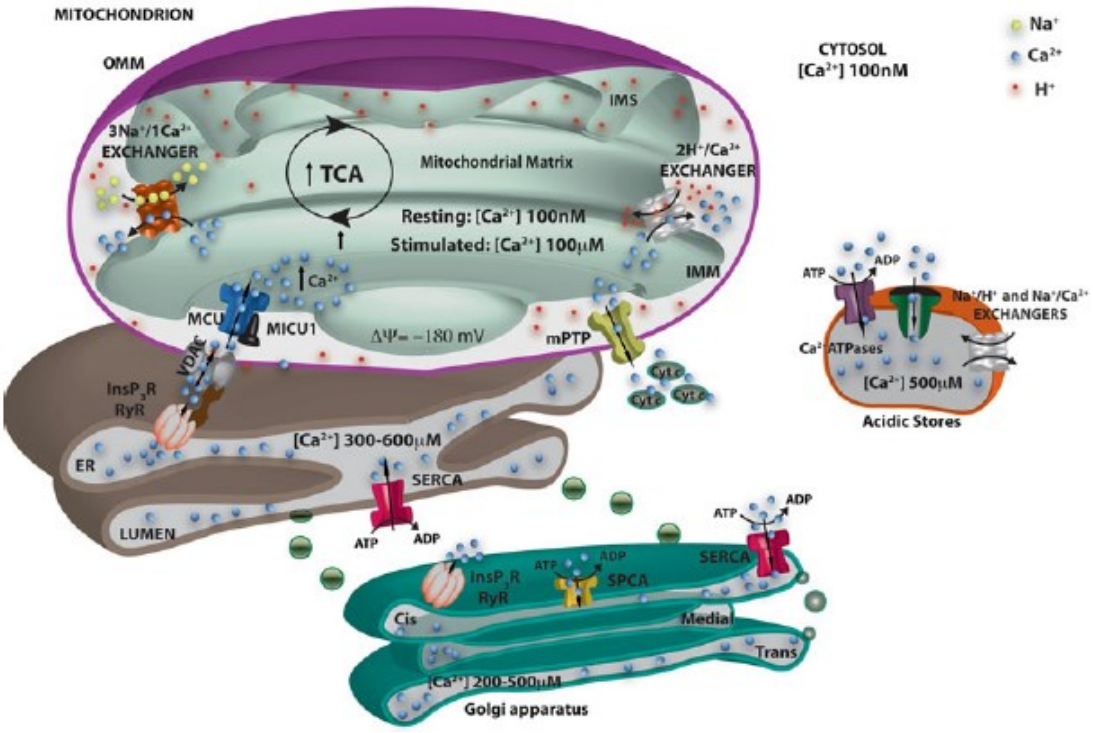

Figure 72: Schematic representation of Ca2+-handling organelles (Source: Brini et al., 2013) (originally in colour)

9.4 Mitochondria and programmed cell death

Another main role of mitochondria is the regulation of the programmed cell death mechanism, also called apoptosis.[196] Cell death mechanisms have central importance in development, homeostasis and tumor surveillance. Apoptosis is initiated by two principal pathways.

The extrinsic pathway is activated by the ligation of death receptors. The most characterized receptors are CD95 (APO-1/FAS), TNF receptor 1, TNF-related apoptosis-inducing ligand-receptor 1 (TRAILR1), and TRAILR2. For example, because FAS is able to bind FAS ligand, a transmembrane receptor, it can activate procaspase 8 into caspase 8. Once activated, these cysteine proteases activate downstream effector caspases such as caspase 3.[197]

Caspases are also called cysteine–aspartic proteases, because of their cysteine abilities to cleave a target protein only at the C-terminal of an aspartic acid amino acid. They are mainly distinguished into initiator caspases, able to activate the cascade, such as caspase 8 and 9, and effector caspases, such as 3, 6 and 7, responsible for the induction of apoptosis. Because of their important role in cell death, they are normally in an inactive form, called procaspase, which can be cleaved into the active form.

The intrinsic pathway, also named the mitochondria-mediated pathway, leads to the process of mitochondrial outer membrane permeabilization (MOMP) as a result of uncompensated cell stress signalling. The main cause seems to be a Mitochondrial Permeability Transition (MPT), leaded by the stimulation of the supramolecular channel called mitochondrial permeability transition pore (mPTP) or permeability transition pore complex (PTPC) (Figure 73).[193]

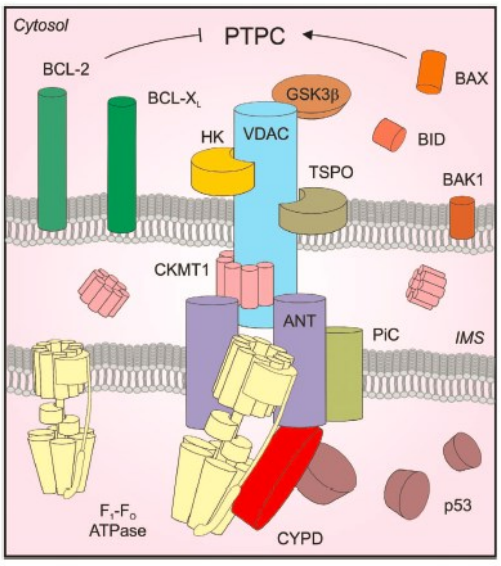

Figure 73: Possible configuration of PTPC (Source: Bonora et al., 2014) (originally in colour)

Actually, mPTP consists in the aggregation of different mitochondrial proteins through the IMM and the OMM such as cyclophilin D (mCypD), ANT (Adenine Nucleotide Translocator) protein,

voltage dependent anion channel (VDAC) and ATPase. The last one mentioned seems to form a dimer complex, in which the c-ring is active not only in the mPTP opening, but also in its aggregation. However, when it is open, mPTP leads to a nonspecific permeability transition of low molecular weight solutes (no more than 1.5 kDa).

The most important effect of this opening is the accumulation of Ca^{2+} into the matrix (Figure 74) and, hence, a decrease in the IMM transmembrane potential, $\Delta\psi$. The dissipation of the $\Delta\psi$, virtually abolish mitochondrial ATP synthesis and several other $\Delta\psi$-dependent mitochondrial functions. As stated before, if there is no proton motive force, ATPase start to be active in hydrolyzing ATP into ADP and Pi, hence, not producing functional energy for the cell.
However, mPTP also changes the mitochondrial osmotic force, hence, high rates of water pass freely through the IMM into the matrix, initiating mitochondrial swelling.

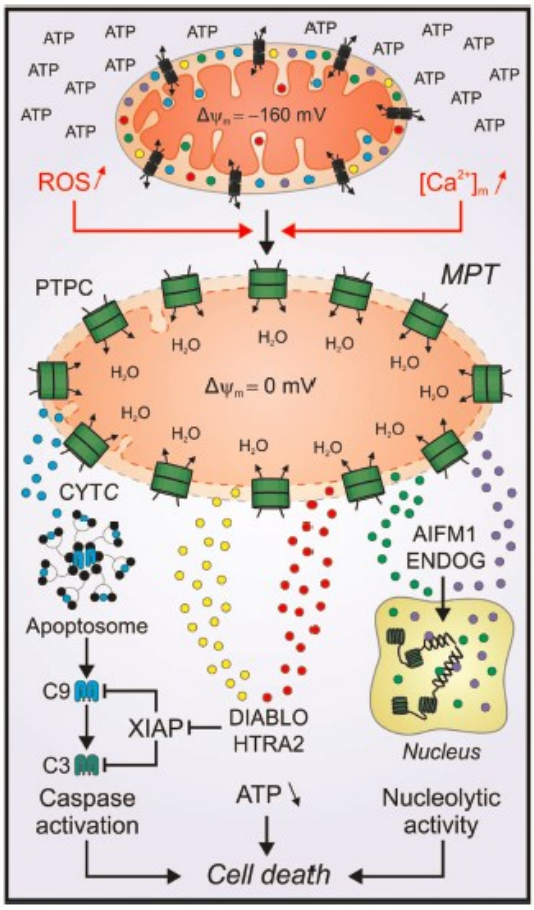

Figure 74: Lethal effect of MPT (Source: Bonora et al., 2014) (originally in colour)

Another important role in the induction of apoptosis and in the mPTP opening is played by ROS, which are generated as side product of ETC or during ischemia reperfusion injury.
ROS are able to induce lipid peroxidation and, hence, the rupture of OMM, leading the release of a number of apoptosis activators, that can initiate proapoptotic pathways out of mitochondria, such as cytochrome C, apoptosis inducing factor (AIF), Endo G and SMAC/DIABLO.

One of apoptosis activators released by OMM disrupt the cytochrome C, which is active in complex III of ETC. In physiological activity, cytochrome C leads to the transfer of one electron from ubiquinol to oxygen through complex III and IV and it is normally bind to cardiolipin, therefore, it cannot be extruded out of mitochondria. During ROS and Ca^{2+} induction, cardiolipin is oxidized and released cytochrome C out of OMM. Cytochrome C released bind itself to APAF-1, generating a multimolecular holoenzyme complex which is called apoptosome. Apoptosome is particularly important during apoptosis, because is able to activate procaspase 9 into caspase 9, thus inducing caspase cascade activity in an intrinsic way.

Other important factors are released by the OMM, such as AIF and Endo G. They are called even caspases-independent apoptosis effector, because of their role in induction of programmed cell death, being active in DNA degradation into nucleus and in chromatine condensation.
Finally, release of SMAC (second mitochondria-derived activator of caspases), which is also called DIABLO (direct IAP-binding protein with low PI) inhibit cytosolic inhibitor of apoptosis (IAP) proteins thus freeing caspases to activate apoptosis.[198]

10. Ischemia and Reperfusion Injury (IRI)

Ischemia is a state of limitation of the blood circulation, which causes an inadequate oxygen and glucose supply to tissues. Thus, a number of modifications are induced (Figure 75). As stated before, the hypoxic state impact on mitochondrial energy production, inducing the activation of the anaerobic glycolysis.

In aerobic conditions, during glycolysis glucose is converted into pyruvate. Afterwards, pyruvate is transformed into acetyl-CoA, hence, being able to take part to the citric cycle and ETC into mitochondria. The total production of this process is up to 30 molecules of ATP for every glucose molecule.

In anaerobic conditions, the absence of oxygen inhibits the regeneration of electron transport systems and pyruvate is reduced to lactate, regenerating NAD^+ from NADH. This leads to the production of only 2 ATP per glucose molecule.

During ischemia, ATP synthesis is inhibited, and existing ATP is cleaved into ADP and phosphate. Since oxidative phosphorylation is interrupted, proton ions accumulate into mitochondrial matrix and pH quickly decreases. In order to raise the pH, Na^+-H^+ exchanger is activated and there is an influx of Na^+ into mitochondrial matrix. However, since Na^+-K^+ ATPase is also inactive during ischemia, the accumulation of Na^+ induces Na^+-Ca^{2+} antiporter with reverse activity. The final result is a Ca^{2+} accumulation into mitochondria and its inhibited reuptake by ER.[199]

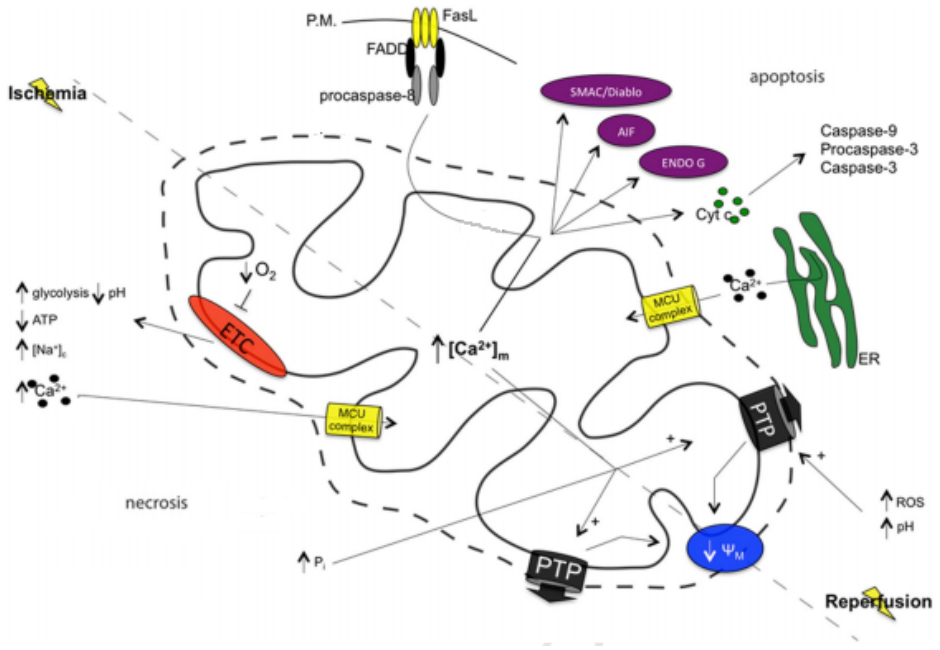

Figure 75: Mitochondrial involvement in cell death during IRI (Source: Morciano et al., 2015) (originally in colour)

All these conditions lead to a predominance of necrosis during ischemia, caused by alteration in electrolyte levels, which results in the depletion of high-energy stores and disruption of cellular membrane. Moreover, Ca^{2+}, adenine nucleotide and phosphate are known to be inductor of mPTP complex opening.

Reperfusion is critical to salvage cells, however, the process also triggers necrosis (i.e., IR injury). The cellular events that underlie this necrosis are thought to be triggered by the abrupt changes in the pH that immediately follow reperfusion. This occurs because as soon as capillary flow resumes, the catabolites that have accumulated are cleared and pH rises abruptly. However, as state before, when ETC is still inactive, yet exposed to oxygen, ROS are generated. As ROS are again inductor of mPTP opening, they contribute to the decrease of IMM transmembrane potential, hence, the induction of apoptosis via intrinsic pathway. Thus, during reperfusion, apoptosis is mainly active.

Ischemia-Reperfusion injury (IRI) is mainly connected with microvascular dysfunction in most organs and it is a potentially serious problem during a variety of standard medical and surgical procedures, such as thrombolytic therapy, organ transplantation, coronary angioplasty, and cardiopulmonary bypass.

For instance, one of the most important kind of ischemia is the ischemic heart disease (IHD). Primary percutaneous coronary intervention (PCI) is normally used if this is the case. As Morciano et al. well summarizes,[200] a number of consequences outcome after this mechanical reperfusion, resulting in IRI-related myocardial infarction (segment elevation myocardial infarction or STEMI) and left ventricular remodeling, which are also used as predictor of prognosis. One of them is cardiomyocytes and endothelial cells necrosis secondary to myocardial reperfusion, which is due to both cell necrosis and apoptosis induced by IRI. In this dramatic symptom, the mPTP opening seems to be involved with a key role. Thus, mPTP opening could be a great potential target for cardio-protection.

10.1 Known molecules active as IRI inhibitors

Nowadays, one of the most important approach for cardio-protection is the pre-conditioning, based on the theory that brief episodes of ischemia/reperfusion applied prior to a longer coronary artery occlusion reduce myocardial infarct size. The effects of ischemic preconditioning (IP) are pronounced; preconditioned hearts are less susceptible to the reperfusion injury, the extent of necrosis is lessened by approximately 75 %, and the hemodynamic performances recover more easily. This beneficial effects of IP were attributed to changes in energy metabolism, since recent studies highlighted that the size of the myocardial injury correlates with the ATP content of the heart and the preconditioned hearts display slower ATP decline during ischemia.[201]

An alternative to pre-conditioning is the inhibition of mPTP opening, which could be used for cardio-protection. Up to now, few agents are known to be only indirectly active as mPTP inhibitors: e.g. Bendavia, which interact with cardiolipin and is able to reduce ROS production and to maintain ETC activity during reperfusion, avoiding disproportion with gradient equilibrium. However, very few agents are known as directly inhibitors of mPTP opening. One of them is Cyclosporin A (CsA), known since 1990 to bind mitochondrial cyclophilin D (mCypD), one of the most important member of mPTP, which is, hence, inhibited.

Recently, cypD has been shown to interact with and regulate the F1F0 ATP-synthase, the main molecular motor of chemiosmotic ATP production in the mitochondrion.[202] Recently, Bonora et al. (2013), demonstrated that the propensity of mPT highly correlates with the subunit c expression levels of the F_O unit.[203]

Oligomycin, which has been long recognized as a potent inhibitor of the mitochondrial ATP synthase,[204] is a macrolide with a 26 membered lactone ring, isolated from *Streptomyces diastatochromogenes.* It is one of the most important F_O inhibitors, binding itself on the interface of subunit a and c-ring and blocking the rotary proton translocation in F_O. If the enzyme is well-coupled, the activity of F_1 is also blocked. Because of the latter mechanism, a subunit of mitochondrial F_1-portion that connects F_1 with F_O was named oligomycin-sensitivity conferring protein (OSCP). This subunit is essential for good coupling between F_1 and F_O and makes the ATPase activity of F_1 sensitive to F_O inhibitor oligomycin, hence the name.

Oligomycin binds to the surface of the c10 ring making contact with two neighboring molecules at a position that explains the inhibitory effect on ATP synthesis. The carboxyl side chain of Glu 59, which is essential for proton translocation, forms an H-bond with oligomycin via a bridging water molecule but is otherwise shielded from the aqueous environment. The remaining contacts between oligomycin and subunit c are primarily hydro- phobic (Figure 77).[205]

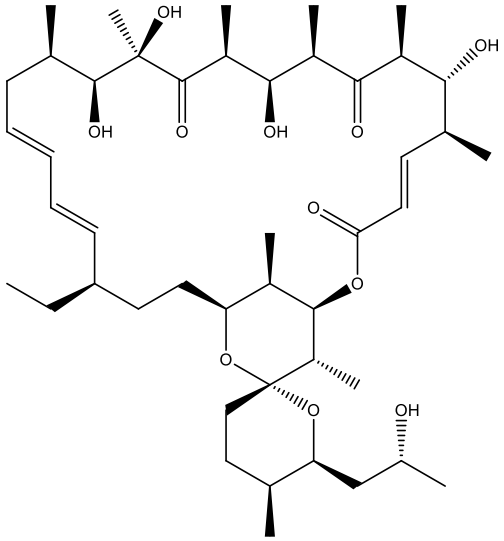

Figure 76: Oligomycin A structure

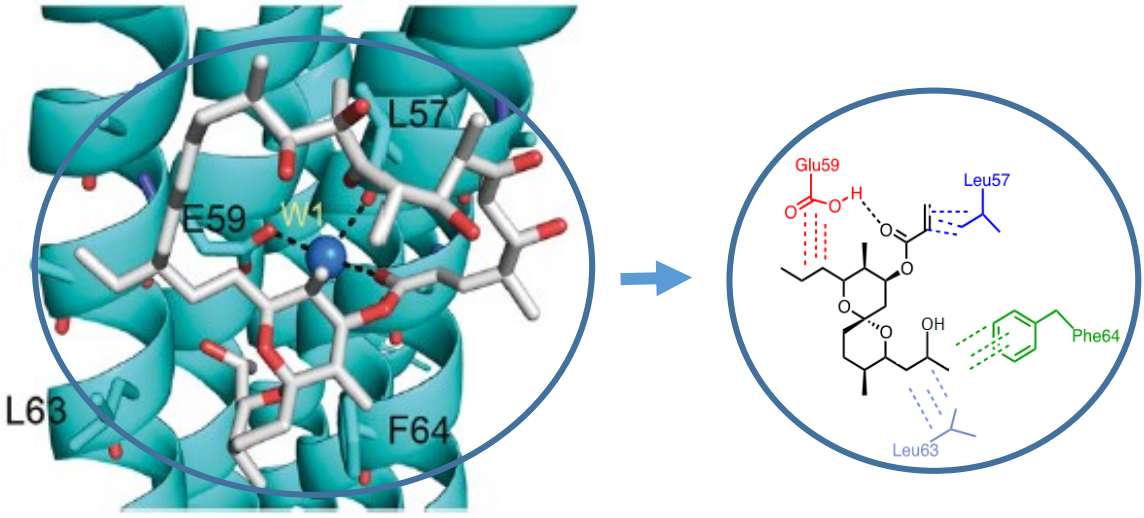

Figure 77: Oligomycin A binding with ATP synthase (adapted from Symersky et al., 2012) (originally in colour)

Carbodiimides are compounds containing a N=C=O functional group, which can inhibit ATP synthase by modifying carboxyl residues residing within F_1, F_0, or both.[206]

Dicyclohexylcarbodiimmide (DCC) is a small organic molecule (Figure 78) that can covalently modify protonated carboxyl groups, hence, inducing irreversible inhibition (Figure 79). When added to ATP synthase at pH above 8, DCC almost exclusively reacts with the carboxyl group of the amino acid residue of subunit c that has elevated pK and can therefore be protonated at such a high pH. Modification of the carboxyl group in a single c-subunit is enough to render the whole c-ring oligomer inactive. In fact, at lower pH (<7) DCC modifies several carboxyl groups in F_1 and inactivates it. However, inhibition of F_O is highly specific, well-defined, and requires much lower DCC concentration.

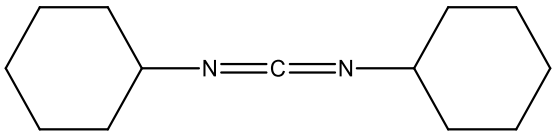

Figure 78: Dicyclohexylcarbodiimmide (DCC)

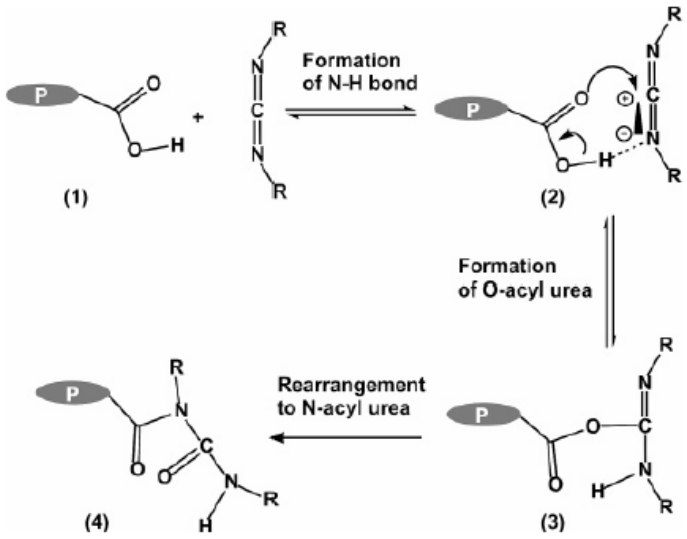

Figure 79: Proposed mechanism for the modification of the c residue with DCCD (Source: von Ballmoos, 2007)

11. Biological Evaluation

To measure mPTP opening inhibition the Co^{2+}-calcein assay has been performed, following the reported protocol, by the research group of professor P. Pinton at the Dept. of Morphology, Surgery and Experimental Medicine, Section of Pathology, Oncology and Experimental Biology of the University of Ferrara.[209] The analysis protocol is based on the decrease in calcein fluorescence, which is directly related to the mPTP opening.

As stated before, mPTP opening occurs both in physiological and in pathological conditions. In physiological conditions mPTP exists in a low-conductance state, in which permeability is limited to molecules under 300Da.

However, a high-conductance state can be initiated by a number of different stimuli (See Chapters 9.3 and 9.4). On these terms, non-specific movement through the pore and IMM is allowed for molecules under 1.5kDa, which leads to the final mitochondrial swelling.

Calcein AM (Figure 80), a non-fluorescent acetomethoxy derivate of calcein, is used in this protocol. Calcein AM can freely diffuse into cellular compartments, where it is hydrolyzed by esterases. After hydrolysis calcein, in its carboxylate form, is no longer able to diffuse, remaining trapped. The ion has green fluorescence properties, hence, it is visible under fluorescence microscopy.

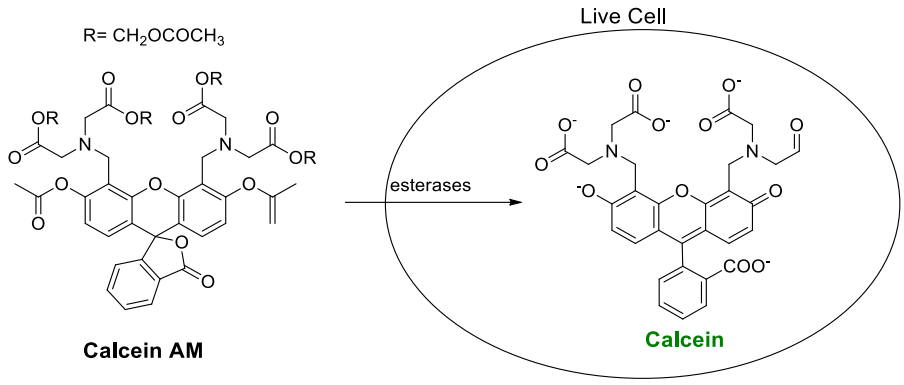

Figure 80: Calcein AM and hydrolyzed calcein

As this protocol is applied to tumoral HeLa intact cells, there is the need to selectively visualize mitochondrial calcein fluorescence. Positive ions (e.g. Ca^{2+}, Fe^{3+}) bind to calcein quenching its fluorescence and can be exploited for detecting the opening of the mitochondrial permeability transition pore and for measuring cell volume changes.[210]

Co^{2+} can be used as well, since it is able to abolish calcein emission and it is not connected with mPTP opening pathway. When mPTP is closed, Co^{2+} is not able to influx into mitochondria. Else, mPTP opening induce Co^{2+} entry into mitochondria, hence, promoting a decrease in calcein fluorescence.

For this reason, the administration of a mPTP opening stimulus (i.e. Ionomycin-mediated Ca^{2+} influx) is used and the system monitored as vehicle and control. (Figure 81)

However, when a mPTP opening inhibitor have been pre-administrated to the system, as cyclosporine A (CsA), this results in a neat inhibition of calcein decrease.

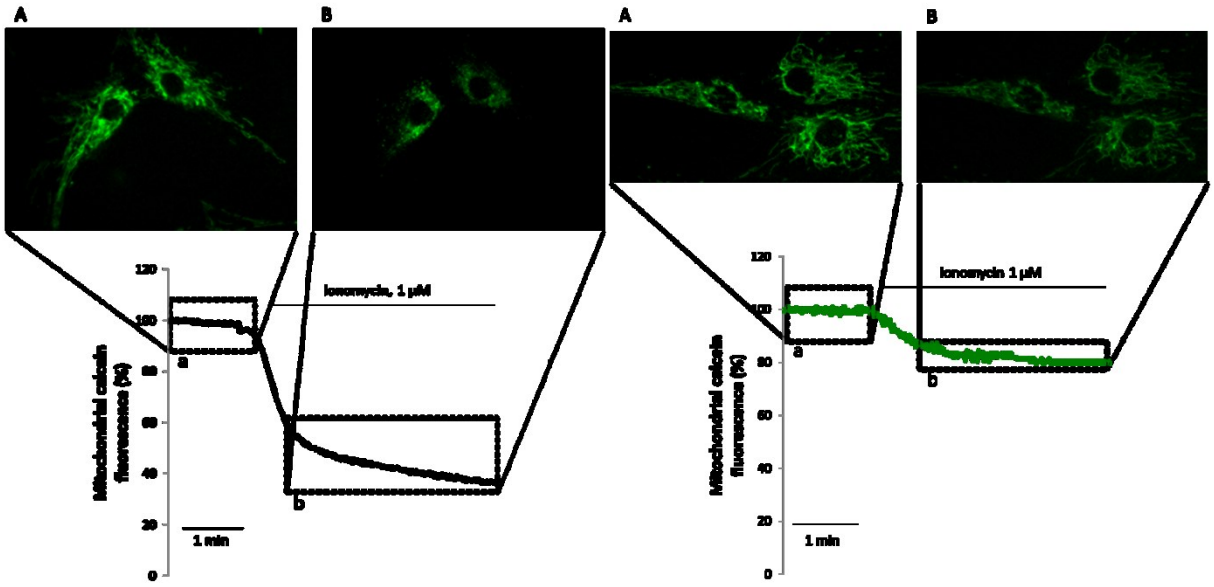

Figure 81: Kinetics of HeLa cells stained with Co^{2+}-calcein technique without (black line) or with (green line) pre-treatment with administration of CsA (Source Bonora et al., 2016) (originally in colour)

12. Research Project: Aim, problems and objectives

Considering the lack in treatments for ischemic-reperfusion injury (IRI), there is a urgent need for new compounds able to avoid reperfusion damages. According to present evidences, mitochondria permeability transition pore (mPTP) is the main target for the prevention of IRI. Since Ca^{2+} is the primary inductor of mPTP opening, it is also important to inhibit Ca^{2+} accumulation. In order to avoid Ca^{2+} accumulation, is crucial to inhibit ATP synthase, for example, by blocking the rotary proton translocation in F_O. For these previous reasons, this project aims to develop molecules able to either inhibit mPTP opening or ATP synthase.

Two different known ATP synthase inhibitors have been chosen as model for two potential classes of mPTP and ATP synthase inhibitors, dicyclohexylcarbodiimide (DCC) and oligomycin A.

DCC has been considered as a starting point for the design of new mPTP inhibitors, because of its suppose capability of binding glutamic acid residue (Glu 59) of c-ring of ATP synthase.

However, DCC in aqueous solution is partially hydrated to the corresponding dicyclohexylurea (DCU) (Figure 82), hence DCU has been tested as mPTP inhibitor and resulted in a greater inhibition effect (IC_{50} = 1µM) compared to DCC (IC_{50} = 15µM). However, to date, the lack of molecular modeling investigation does not allow us to establish the exact mechanism of such inhibition.

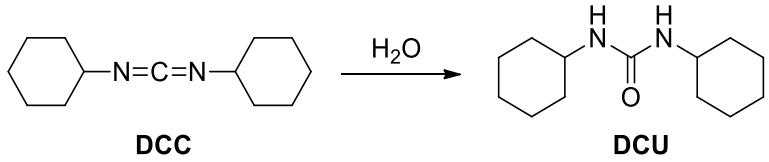

Figure 82: DCC reacts with water to form DCU

Considering these previous results, DCU has been chosen as a promising hit compound suitable for structure-activity optimization. As there are no previous evidences for c-ring inhibition by urea derivatives, compounds **1 - 18** (Table 2) have been synthesized in order to obtain useful information about the relevance of different substituents for interactions within mitochondria. Consequently, punctual modifications have been introduced either to the urea moiety or to the N/N' substitutions (Figure 83).

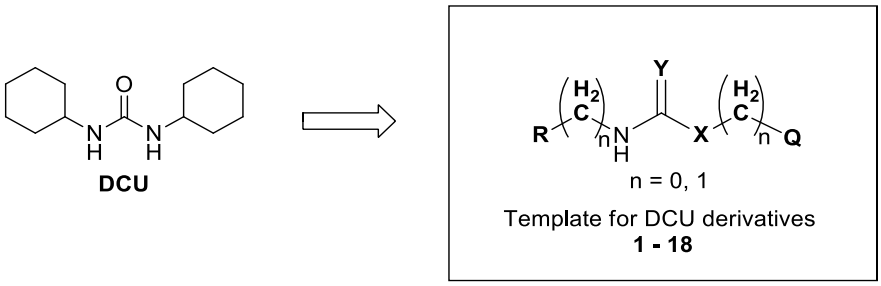

Figure 83: Template for DCU derivatives

Therefore, five classes of DCU derivatives have been synthesized. Firstly, the intact urea moiety has been maintained and a number of symmetric (compounds **1**-**7**) or asymmetric (**8**-**13**) N/N' modifications were introduced by combination of different alkyl/cycloalkyl/(substituted)aryl/benzyl groups (Figure 84).

Secondly, the urea function has been substituted with a thiourea group so to evaluate the effect of the removal of a potential hydrogen bond acceptor. Even in this case, symmetric (**14**, **15**) and asymmetric (**16**) compounds have been prepared (Figure 85).

Lastly, two carbamates derivatives were produced (**17**-**18**), in order to understand how the activity is influenced by a hydrogen bond acceptor in the place for a donor one (Figure 86).

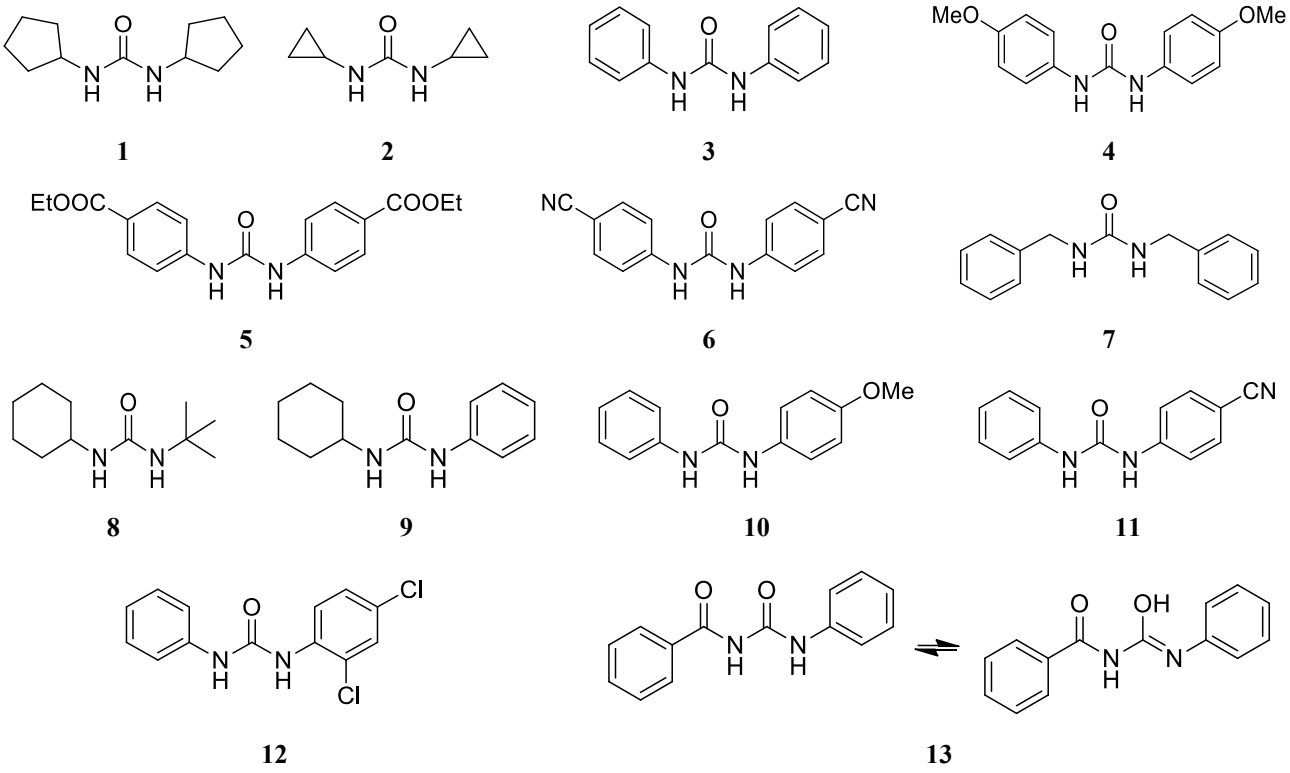

Figure 84: Symmetric and asymmetric ureas synthesized

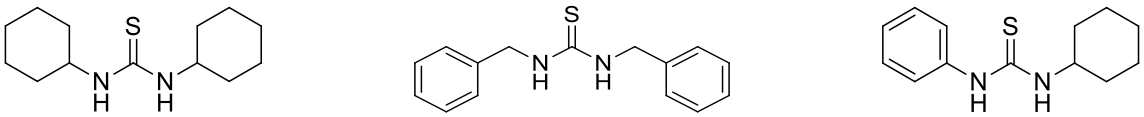

14 **15** **16**

Figure 85: Symmetric and asymmetric thioureas synthesized

17 **18**

Figure 86: Carbamates synthesized

The second mPTP opening inhibitor chosen as reference compound for this project is oligomycin A. As stated before, oligomycin A is known to create a number of Van der Wall's interactions with the c subunits of ATP synthase, thus blocking its activity. Even if oligomycin A derivatives have already been synthesized,[207,208] spiro ring steric supposed recognition could be an interesting starting point for the construction of new compounds libraries. Subsequently, the 1,7-dioxaspiro[5.5]undecane portion of Oligomycin A. was taken into consideration for the design of easy-accessible and low cost molecules (Figure 87).

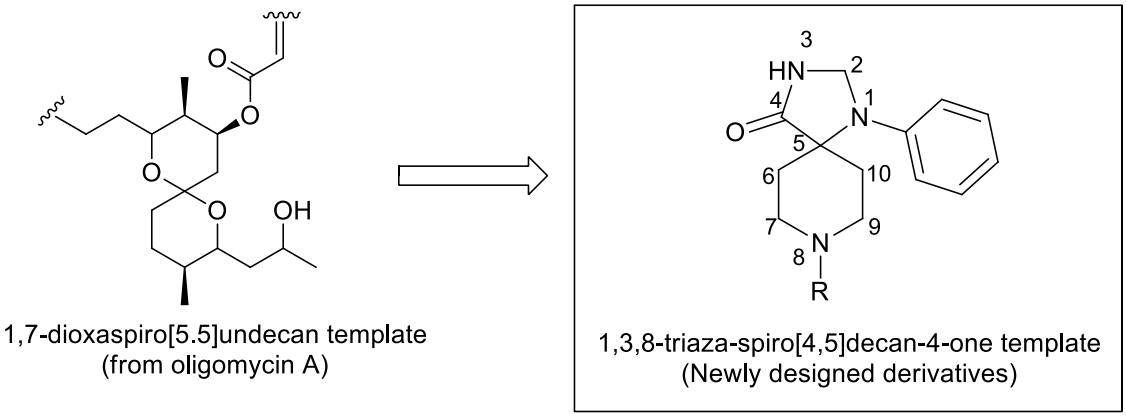

Figure 87: 1-phenyl-1, 3, 8-triaza-spiro[4,5]decan-4-one template

Notably, the carbonyl group of the lactam ring could maintain the ability to create a hydrogen bond, as it happens in oligomycin A, which creates the water bridge with Glu 59 and Leu 57.

Moreover, the aromatic ring at *N*-1 position will mimic the double bond of unsaturated ester present in oligomycin A.

The structure of this scaffold give the opportunity for easy and multiple functionalization at the 1-, 3-, and 8-positions. In this study a versatile synthetic approach was developed to realise a first series of compounds variably modified at the *N*-8 position of the 1-phenyl-1, 3, 8-triaza-spiro[4,5]decan-4-one core (compounds **19**-**24**) (Figure 88).

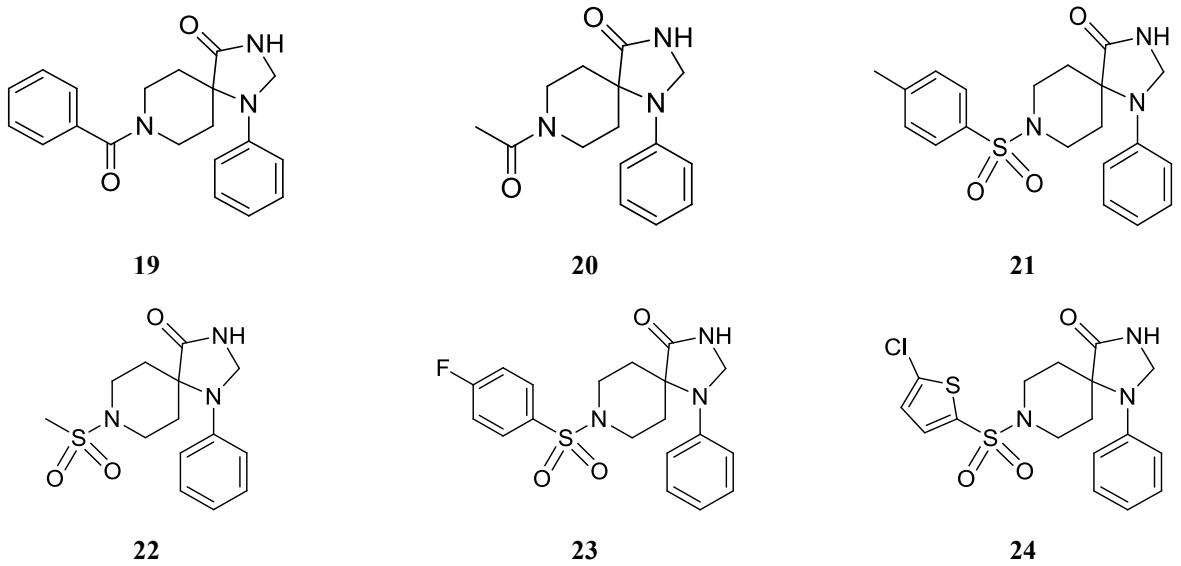

Figure 88: Derivatives of 1-phenyl-1, 3, 8 – triaza-spiro[4,5]decan-4-one with substitution in N-8

Finally, both urea and thiourea function was incorporated into 1-phenyl-1, 3, 8-triaza-spiro[4,5]decan-4-one structure to evaluate possible effects resulting from the combination of the two different moieties (compounds **25-27**) (Figure 89).

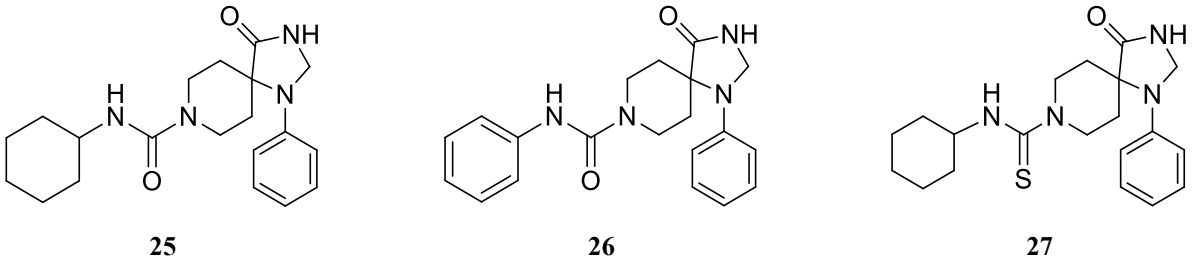

Figure 89: Derivatives of 1-phenyl-1, 3, 8 – triaza-spiro[4,5]decan-4-one with urea and thiourea moiety

13. Materials and equipment

13.1 Materials & reagents

All the chemicals were brought from Sigma Aldrich and used as received. All purity percentages are given as a weight percentage.
Deuterated chloroform (99.8% atom D) and deuterated DMSO (≥99.9%) were used as such for NMR analysis. Both were purchased from Sigma Aldrich.

13.2 Equipment

NMR

1H-NMR and 13C-NMR were registered with Varian spectrometers at 300 MHz and 400 MHz at room temperature. Chemical shifts (δ) are reported with respect to trimethylsilane in the following manner: chemical shift (multiplicity; coupling constants; proton integration).
Signal multiplicity are shortened in the following manner: s for singlet; d for doublet; t for triplet; q for quartet; br for broad signal; m for multiplet; dd for double doublet. The program used to elaborate the spectra was MestReNova 6.0.2.

Mass-Spectrometer

Mass spectral analyses were performed by ESI MICROMASS ZMD 2000 electrospray mass spectrometer, after dissolution of compounds in a solution composed by 40:60:0.1 of H_2O:CH_3CN:TFA.

High-performance Liquid Chromatography

For analytical controls Beckmann System Gold 168 HPLC have been used with LC column Kinetex 5 µm EVO C18 100Å (250 X 4.6mm) and a variable wavelength UV detector fixed to 220nm. Analysis were conducted using two solution A and B containing, respectively, 100:0.1 H_2O:TFA and 40:60:0.1 of H_2O:CH_3CN:TFA with gradient eluition of 0->50 of solution B in 30 minutes (except for compound 33). For purification Waters Delta Prep 3000 HPLC have been used with column Jupiter 10µm C18 AXIA (100 x 30.00 mm).

14. Experimental Section

14.1 Symmetric ureas

Symmetric ureas **1–7** have been produced by reaction between carbonyldiimidazole (CDI) and two equivalents of aromatic or aliphatic primary amines. The basic reaction mechanism (Figure 90) involves the attack by the lone pair of the primary amine to the carbonyl group of CDI. The tetrahedral intermediate rearranges to the mono-substituted product, with the loss of one imidazole. The mono-substituted intermediate may rearrange producing an isocyanate, which can react with another amine molecule, giving the symmetric urea.

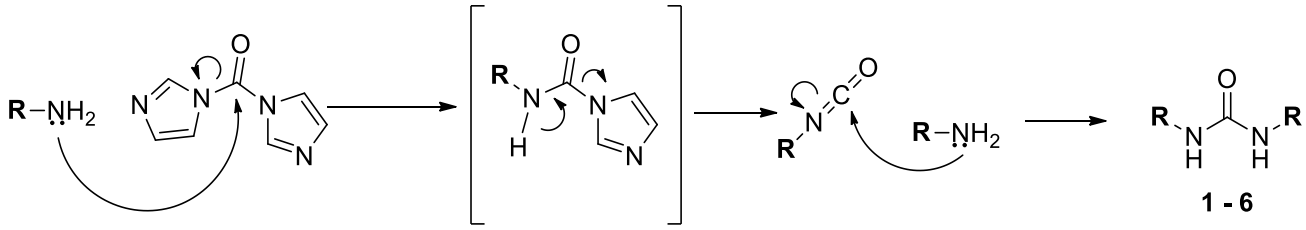

Figure 90: Proposed reaction mechanism for symmetric ureas synthesis

The standard procedure was as follow: to a solution of primary amine (7.54 mmol) in CH_2Cl_2 or THF (10 mL) was added carbodiimidazole (CDI) (0.6 g, 3.77 mmol). The solution was magnetically stirred at room temperature or under mild reflux for 3-18 hours. After the reaction was complete, as indicated by TLC, the precipitate was filtered and washed with Et_2O to afford the product as a white solid

Synthesis of 1,3-dicyclopentylurea (1)

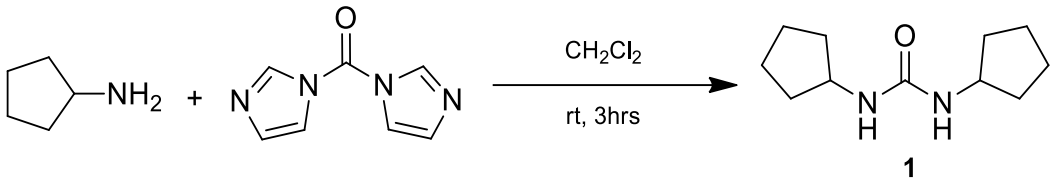

Yield: 80%

Melting point: 235-240 °C

MS (ESI): $[M+H]^+ = 197.10$

^{1}H NMR (400 MHz, DMSO) δ 5.60 (d, *J* = 7.3 Hz, 2H, 2NH), 3.88 – 3.73 (m, 2H, 2CH-NH), 1.72 (td, J = 11.9, 6.8 Hz, 4H, 4CH_2-CH), 1.63 – 1.39 (m, 8H, 4CH_2-CH; 4CH_2-CH_2-CH), 1.30 – 1.13 (m, 4H, 4CH_2-CH_2-CH).

^{13}C NMR (101 MHz, DMSO) δ 157.30 (CO), 50.82 (2CH), 33.01 (4CH_2-CH), 23.12 (4CH_2-CH_2-CH).

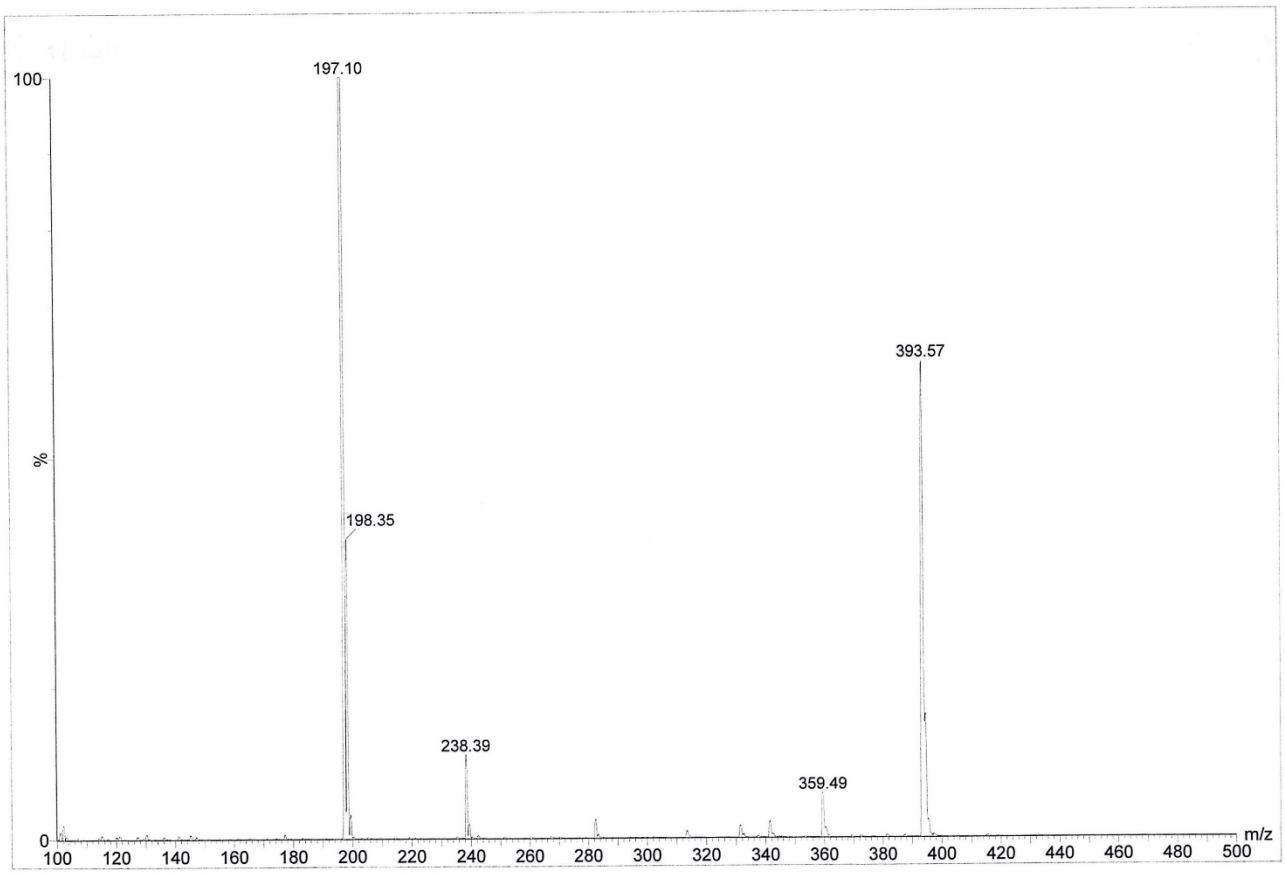

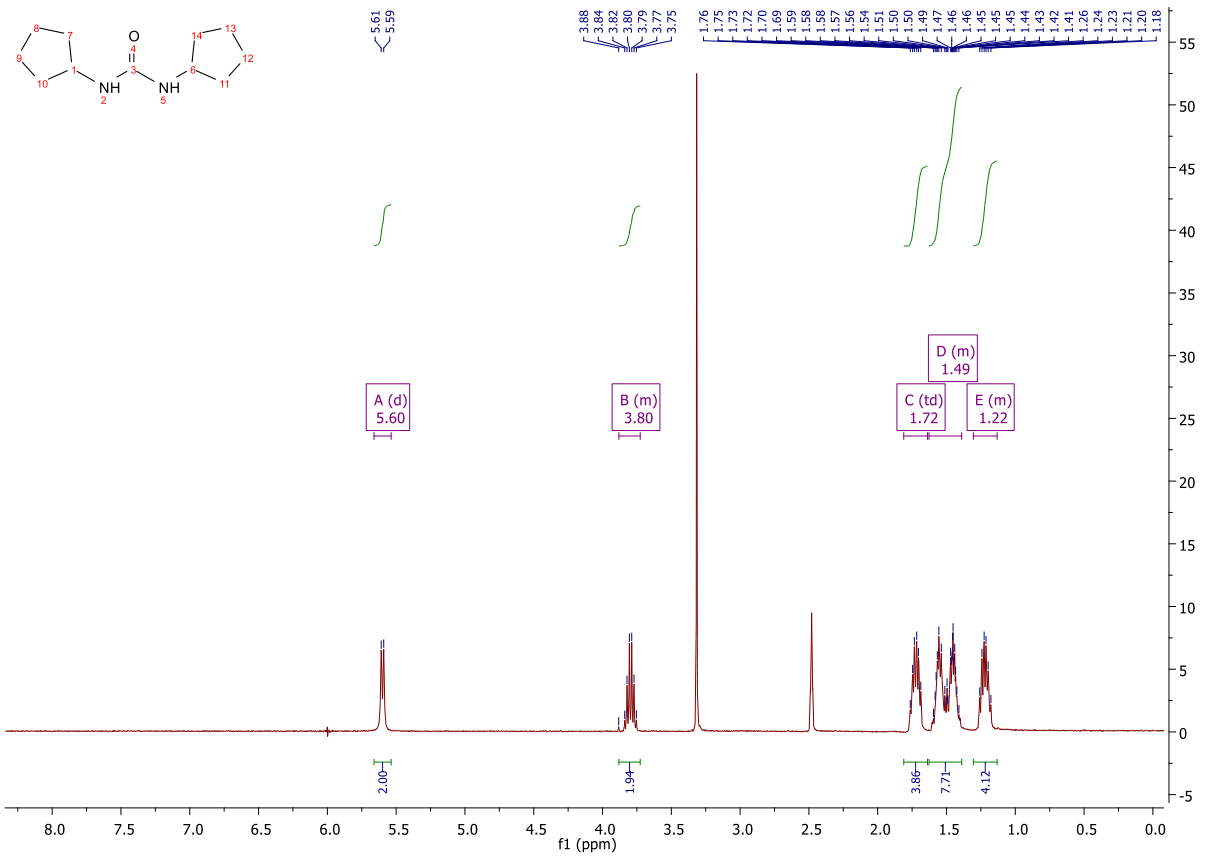
A (d)
5.60
B (m)
3.80
C (td)
1.72
D (m)
1.49
E (m)
1.22
f1 (ppm)

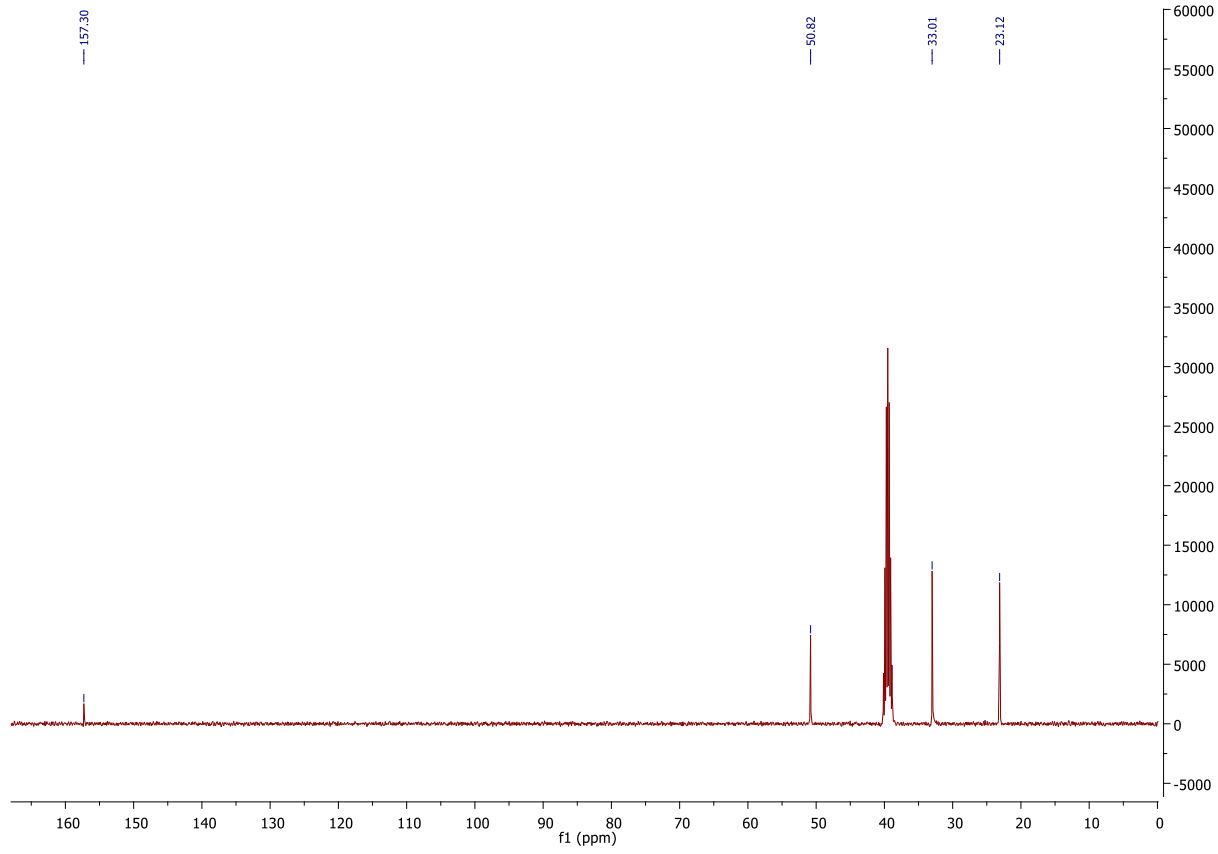
157.30
50.82
33.01
23.12
f1 (ppm)

Synthesis of 1,3-dicyclopropylurea (2)

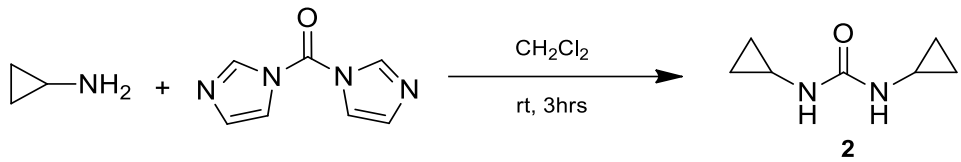

2

Yield: 63%

Melting point: 168-173°C

MS (ESI): $[M+H]^+ = 141.29$

^{1}H NMR (400 MHz, DMSO) δ 6.01 (s, 2H, 2NH), 2.42 – 2.25 (m, 2H, 2CH-NH), 0.58 – 0.44 (m, 4H, 4CH_2-CH), 0.38 – 0.22 (m, 4H, 4CH_2-CH).

^{13}C NMR (101 MHz, DMSO) δ 159.41 (CO), 22.46 (2CH), 6.46 (2CH_2-CH).

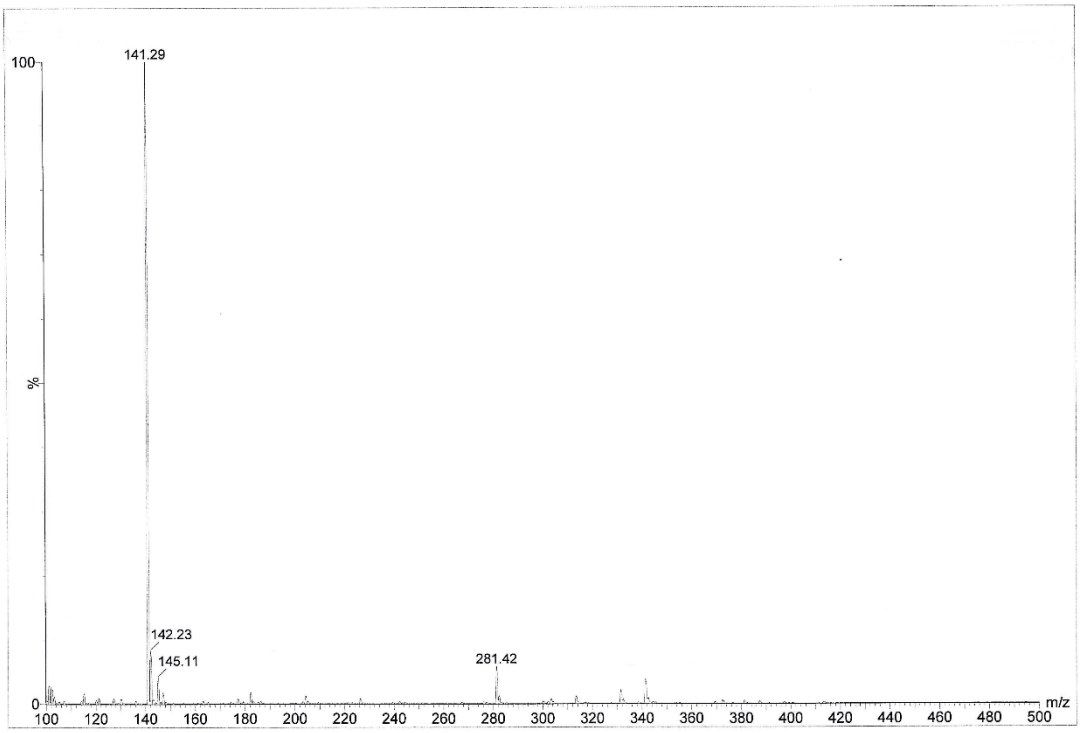

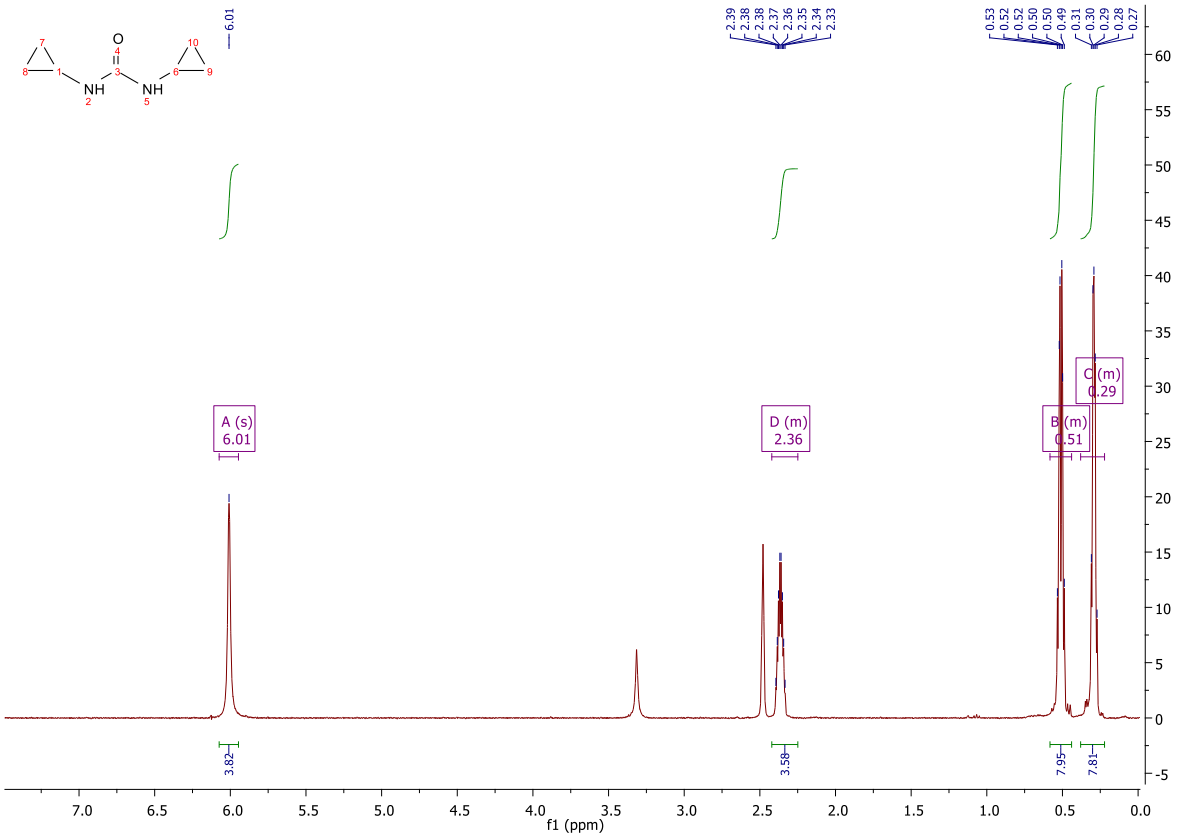
A (s)
6.01
D (m)
2.36
B (m)
0.51
C (m)
0.29
3.82
3.58
7.95
7.81
f1 (ppm)

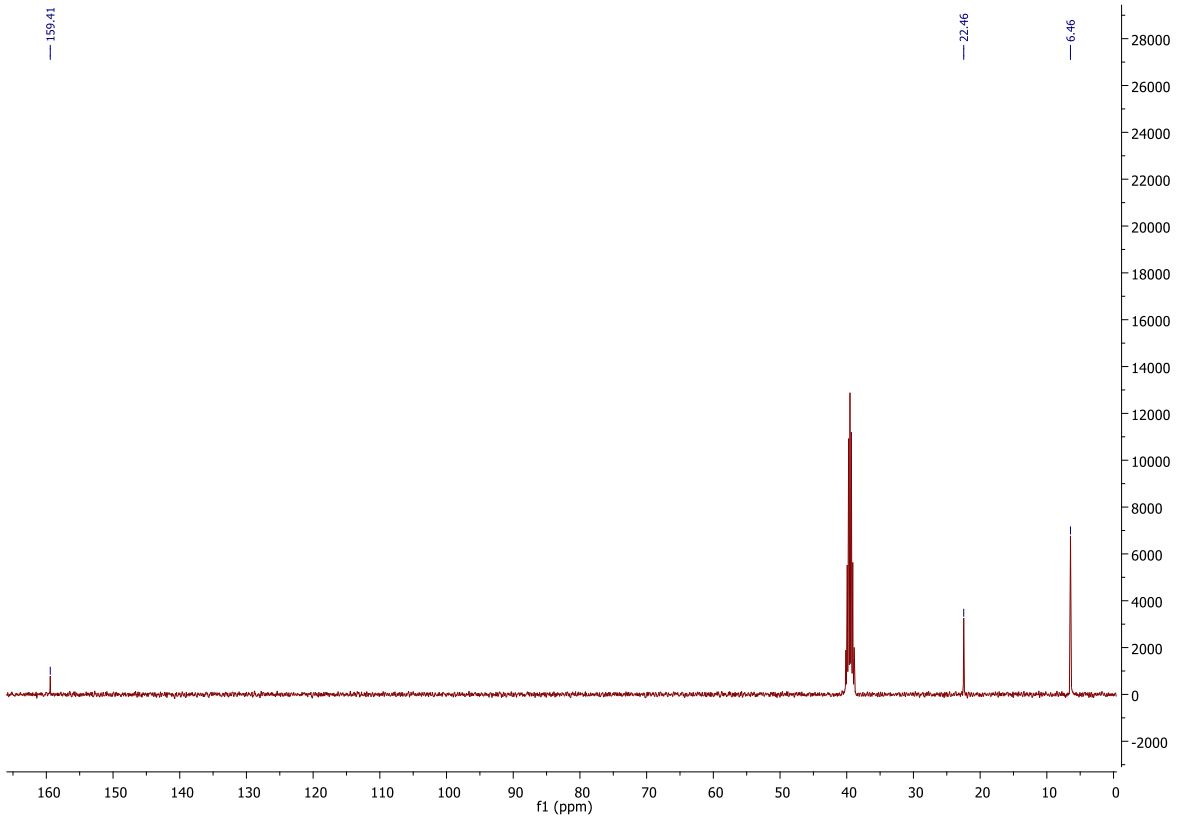
159.41
22.46
6.46
f1 (ppm)

Synthesis of 1,3-diphenylurea (3)

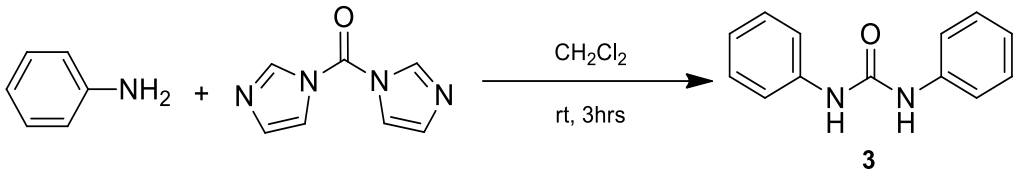

Yield: 89%

Melting point: 257-261°C

MS (ESI): $[M+H]^+ = 213.34$

^{1}H NMR (400 MHz, DMSO) δ 8.64 (s, 2H, 2N<u>H</u>), 7.43 (dd, J = 8.6, 1.0 Hz, 4H, 4Cq$_{Ar}$-C<u>H$_{Ar}$</u>), 7.26 (m, 4H, 4Cq-CH$_{Ar}$-C<u>H$_{Ar}$</u>), 7.01 – 6.88 (m, 2H, CH$_{Ar}$- CH$_{Ar}$-C<u>H$_{Ar}$</u>).

^{13}C NMR (101 MHz, DMSO) δ 152.50 (<u>C</u>O), 139.69 (<u>2Cq$_{Ar}$</u>), 128.78 (<u>4C</u>H$_{Ar}$-CH$_{Ar}$-Cq$_{Ar}$), 121.79 (<u>2C</u>H$_{Ar}$-CH$_{Ar}$-CH$_{Ar}$-Cq$_{Ar}$), 118.14 (<u>4C</u>H$_{Ar}$-CqAr).

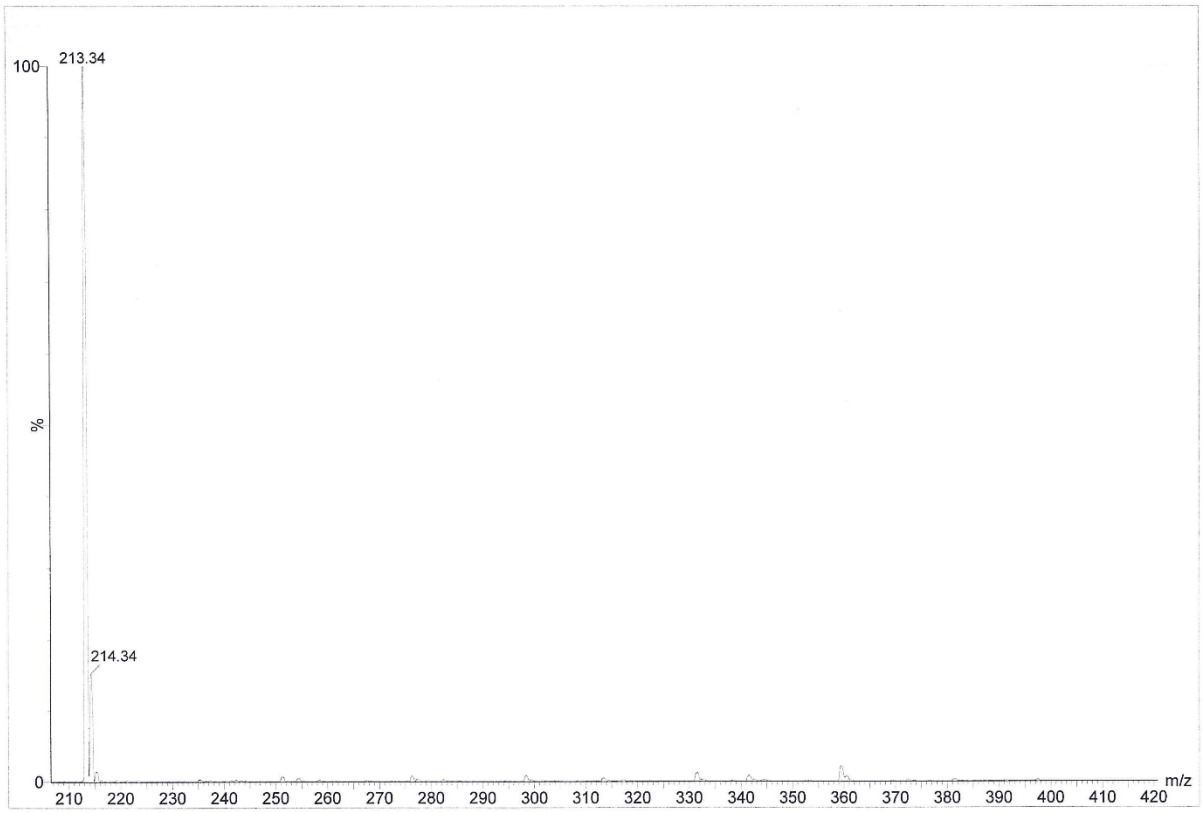

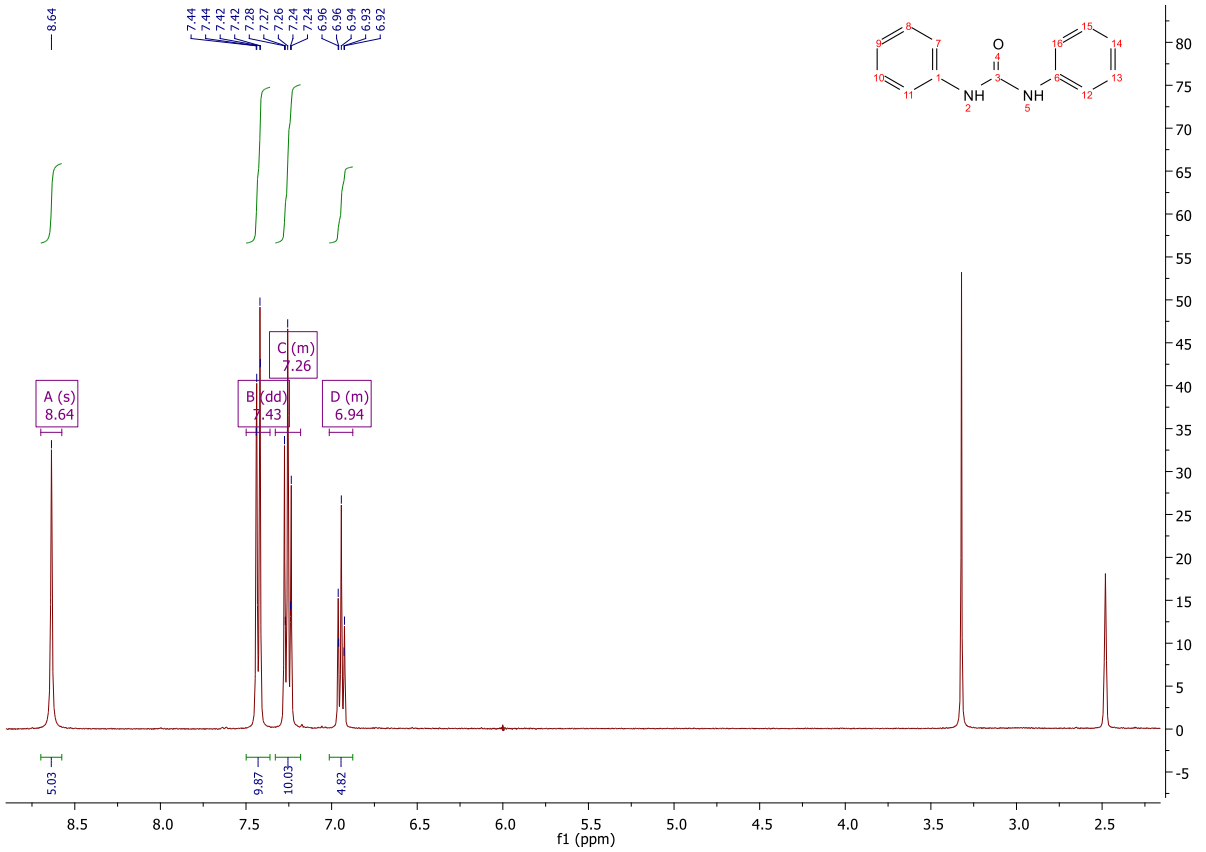
8.64
7.44
7.44
7.42
7.42
7.28
7.27
7.26
7.24
7.24
6.96
6.96
6.94
6.93
6.92
A (s)
8.64
B (dd)
7.43
C (m)
7.26
D (m)
6.94
5.03
9.87
10.03
4.82
f1 (ppm)

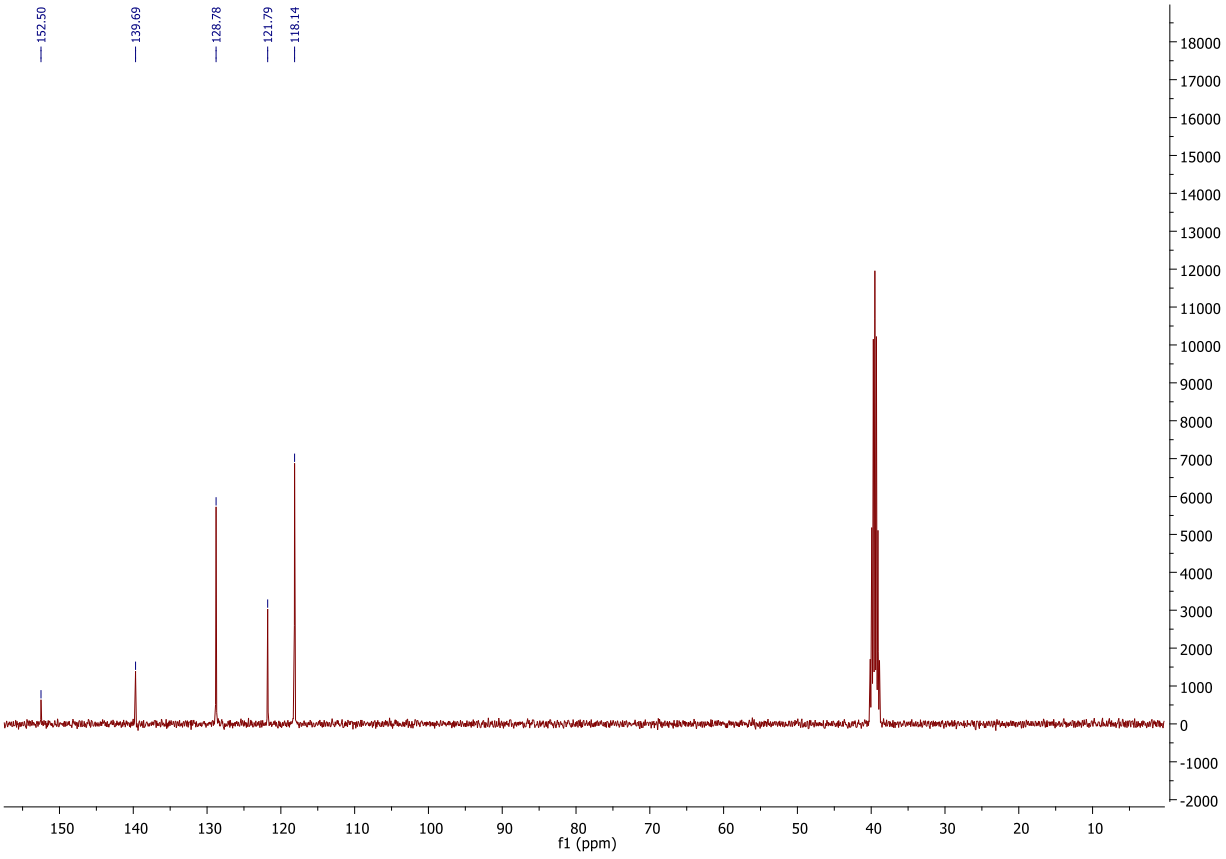
152.50
139.69
128.78
121.79
118.14
f1 (ppm)

Synthesis of 1,3-bis(4-methoxyphenyl)urea (4)

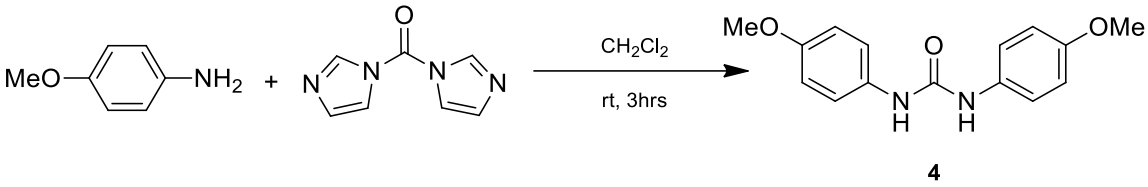

4

Yield: 85%

Melting point: 250-253°C

MS (ESI): $[M+H]^+ = 273.34$

^{1}H NMR (400 MHz, DMSO) δ 8.36 (s, 2H, 2NH), 7.38 – 7.24 (m, 4H, 4CH_{Ar}-Cq_{Ar}-NH), 6.83 (d, *J* = 9.0 Hz, 4H, 4CH_{Ar}-CH_{Ar}-Cq_{Ar}), 3.69 (s, 6H, 2CH_3-O).

^{13}C NMR (101 MHz, DMSO) δ 154.29 (2Cq_{Ar}-OCH_3), 152.94 (CO), 132.94 (2Cq_{Ar}-NH), 119.86 (2CH_{Ar}-Cq_{Ar}-$NH_)$, 113.94 (2CH_{Ar}-Cq_{Ar}-$OCH_{3)}$, 55.15 (2CH_3-O).

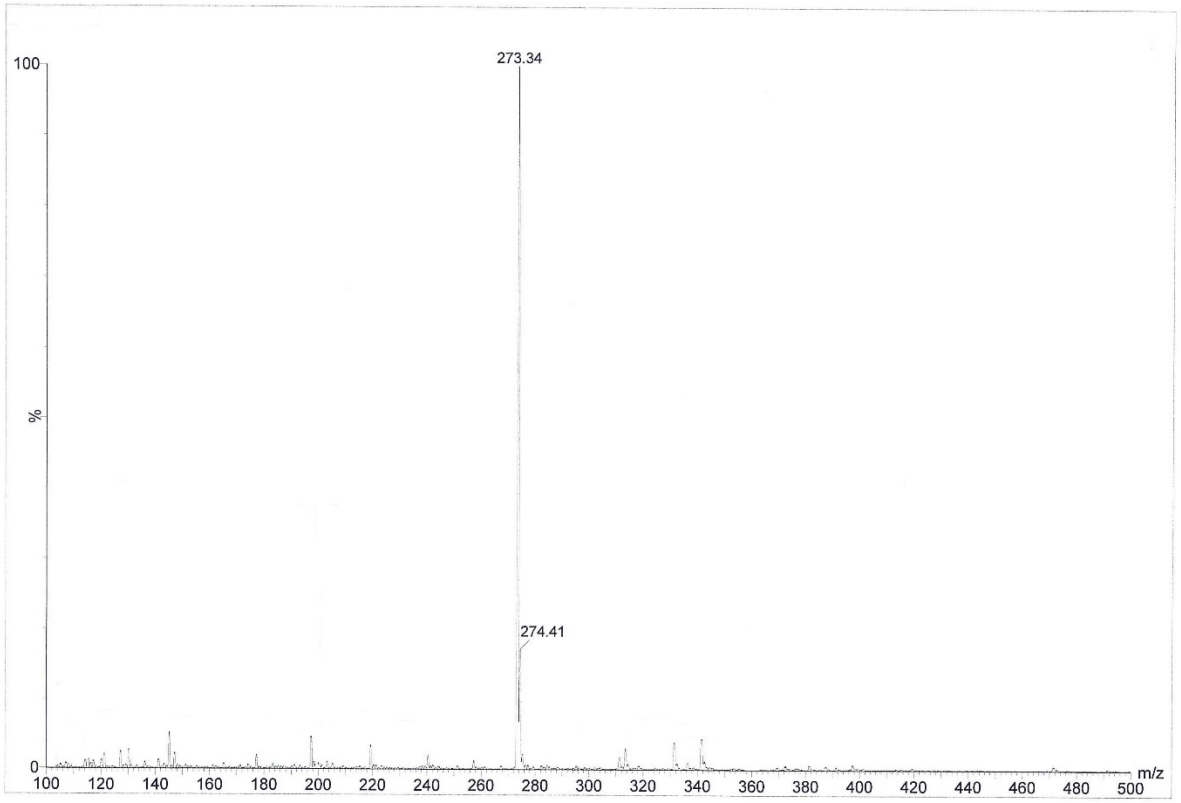

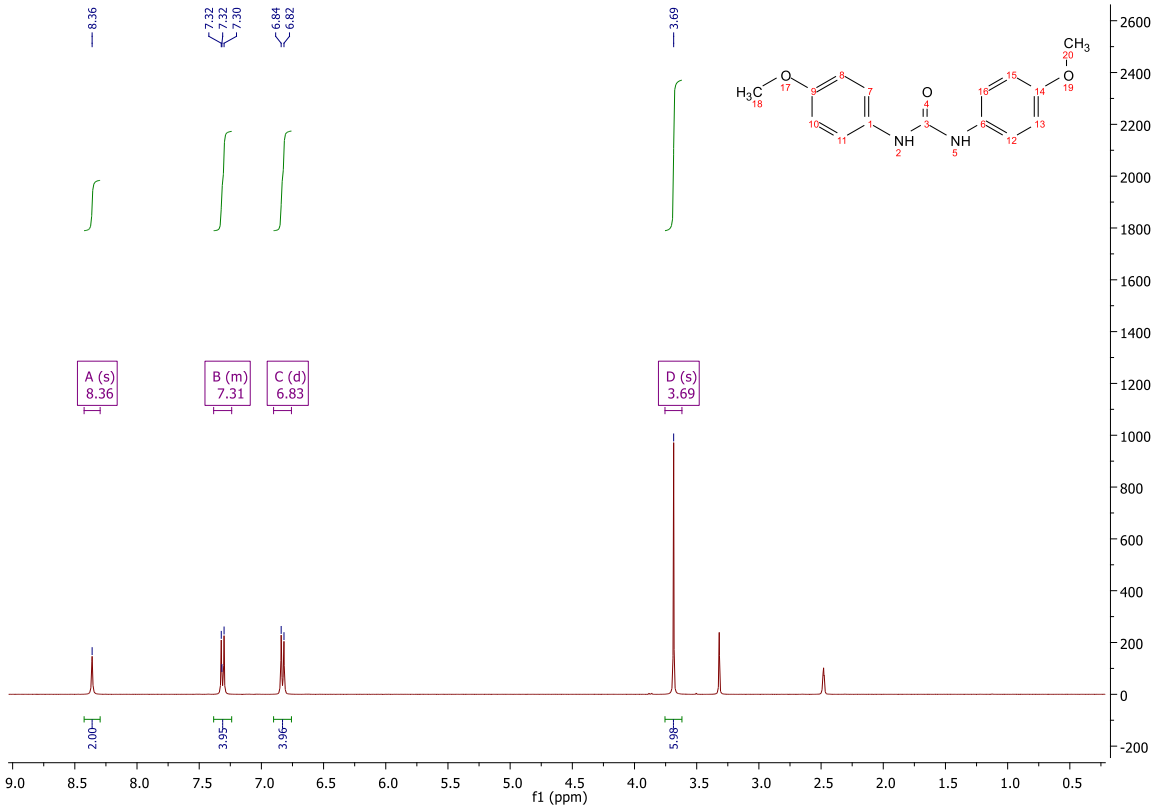
8.36
7.32
7.32
7.30
6.84
6.82
3.69
A (s)
8.36
B (m)
7.31
C (d)
6.83
D (s)
3.69
2.00
3.95
3.96
5.98
f1 (ppm)

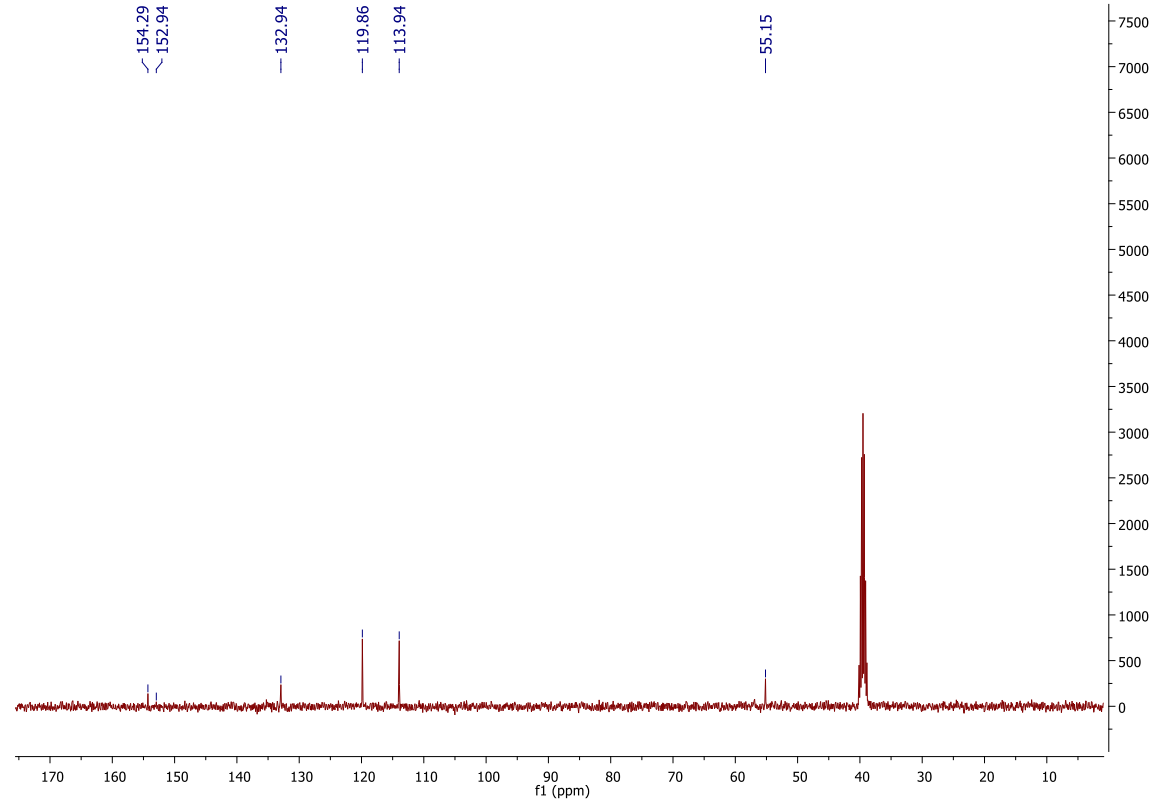
154.29
152.94
132.94
119.86
113.94
55.15
f1 (ppm)

Synthesis of Diethyl 4,4'-(carbonylbis(azanediyl)) dibenzoate (5)

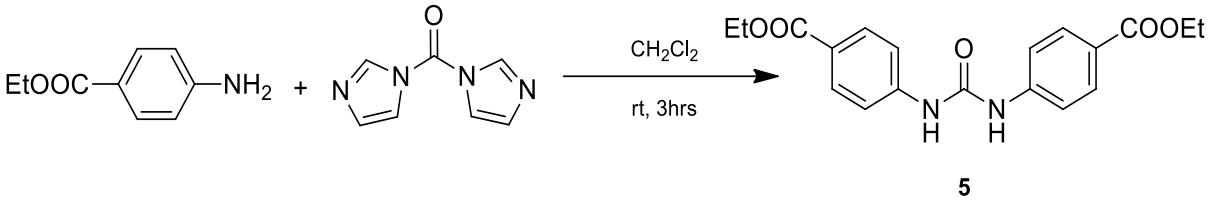

5

Yield: 81%

Melting point: 225-228°C

MS (ESI): $[M+H]^+ = 357.35$

^{1}H NMR (400 MHz, DMSO) δ 9.28 (s, 2H, 2NH), 7.94 – 7.81 (m, 4H, 4CH_{Ar}-Cq_{Ar}-CO), 7.65 – 7.52 (m, 4H, 4CH_{Ar}-Cq_{Ar}-NH), 4.26 (q, *J* = 7.1 Hz, 4H, 2CH_2-O), 1.29 (t, *J* = 7.1 Hz, 6H, 2CH_3-CH_2).

^{13}C NMR (101 MHz, DMSO) δ 165.38 (CO-OCH_2), 151.89 (CO-OCH_2), 143.94 (2Cq_{Ar}-NH), 130.38 (2CH_{Ar}-Cq_{Ar}-CO), 123.05 (2Cq_{Ar}-CO), 117.48 (2CH_{Ar}-Cq_{Ar}-NH), 60.34 (2CH_2O), 14.26 (2CH_3-CH_2).

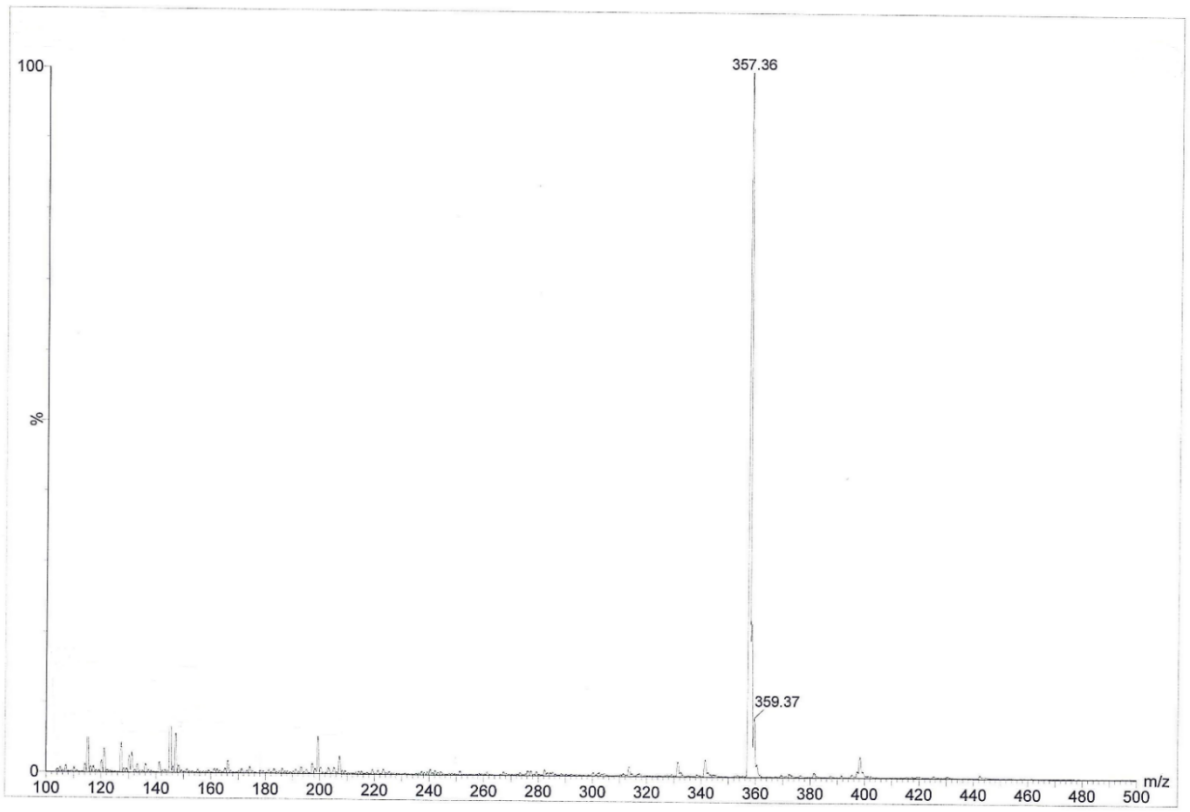

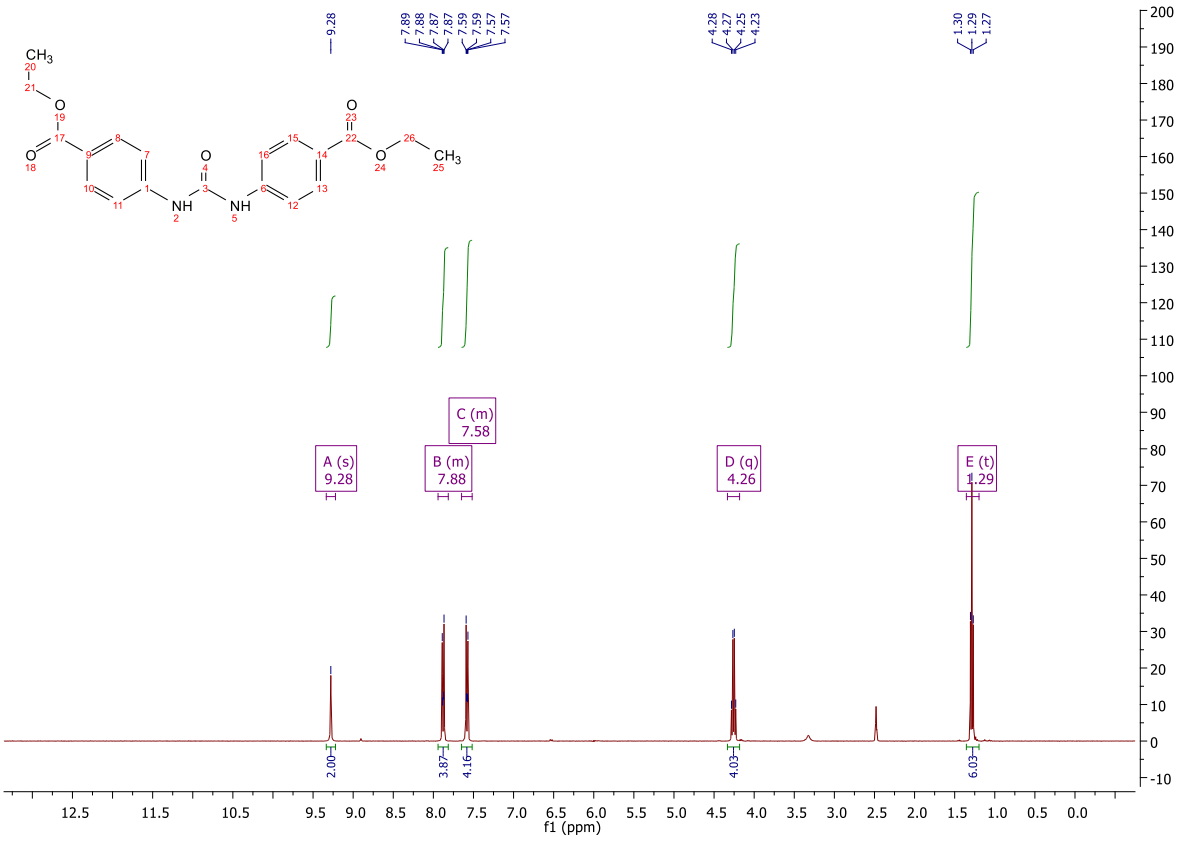
9.28
7.89
7.88
7.87
7.87
7.59
7.57
7.57
4.28
4.27
4.25
4.23
1.30
1.29
1.27
A (s) 9.28
B (m) 7.88
C (m) 7.58
D (q) 4.26
E (t) 1.29
2.00
3.87
4.16
4.03
6.03
f1 (ppm)

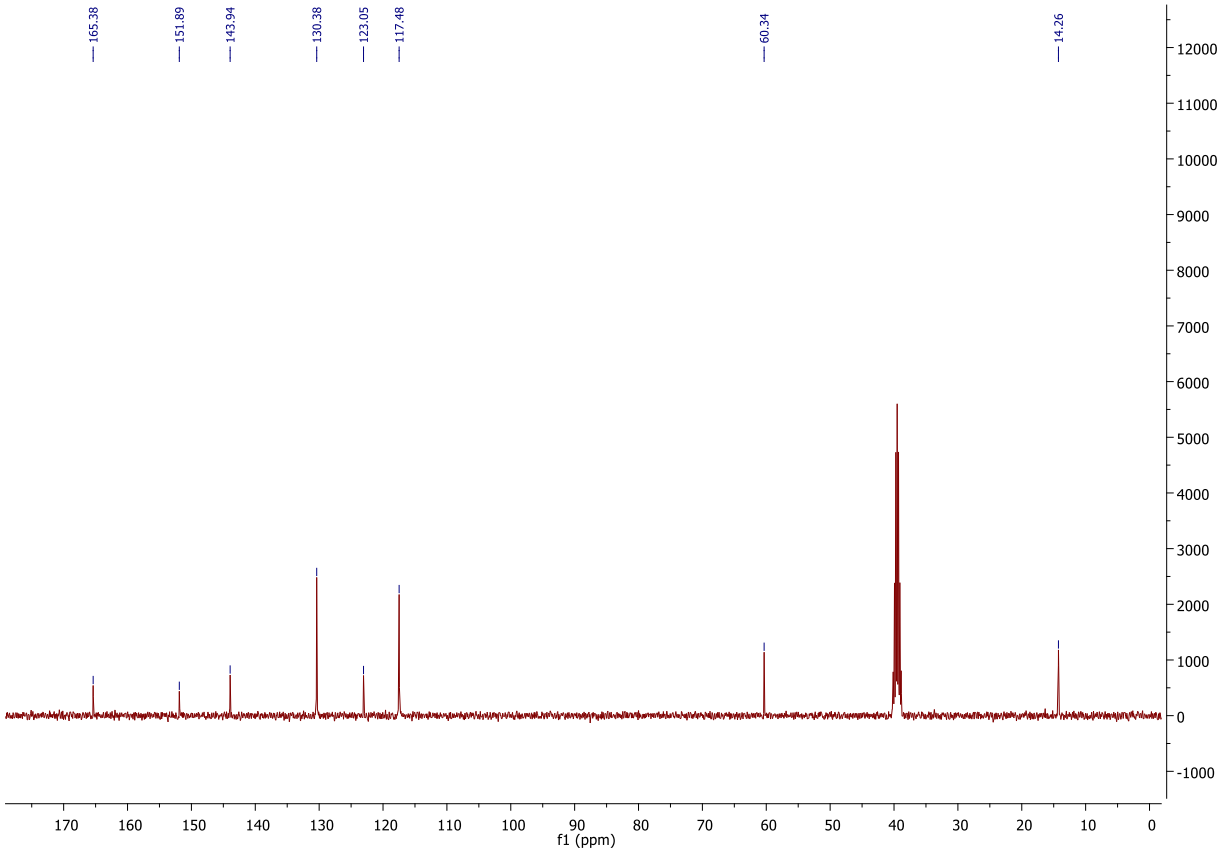
165.38
151.89
143.94
130.38
123.05
117.48
60.34
14.26
f1 (ppm)

Synthesis of 1,3-bis(4'-cyanophenyl)urea (6)

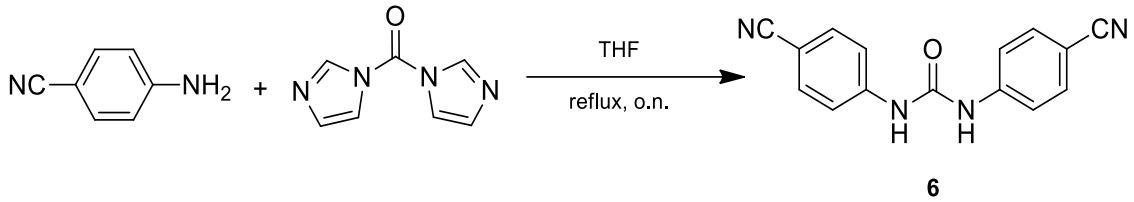

6

Yield: 27%

Melting point: 266-269°C

MS (ESI): $[M+H]^+ = 263.32$

^{1}H NMR (400 MHz, DMSO) δ 9.38 (s, 2H, 2NH), 7.76 – 7.71 (m, 4H, 2C$\underline{H_{Ar}}$-Cq_{Ar}-NH), 7.64 – 7.60 (m, 4H, 2C$\underline{H_{Ar}}$-Cq_{Ar}-NH).

^{13}C NMR (101 MHz, DMSO) δ 151.80 (CO), 143.70 (2C$\underline{q_{Ar}}$-CO), 133.34 (2C$\underline{H_{Ar}}$-Cq_{Ar}-CN), 119.22 (C$\underline{H_{Ar}}$-CH_{Ar}-CH_{Ar}-Cq_{Ar}), 118.37 (2C$\underline{H_{Ar}}$-CH_{Ar}-Cq_{Ar}-CN), 103.79 (2C$\underline{q_{Ar}}$-CN).

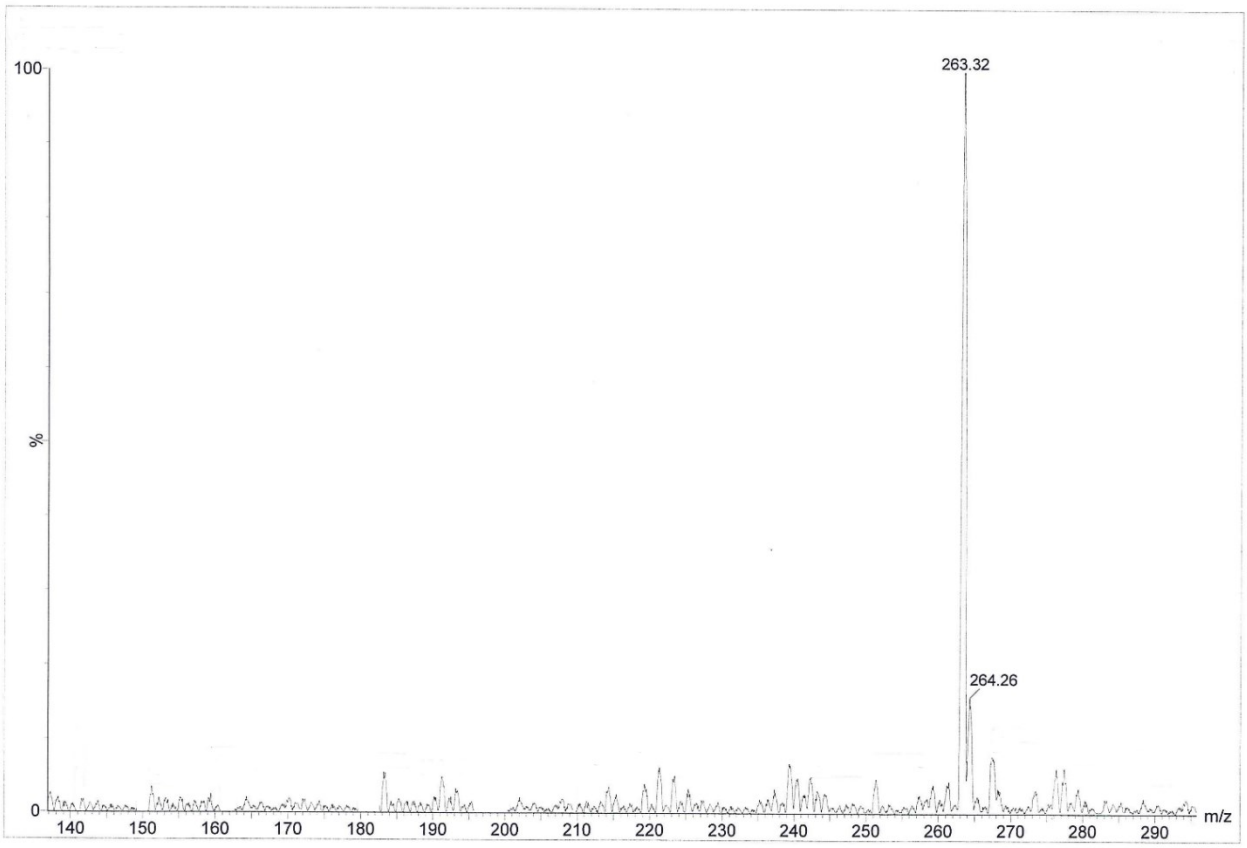

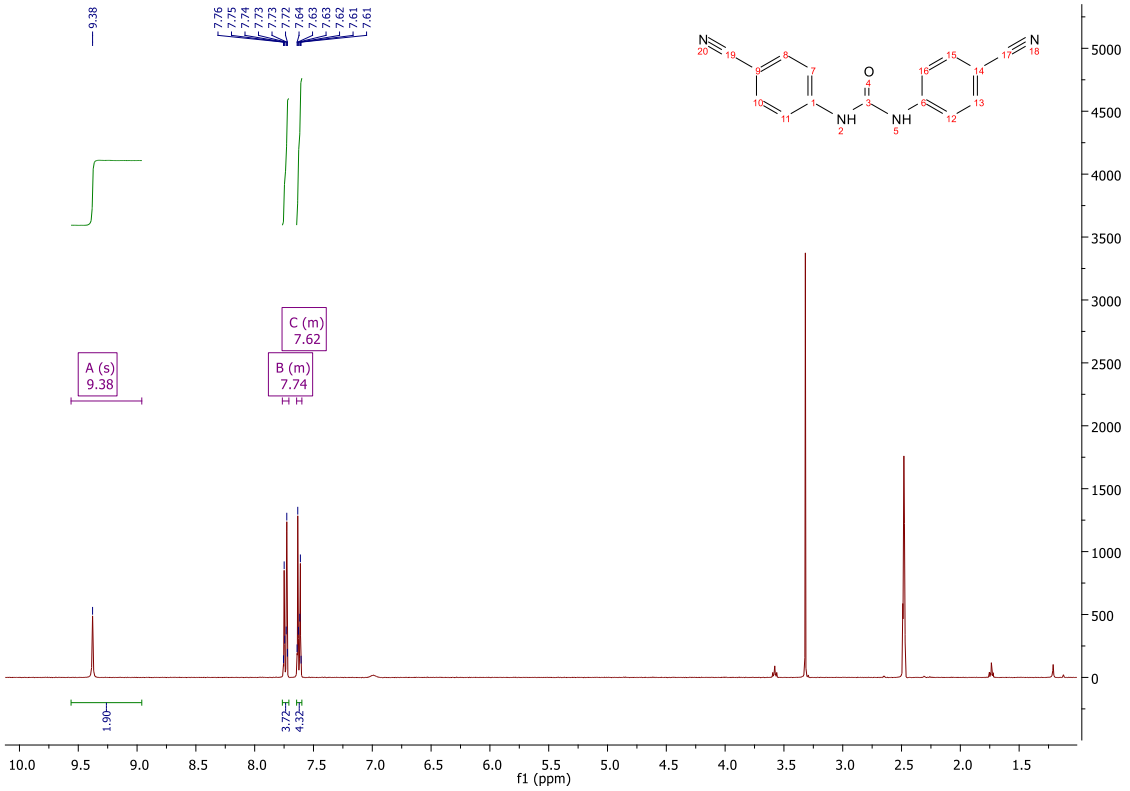
9.38
7.76
7.75
7.74
7.73
7.72
7.64
7.63
7.62
7.61
7.61
A (s)
9.38
C (m)
7.62
B (m)
7.74
1.90
3.72
4.32
f1 (ppm)

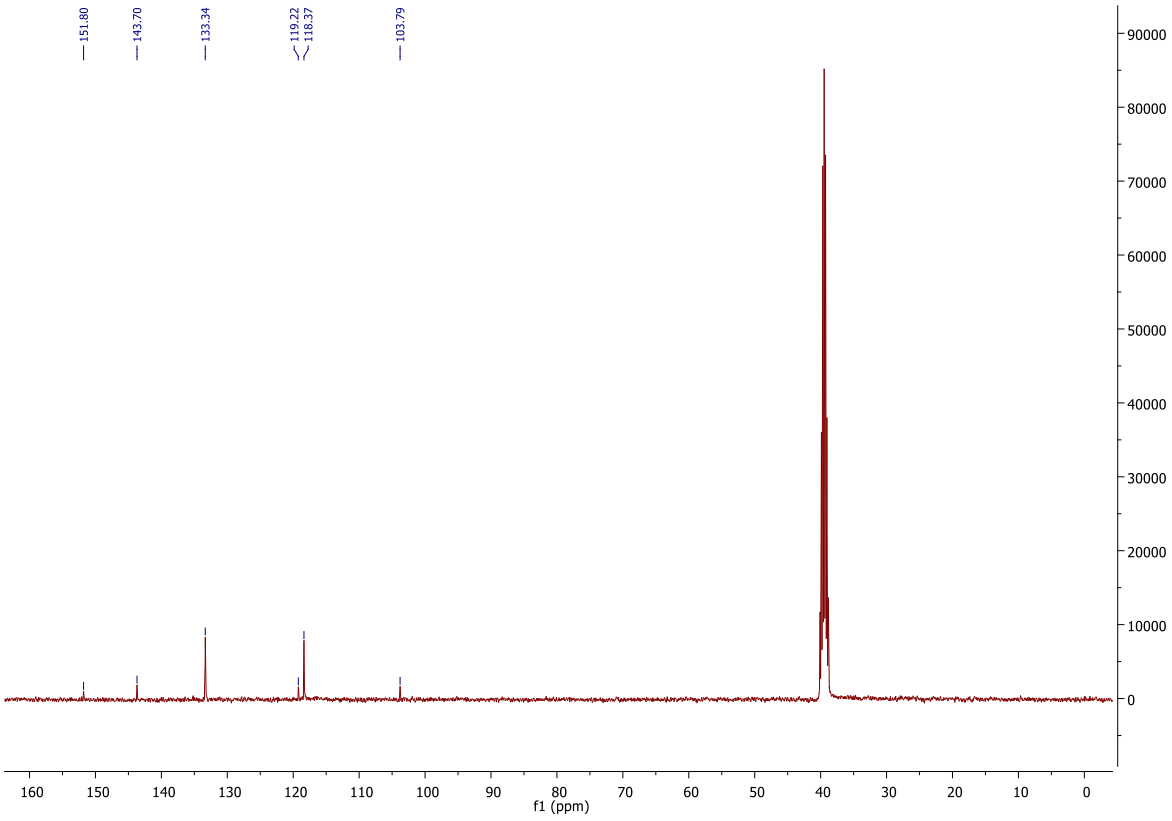
151.80
143.70
133.34
119.22
118.37
103.79
f1 (ppm)

Synthesis of 1,3-dibenzylurea (7)

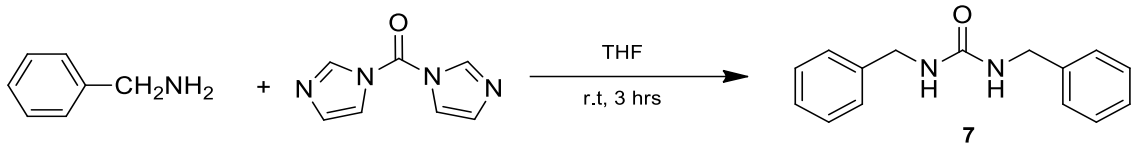

Yield: 89%

Melting point: 169-173°C

MS (ESI): $[M+H]^+ = 241.08$

^{1}H NMR (400 MHz, DMSO) δ 7.36 – 7.14 (m, 10H, 10 C$\underline{H}_{Ar}$), 6.42 (t, *J* = 6.0 Hz, 2H, 2N$\underline{H}$), 4.21 (d, *J* = 6.0 Hz, 4H, 2C$\underline{H}_2$-NH).

^{13}C NMR (101 MHz, DMSO) δ 158.08 (CO), 140.91 ($\underline{Cq}_{Ar}$), 128.21 (2$\underline{C}H_{Ar}$-CH_{Ar}-Cq_{Ar}), 126.99 (2CH_{Ar}-Cq_{Ar}), 126.55 (2$\underline{C}H_{Ar}$-CH_{Ar}-CH_{Ar}), 42.96 ($\underline{C}H_2$).

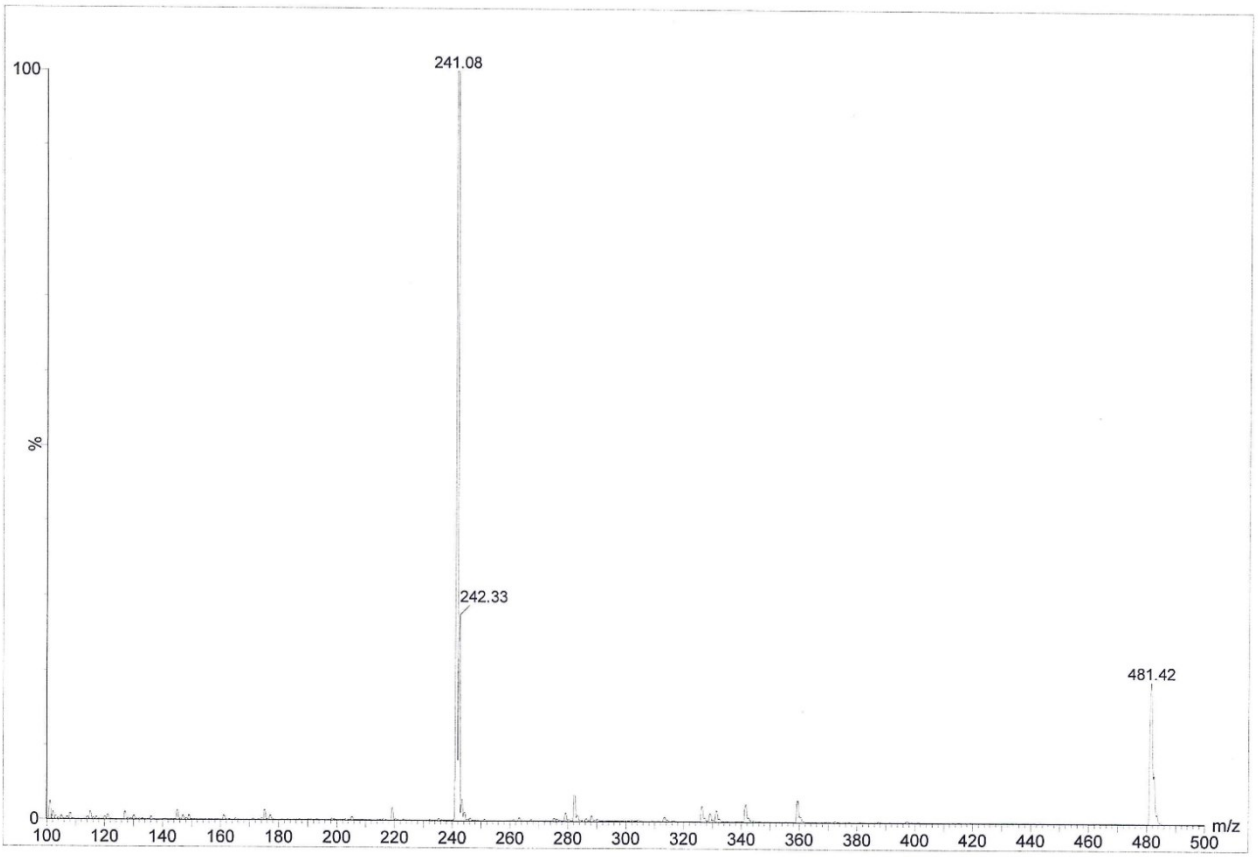

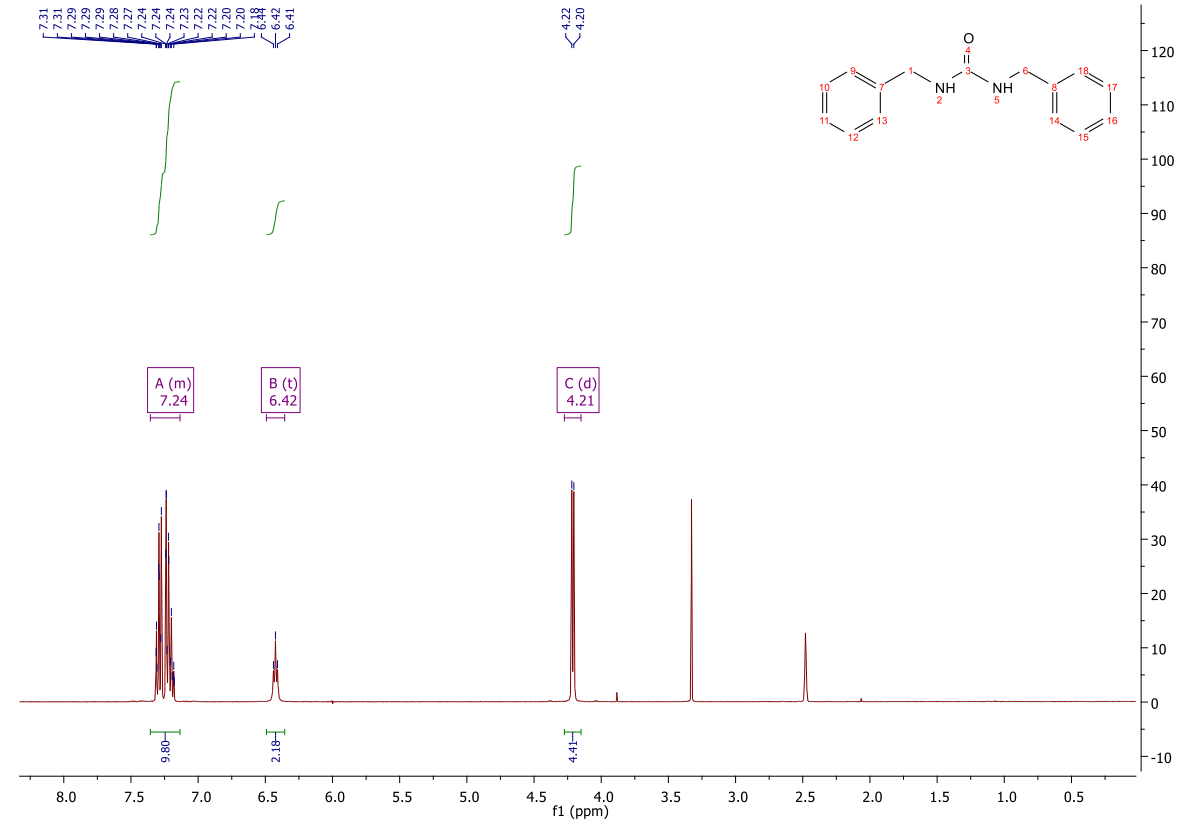
7.31
7.31
7.29
7.29
7.29
7.28
7.27
7.24
7.24
7.24
7.23
7.22
7.22
7.20
7.20
7.18
6.44
6.42
6.41
4.22
4.20
A (m)
7.24
B (t)
6.42
C (d)
4.21
9.80
2.18
4.41
f1 (ppm)

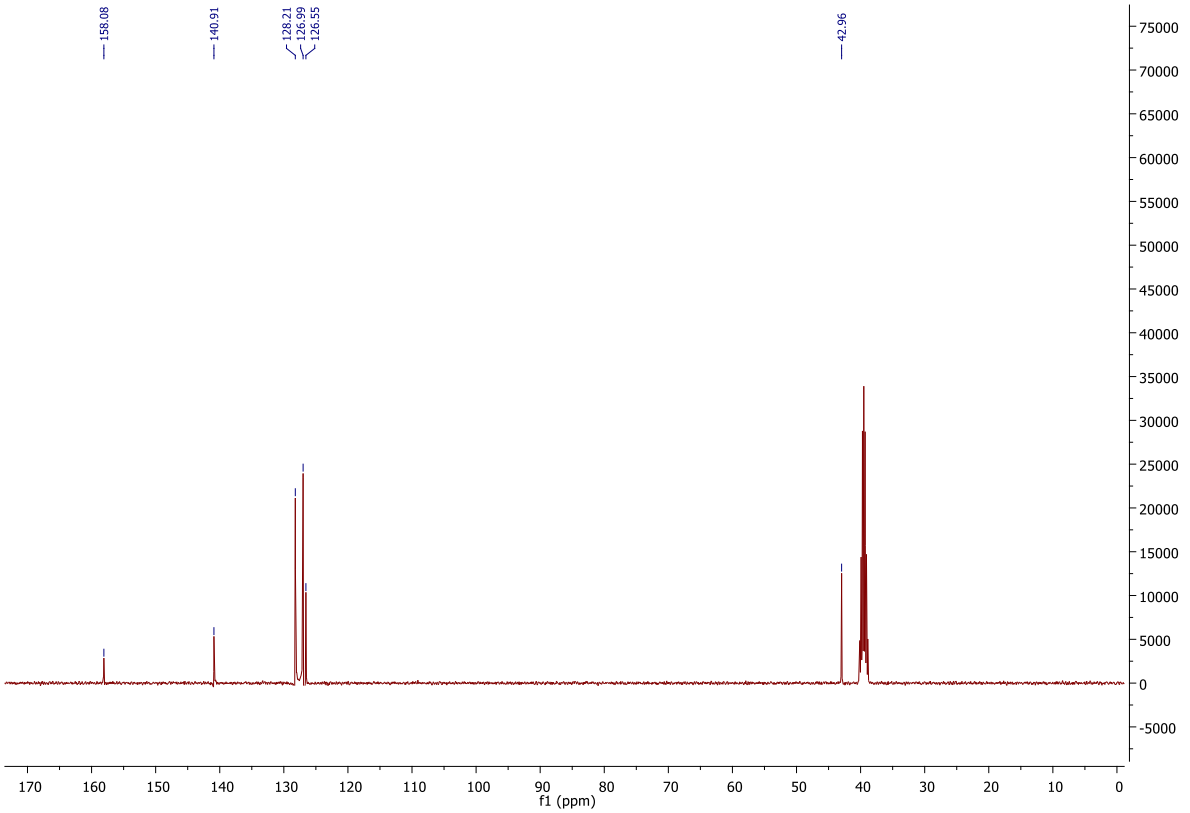
158.08
140.91
128.21
126.99
126.55
42.96
f1 (ppm)

14.2 Asymmetric ureas and thioureas

Even if it is possible to produce asymmetric ureas using CDI and one equivalent of each amine, the isocyanate intermediate is too reactive to be easily isolated, and symmetric ureas are produced as well. For this reason, asymmetric ureas, and even thioureas, have been produced by another synthetic pathway (Figure 91). Noticeably, reactions with isothiocyanates required longer time under reflux conditions.

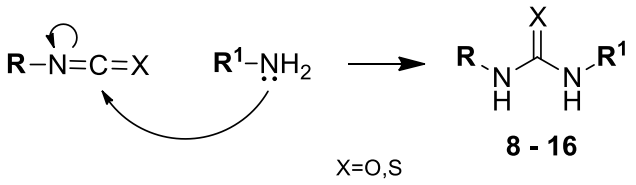

Figure 91: Reaction mechanism for synthesis of asymmetric ureas

The standard procedure was as follow: to solution of amine (4.8 mmol) in 1,2 dichlorethane (1,2-DCE) or THF (30 mL) was added isocyanate/isothiocyanate (4.8 mmol). The solution was then stirred at room temperature for 18 hours. After the reaction was complete as indicated by TLC, the solution was evaporated and washed two times with Et_2O to afford the product as a white solid.

Synthesis of 1-(*tert*-butyl)-3-cyclohexylurea (8)

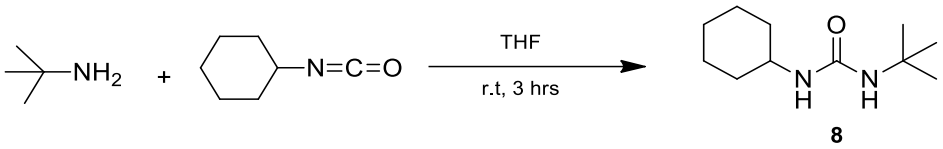

8

Yield: 84%

Melting point: 225°C

MS (ESI): $[M+H]^+ = 199.23$

^{1}H NMR (400 MHz, DMSO) δ 5.50 (d, *J* = 8.1 Hz, 1H, NH-CH), 5.47 (s, 1H, NH-Cq), 3.29 – 3.21 (m, 1H, NH-CH), 1.72 – 1.64 (m, 2H, 2NH-CH-CH$_2$), 1.63 – 1.56 (m, 2H, 2NH-CH-CH$_2$), 1.52 – 1.44 (m, 1H, CH-CH$_2$-CH$_2$-CH$_2$), 1.28 – 1.20 (m, 2H, 2CH-CH$_2$-CH$_2$), 1.17 (s, 9H, 3Cq-CH$_3$), 1.15 – 1.07 (m, *J* = 11.8 Hz, 1H, CH-CH$_2$-CH$_2$-CH$_2$), 1.04 – 0.93 (m, 2H, 2CH-CH$_2$-CH$_2$).

^{13}C NMR (101 MHz, DMSO) δ 156.69 (CO), 48.88 (NH-Cq), 47.19 (NH-CH), 33.40 (CH-CH$_2$-CH$_2$-CH$_2$), 29.36 (3CH$_3$-Cq), 25.34 (2CH$_2$-CH), 24.47 (2CH$_2$-CH$_2$-CH).

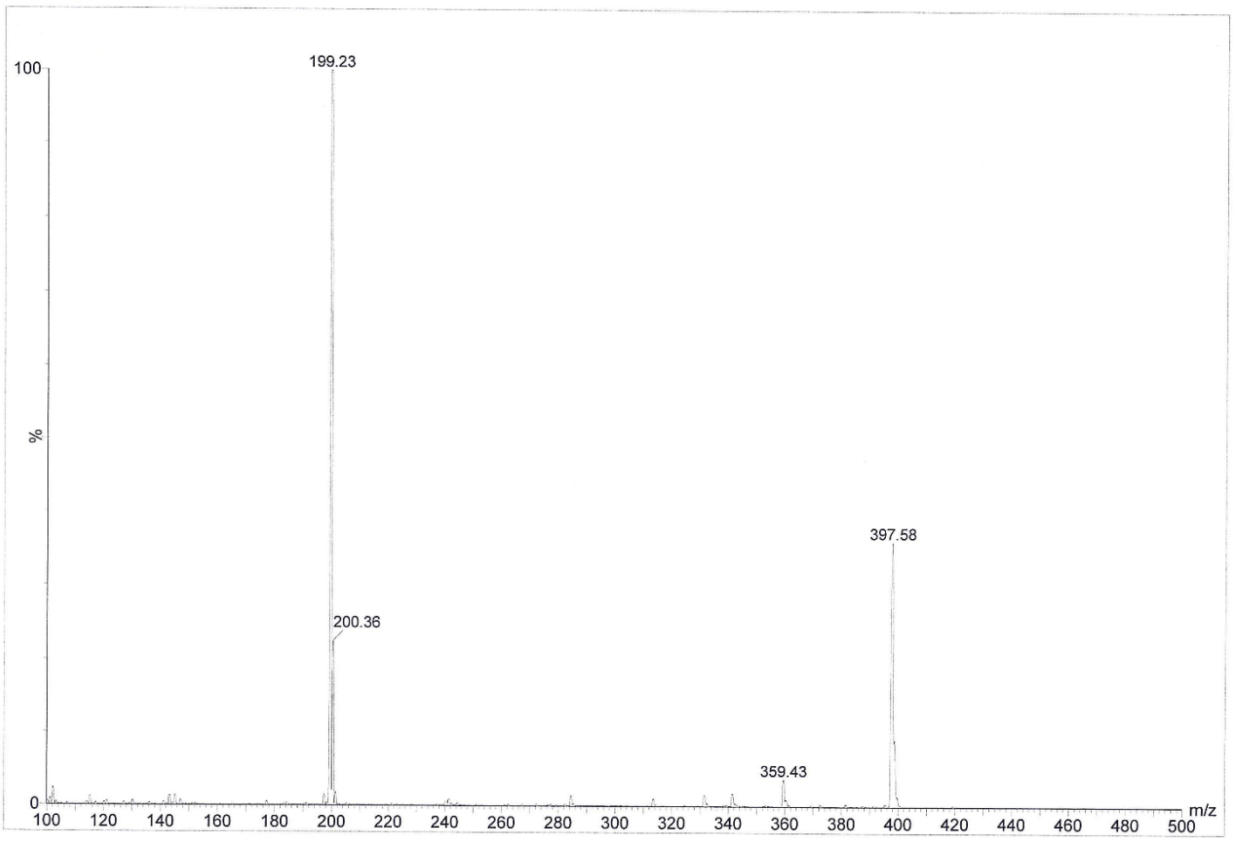

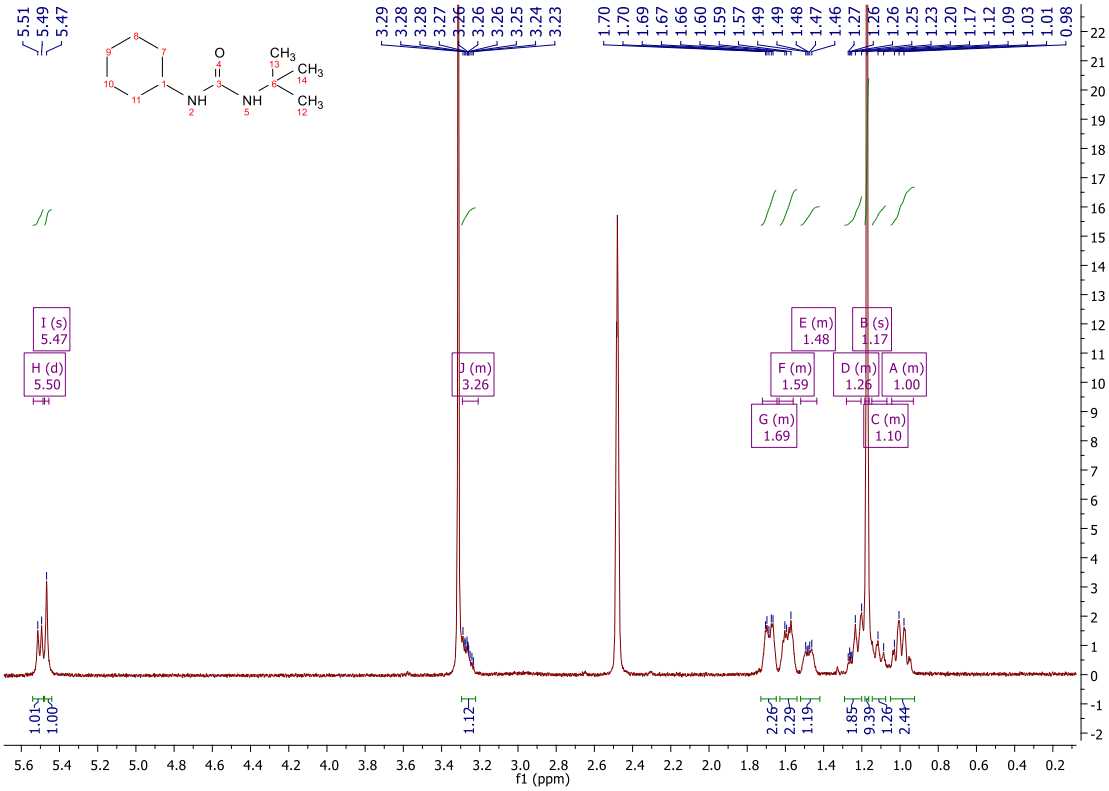
I (s)
5.47
H (d)
5.50
J (m)
3.26
E (m)
1.48
B (s)
1.17
F (m)
1.59
D (m)
1.26
A (m)
1.00
G (m)
1.69
C (m)
1.10
f1 (ppm)

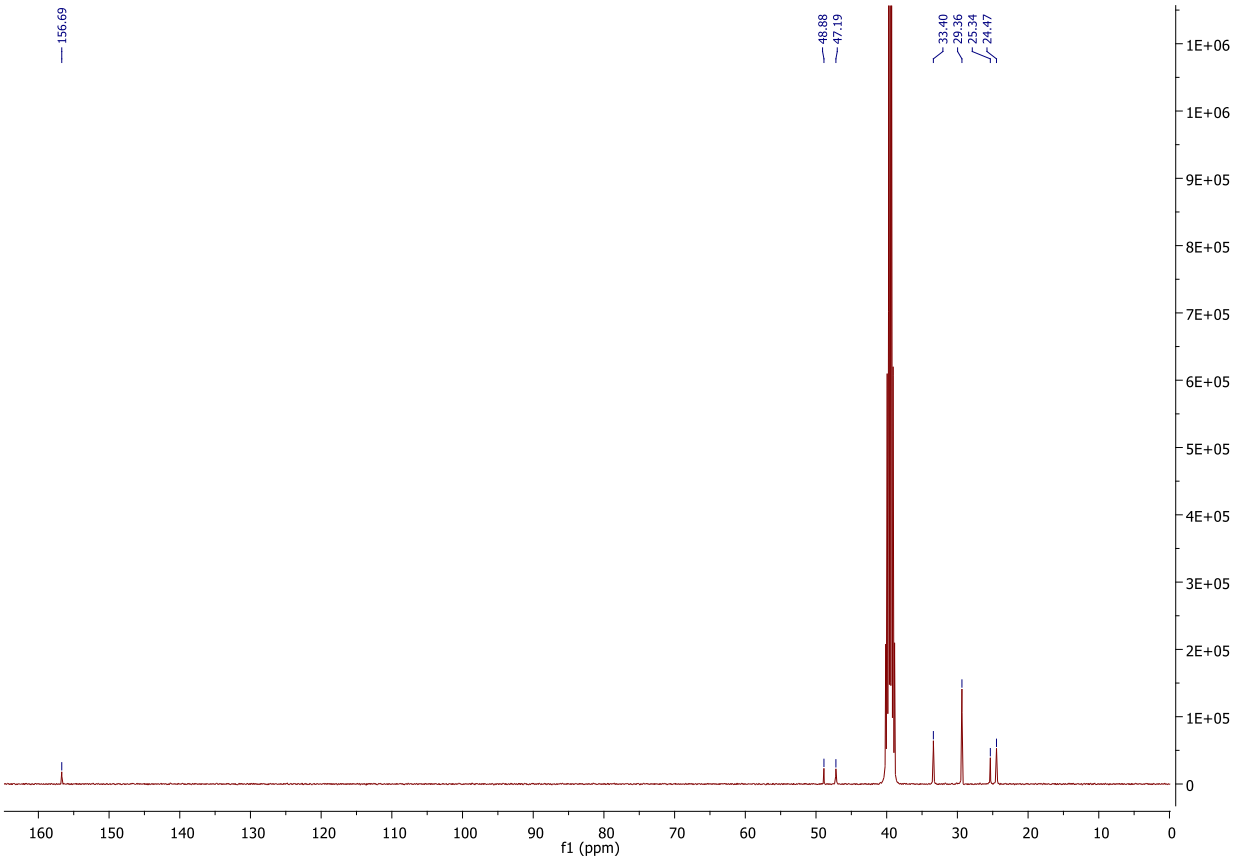
156.69
48.88
47.19
33.40
29.36
25.34
24.47
f1 (ppm)

Synthesis of 1-cyclohexyl-3-phenylurea (9)

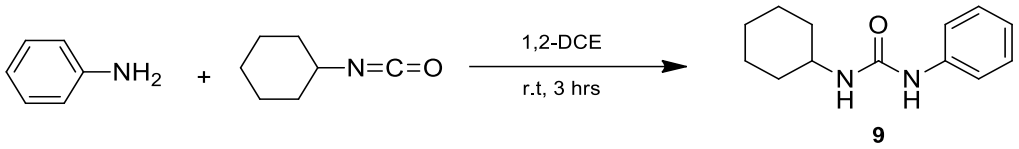

9

Yield: 87%

Melting point: 188-190°C

MS (ESI): $[M+H]^+ = 219.09$

^{1}H NMR (400 MHz, DMSO) δ 8.25 (s, 1H, N<u>H</u>-Cq$_{Ar}$), 7.33 (dd, *J* = 8.6, 1.1 Hz, 2H, 2C<u>H$_{Ar}$</u>-Cq$_{Ar}$), 7.24 – 7.11 (m, 2H, 2C<u>H$_{Ar}$</u>-CH$_{Ar}$-Cq$_{Ar}$), 6.84 (t, *J* = 7.3 Hz, 1H, C<u>H$_{Ar}$</u>-CH$_{Ar}$-CH$_{Ar}$-Cq$_{Ar}$), 6.03 (d, *J* = 7.8 Hz, 1H, N<u>H</u>-CH), 3.50 – 3.35 (m, 1H, NH-C<u>H</u>), 1.82 – 1.71 (m, 2H, 2CH-C<u>H$_2$</u>), 1.68 – 1.59 (m, 2H, 2CH-C<u>H$_2$</u>), 1.56 – 1.45 (m, 1H, CH-CH$_2$-CH$_2$-C<u>H$_2$</u>), 1.34 – 1.23 (m, 2H, 2 CH-CH$_2$-C<u>H$_2$</u>), 1.21 – 1.06 (m, 3H, 2CH-CH$_2$-C<u>H$_2$</u>; CH-CH$_2$-CH$_2$-C<u>H$_2$</u>).

^{13}C NMR (101 MHz, DMSO) δ 154.38 (<u>C</u>O), 140.56 (<u>Cq$_{Ar}$</u>-NH), 128.64 (<u>C</u>H$_{Ar}$-CH$_{Arr}$-Cq$_{Ar}$), 120.85 (<u>C</u>H$_{Ar}$-CH$_{Ar}$-CH$_{Ar}$-Cq$_{Ar}$), 117.42 (<u>C</u>H$_{Ar}$-Cq$_{Ar}$), 47.54 (<u>C</u>H-NH), 32.99 (<u>C</u>H$_2$-CH), 25.25 (<u>C</u>H$_2$-CH$_2$-CH$_2$-CH), 24.36 (<u>C</u>H$_2$-CH$_2$-CH).

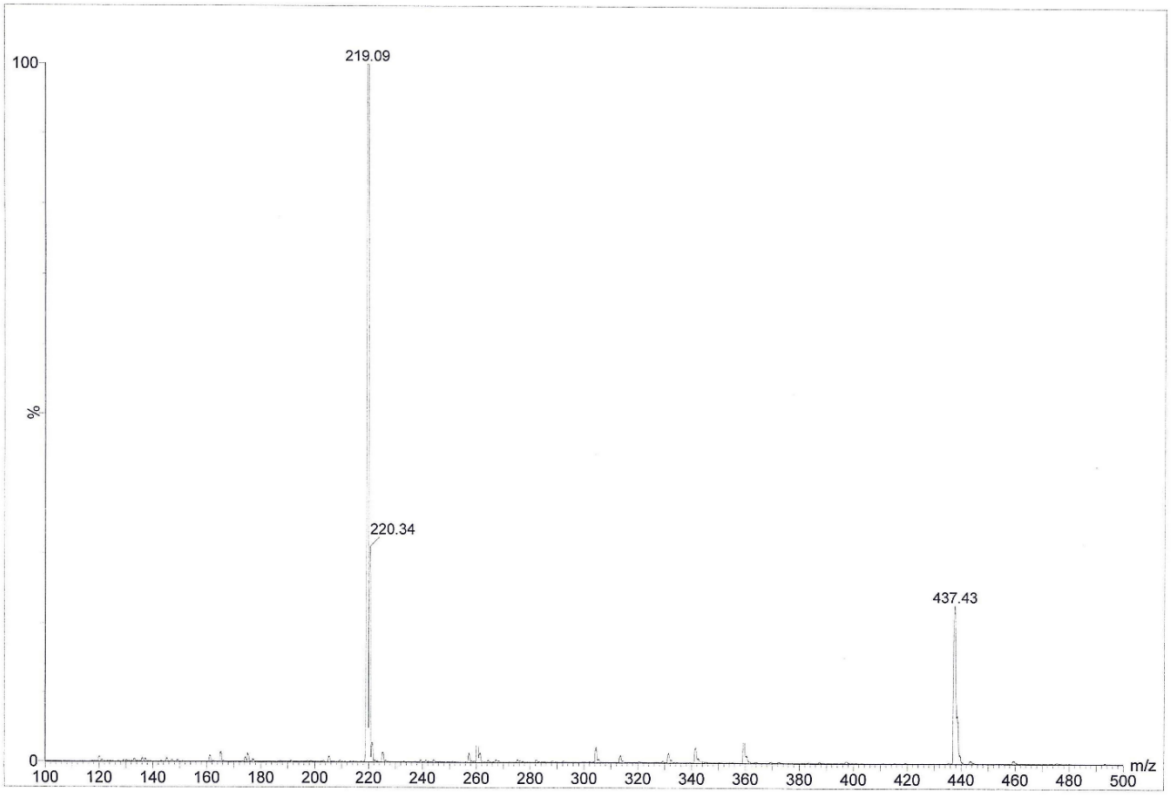

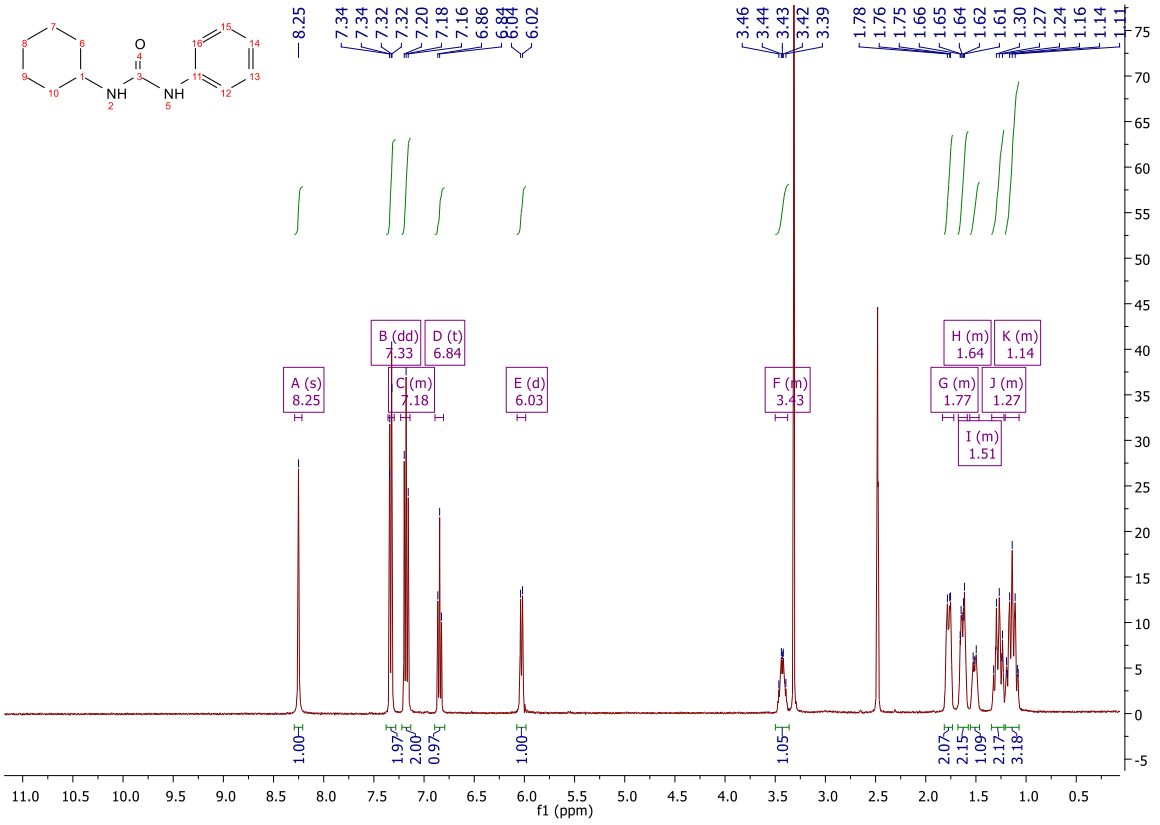
8.25
7.34
7.34
7.32
7.32
7.20
7.18
7.16
6.86
6.84
6.84
6.02
3.46
3.44
3.43
3.42
3.39
1.78
1.76
1.75
1.66
1.65
1.64
1.62
1.61
1.30
1.27
1.24
1.16
1.14
1.11
A (s) 8.25
B (dd) 7.33
C (m) 7.18
D (t) 6.84
E (d) 6.03
F (m) 3.43
G (m) 1.77
H (m) 1.64
I (m) 1.51
J (m) 1.27
K (m) 1.14
1.00
1.97
2.00
0.97
1.00
1.05
2.07
2.15
1.09
2.17
3.18
f1 (ppm)

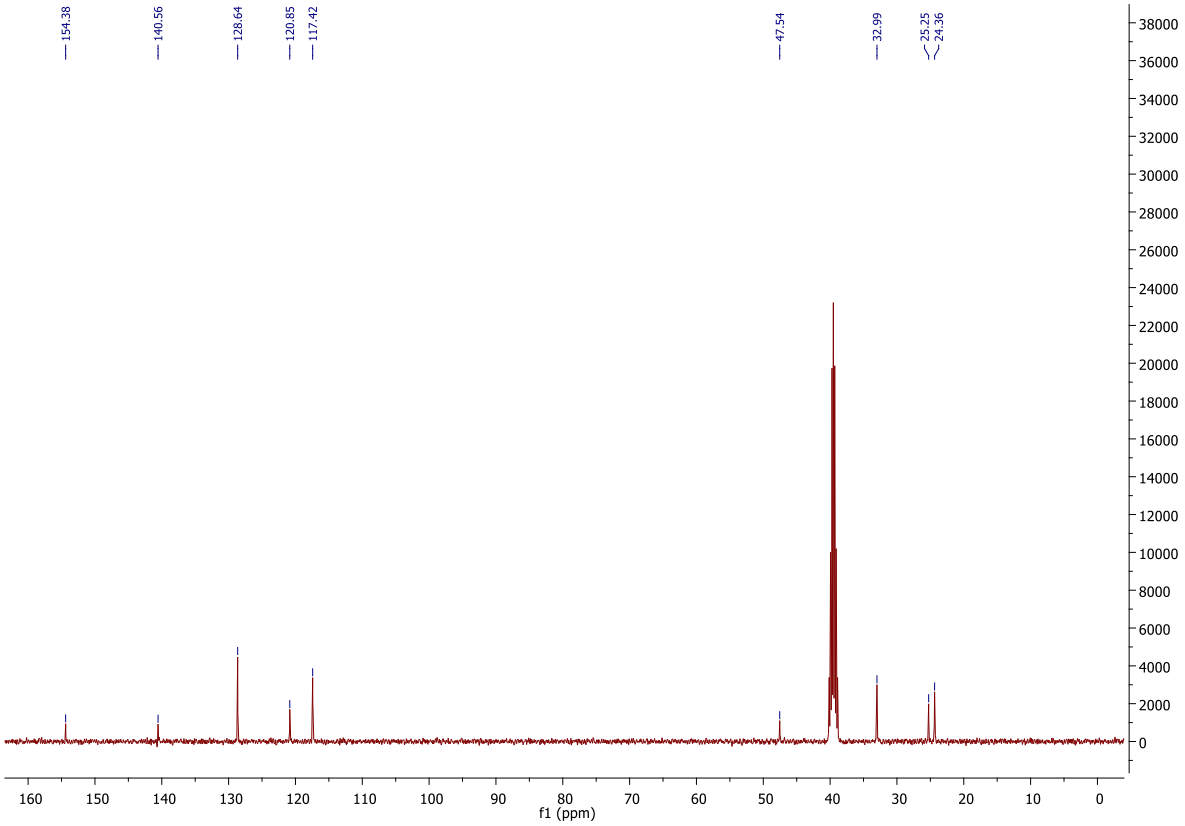
154.38
140.56
128.64
120.85
117.42
47.54
32.99
25.25
24.36
f1 (ppm)

Synthesis of 1-(4-methoxyphenyl)-3-phenylurea (10)

10

Yield: 86%

Melting point: 194-199°C

MS (ESI): $[M+H]^+ = 243.33$

^{1}H NMR (400 MHz, DMSO) δ 8.55 (s, 1H, CO-N<u>H</u>), 8.44 (s, 1H, CO-N<u>H</u>), 7.41 (dd, *J* = 8.7, 1.1 Hz, 2H, C<u>H$_{Ar}$</u>-Cq$_{Ar}$), 7.35 – 7.30 (m, 2H, 2C<u>H$_{Ar}$</u>-Cq$_{Ar}$-OCH$_3$), 7.28 – 7.21 (m, 2H, 2C<u>H$_{Ar}$</u>-CH$_{Ar}$-Cq$_{Ar}$), 6.96 – 6.89 (m, 1H, C<u>H$_{Ar}$</u>-CH$_{Ar}$-CH$_{Ar}$-Cq$_{Ar}$), 6.88 – 6.81 (m, 2H, 2C<u>H$_{Ar}$</u>- CH$_{Ar}$-Cq$_{Ar}$-OCH$_3$), 3.69 (s, 3H, OC<u>H$_3$</u>).

^{13}C NMR (101 MHz, DMSO) δ 154.42 (<u>Cq$_{Ar}$</u>-OMe), 152.71 (<u>C</u>O), 139.90 (<u>Cq$_{Ar}$</u>-NH), 132.71 (<u>Cq$_{Ar}$</u>-NH), 128.75 (<u>C</u>H$_{Ar}$-CH$_{Ar}$-Cq$_{Ar}$-NH), 121.59 (<u>C</u>H$_{Ar}$-CH$_{Ar}$--CH$_{Ar}$-Cq$_{Ar}$), 119.98 (<u>C</u>H$_{Ar}$-Cq$_{Ar}$-NH), 118.04 (<u>C</u>H$_{Ar}$-CH$_{Ar}$-Cq$_{Ar}$-OCH$_3$), 113.98 (<u>C</u>H$_{Ar}$-Cq$_{Ar}$-OCH$_3$), 55.17 (O<u>C</u>H$_3$).

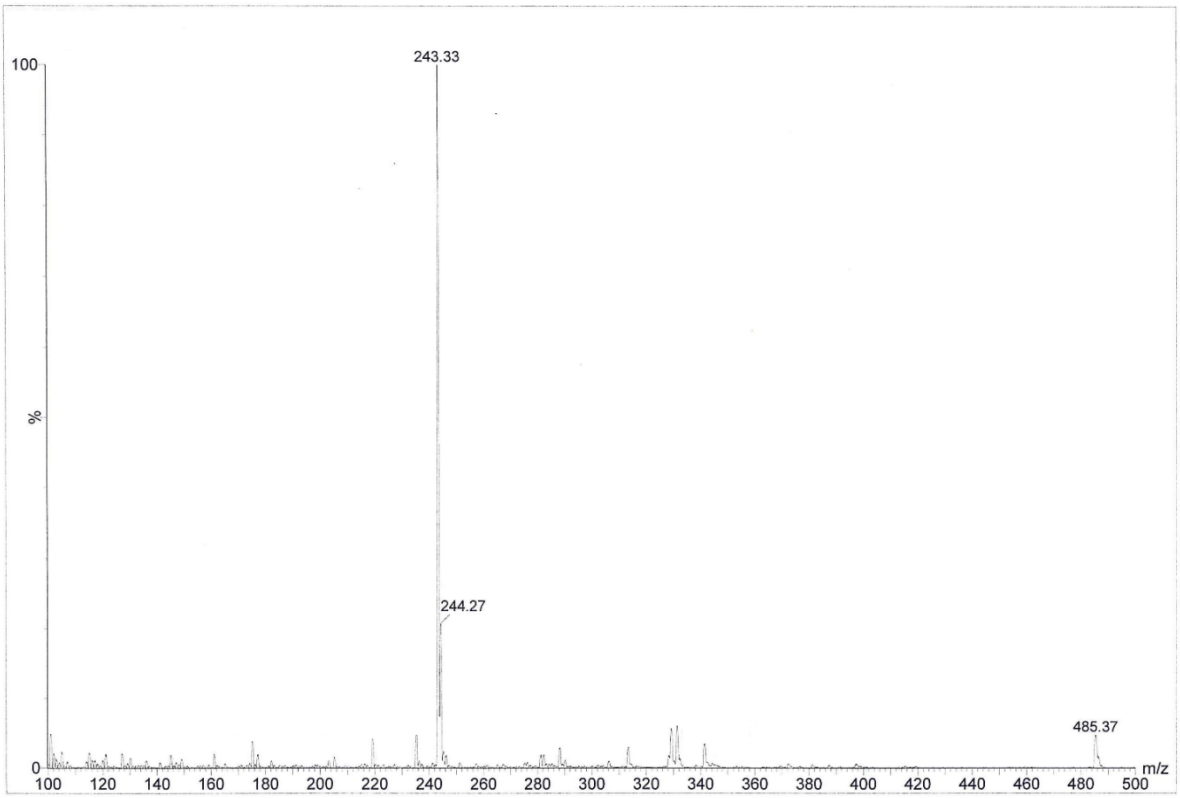

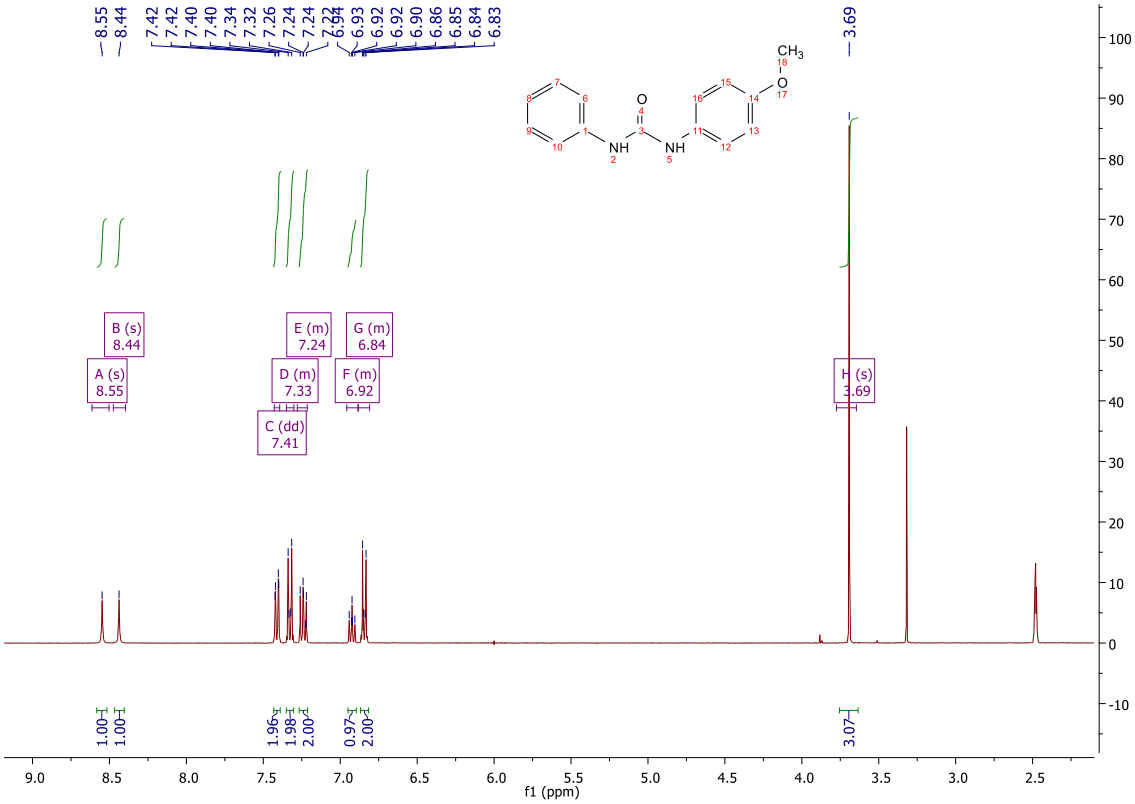
8.55
8.44
7.42
7.42
7.40
7.40
7.34
7.32
7.26
7.24
7.24
7.22
6.94
6.93
6.92
6.92
6.90
6.86
6.85
6.84
6.83
3.69
B (s) 8.44
A (s) 8.55
E (m) 7.24
G (m) 6.84
D (m) 7.33
F (m) 6.92
C (dd) 7.41
H (s) 3.69
1.00
1.00
1.96
1.98
2.00
0.97
2.00
3.07
f1 (ppm)

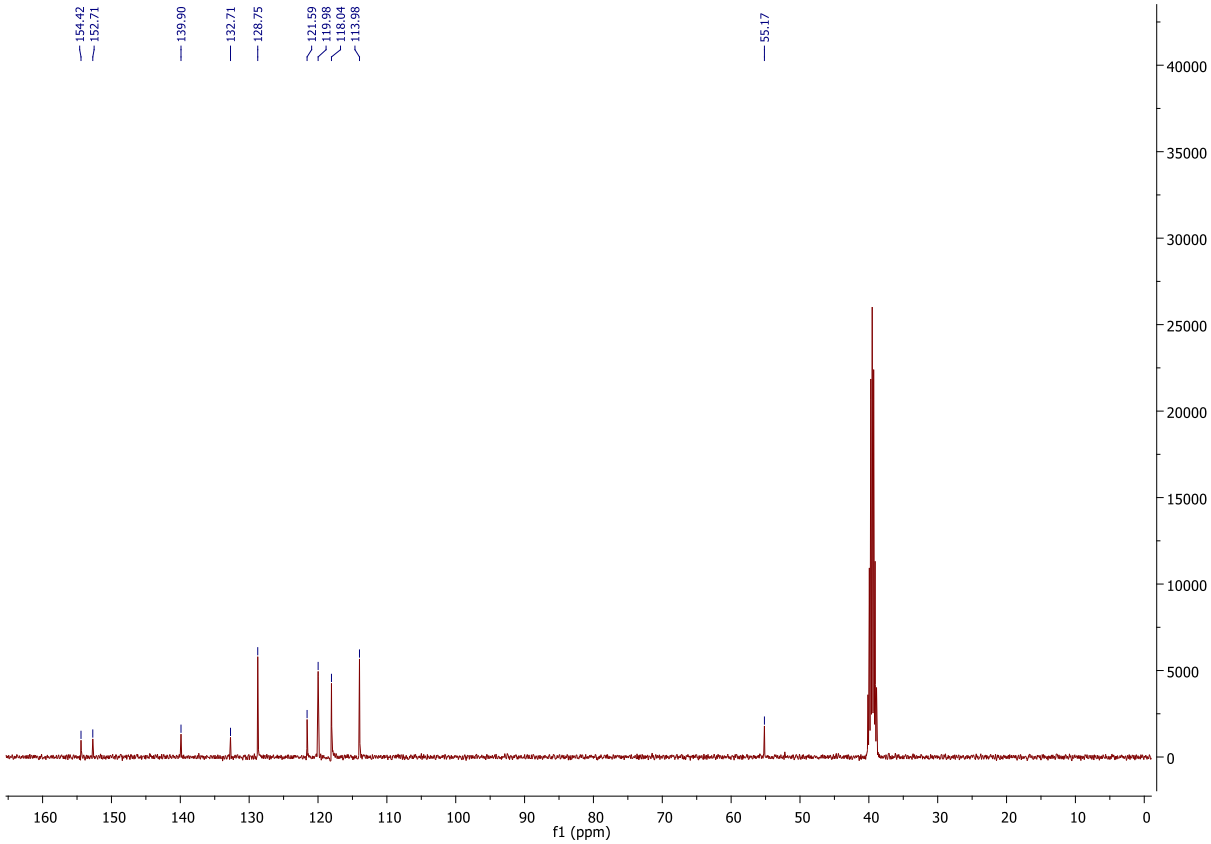
154.42
152.71
139.90
132.71
128.75
121.59
119.98
118.04
113.98
55.17
f1 (ppm)

Synthesis of 1-(4-cyanophenyl)-3-phenylurea (11)

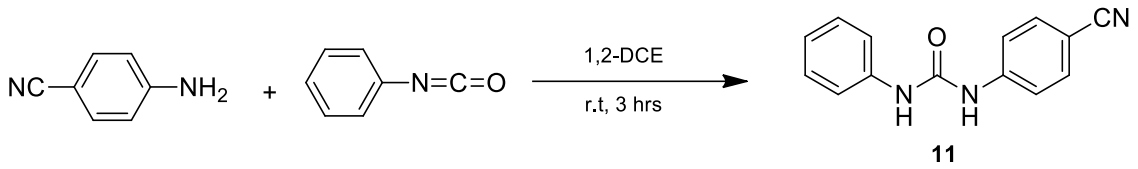

11

Yield: 11%

Melting point: 196-200°C

MS (ESI): $[M+H]^+ = 238.32$

^{1}H NMR (400 MHz, DMSO) δ 9.18 (s, 1H, CO-N<u>H</u>), 8.84 (s, 1H, CO-N<u>H</u>), 7.71 (d, *J* = 8.8 Hz, 2H, 2C<u>H$_{Ar}$</u>-CH$_{Ar}$-Cq$_{Ar}$-CN), 7.61 (d, *J* = 8.8 Hz, 2H, 2CH$_{Ar}$-Cq$_{Ar}$-CN), 7.44 (d, *J* = 7.6 Hz, 2H, 2C<u>H$_{Ar}$</u>-Cq$_{Ar}$), 7.28 (t, *J* = 7.9 Hz, 2H, 2C<u>H$_{Ar}$</u>-CH$_{Ar}$-Cq$_{Ar}$), 6.98 (t, *J* = 7.4 Hz, 1H, C<u>H$_{Ar}$</u>-CH$_{Ar}$-CH$_{Ar}$).

^{13}C NMR (101 MHz, DMSO) δ 152.09 (<u>C</u>O), 144.23 (<u>Cq$_{Ar}$</u>-NH), 139.14 (<u>Cq$_{Ar}$</u>-NH), 133.31 (2<u>C</u>H$_{Ar}$-Cq$_{Ar}$-CN), 128.86 (2<u>C</u>H$_{Ar}$-CH$_{Ar}$-Cq$_{Ar}$-NH), 122.37 (<u>C</u>H$_{Ar}$-CH$_{Ar}$-CH$_{Ar}$-Cq$_{Ar}$), 119.34 (2CH$_{Ar}$-Cq$_{Ar}$), 118.51 (2<u>C</u>H$_{Ar}$-CH$_{Ar}$-Cq$_{Ar}$-CN), 118.00 (<u>C</u>N), 103.18 (<u>Cq$_{Ar}$</u>-CN).

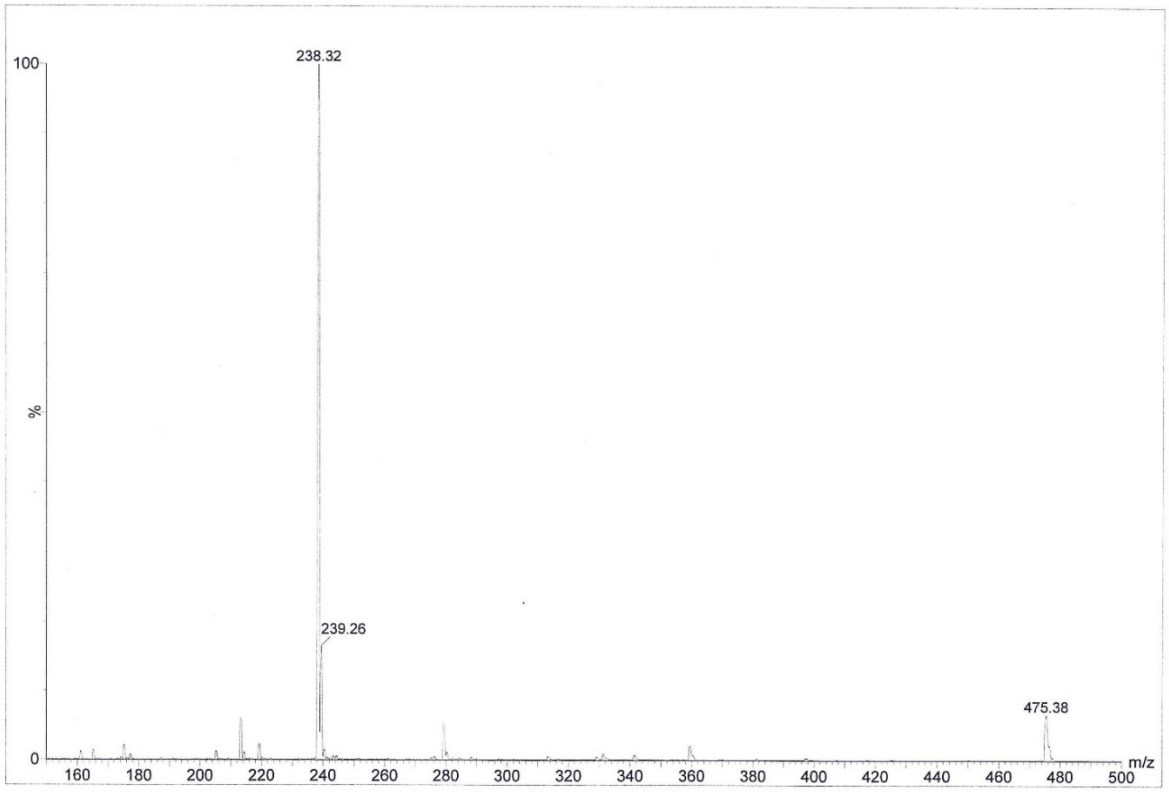

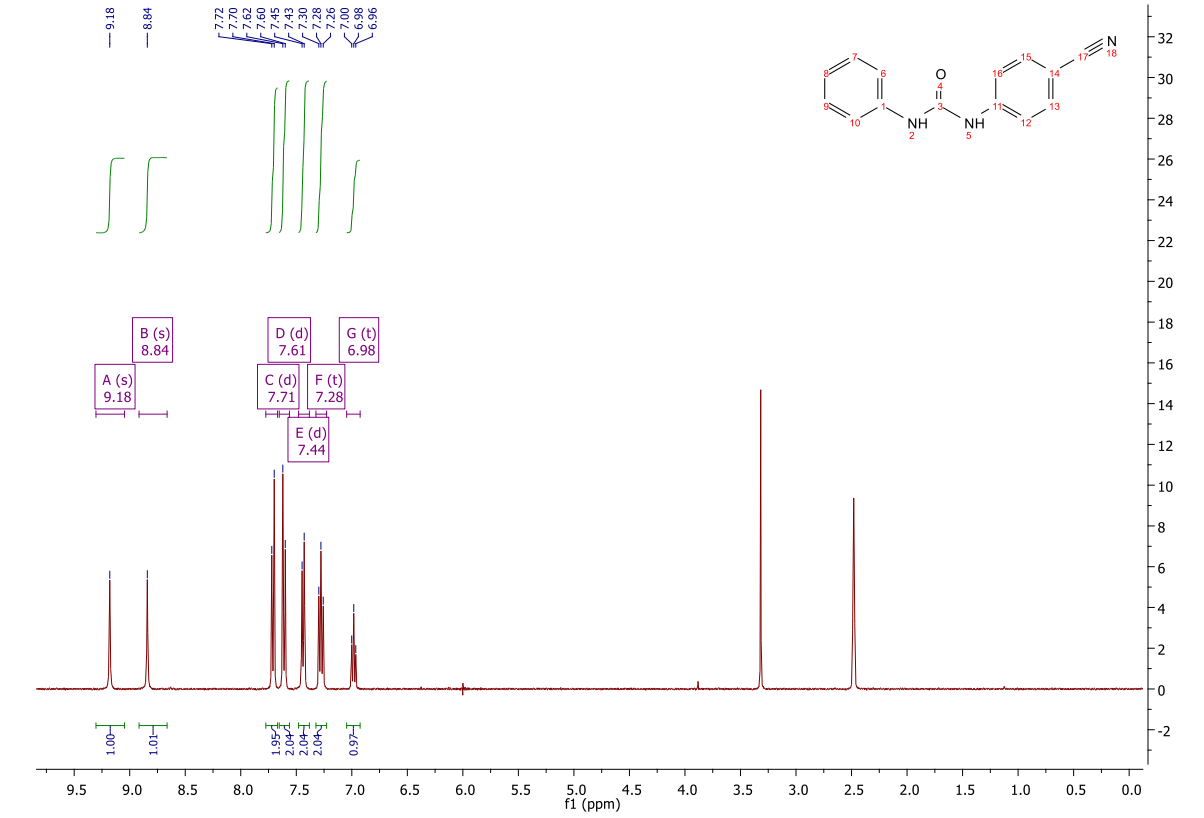
9.18
8.84
7.72
7.70
7.62
7.60
7.45
7.43
7.30
7.28
7.26
7.00
6.98
6.96
A (s) 9.18
B (s) 8.84
C (d) 7.71
D (d) 7.61
E (d) 7.44
F (t) 7.28
G (t) 6.98
1.00
1.01
1.95
2.04
2.04
2.04
0.97
f1 (ppm)

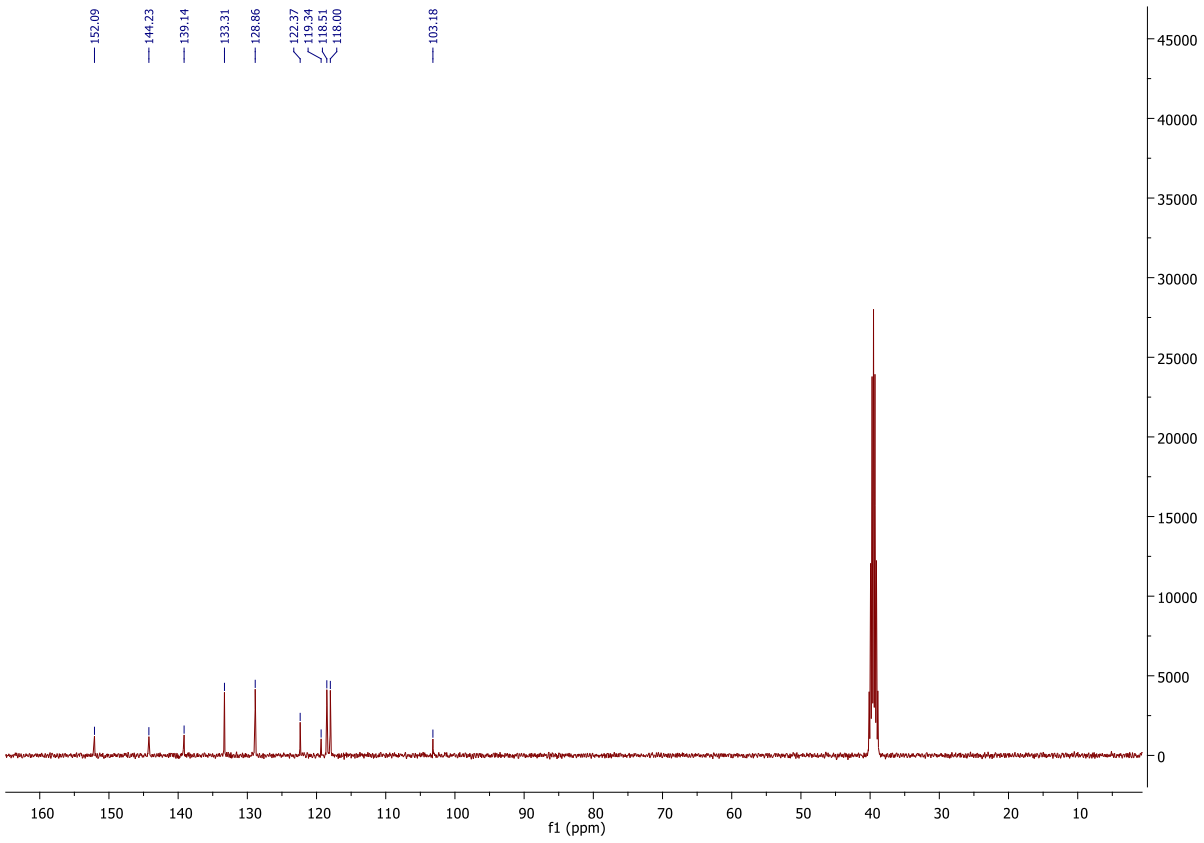
152.09
144.23
139.14
133.31
128.86
122.37
119.34
118.51
118.00
103.18
f1 (ppm)

Synthesis of 1-(2,4-dichlorophenyl)-3-phenylurea (12)

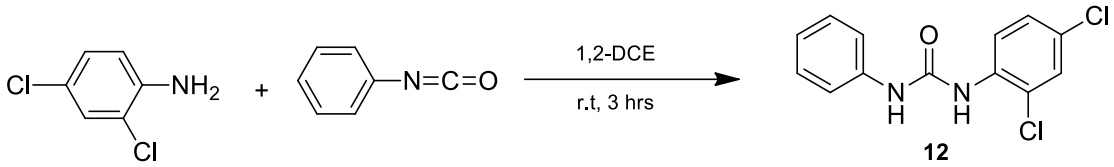

Yield: 48%

Melting point: 223-226°C

MS (ESI): $[M+H]^+ = 281.27$

^{1}H NMR (400 MHz, DMSO) δ 9.42 (s, 1H, N<u>H</u>-Cq$_{Ar}$-Cq$_{Ar}$-Cl), 8.37 (s, 1H, N<u>H</u>-Cq$_{Ar}$-CH$_{Ar}$), 8.19 (d, *J* = 9.0 Hz, 1H, C<u>H$_{Ar}$</u>-Cq$_{Ar}$-Cl), 7.60 (d, *J* = 2.4 Hz, 1H, C<u>H$_{Ar}$</u>-Cq$_{Ar}$- Cq$_{Ar}$-Cl), 7.46 – 7.41 (m, 2H, 2C<u>H$_{Ar}$</u>-Cq$_{Ar}$-NH), 7.36 (dd, *J* = 9.0, 2.5 Hz, 1H, C<u>H$_{Ar}$</u>-CH$_{Ar}$-Cq$_{Ar}$- Cq$_{Ar}$-Cl), 7.32 – 7.24 (m, 2H, 2C<u>H$_{Ar}$</u>-CH$_{Ar}$-Cq$_{Ar}$-NH), 7.02 – 6.94 (m, 1H, C<u>H$_{Ar}$</u>-CH$_{Ar}$-CH$_{Ar}$-Cq$_{Ar}$).

^{13}C NMR (101 MHz, DMSO) δ 151.97 (<u>C</u>O), 139.24 (<u>Cq$_{Ar}$</u>-NH-CO), 135.23 (<u>Cq$_{Ar}$</u>-Cq$_{Ar}$-Cl), 128.93 (CH$_{Ar}$-CH$_{Ar}$-<u>Cq$_{Ar}$</u>-Cl), 128.56 (2<u>C</u>H$_{Ar}$-CH$_{Ar}$-Cq$_{Ar}$-NH), 127.65 (Cl-Cq$_{Ar}$-<u>C</u>H$_{Ar}$-Cq$_{Ar}$-Cl), 126.03 (<u>Cq$_{Ar}$</u>-Cl), 122.54 (<u>C</u>H$_{Ar}$-CH$_{Ar}$-CH$_{Ar}$-Cq$_{Ar}$), 122.28 (<u>C</u>H$_{Ar}$-CH$_{Ar}$-Cq$_{Ar}$-Cl), 122.05 (2<u>C</u>H$_{Ar}$-Cq$_{Ar}$-NH), 118.23 (<u>C</u>H$_{Ar}$-Cq$_{Ar}$-Cl).

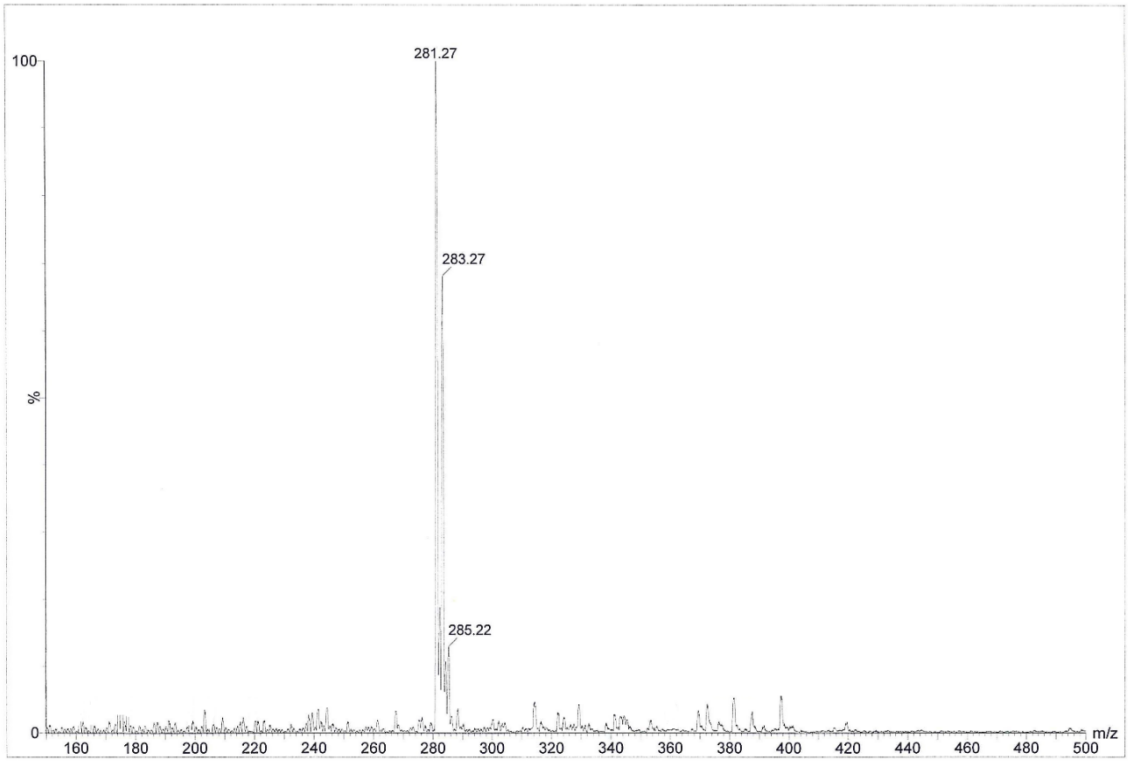

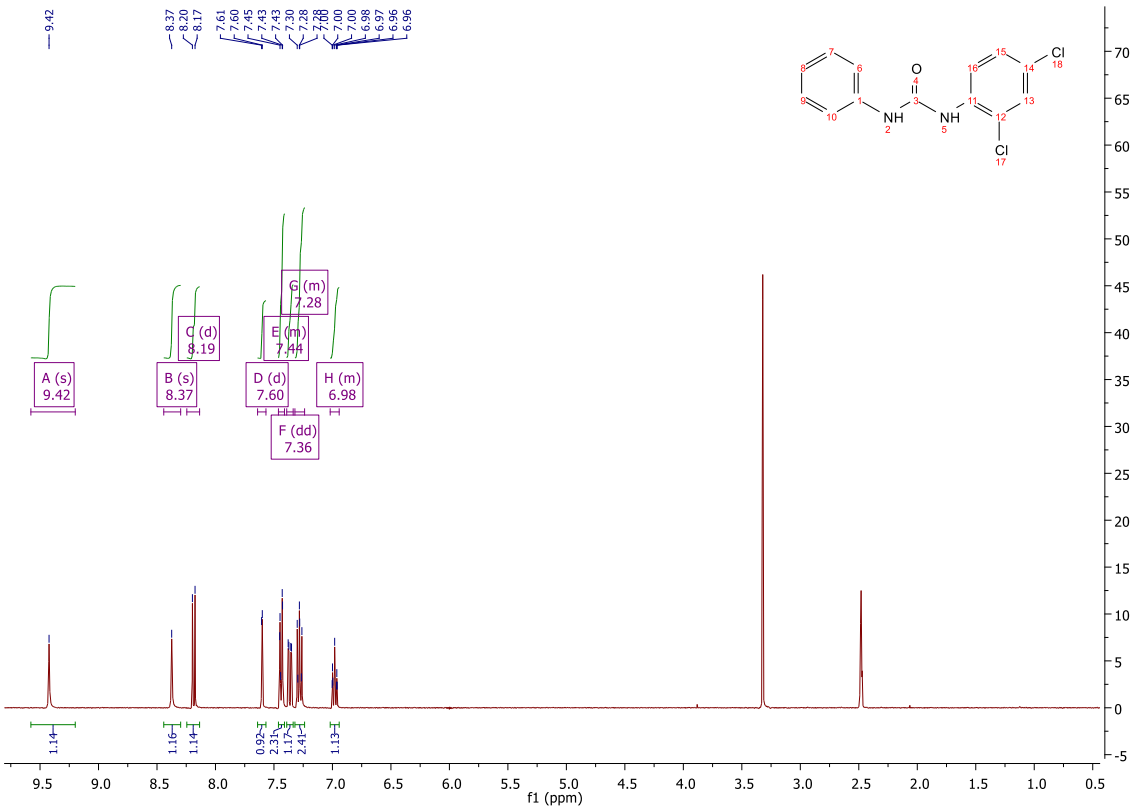
9.42
8.37
8.20
8.17
7.61
7.60
7.45
7.43
7.30
7.28
7.00
6.98
6.97
6.96
A (s) 9.42
B (s) 8.37
C (d) 8.19
D (d) 7.60
E (m) 7.44
F (dd) 7.36
G (m) 7.28
H (m) 6.98
f1 (ppm)

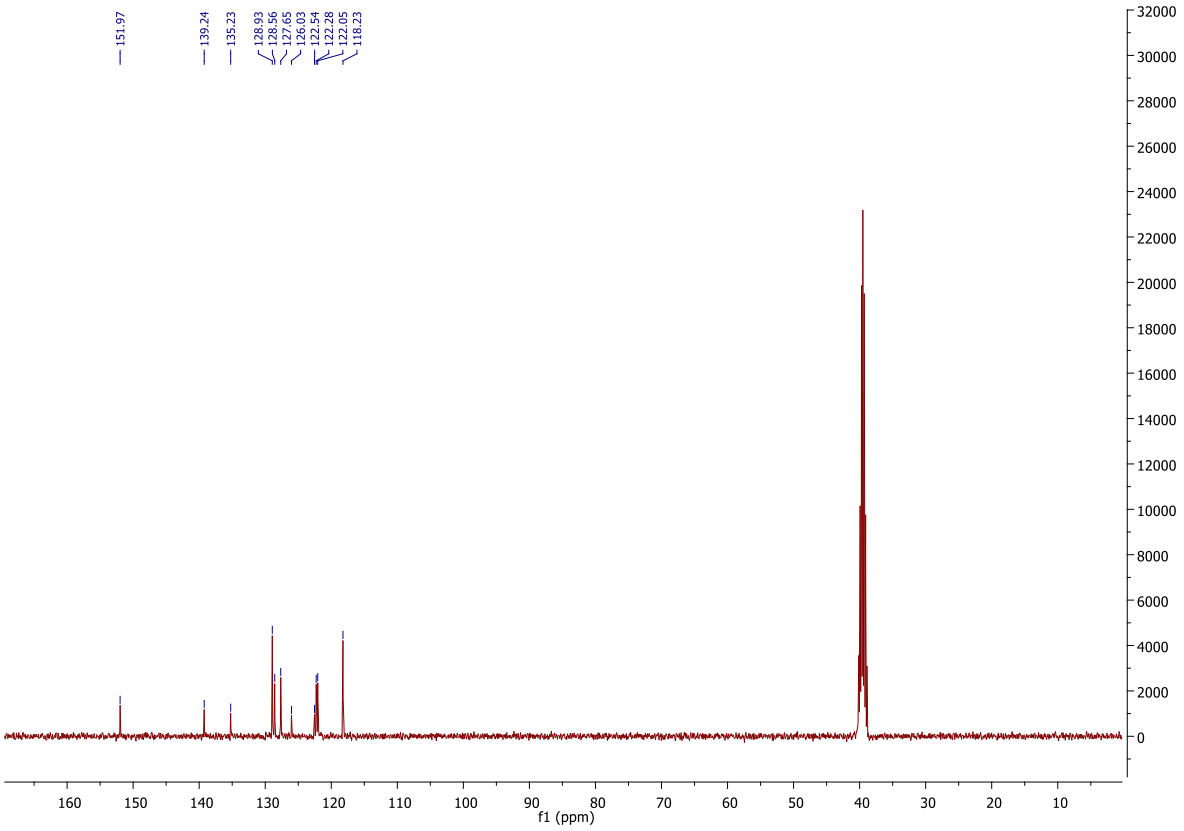
151.97
139.24
135.23
128.93
128.56
127.65
126.03
122.54
122.28
122.05
118.23
f1 (ppm)

Synthesis of [(Phenylamino)carbonyl]-benzamide (13)

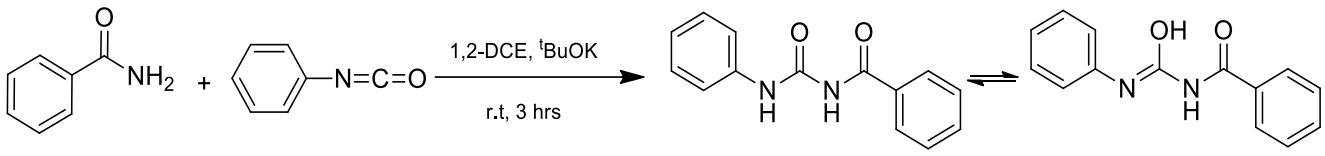

13

Yield: 68%

Melting point: 208-211°C

MS (ESI): $[M+H]^+ = 241.27$

^{1}H NMR (400 MHz, DMSO) δ 11.03 (s, 1H), 10.82 (s, 1H), 10.23 (s, 1H), 8.01 (d, *J* = 7.4 Hz, 2H), 7.93 (d, *J* = 7.1 Hz, 2H), 7.76 (d, *J* = 7.8 Hz, 2H), 7.64 (t, *J* = 7.4 Hz, 1H), 7.60 – 7.46 (m, 7H), 7.34 (td, *J* = 7.8, 4.4 Hz, 4H), 7.09 (dd, *J* = 13.2, 7.1 Hz, 2H).

^{13}C NMR (101 MHz, DMSO) δ 168.61, 165.45, 151.01, 139.07, 137.52, 134.88, 132.97, 132.18, 131.46, 128.91, 128.50, 128.29, 128.21, 127.55, 123.67, 123.55, 120.23, 119.74.

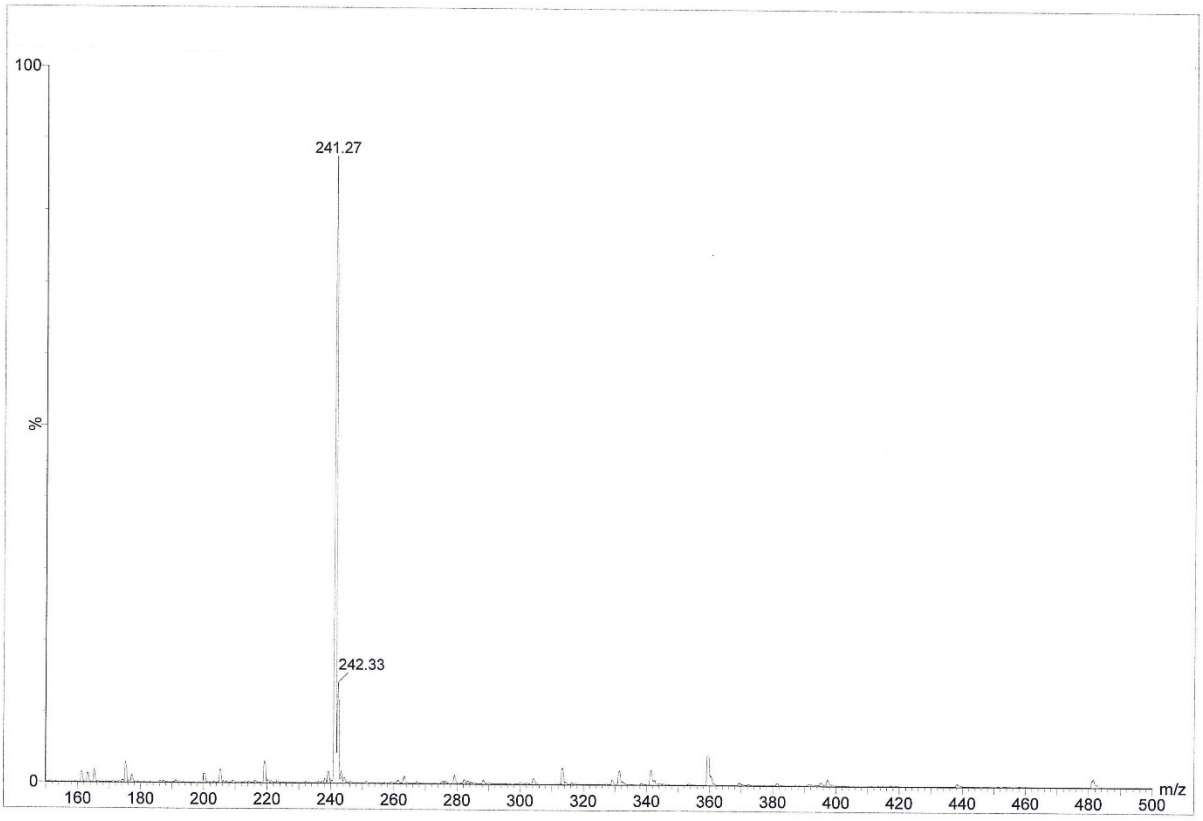

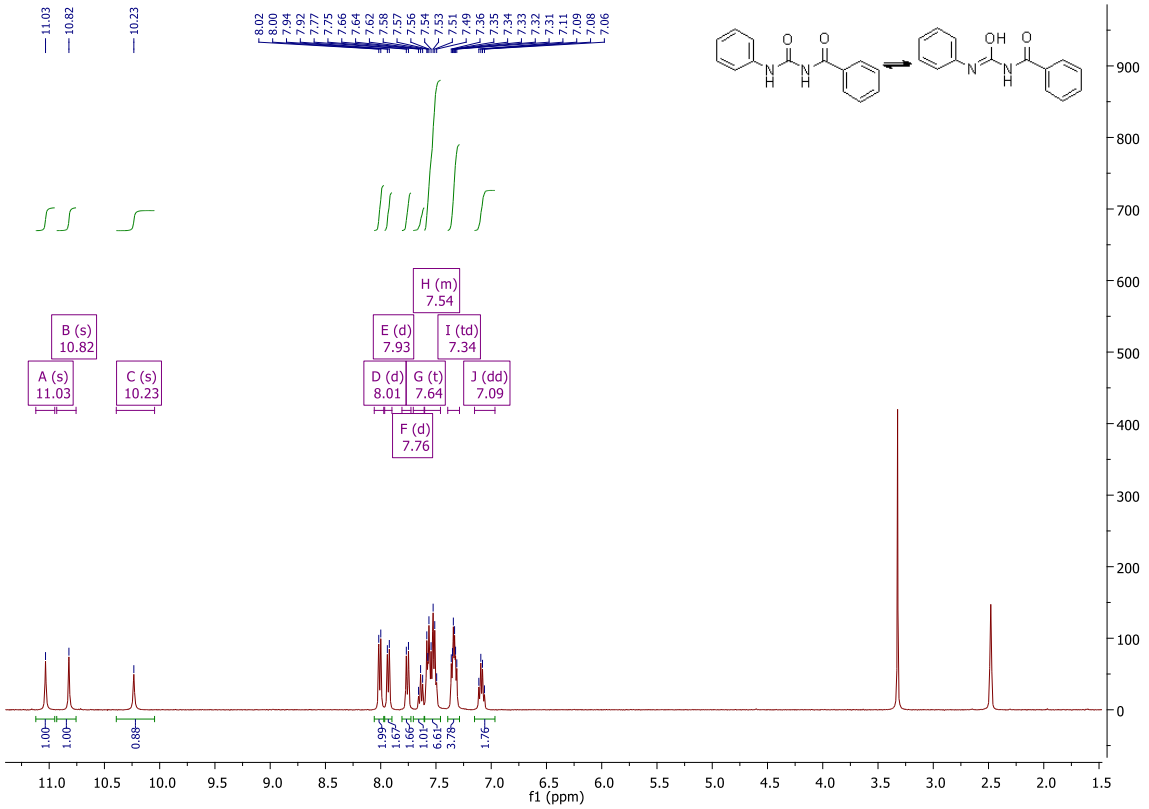
11.03
10.82
10.23
8.02
8.00
7.94
7.92
7.77
7.75
7.66
7.64
7.62
7.58
7.57
7.56
7.54
7.53
7.51
7.49
7.36
7.35
7.34
7.33
7.32
7.31
7.11
7.09
7.08
7.06
H (m) 7.54
B (s) 10.82
E (d) 7.93
I (td) 7.34
A (s) 11.03
C (s) 10.23
D (d) 8.01
G (t) 7.64
J (dd) 7.09
F (d) 7.76
1.00
1.00
0.88
1.99
1.67
1.66
1.01
6.61
3.78
1.76
f1 (ppm)

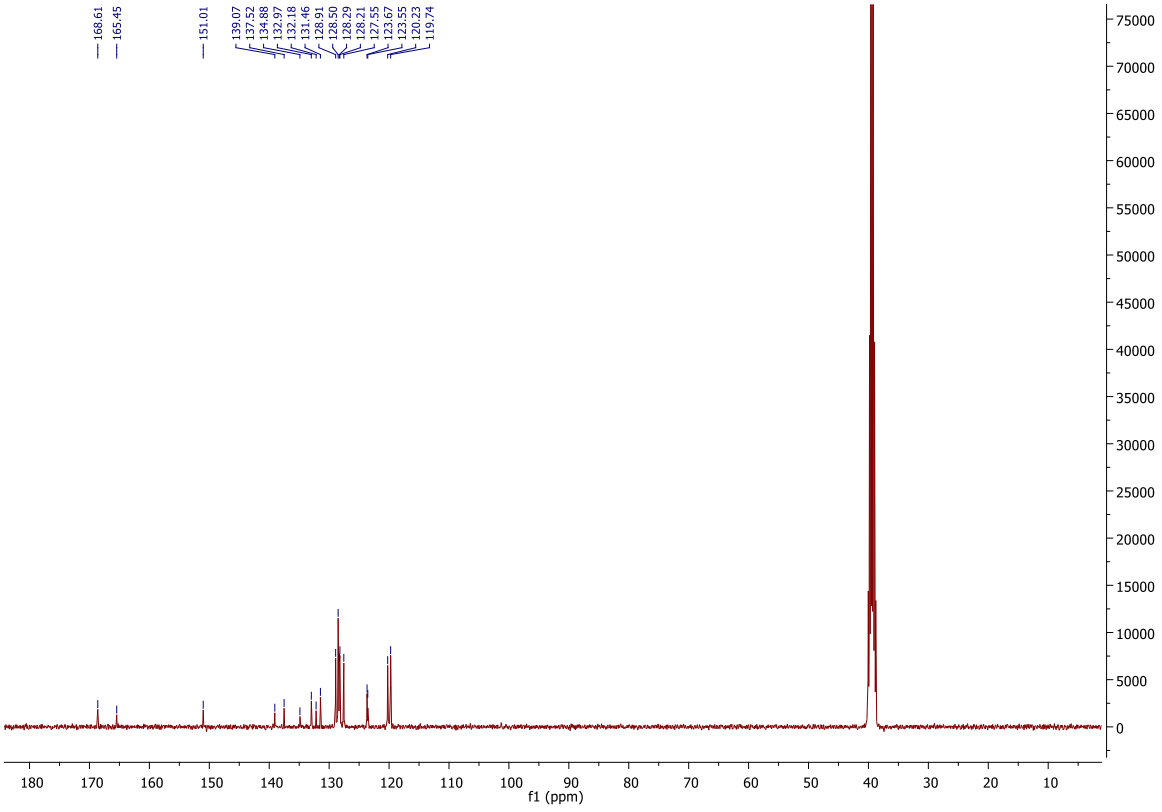
168.61
165.45
151.01
139.07
137.52
134.88
132.97
132.18
131.46
128.91
128.50
128.29
128.21
127.55
123.67
123.55
120.23
119.74
f1 (ppm)

Synthesis of 1,3-Dicyclohexylthiourea (14)

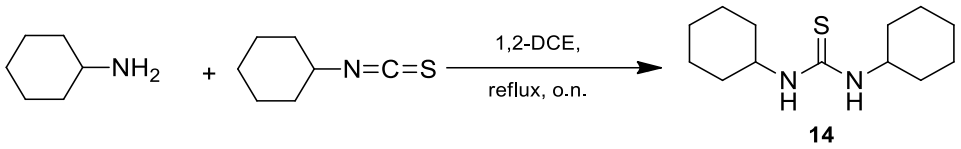

14

Yield: 88%

Melting point: 184-187°C

MS (ESI): $[M+H]^+ = 241.02$

^{1}H NMR (400 MHz, DMSO) δ 7.07 (d, *J* = 7.9 Hz, 2H, 2NH), 3.93 (s, 2H, 2CH-NH), 1.91 – 1.75 (m, 4H, 4CH_2-CH-NH), 1.69 – 1.58 (m, 4H, 4CH_2-CH-NH), 1.56 – 1.44 (m, 2H, 2CH_2-CH_2-CH_2-CH), 1.32 – 1.02 (m, 10H, 4CH_2-CH_2-CH; 2CH_2-CH_2-CH_2-CH).

^{13}C NMR (101 MHz, DMSO-d_6) δ 179.93 (CS), 51.47 (2CH-NH), 32.37 (2CH_2-CH), 25.22 (2CH_2-CH_2-CH_2-CH), 24.51 (2CH_2-CH_2-CH).

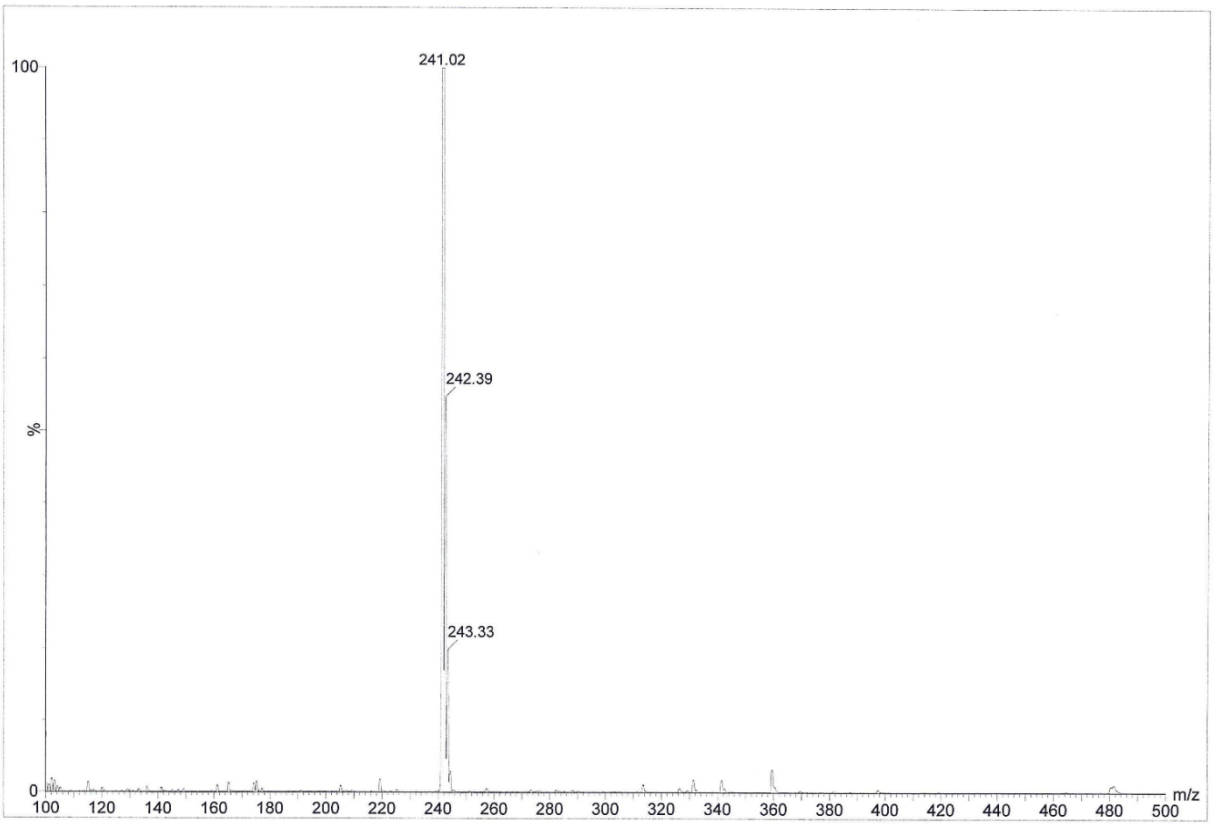

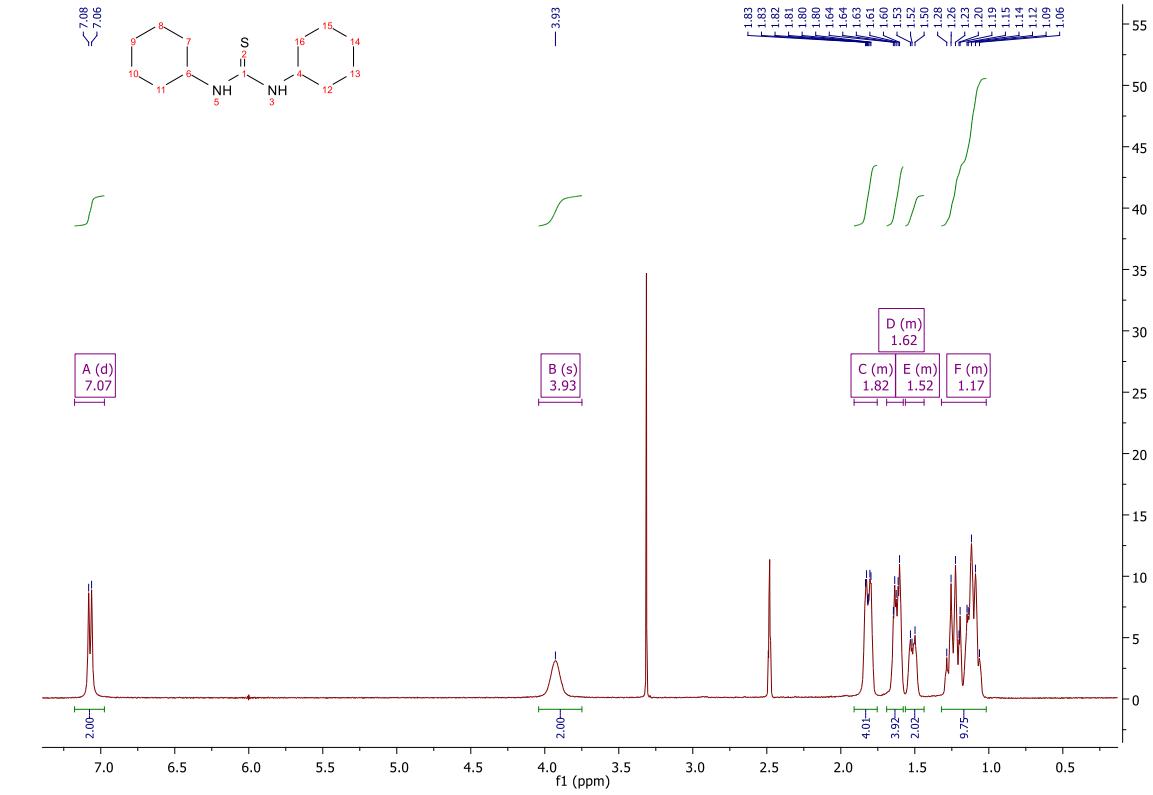
7.08
7.06
3.93
1.83
1.82
1.81
1.80
1.64
1.63
1.61
1.60
1.53
1.52
1.50
1.28
1.26
1.23
1.20
1.19
1.15
1.14
1.12
1.09
1.06
A (d)
7.07
B (s)
3.93
D (m)
1.62
C (m)
1.82
E (m)
1.52
F (m)
1.17
2.00
2.00
4.01
3.92
2.02
9.75
f1 (ppm)

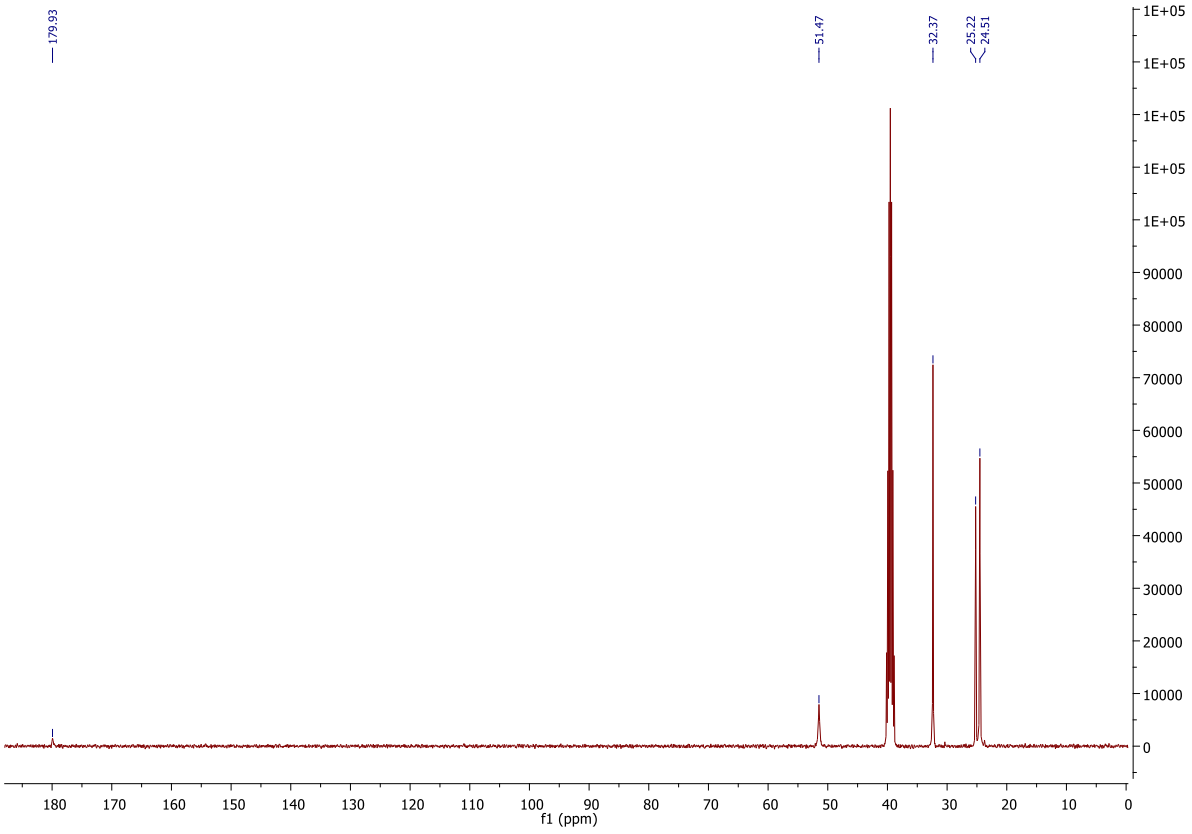
179.93
51.47
32.37
25.22
24.51
f1 (ppm)

Synthesis of 1,3-dibenzyl-thiourea (15)

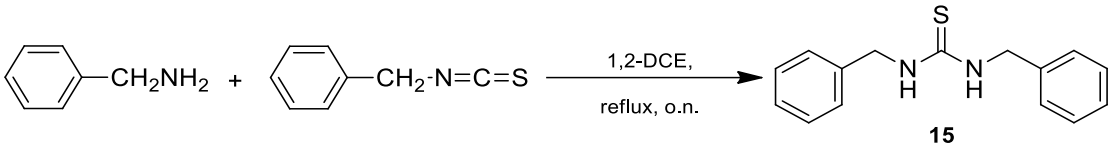

Yield: 89%

Melting point: 169-173°C

MS (ESI): $[M+H]^+ = 257.07$

^{1}H NMR (400 MHz, DMSO) δ 7.96 (s, 2H, 2NH), 7.48 – 7.04 (m, 10H, 10CH_{Ar}), 4.68 (s, 4H, 2CH_2-NH).

^{13}C NMR (101 MHz, DMSO) δ 171.25 (CS), 139.15 (2Cq_{Ar}), 128.15 (4CH_{Ar}-CH_{Ar}-Cq_{Ar}), 127.10 (4CH_{Ar}-Cq_{Ar}), 126.72 (2CH_{Ar}-CH_{Ar}-CH_{Ar}-Cq_{Ar}), 46.95 (2CH_2).

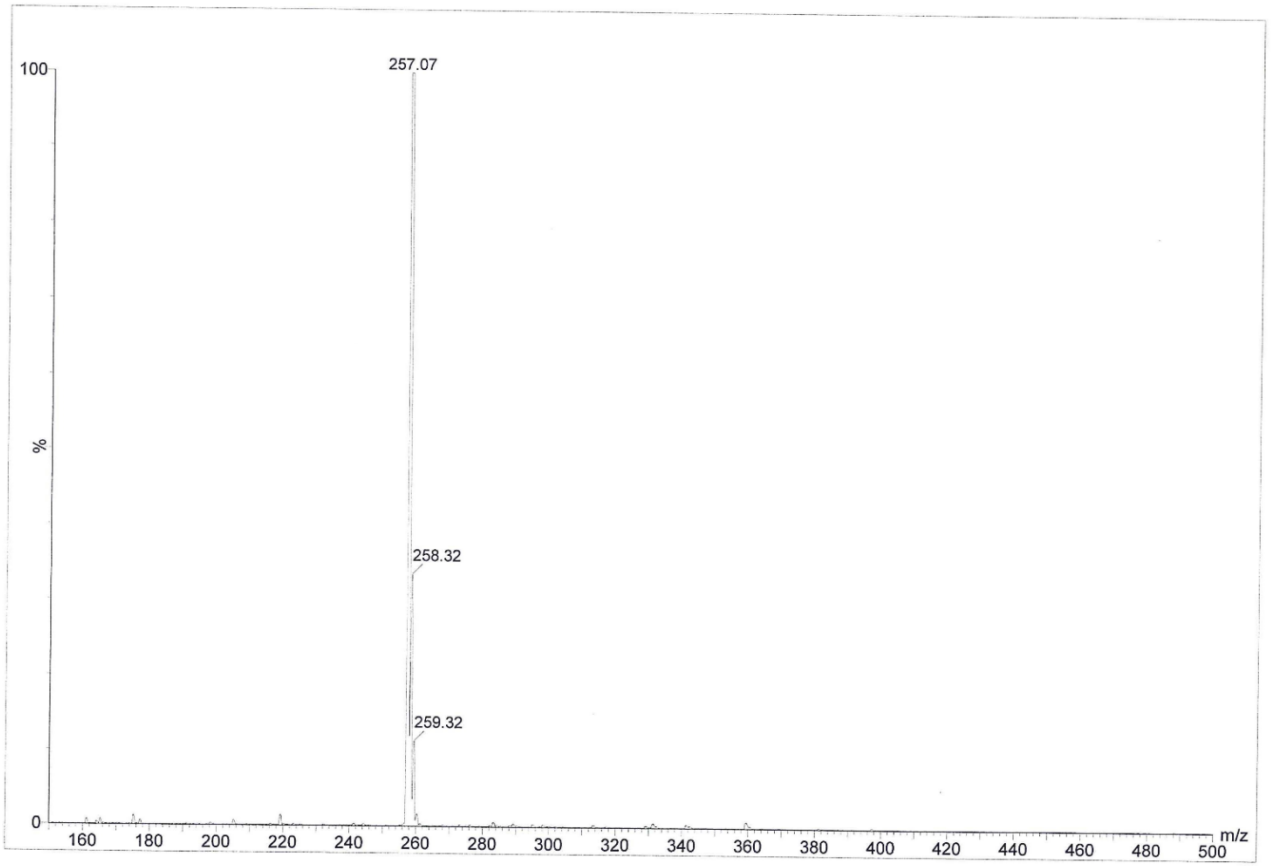

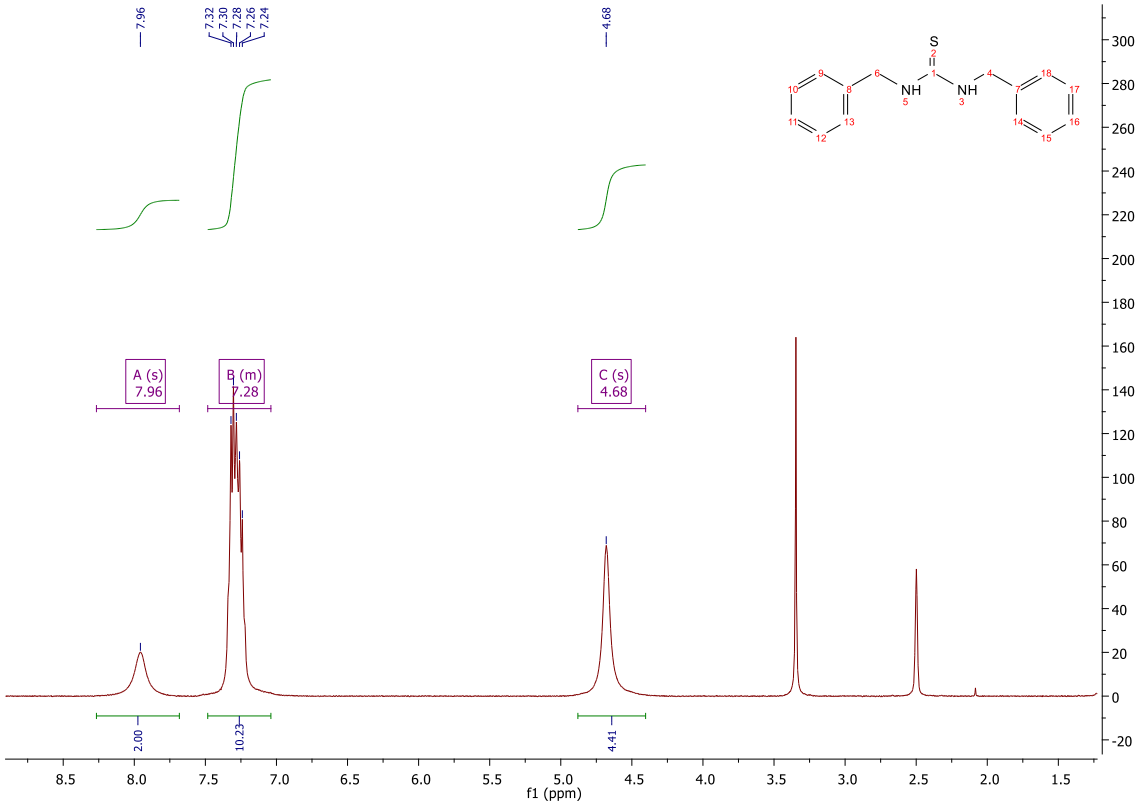
7.96
7.32
7.30
7.28
7.26
7.24
4.68
A (s)
7.96
B (m)
7.28
C (s)
4.68
2.00
10.23
4.41
f1 (ppm)

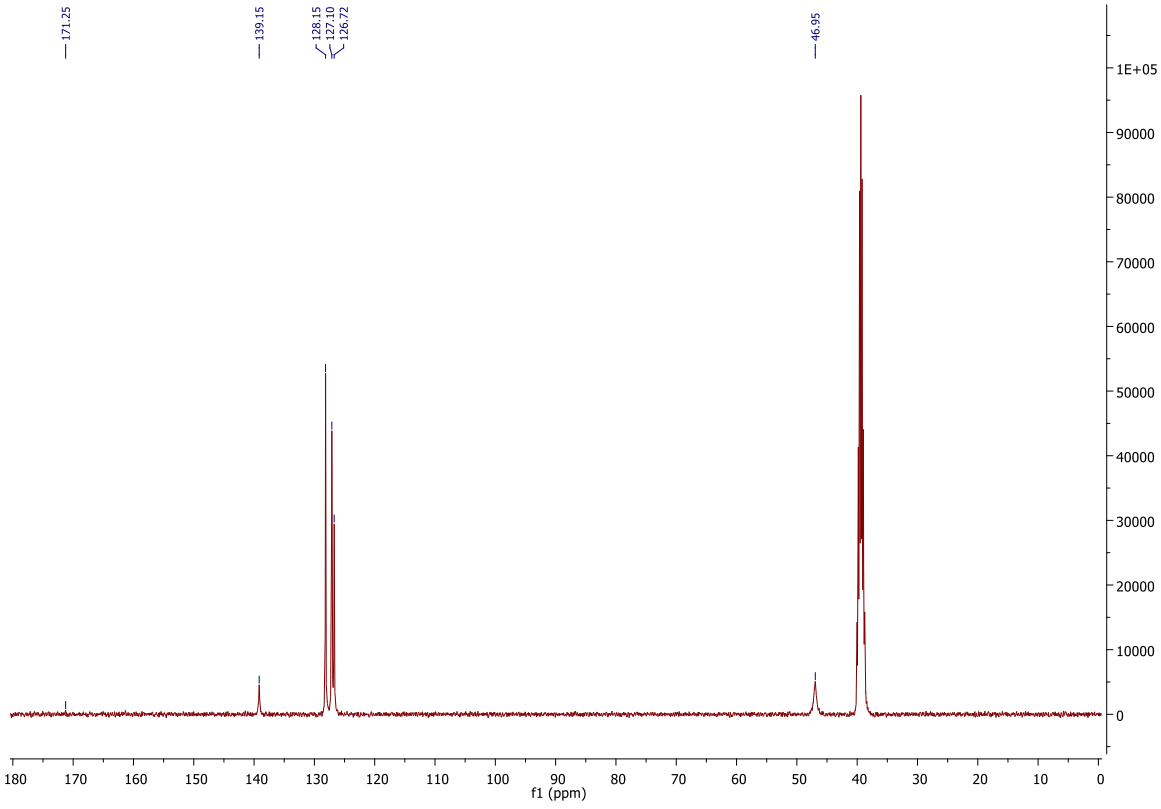
171.25
139.15
128.15
127.10
126.72
46.95
f1 (ppm)

Synthesis of 1-cyclohexyl-3-phenyl-thiourea (16)

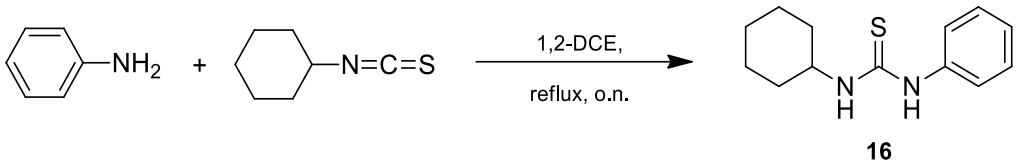

16

Yield: 15%

Melting point: 143-148°C

MS (ESI): $[M+H]^+ = 235.32$

^{1}H NMR (400 MHz, DMSO) δ 9.36 (s, 1H, N<u>H</u>-Cq$_{Ar}$), 7.64 (d, *J* = 8.2 Hz, 1H, N<u>H</u>-CH), 7.43 (d, *J* = 7.9 Hz, 2H, 2C<u>H$_{Ar}$</u>-Cq$_{Ar}$), 7.27 (t, *J* = 7.8 Hz, 2H, 2C<u>H$_{Ar}$</u>-CH$_{Ar}$-Cq$_{Ar}$), 7.05 (t, *J* = 7.2 Hz, 1H, C<u>H$_{Ar}$</u>-CH$_{Ar}$-CH$_{Ar}$-Cq$_{Ar}$), 4.06 (s, 1H, C<u>H</u>-NH), 1.88 (d, *J* = 9.5 Hz, 2H, 2C<u>H$_2$</u>-CH), 1.66 (dd, *J* = 8.8, 3.0 Hz, 2H, 2C<u>H$_2$</u>-CH), 1.54 (d, *J* = 13.0 Hz, 1H, C<u>H$_2$</u>-CH$_2$-CH$_2$-CH), 1.35 – 1.05 (m, 5H, 2C<u>H$_2$</u>-CH$_2$-CH; C<u>H$_2$</u>-CH$_2$-CH$_2$-CH).

^{13}C NMR (101 MHz, DMSO) δ 179.15 (<u>C</u>S), 139.59 (<u>Cq$_{Ar}$</u>), 128.42 (2<u>C</u>H$_{Ar}$-CH$_{Ar}$-Cq$_{Ar}$), 123.73 (<u>C</u>H$_{Ar}$-CH$_{Ar}$-CH$_{Ar}$-Cq$_{Ar}$), 122.61 (2<u>C</u>H$_{Ar}$-Cq$_{Ar}$), 52.09 (<u>C</u>H-NH), 31.86 (2<u>C</u>H$_2$-CH), 25.17(<u>C</u>H$_2$-CH$_2$-CH$_2$-CH), 24.53(2<u>C</u>H$_2$-CH$_2$-CH).

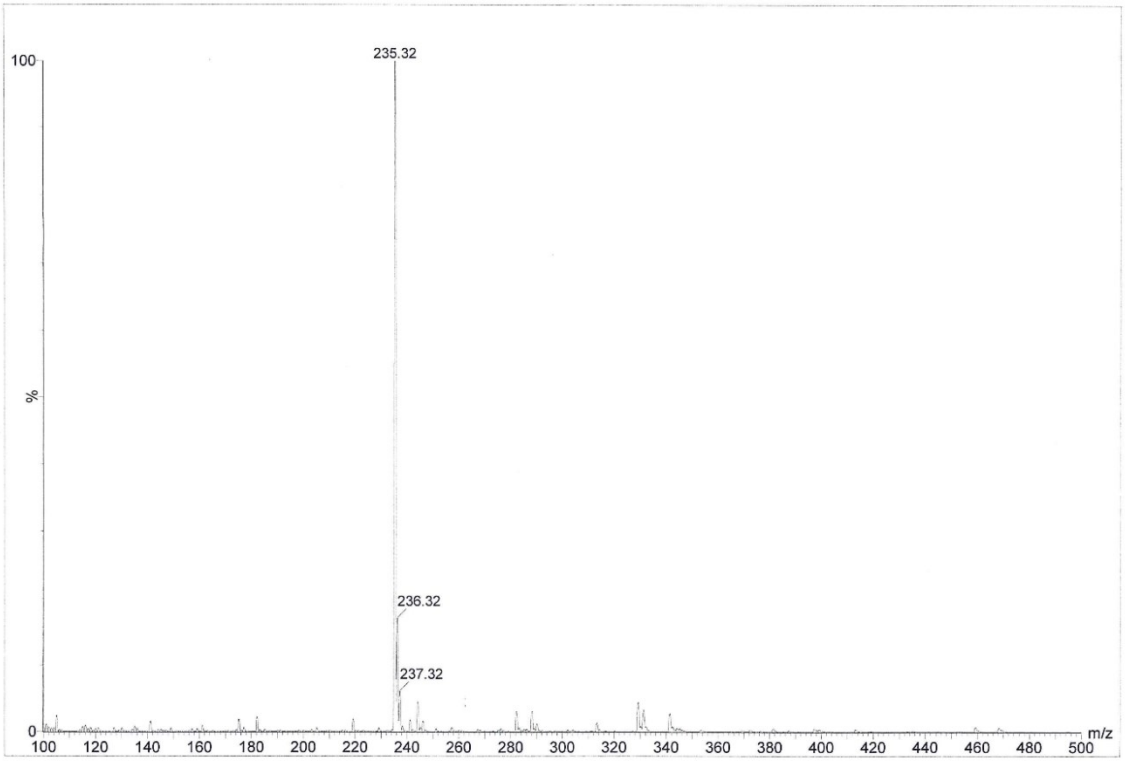

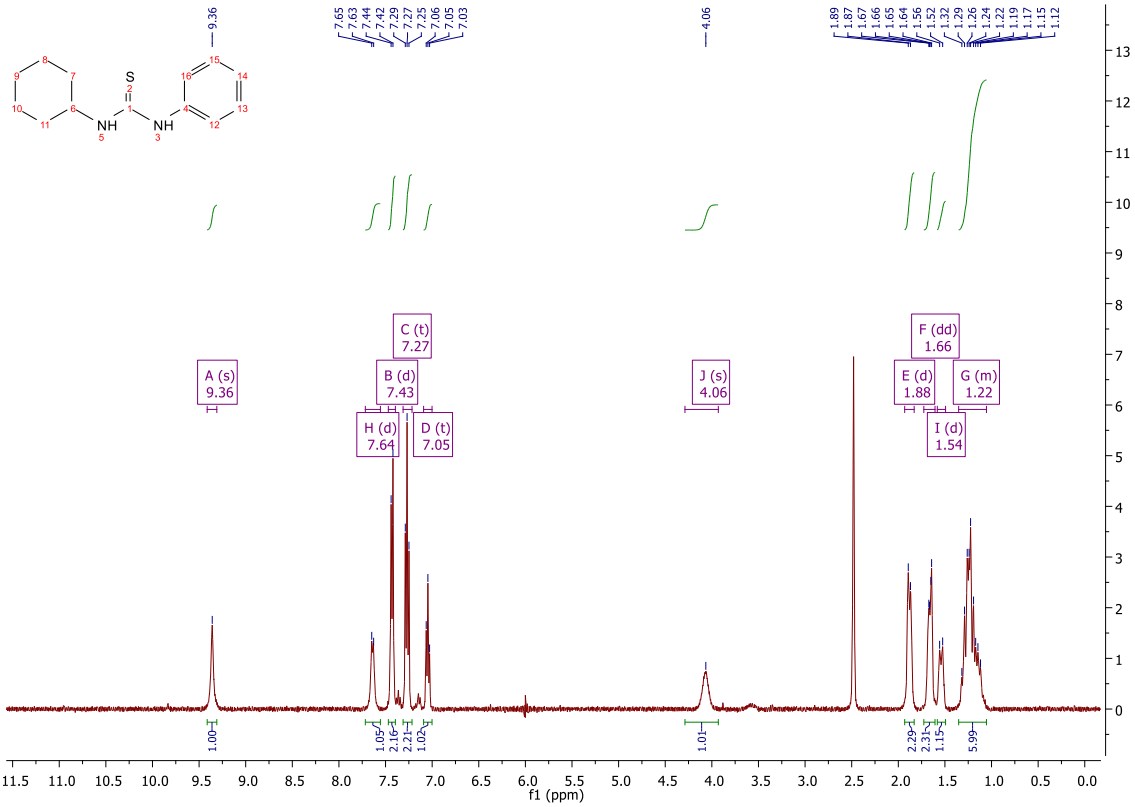
A (s)
9.36
B (d)
7.43
C (t)
7.27
D (t)
7.05
H (d)
7.64
J (s)
4.06
E (d)
1.88
F (dd)
1.66
G (m)
1.22
I (d)
1.54
f1 (ppm)

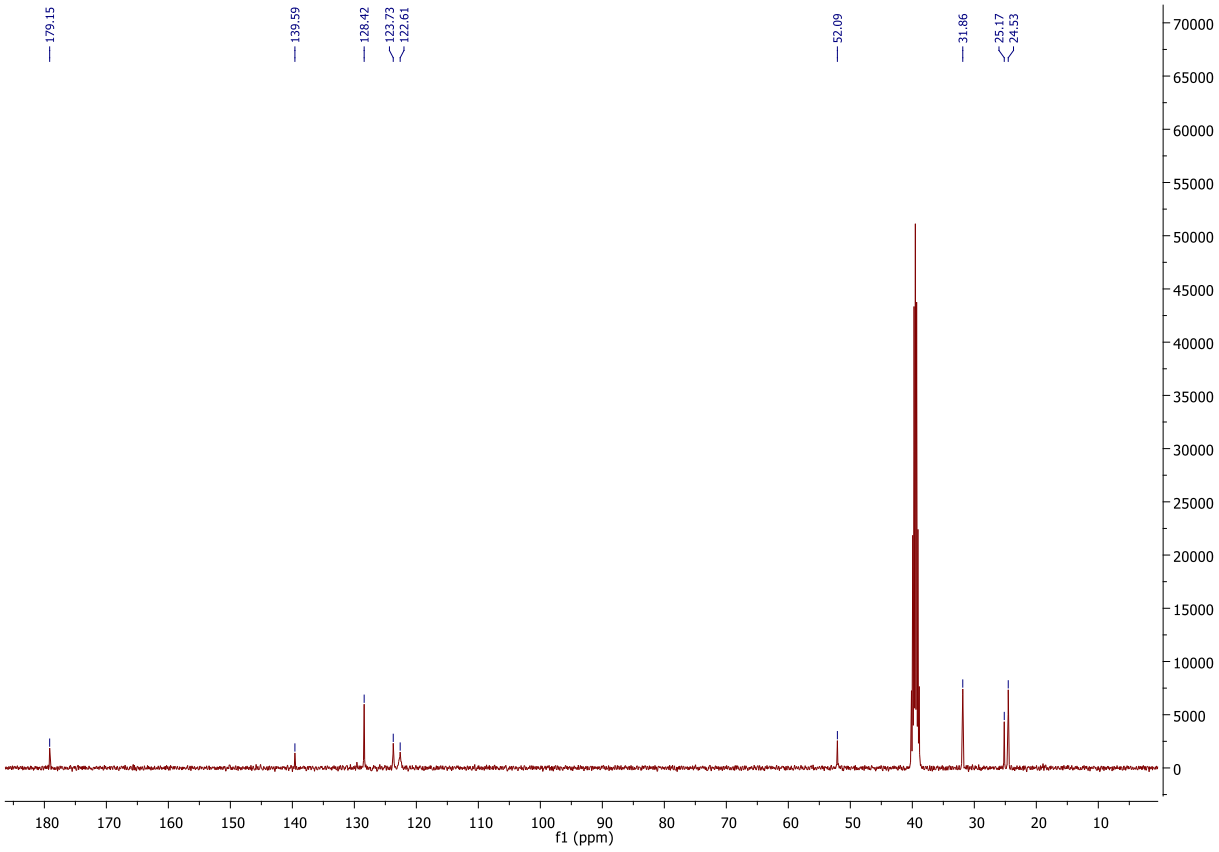
179.15
139.59
128.42
123.73
122.61
52.09
31.86
25.17
24.53
f1 (ppm)

14.3 Carbamates

Carbamates **17** and **18** were produced by reaction of either aryl- or cyclohexyl-amine with di-*tert*-butyl dicarbonate (Figure 92). The nitrogen lone pair in primary amine attacks a carbonyl group of di-*tert*-butyl dicarbonate. The leaving group, the *tert*-butyl carbonate anion, decomposes to give carbon dioxide and *tert*-butanol.

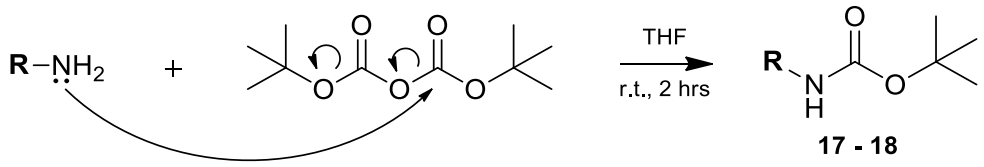

Figure 92: Reaction mechanism for synthesis of carbamates

The general procedure of carbamates synthesis was as follow: to solution of amine (1 eq) in THF (10 mL) was added di-*tert*-butyl dicarbonate (0.5720 g, 2.62 mmol, 1 eq). The solution was then stirred at room temperature for 2 hours. After the reaction was complete as indicated by TLC, the solution was evaporated to afford the product as a white solid.

Synthesis of *tert*-butyl cyclohexylcarbamate (17)

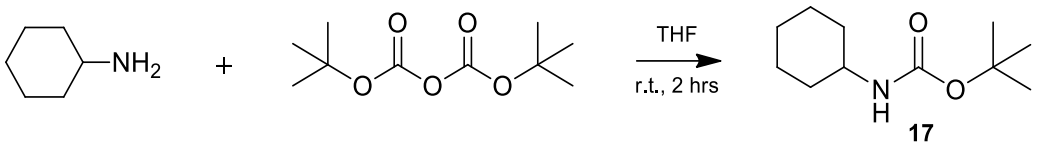

17

Yield: 88%

Melting point: 78-80°C

MS (ESI): $[M+H]^+ = 200.36$

^{1}H NMR (400 MHz, $CDCl_3$) δ 4.45 (s, 1H, NH), 3.58 – 3.13 (m, 1H, CH), 1.98 – 1.76 (m, *J* = 12.3, 3.0 Hz, 2H, 2CH_2-CH), 1.74 – 1.60 (m, 2H, 2CH_2-CH), 1.58 – 1.51 (m, 1H, CH_2-CH_2-CH_2-CH), 1.39 (s, 9H, 3CH_3), 1.34 – 1.19 (m, 2H, 2CH_2-CH_2-CH), 1.16 – 0.98 (m, 3H, 2CH_2-CH_2-CH; CH_2-CH_2-CH_2-CH).

^{13}C NMR (101 MHz, $CDCl_3$) δ 155.14 (CO), 78.84 (Cq-O-CO), 49.36 (CH-NH-CO), 33.49 (2CH_2-CH), 28.38 (3CH_3), 25.49 (CH_2-CH_2-CH_2-CH), 24.87 (2CH_2-CH_2-CH).

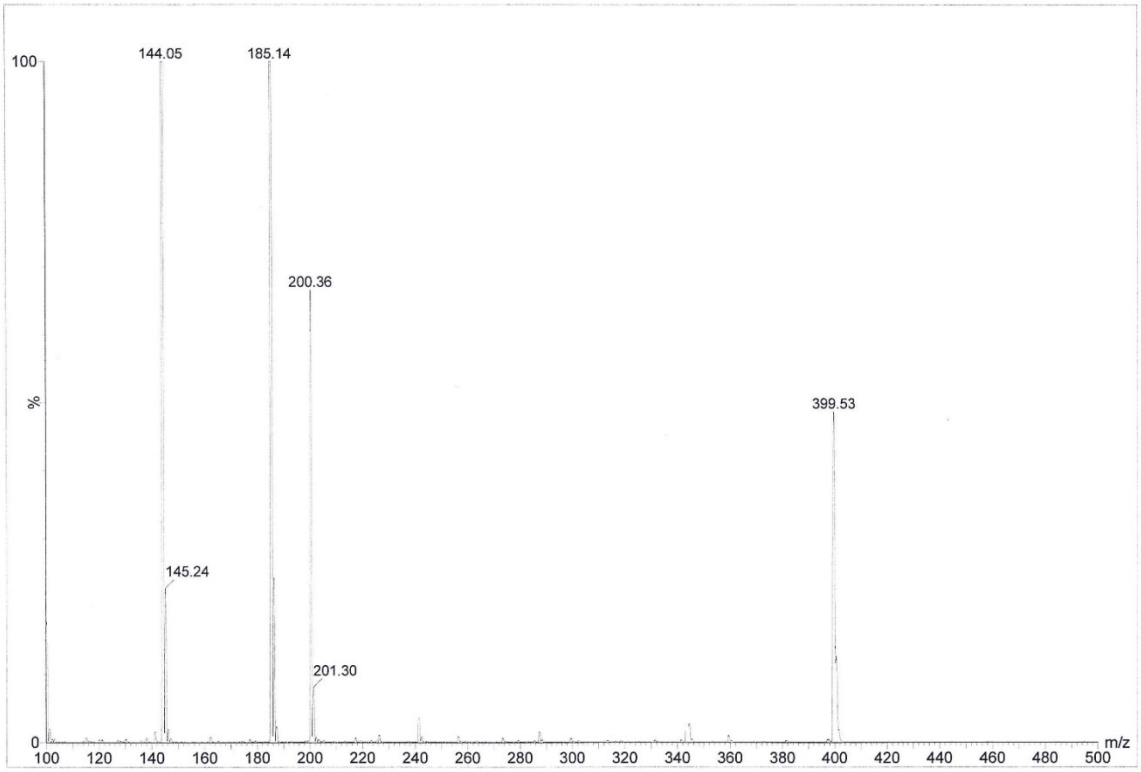

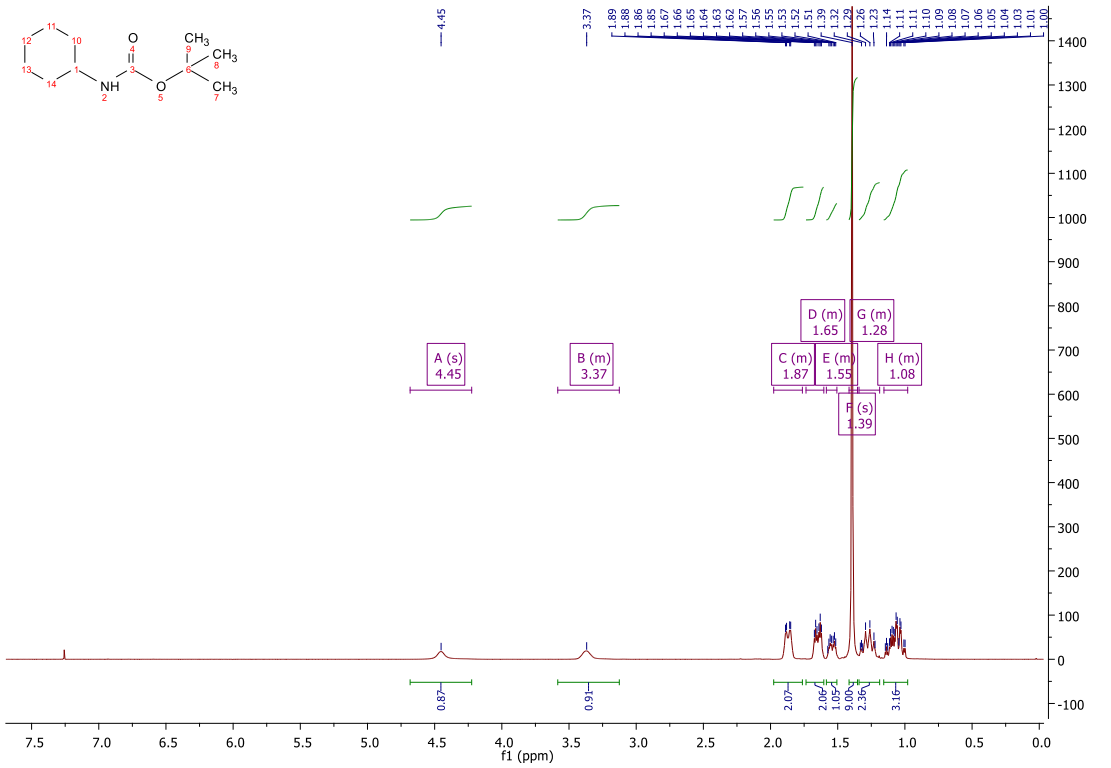
4.45
3.37
A (s) 4.45
B (m) 3.37
C (m) 1.87
D (m) 1.65
E (m) 1.55
F (s) 1.39
G (m) 1.28
H (m) 1.08
0.87
0.91
2.07
2.06
1.05
9.00
2.36
3.16
f1 (ppm)

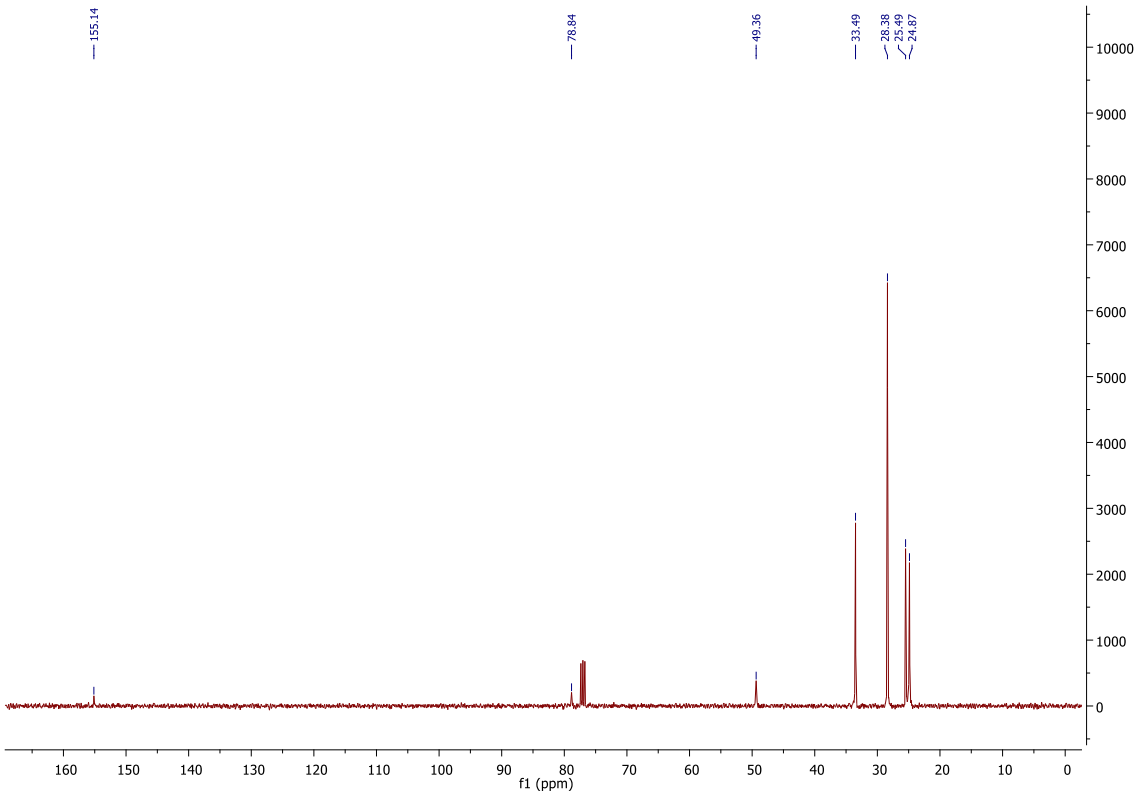
155.14
78.84
49.36
33.49
28.38
25.49
24.87
f1 (ppm)

Synthesis of *tert*-butyl phenylcarbamate (18)

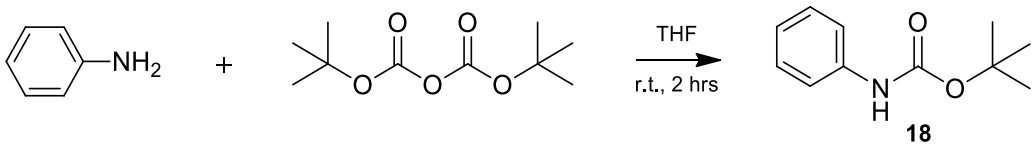

18

Yield: 82%

Melting point: 135-137°C

MS (ESI): $[M+H]^+ = 194.28$

^{1}H NMR (400 MHz, DMSO) δ 9.32 (s, 1H, N<u>H</u>-Cq$_{Ar}$), 7.44 (d, *J* = 7.8 Hz, 2H, 2C<u>H$_{Ar}$</u>-Cq$_{Ar}$), 7.27 – 7.19 (m, 2H, 2C<u>H$_{Ar}$</u>-CH$_{Ar}$-Cq$_{Ar}$), 6.98 – 6.90 (m, 1H, C<u>H$_{Ar}$</u>-CH$_{Ar}$-CH$_{Ar}$-Cq$_{Ar}$), 1.47 (s, 9H, 3CH$_3$).

^{13}C NMR (101 MHz, DMSO) δ 152.64 (<u>C</u>O), 139.39 (<u>Cq$_{Ar}$</u>-NH), 128.49 (2<u>C</u>H$_{Ar}$-CH$_{Ar}$-Cq$_{Ar}$), 121.87 (<u>C</u>H$_{Ar}$-CH$_{Ar}$-CH$_{Ar}$-Cq$_{Ar}$), 117.94 (2<u>C</u>H$_{Ar}$-Cq$_{Ar}$), 78.84 (<u>Cq</u>-O), 28.02 (3<u>C</u>H$_3$).

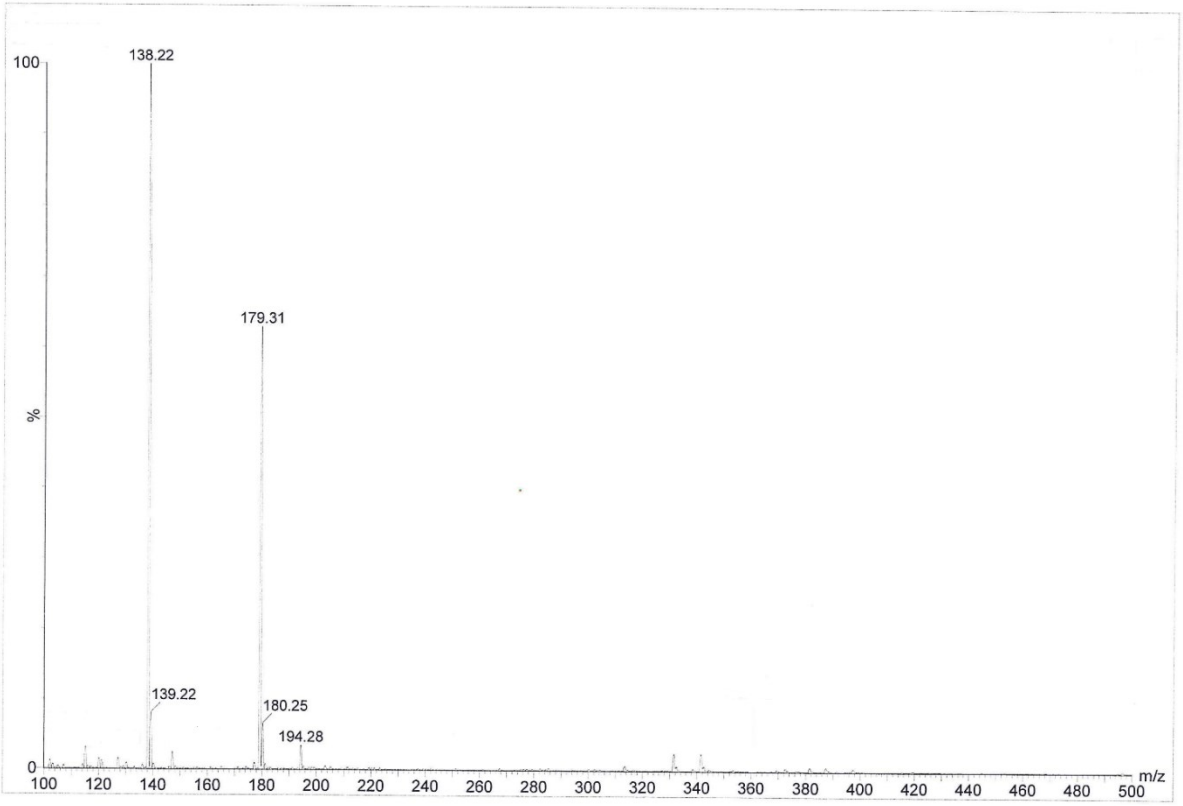

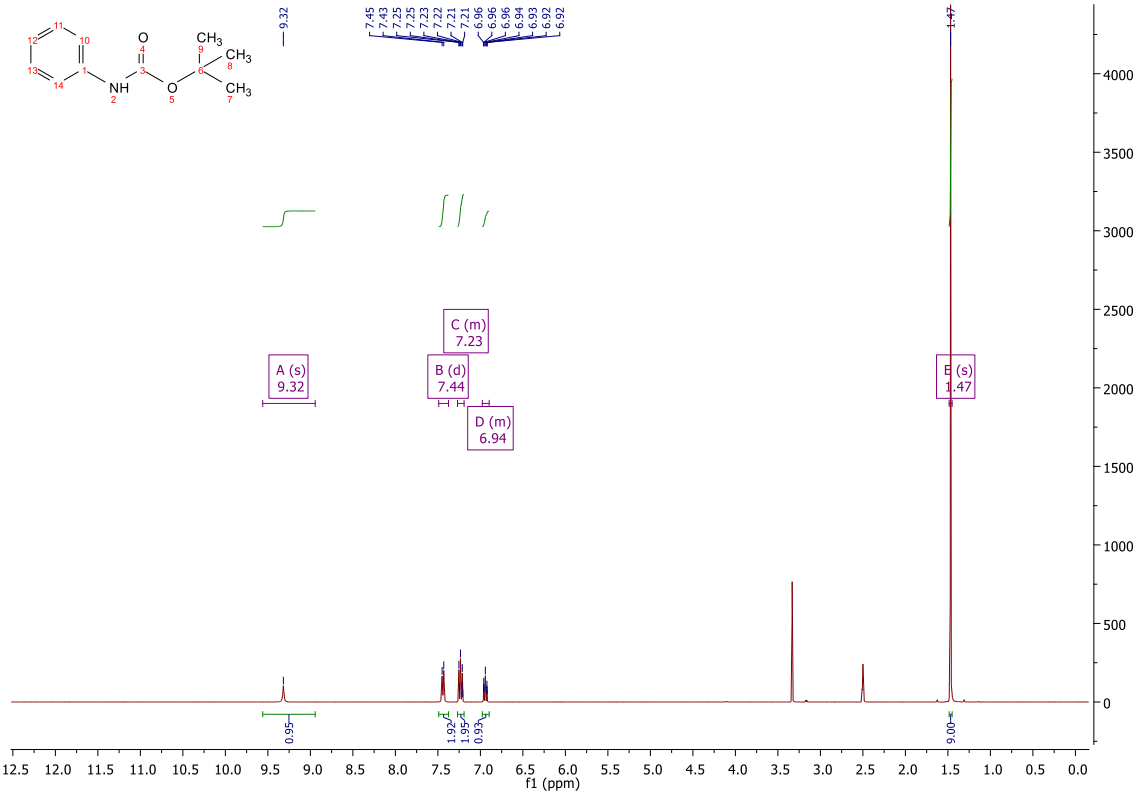
9.32
7.45
7.43
7.25
7.25
7.25
7.23
7.22
7.21
7.21
6.96
6.96
6.96
6.94
6.93
6.92
6.92
1.47
A (s)
9.32
C (m)
7.23
B (d)
7.44
D (m)
6.94
E (s)
1.47
0.95
1.92
1.95
0.93
9.00
f1 (ppm)

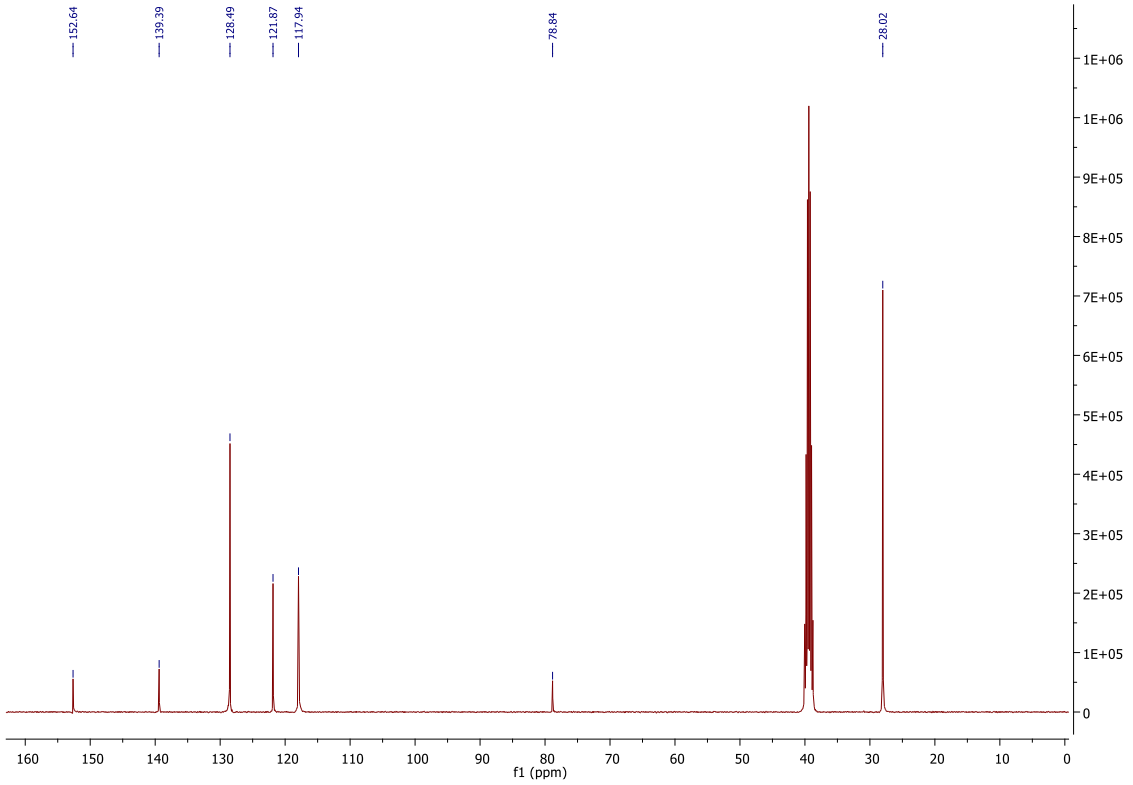
152.64
139.39
128.49
121.87
117.94
78.84
28.02
f1 (ppm)

14.4 Phenyl-1, 3, 8-triaza-spiro[4,5]decan-4-one derivatives

In order to introduce substitutions at the N-8 position, reactions with commercially available 1-phenyl-1, 3, 8–triaza-spiro[4,5]decan-4-one **28** (Figure 93) was taken into consideration. All these reactions involve economic and green reagents, are easily to conduct and purify and almost all of the reactions lead to high yields (>70%).

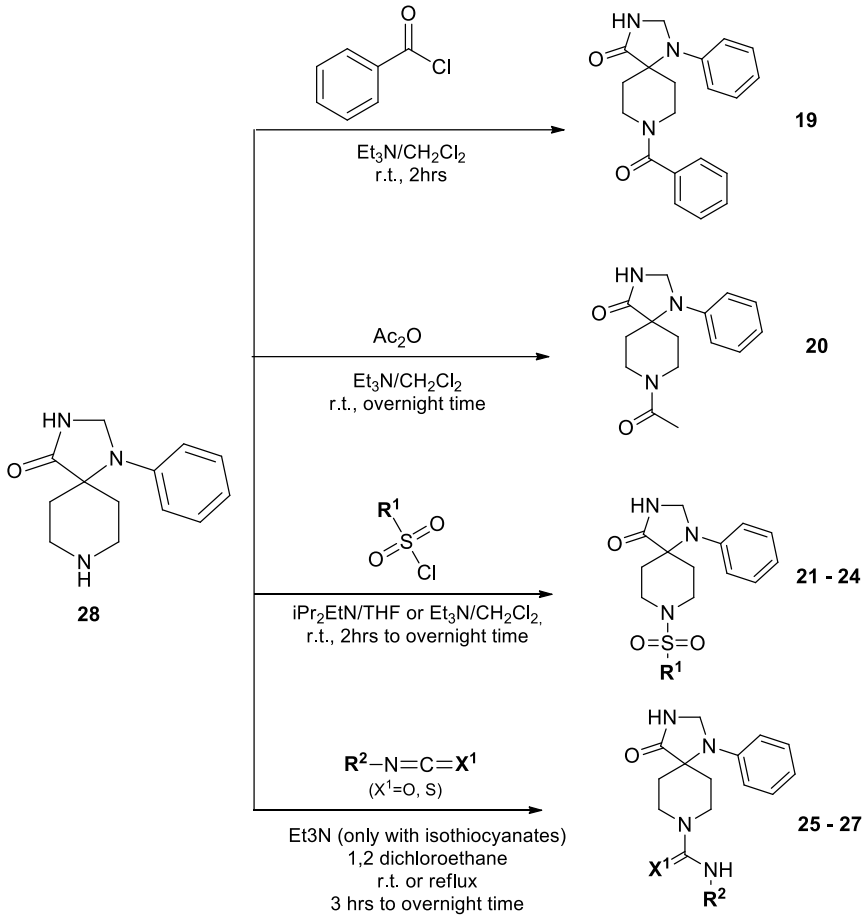

Figure 93: Different reaction pathways for the synthesis of 1-phenyl-1, 3, 8–triaza-spiro[4,5]decan-4-one derivatives

Synthesis of 1-phenyl-8-benzoyl-1, 3, 8–triaza-spiro[4,5]decan-4-one (19)

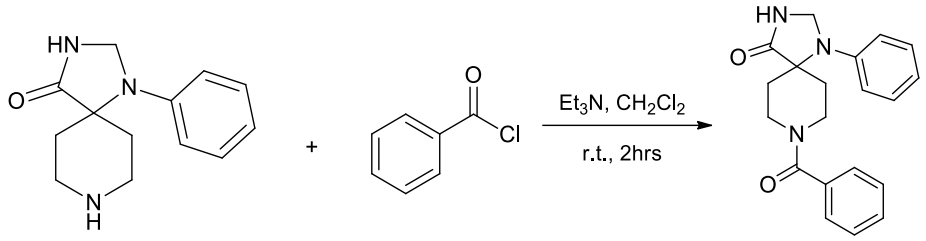

To a solution of 1-phenyl-1, 3, 8–triaza-spiro[4,5]decan-4-one (1 eq, 0.1 g, 0.4 mmol) in CH_2Cl_2 (10 ml) was added triethylamine (1.25 eq) and then benzoylchloride (1 eq). The solution was stirred at room temperature for 2 hours. After the reaction was complete as indicated by TLC, it was diluted in 30 mL of CH_2Cl_2 and washed with 1M HCl, water and brine. After anhydrification with anhydrous sodium sulfate, the solution was evaporated under reduced pressure to give compound **19** as a white solid.

Yield: 80%

Melting point: 215-225°C

MS (ESI): $[M+H]^+ = 336.29$

^{1}H NMR (400 MHz, CD_3OD) δ 7.53 – 7.36 (m, 5H, CH_{Ar}), 7.35 – 7.20 (m, 2H, CH_{Ar}), 6.97 – 6.75 (m, 3H, CH_{Ar}), 4.70 (m, 2H, NH-CH_2), 4.52 (m, 1H, CH-N-CO), 3.87 (m, 1H, CH-N-CO), 3.69 (m, 2H, CH_2-N-CO), 2.75 – 2.54 (m, 1H, CH-Cq), 2.39 (td, J = 13.3, 5.0 Hz, 1H, CH-Cq), 1.86 (m, 1H, CH-Cq), 1.68 (m, 1H, CH-Cq).

^{13}C NMR (101 MHz, CD_3OD) δ 177.35 (CO-NH), 171.52 (CO-Cq$_{Ar}$), 143.00 (Cq$_{Ar}$-N), 135.54 (Cq$_{Ar}$-CO), 129.73 (CH_{Ar}), 128.93 (2CH_{Ar}), 128.41 (2CH_{Ar}), 126.35 (2CH_{Ar}), 119.36 (CH_{Ar}), 115.78 (2CH_{Ar}), 59.39 (N-Cq-CO), 59.25 (NH-CH_2-N), 44.22 (CH_2-N), 38.86 (CH_2-N), 29.36 (CH_2-Cq), 28.54 (CH_2-Cq).

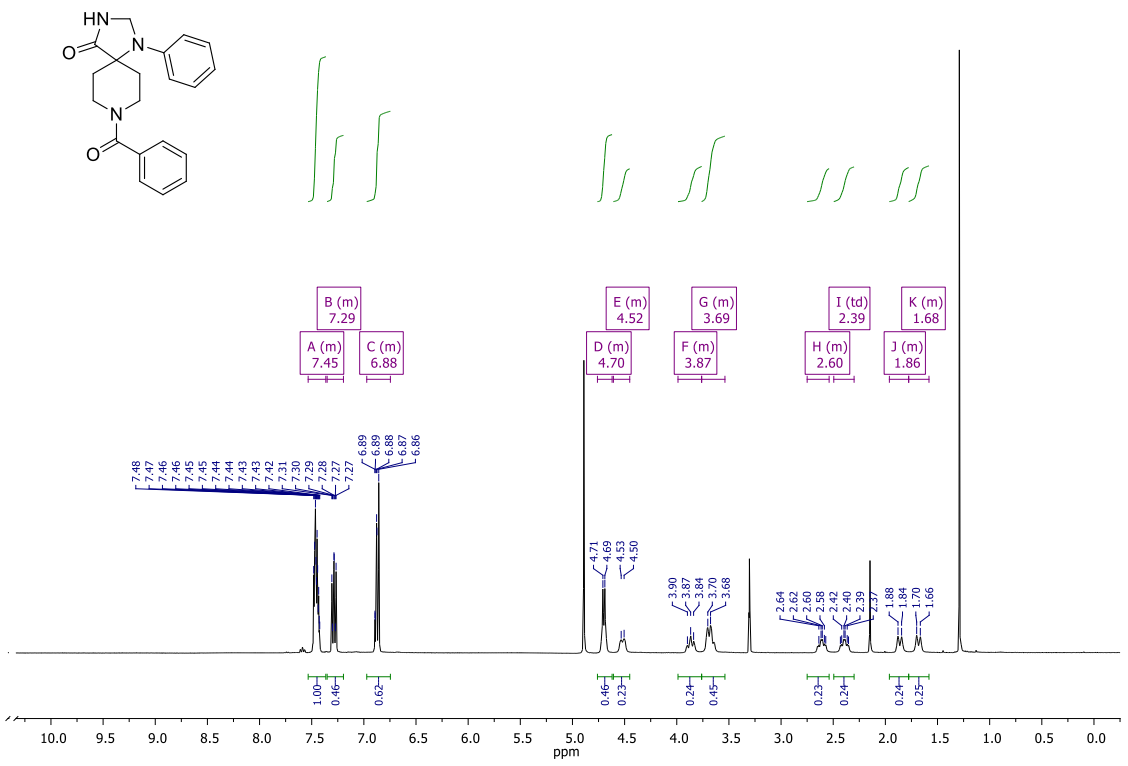
HN
O
N
N
O
B (m) 7.29
A (m) 7.45
C (m) 6.88
E (m) 4.52
D (m) 4.70
G (m) 3.69
F (m) 3.87
I (td) 2.39
H (m) 2.60
K (m) 1.68
J (m) 1.86
7.48 7.47 7.46 7.46 7.45 7.45 7.44 7.43 7.43 7.42 7.31 7.30 7.29 7.28 7.27 7.27
6.89 6.89 6.88 6.87 6.86
4.71 4.69 4.53 4.50
3.90 3.87 3.84 3.70 3.68
2.64 2.62 2.60 2.58 2.42 2.40 2.39 2.37
1.88 1.84 1.70 1.66
1.00 0.46 0.62 0.46 0.23 0.24 0.45 0.23 0.24 0.24 0.25
10.0 9.5 9.0 8.5 8.0 7.5 7.0 6.5 6.0 5.5 5.0 4.5 4.0 3.5 3.0 2.5 2.0 1.5 1.0 0.5 0.0
ppm

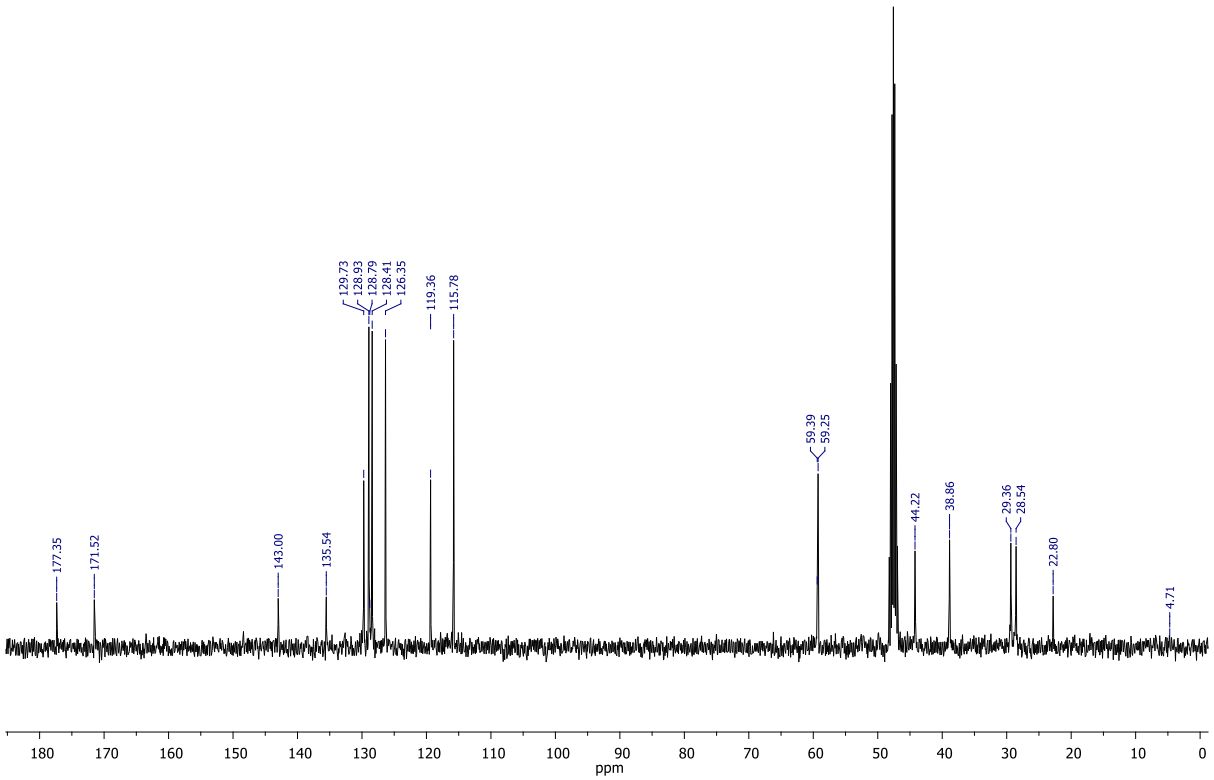
129.73
128.93
128.79
128.41
126.35
119.36
115.78
177.35
171.52
143.00
135.54
59.39
59.25
44.22
38.86
29.36
28.54
22.80
4.71
180 170 160 150 140 130 120 110 100 90 80 70 60 50 40 30 20 10 0
ppm

Synthesis of 1-phenyl-8-acetyl-1, 3, 8-triaza-spiro[4,5]decan-4-one (20)

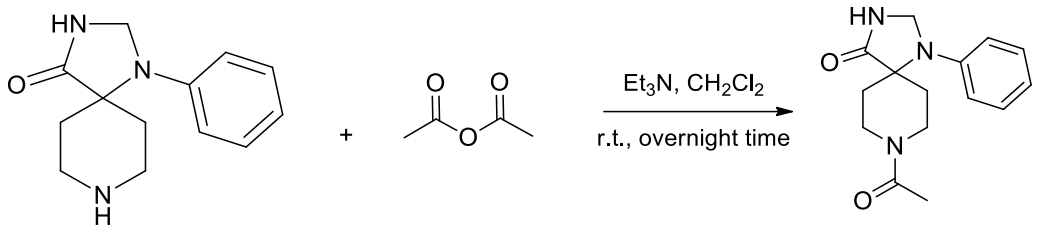

28 **20**

To a solution of 1-phenyl-1, 3, 8-triaza-spiro[4,5]decan-4-one (1 eq, 0.1 g, 0.4 mmol) in CH_2Cl_2 (25 mL) was added TEA (1 eq) and then Ac_2O (1 eq). The solution was stirred at R.T. for 3 h. After the reaction was complete as indicated by TLC, it was diluted in 30 mL of CH_2Cl_2 and washed with 1M HCl, water and brine. After anhydrification with anhydrous sodium sulfate, the solution was evaporated under reduced pressure to give compound **20** as a white solid.

Yield: 93%

Melting point: 197-200°C

MS (ESI): $[M+H]^+ = 274.32$

^{1}H NMR (400 MHz, CD_3OD) δ 7.34 – 7.14 (m, 2H, C$\underline{H}_{Ar}$), 6.83 (m, 3H, C$\underline{H}_{Ar}$), 4.88 (s, 2H, NH-C$\underline{H}_2$-N), 4.47 – 4.27 (m, 1H, C$\underline{H}_2$-N), 3.97 – 3.78 (m, 2H, C$\underline{H}_2$-N), 3.45 (td, J = 12.8, 3.6 Hz, 1H, C$\underline{H}_2$-N), 2.59 – 2.30 (m, 2H, C$\underline{H}_2$-Cq), 2.14 (s, 3H, C$\underline{H}_3$-CO), 1.86 – 1.68 (m, 2H, C$\underline{H}_2$-Cq).

^{13}C NMR (101 MHz, CD_3OD) δ 177.43 (C$\underline{O}$-NH), 170.36 (C$\underline{O}$-CH_3), 143.04 (C$\underline{q}_{Ar}$-N), 128.88 (C$\underline{H}_{Ar}$), 119.30 (2C$\underline{H}_{Ar}$), 115.82 (2C$\underline{H}_{Ar}$), 59.37 (N-C$\underline{q}$-CO), 59.22 (NH-C$\underline{H}_2$-N), 42.73 (C$\underline{H}_2$-N), 38.05 (C$\underline{H}_2$-N), 29.38 (C$\underline{H}_2$-Cq), 28.49 (C$\underline{H}_2$-Cq), 19.74 (C$\underline{H}_3$-CO).

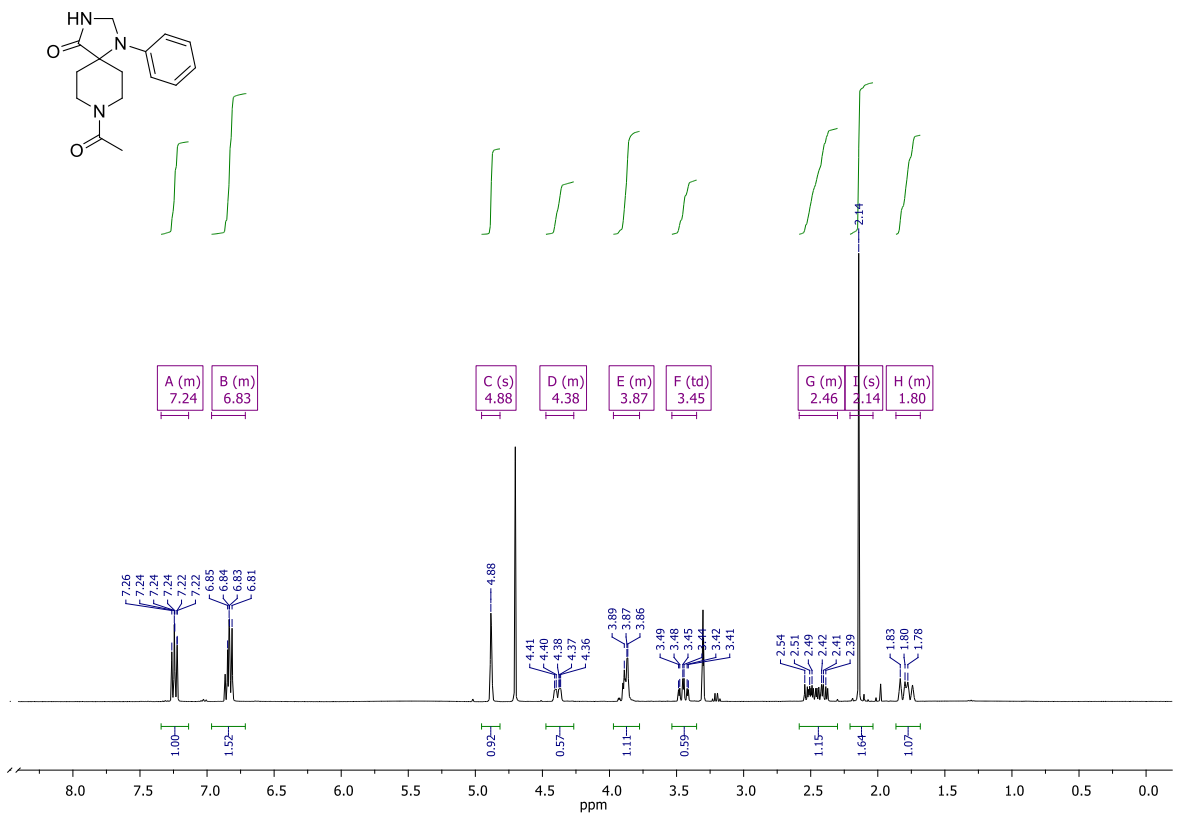
HN
O
N
N
O
A (m) 7.24
B (m) 6.83
C (s) 4.88
D (m) 4.38
E (m) 3.87
F (td) 3.45
G (m) 2.46
I (s) 2.14
H (m) 1.80
7.26 7.24 7.24 7.24 7.22 7.22 6.85 6.84 6.83 6.81
4.88
4.41 4.40 4.38 4.37 4.36
3.89 3.87 3.86
3.49 3.48 3.45 3.44 3.42 3.41
2.54 2.51 2.49 2.42 2.41 2.39
1.83 1.80 1.78
2.14
1.00 1.52 0.92 0.57 1.11 0.59 1.15 1.64 1.07
8.0 7.5 7.0 6.5 6.0 5.5 5.0 4.5 4.0 3.5 3.0 2.5 2.0 1.5 1.0 0.5 0.0
ppm

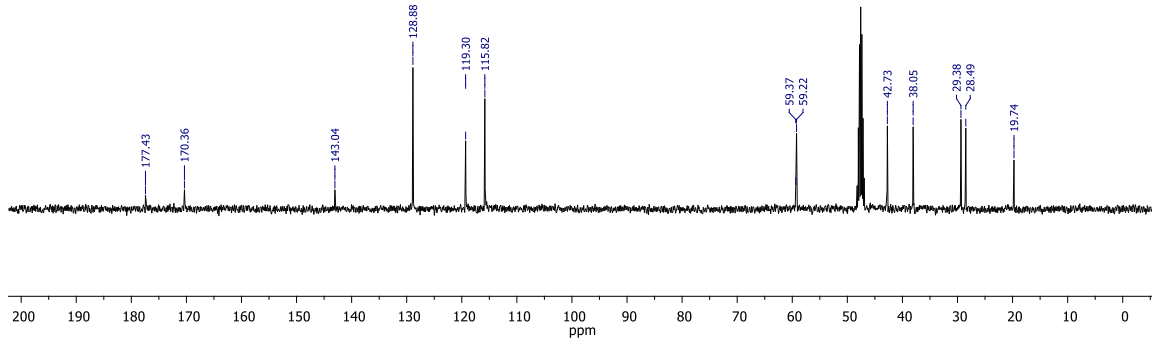
177.43
170.36
143.04
128.88
119.30
115.82
59.37
59.22
42.73
38.05
29.38
28.49
19.74
200 190 180 170 160 150 140 130 120 110 100 90 80 70 60 50 40 30 20 10 0
ppm

Synthesis of 1-phenyl-8-tosyl-1, 3, 8–triaza-spiro[4,5]decan-4-one (21)

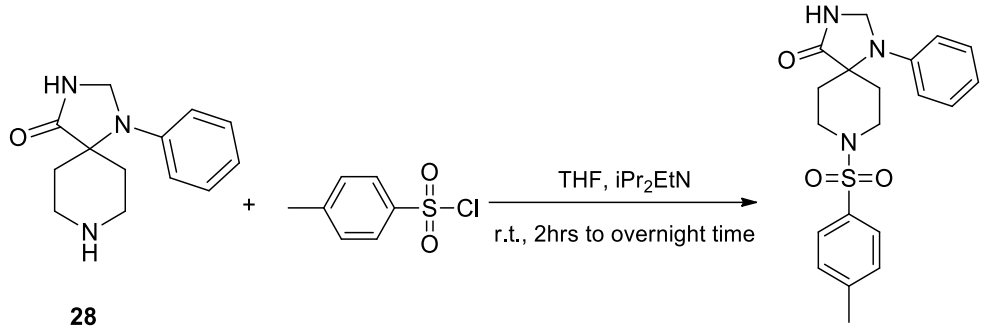

28 **21**

To a solution of 1-phenyl-1, 3, 8 – triaza-spiro[4,5]decan-4-one (1 eq, 0.1 g, 0.4 mmol) in THF (5 mL) was added DIPEA (1 eq) and tosyl chloride (1.2 eq). The solution was then stirred at room temperature for 18 hours. After the reaction was complete as indicated by TLC, the solution was diluted with EtOAc and extracted with water and brine. After anhydrification, the organic layer was evaporated under reduced pressure to give **21** as white solids.

Yield: 72%

Melting point: 250-254°C

MS (ESI): $[M+H]^+ = 386.40$

^{1}H NMR (400 MHz, DMSO) δ 8.78 (s, 1H, CO-N<u>H</u>), 7.66 (d, J = 8.2 Hz, 2H, C<u>H$_{Ar}$</u>-Cq-SO$_2$), 7.47 (d, J = 8.1 Hz, 2H, C<u>H$_{Ar}$</u>-Cq-CH$_3$), 7.23 (t, J = 7.9 Hz, 2H, C<u>H$_{Ar}$</u>), 6.84 – 6.66 (m, 3H, C<u>H$_{Ar}$</u>), 4.56 (s, 2H, NH-C<u>H$_2$</u>-N), 3.65 (d, J = 6.8 Hz, 2H, C<u>H$_2$</u>-N-SO$_2$), 3.02 (m, 2H, C<u>H$_2$</u>-Cq), 2.52-2.47 (m, 5H, C<u>H$_3$</u>-Cq$_{Ar}$, C<u>H$_2$</u>-N-SO$_2$), 1.68 (d, J = 13.8 Hz, 2H, C<u>H$_2$</u>-Cq).

^{13}C NMR (101 MHz, DMSO) δ 175.14 (<u>C</u>O-NH), 143.39 (<u>Cq$_{Ar}$</u>-SO$_2$), 142.88 (<u>Cq$_{Ar}$</u>-N), 133.15 (Cq<u>$_{Ar}$</u>-CH$_3$), 129.82 (<u>2C</u>H$_{Ar}$), 129.04 (<u>2C</u>H$_{Ar}$), 127.30 (<u>2C</u>H$_{Ar}$-Cq$_{Ar}$-SO$_2$), 117.98 (<u>C</u>H$_{Ar}$), 114.22 (<u>2C</u>H$_{Ar}$-Cq$_{Ar}$-N), 58.63 (N-<u>Cq</u>-CO), 57.44 (<u>C</u>H$_2$-N), 42.66 (<u>C</u>H$_2$-N), 27.99 (<u>C</u>H$_2$-Cq), 20.96 (<u>C</u>H$_3$-Cq$_{Ar}$).

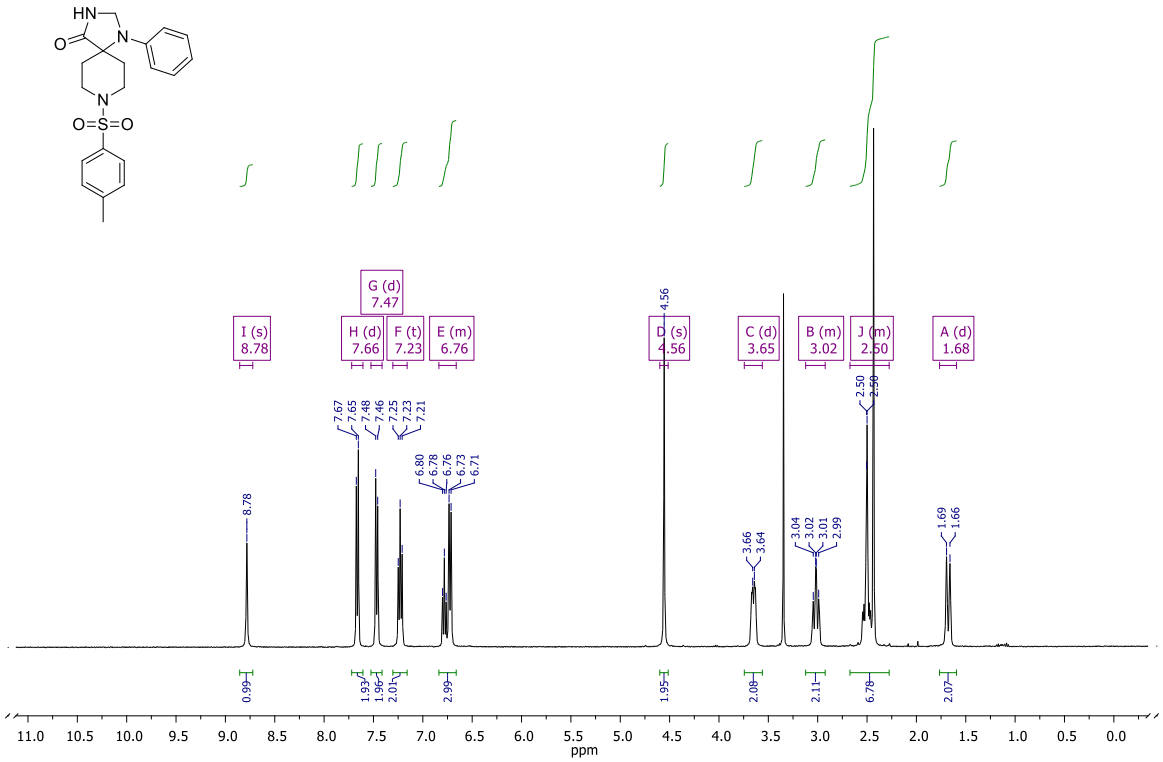
HN
O
N
N
O=S=O
I (s) 8.78
H (d) 7.66
G (d) 7.47
F (t) 7.23
E (m) 6.76
D (s) 4.56
C (d) 3.65
B (m) 3.02
J (m) 2.50
A (d) 1.68
ppm

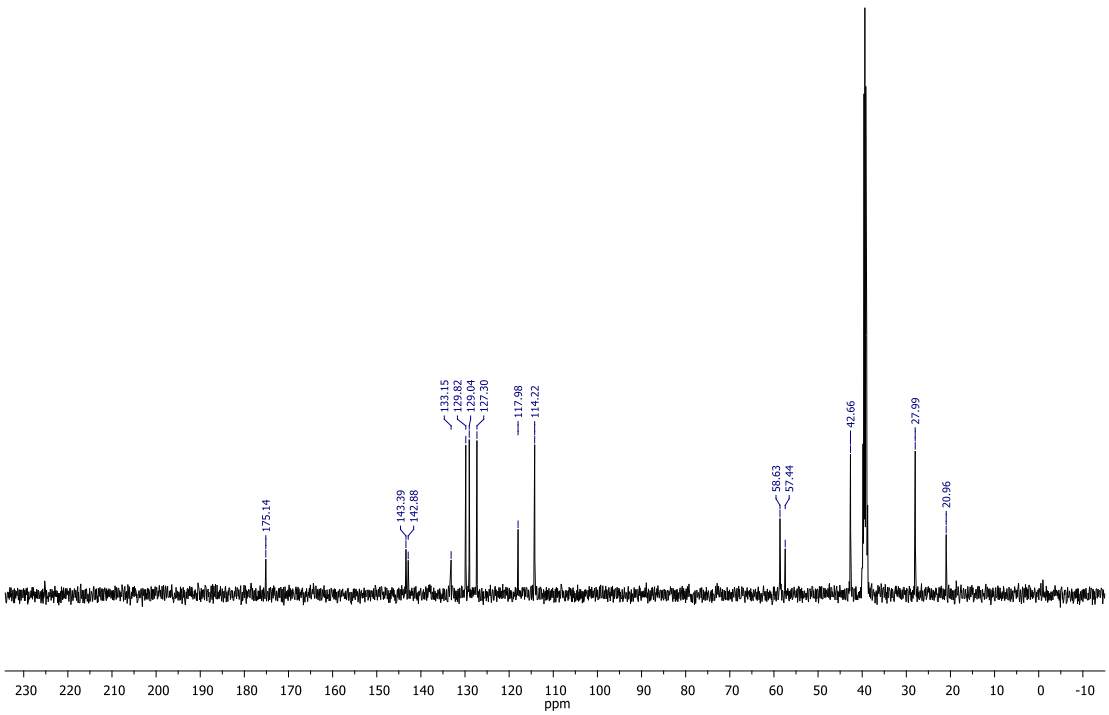
175.14
143.39
142.88
133.15
129.82
129.04
127.30
117.98
114.22
58.63
57.44
42.66
27.99
20.96
ppm

Synthesis of 1-phenyl-8-mesyl-1, 3, 8–triaza-spiro[4,5]decan-4-one (22)

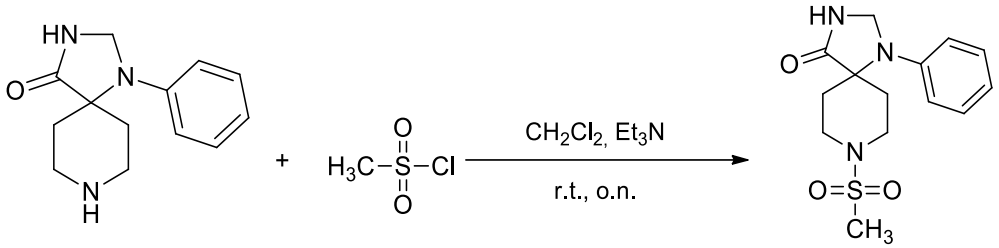

28 **22**

To a solution of 1-phenyl-1, 3, 8–triaza-spiro[4,5]decan-4-one (1 eq, 0.1 g, 0.4 mmol) in CH_2Cl_2 (5 mL) was added TEA (1 eq) and methanesulfonyl chloride (1.2 eq). The solution was then stirred at room temperature for 18 hours. After the reaction was complete as indicated by TLC, the solution was diluted with EtOAc and extracted with water and brine. After anhydrification, the organic layer was evaporated under reduced pressure to give **22** as white solids.

Yield: 87%

Melting point: 248-252°C

MS (ESI): $[M+H]^+ = 310.25$

^{1}H NMR (400 MHz, DMSO) δ 8.90 (s, 1H, CO-N$\underline{H}$), 7.25 (t, J = 8.0 Hz, 2H, C$\underline{H}_{Ar}$), 6.80 (m, 3H, C$\underline{H}_{Ar}$), 4.61 (s, 2H, NH-C$\underline{H}_2$-N), 3.57 (m, 2H, C$\underline{H}_2$-N-SO_2), 3.47 - 3.39 (m, 2H, C$\underline{H}_2$-N-SO_2), 2.92 (s, 3H, C$\underline{H}_3$-SO_2), 2.58 – 2.45 (m, 2H, C$\underline{H}_2$-Cq), 1.74 (d, J = 13.9 Hz, 2H, C$\underline{H}_2$-Cq).

^{13}C NMR (101 MHz, DMSO) δ 175.40 ($\underline{C}$O-NH), 142.97 ($\underline{Cq}_{Ar}$-N), 129.08 ($\underline{2C}H_{Ar}$), 117.95 ($\underline{C}H_{Ar}$), 114.23 ($\underline{2C}H_{Ar}$-Cq_{Ar}), 58.71 (N-$\underline{Cq}$-CO), 57.62 ($\underline{C}H_2$-N), 42.44 ($\underline{C}H_2$-N), 34.18 ($\underline{C}H_3$-SO_2), 28.21 ($\underline{C}H_2$-Cq).

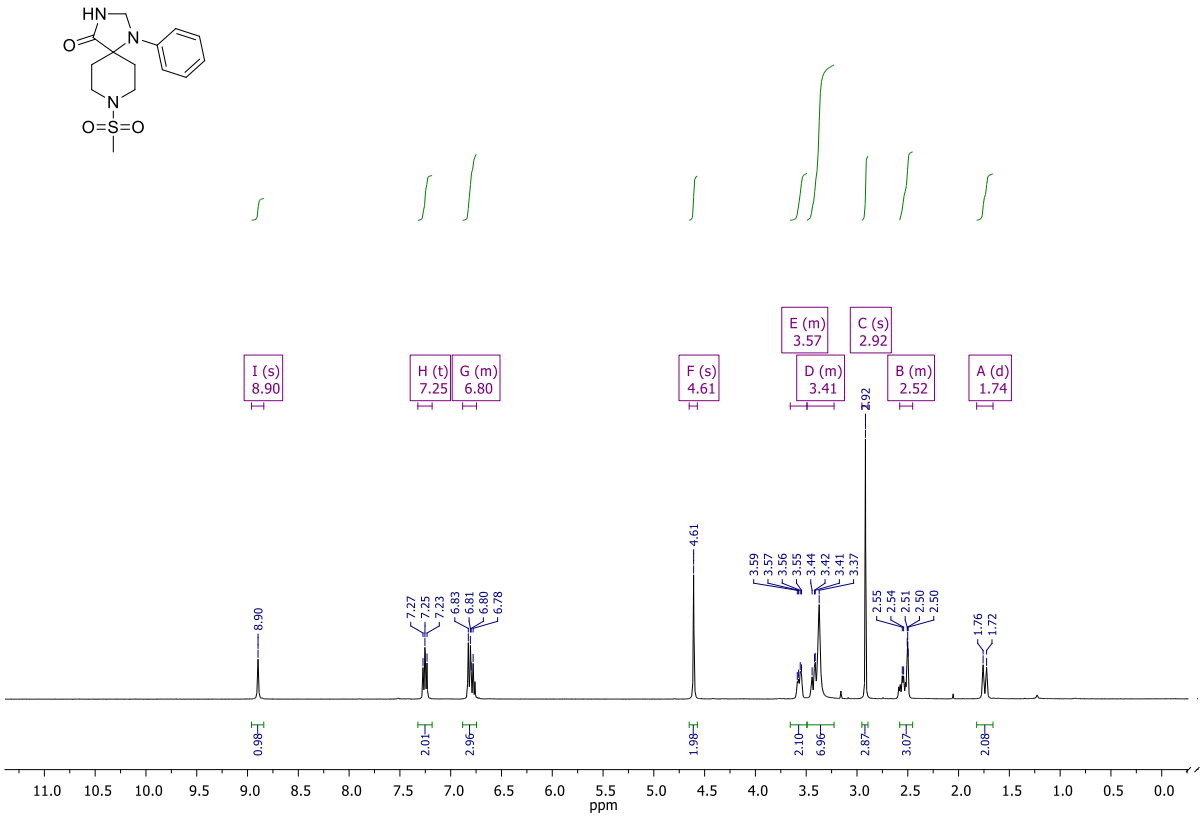
HN
O
N
N
O=S=O
I (s) 8.90
H (t) 7.25
G (m) 6.80
F (s) 4.61
E (m) 3.57
D (m) 3.41
C (s) 2.92
B (m) 2.52
A (d) 1.74
8.90
7.27
7.25
7.23
6.83
6.81
6.80
6.78
4.61
3.59
3.57
3.56
3.55
3.44
3.42
3.41
3.37
2.92
2.55
2.54
2.51
2.50
2.50
1.76
1.72
0.98
2.01
2.96
1.98
2.10
6.96
2.87
3.07
2.08
ppm

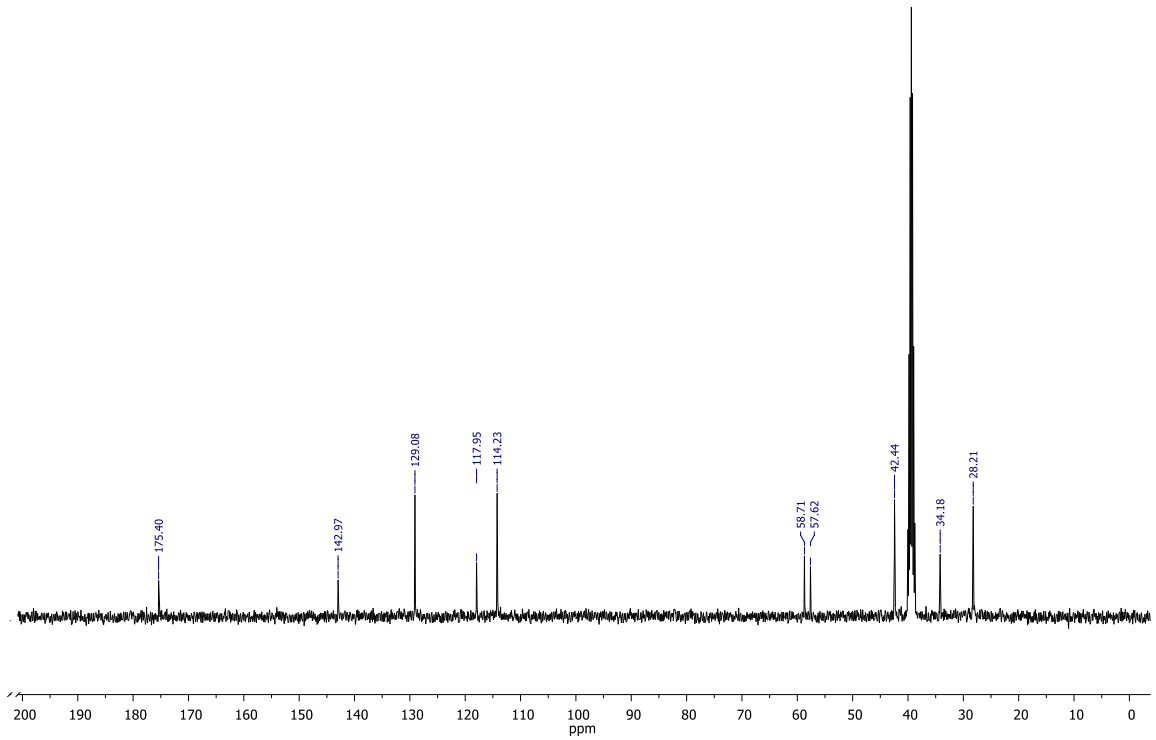
175.40
142.97
129.08
117.95
114.23
58.71
57.62
42.44
34.18
28.21
ppm

Synthesis of 1-phenyl-8-(4-fluoro-benzen)-sulfonyl-1, 3, 8–triaza-spiro[4,5]decan-4-one (23)

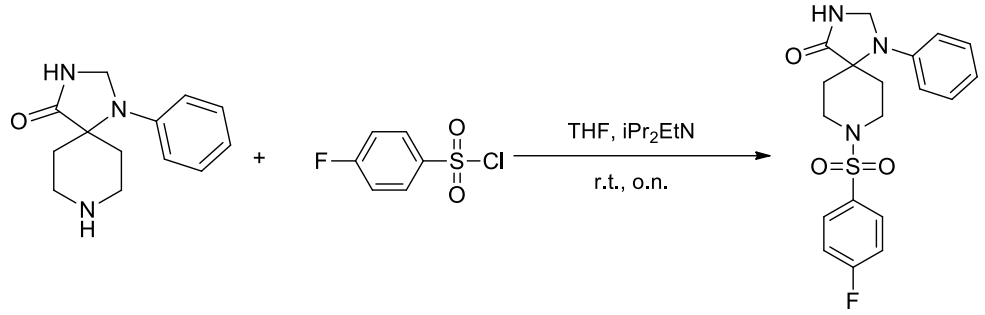

28 **23**

To a solution of 1-phenyl-1, 3, 8–triaza-spiro[4,5]decan-4-one (1 eq, 0.1 g, 0.4mmol) in THF (5 mL) was added DIPEA (1 eq) and, then, 4-fluorobenzenesulfonyl chloride (1.2 eq). The solution was then stirred at room temperature for 16 hours. After the reaction was complete as indicated by TLC, the solution was diluted with EtOAc and extracted with water and brine. After anhydrification, the organic layer was evaporated under reduced pressure to give **23** as white solids.

Yield: 78%

Melting point: 251-254°C

MS (ESI): $[M+H]^+ = 390.38$

^{1}H NMR (400 MHz, DMSO) δ 8.77 (s, 1H, CO-N$\underline{H}$), 7.93 – 7.82 (m, 2H, C$\underline{H}_{Ar}$-Cq-SO_2), 7.51 (m, 2H, C$\underline{H}_{Ar}$-Cq-F), 7.23 (m, 2H, C$\underline{H}_{Ar}$), 6.75 (m, 3H, C$\underline{H}_{Ar}$), 4.56 (s, 2H, NH-C$\underline{H}_2$-N), 3.68 (m, 2H, C$\underline{H}_2$-N-SO_2), 3.07 (m, 2H, C$\underline{H}_2$-N-SO_2), 2.49 (m, 2H, C$\underline{H}_2$-Cq), 1.69 (d, J = 13.8 Hz, 2H, C$\underline{H}_2$-Cq).

^{13}C NMR (101 MHz, DMSO) δ 175.10 (C$\underline{O}$-NH), 165.71 (Cq$_{\underline{Ar}}$-F), 142.88 (Cq$_{\underline{Ar}}$-N), 132.58 (Cq$_{\underline{Ar}}$-SO_2), 130.29 (2C$\underline{H}_{Ar}$-Cq$_{Ar}$-F), 129.02 (2C$\underline{H}_{Ar}$), 118.08 (C$\underline{H}_{Ar}$), 116.70 (2C$\underline{H}_{Ar}$-Cq$_{Ar}$-F), 114.34 (2C$\underline{H}_{Ar}$-Cq$_{Ar}$-N), 58.63 (N-C$\underline{q}$), 57.46 (C$\underline{H}_2$-N), 42.63 (C$\underline{H}_2$-N), 27.95 (C$\underline{H}_2$-Cq).

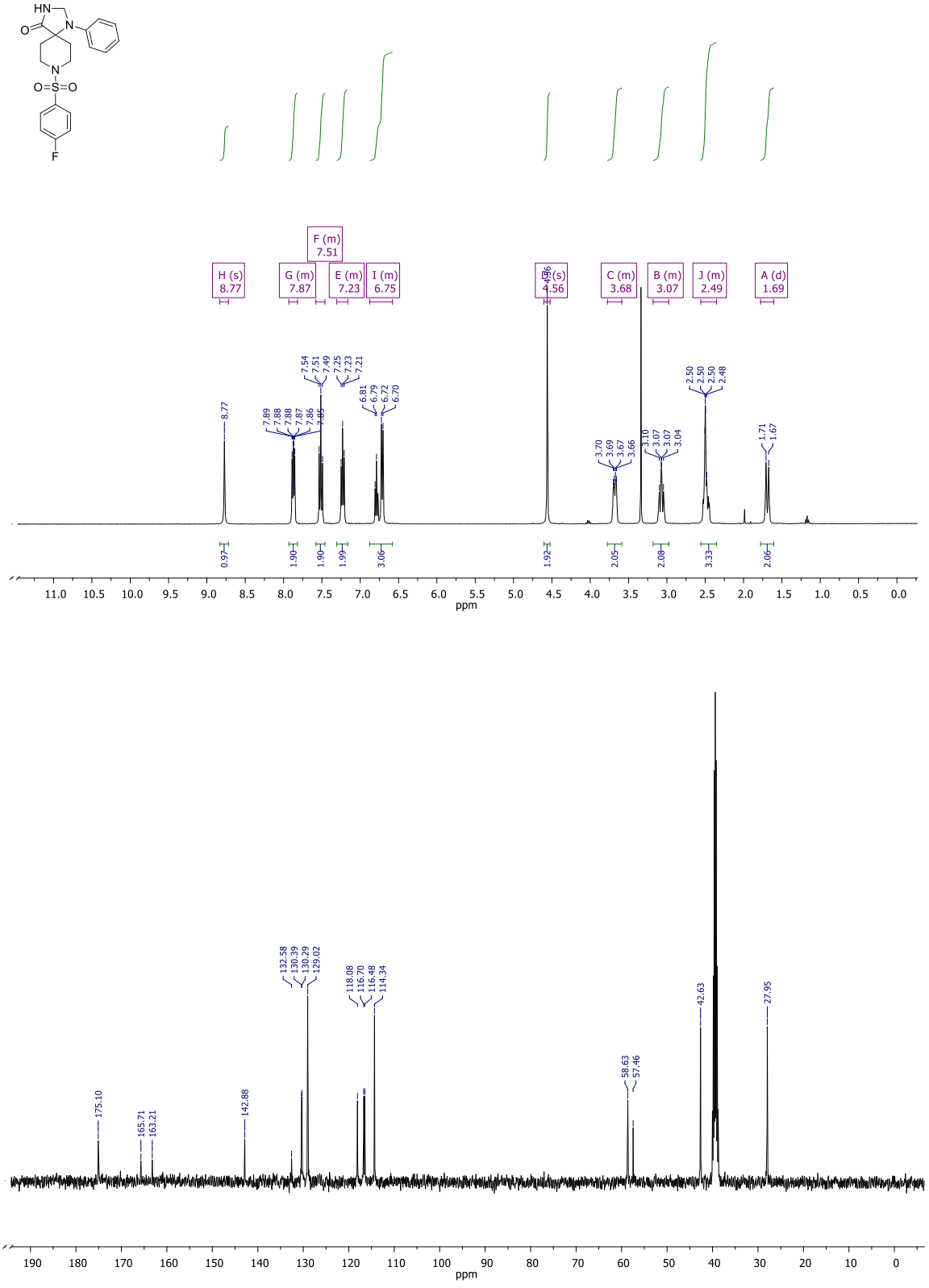
HN
O
N
N
O=S=O
F
H (s) 8.77
G (m) 7.87
E (m) 7.23
F (m) 7.51
I (m) 6.75
D (s) 4.56
C (m) 3.68
B (m) 3.07
J (m) 2.49
A (d) 1.69
8.77
7.89
7.88
7.88
7.87
7.86
7.85
7.54
7.51
7.49
7.25
7.23
7.21
6.81
6.79
6.72
6.70
4.56
3.70
3.69
3.67
3.66
3.10
3.07
3.07
3.04
2.50
2.50
2.50
2.48
1.71
1.67
0.97
1.90
1.90
1.99
3.06
1.92
2.05
2.08
3.33
2.06
ppm
175.10
165.71
163.21
142.88
132.58
130.39
130.29
129.02
118.08
116.70
116.48
114.34
58.63
57.46
42.63
27.95
ppm

Synthesis of 1-phenyl-8-(5-chloro-thiophen)-sulphonyl-1, 3, 8–triaza-spiro[4,5]decan-4-one (24)

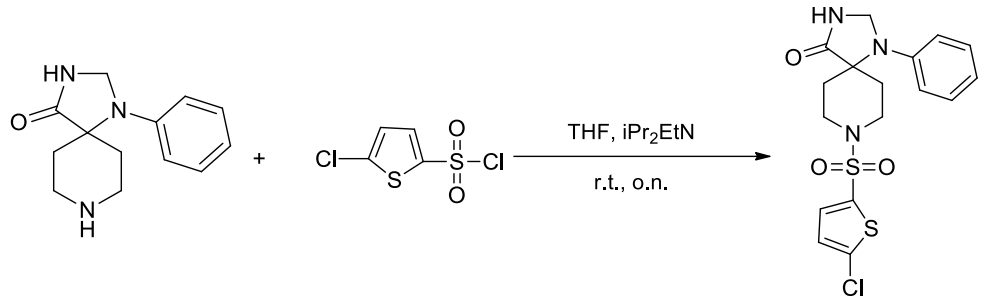

28 **24**

To a solution of 1-phenyl-1, 3, 8–triaza-spiro[4,5]decan-4-one (1 eq, 0.1 g, 0.4 mmol) in THF (5 mL) was added DIPEA (1 eq) and 5-Chlorothiophene-2-sulfonyl chloride (1.2 eq). The solution was then stirred at room temperature for 14 h. After the reaction was complete as indicated by TLC, the solution was diluted with EtOAc and extracted with water and brine. After anhydrification, the organic layer was evaporated under reduced pressure to give **24** as white solids.

Yield: 71%

Melting point: 256-259°C

MS (ESI): $[M+H]^+ = 412.18$

^{1}H NMR (400 MHz, DMSO) δ 8.82 (s, 1H, CO-NH), 7.61 (d, J = 4.1 Hz, 1H, CH-Cq-S), 7.41 (d, J = 4.1 Hz, 1H, CH-Cq-S), 7.25 (dd, J = 8.6, 7.4 Hz, 2H, CH_{Ar}), 6.84 – 6.70 (m, 3H, CH_{Ar}), 4.58 (s, 2H, NH-CH_2-N), 3.66 (m, 2H, CH_2-N), 3.21 (m, 2H, CH_2-N), 2.51 (m, 2H, CH_2-Cq), 1.74 (d, J = 14.1 Hz, 2H, CH_2-Cq).

^{13}C NMR (101 MHz, DMSO) δ 175.07 (CO-NH), 142.87 (Cq_{Ar}-N), 135.33 (S-Cq-Cl), 134.52 (CH-Cq-S), 132.73 (CH-Cq-S), 129.07 ($2CH_{Ar}$), 128.73 (CH-Cq-S), 118.15 (CH_{Ar}), 114.40 ($2CH_{Ar}$-Cq_{Ar}-N), 58.67 (N-Cq), 57.39 (CH_2-N), 42.79 (CH_2-N), 27.87 (CH_2-Cq).

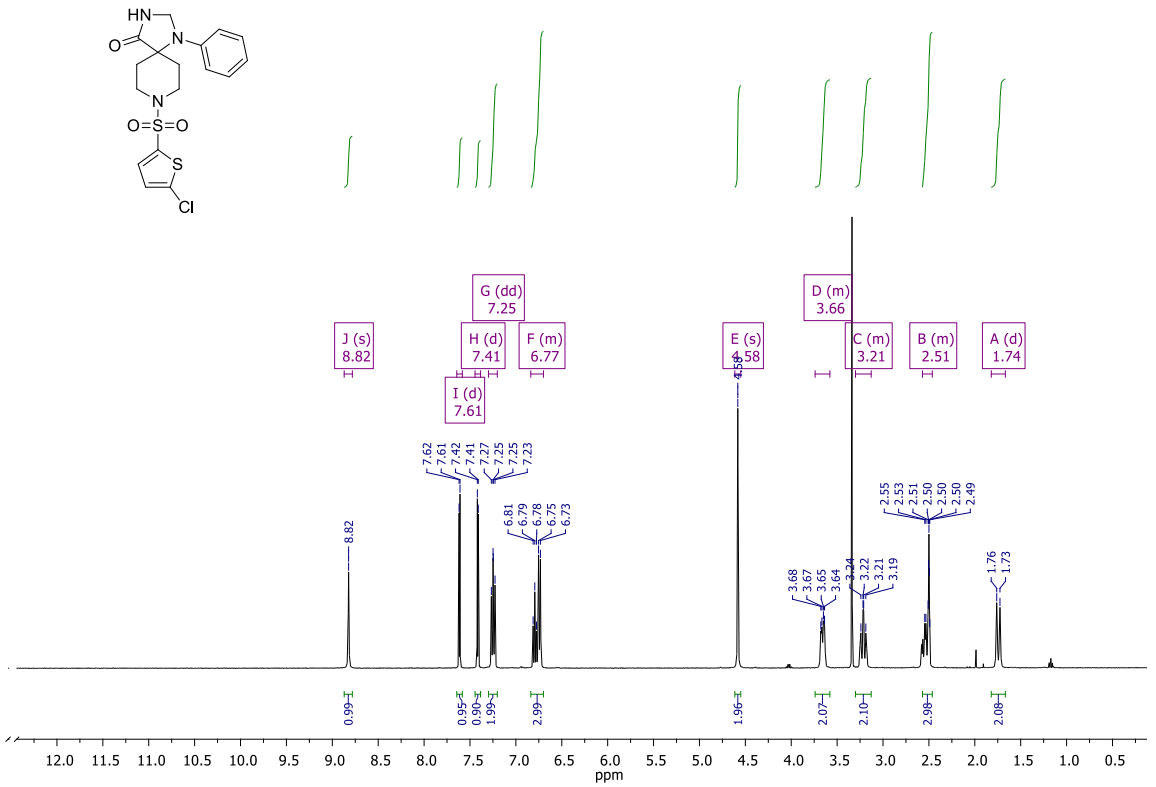
HN
O
N
N
O=S=O
S
Cl
J (s) 8.82
H (d) 7.41
I (d) 7.61
G (dd) 7.25
F (m) 6.77
E (s) 4.58
D (m) 3.66
C (m) 3.21
B (m) 2.51
A (d) 1.74
ppm

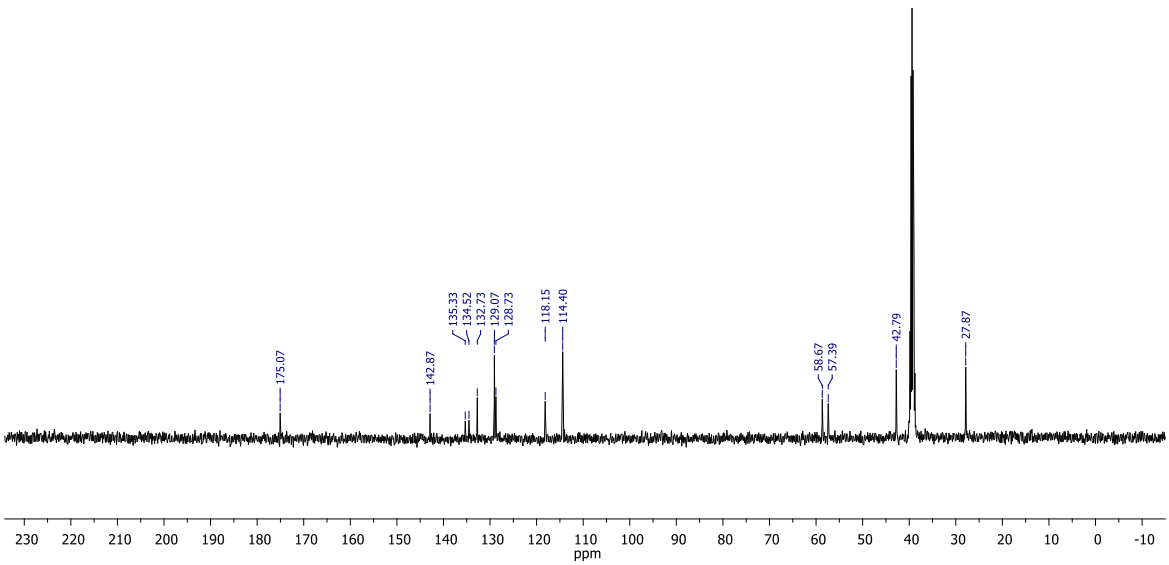
175.07
142.87
135.33
134.52
132.73
129.07
128.73
118.15
114.40
58.67
57.39
42.79
27.87
ppm

Synthesis of 4-oxo-N,1-diphenyl-1, 3, 8-triazaspiro[4.5]decane-8-carboxamide (25)

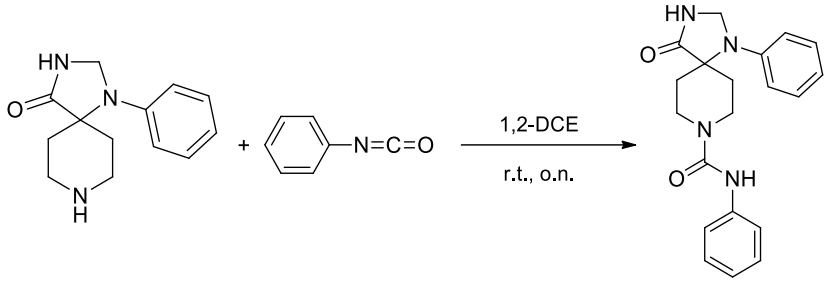

28 **25**

To a solution of 1-phenyl-1, 3, 8–triaza-spiro[4,5]decan-4-one (1 eq, 0.1 g, 0.4 mmol) in 1,2-dichloroethane (20 mL) was added phenyl isocyanate (1 eq). The solution was then stirred at room temperature for 1 hour. After the reaction was complete as indicated by TLC, the precipitate was filtered and washed with Et_2O to give **25** as white solids.

Yield: 72%

Melting point: 250-254°C

MS (ESI): $[M+H]^+ = 351.24$

^{1}H NMR (400 MHz, DMSO) 8.79 (s, 1H, Cq-CO-N<u>H</u>), 8.65 (s, 1H, N-CO-N<u>H</u>), 7.44 (d, *J* = 4.5 Hz, 2H, NH-Cq$_{Ar}$-C<u>H</u>$_{Ar}$), 7.19 (d, *J* = 33.3 Hz, 4H, C<u>H</u>$_{Ar}$), 6.92 (d, *J* = 6.0 Hz, 1H, C<u>H</u>$_{Ar}$), 6.70 (s, 3H, C<u>H</u>$_{Ar}$), 4.59 (s, 2H, NH-C<u>H</u>$_2$-N), 4.04 (d, *J* = 10.3 Hz, 2H, C<u>H</u>$_2$-N-CO), 3.48 (s, 2H, C<u>H</u>$_2$-N-CO), 2.51 (m, 2H, C<u>H</u>$_2$-Cq), 1.60 (d, *J* = 12.5 Hz, 2H, C<u>H</u>$_2$-Cq).

^{13}C NMR (101 MHz, DMSO) δ 175.98 (Cq-<u>C</u>O-NH), 155.38 (NH-<u>C</u>O-NH), 143.00 (<u>Cq</u>$_{Ar}$-N), 140.51 (<u>Cq</u>$_{Ar}$-NH-CO), 128.96 (<u>2C</u>H$_{Ar}$-CH$_{Ar}$-Cq$_{Ar}$-NH), 128.24 (<u>2C</u>H$_{Ar}$-CH$_{Ar}$-Cq$_{Ar}$-N), 121.63 (<u>C</u>H$_{Ar}$), 119.58 (<u>C</u>H$_{Ar}$), 117.63 (<u>C</u>H$_{Ar}$-Cq$_{Ar}$-N), 113.81 (<u>C</u>H$_{Ar}$-Cq$_{Ar}$-N), 58.64 (N-<u>Cq</u>), 58.20 (<u>C</u>H$_2$-N), 41.02 (<u>C</u>H$_2$-N), 27.88 (<u>C</u>H$_2$-Cq).

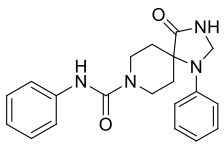
O
NH
H
N
N
N
O

A (m) 8.72
B (s) 7.44
C (m) 7.19
D (m) 6.81
E (s) 4.59
F (s) 4.03
H (s) 3.48
I (s) 2.47
G (d) 1.60
8.79
8.65
7.44
7.24
7.15
6.92
6.70
4.59
4.03
3.48
2.47
1.62
1.59
1.00
0.84
1.68
1.79
0.85
0.91
1.01
1.33
0.91
ppm

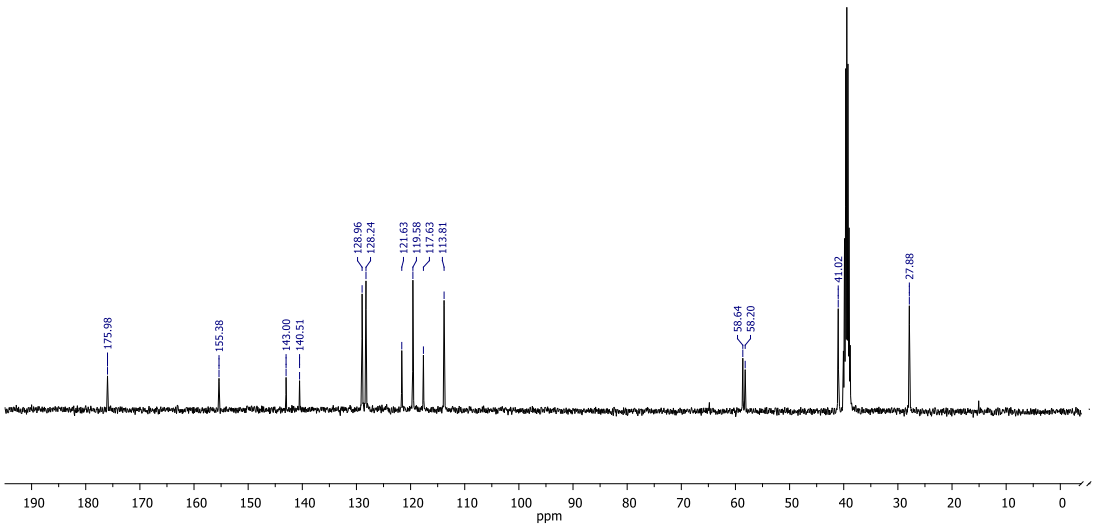
175.98
155.38
143.00
140.51
128.96
128.24
121.63
119.58
117.63
113.81
58.64
58.20
41.02
27.88
ppm

Synthesis of N-cyclohexyl-4-oxo-1-phenyl-1, 3, 8-triazaspiro[4.5]decane-8-carboxamide (26)

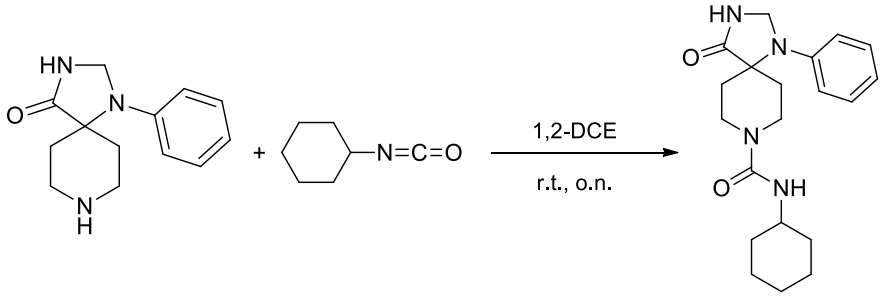

28 **26**

To a solution of 1-phenyl-1, 3, 8–triaza-spiro[4,5]decan-4-one (1 eq, 0.1 g, 0.4 mmol) in 1,2-dichloroethane (20 mL) was added cyclohexyl isocyanate (1 eq). The solution was then stirred at room temperature for 1 to 18 h. After the reaction was complete as indicated by TLC, the precipitate was filtered and washed with Et_2O to give **26** as white solids.

Yield: 72%

Melting point: 255-258°C

MS (ESI): $[M+H]^+ = 357.48$

^{1}H NMR (400 MHz, DMSO) δ 8.74 (s, 1H, CO-N<u>H</u>-CH_2), 7.13 (t, J = 7.9 Hz, 2H, C<u>H</u>$_{Ar}$), 6.80 – 6.51 (m, 3H, C<u>H</u>$_{Ar}$), 6.33 (d, J = 7.6 Hz, 1H, CO-N<u>H</u>-CH), 4.57 (s, 2H, NH-C<u>H</u>$_2$-N), 3.88 (dd, J = 12.8, 3.9 Hz, 2H, CH_2-N-CO), 3.58 – 3.42 (m, 1H, CO-NH-C<u>H</u>), 3.29 (d, J = 3.0 Hz, 2H, CH_2-N-CO), 2.39 (td, J = 13.4, 5.0 Hz, 2H, C<u>H</u>$_2$-Cq), 1.77 (d, *J* = 10.3 Hz, 2H, C<u>H</u>$_2$-Cq), 1.69 (m, 2H, 2C<u>H</u>$_2$-CH-N), 1.56 (m, 1H, C<u>H</u>$_2$-CH_2-C<u>H</u>$_2$), 1.45 (m, 2H, 2C<u>H</u>$_2$-CH-N), 1.34 – 1.13 (m, 4H, CH_2-C<u>H</u>$_2$-CH), 1.13 – 1.00 (m, 1H, C<u>H</u>$_2$-CH_2-CH_2).

^{13}C NMR (101 MHz, DMSO) δ 176.18 (Cq-<u>C</u>O-NH), 157.01 (NH-<u>C</u>O-NH), 142.95 (<u>Cq</u>$_{Ar}$-N), 128.88 (2<u>C</u>H$_{Ar}$), 117.32 (<u>C</u>H$_{Ar}$), 113.31 (2<u>C</u>H$_{Ar}$-Cq$_{Ar}$-N), 58.61 (N-<u>Cq</u>), 58.08 (NH-<u>C</u>H_2-N), 49.06 (<u>C</u>H-N), 40.88 (<u>C</u>H_2-N), 33.15 (<u>C</u>H_2-CH-N), 27.24 (<u>C</u>H_2-Cq), 25.32 (CH_2-<u>C</u>H_2-CH_2-CH), 25.04 (<u>C</u>H_2-CH_2-CH_2-CH).

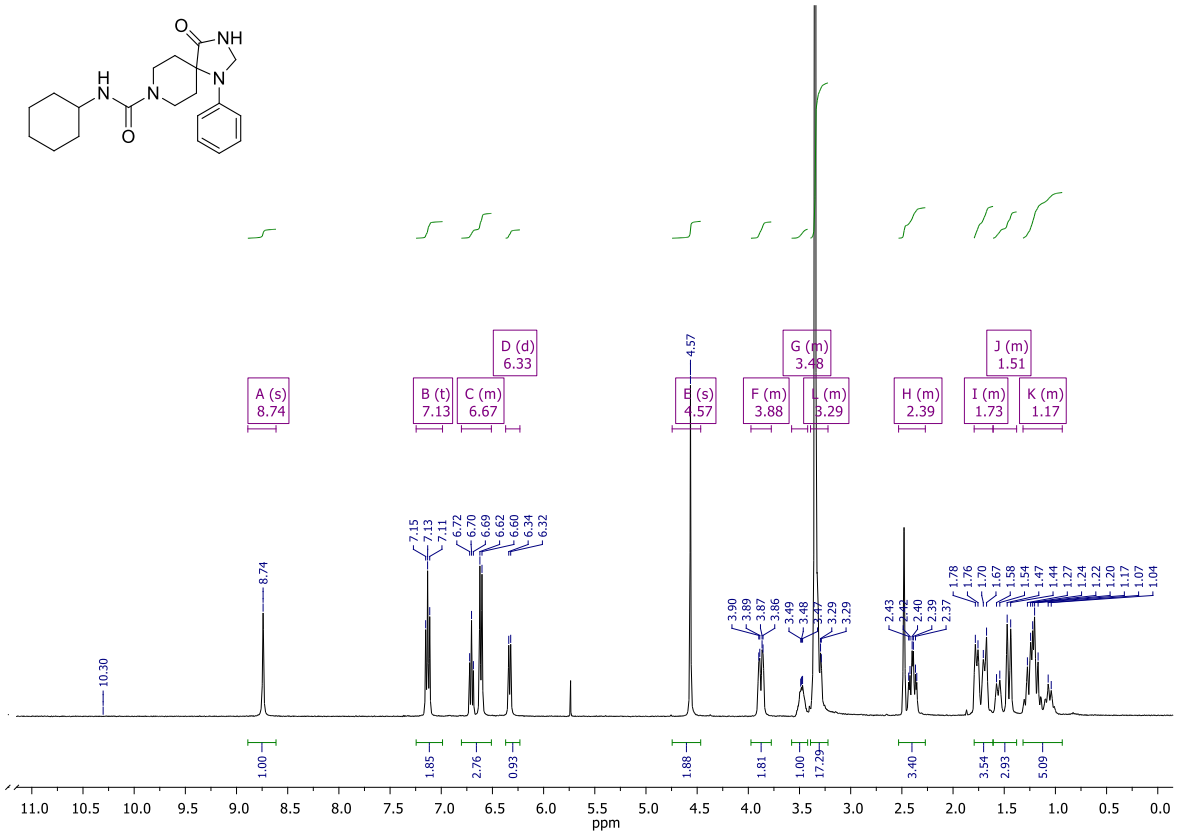
A (s) 8.74
B (t) 7.13
C (m) 6.67
D (d) 6.33
E (s) 4.57
F (m) 3.88
G (m) 3.48
L (m) 3.29
H (m) 2.39
I (m) 1.73
J (m) 1.51
K (m) 1.17
ppm

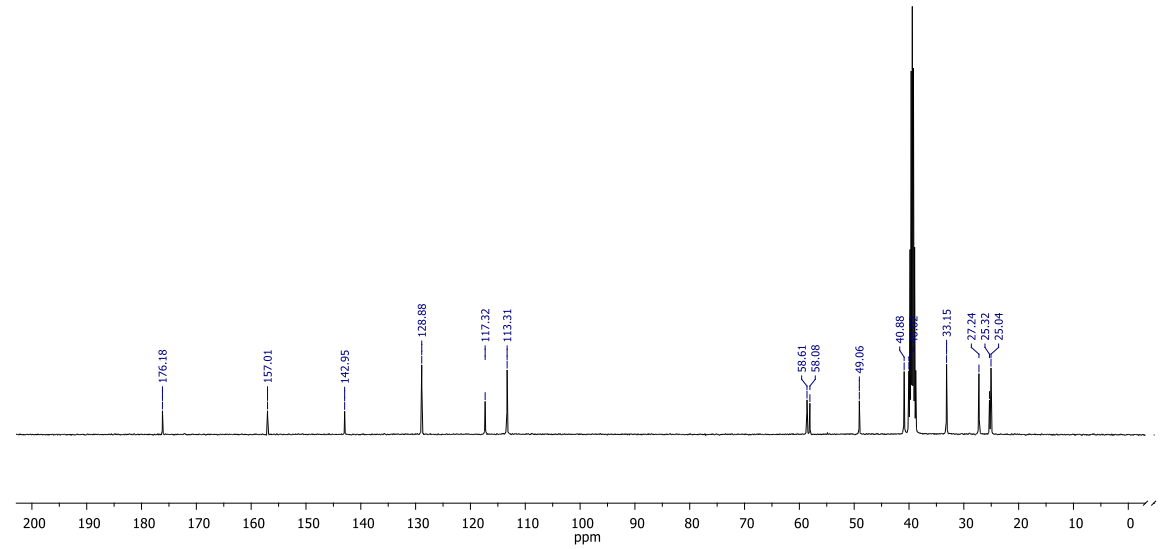
176.18
157.01
142.95
128.88
117.32
113.31
58.61
58.08
49.06
40.88
33.15
27.24
25.32
25.04
ppm

Synthesis of N-cyclohexyl-4-oxo-1-phenyl-1, 3, 8-triazaspiro[4.5]decane-8-carbothioamide (27)

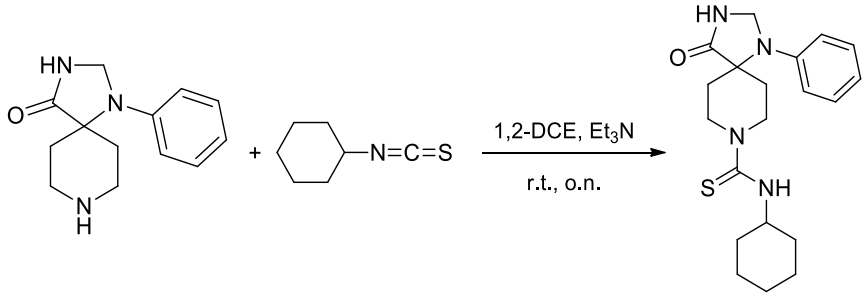

28 **27**

To a solution of 1-phenyl-1, 3, 8–triaza-spiro[4,5]decan-4-one (1 eq, 0.1 g, 0.4 mmol) in 1,2-dichloroethane (20 mL) was added TEA (1 eq) and cyclohexyl isothiocyanate (1 eq). The solution was then stirred under reflux for 18 h. After the reaction was complete as indicated by TLC, the solution was diluted with CH_2Cl_2 and washed with 2N HCl, water and brine. After anhydrification and evaporation, product was further purified by column chromatography (1:2 Petroleum ether: EtOAc) to give **27** as a white solid.

Yield: 70%

Melting point: 250-252°C

MS (ESI): $[M+H]^+ = 373.51$

^{1}H NMR (400 MHz, DMSO) δ 8.81 (s, 1H, CO-N<u>H</u>-CH_2), 7.36 (d, *J* = 7.8 Hz, 1H, N<u>H</u>-CS), 7.13 (dd, *J* = 8.5, 7.4 Hz, 2H, 2C<u>H</u>$_{Ar}$-Cq$_{Ar}$), 6.70 (t, *J* = 7.3 Hz, 1H, C<u>H</u>$_{Ar}$), 6.58 (d, *J* = 8.1 Hz, 2H, 2C<u>H</u>$_{Ar}$), 4.58 (s, 2H, NH-C<u>H</u>$_2$-N), 4.51 (d, *J* = 12.7 Hz, 2H), 4.32 – 4.23 (m, 1H, CS-NH-C<u>H</u>), 3.62 (dd, *J* = 12.7, 10.2 Hz, 2H, C<u>H</u>$_2$-N-CS), 2.54 – 2.43 (m, 2H, CH_2-N-CS), 1.92 – 1.84 (m, 2H, C<u>H</u>$_2$-Cq-CO), 1.75 – 1.66 (m, 2H, C<u>H</u>$_2$-Cq-CO), 1.62 – 1.50 (m, 3H, CH_2-C<u>H</u>$_2$-CH_2; C<u>H</u>$_2$-CH_2-CH_2), 1.30 – 1.19 (m, 6H, CH_2-C<u>H</u>$_2$-CH; CH_2-C<u>H</u>$_2$-CH_2), 1.07 – 0.98 (m, 1H, C<u>H</u>$_2$-CH_2-CH_2).

^{13}C NMR (101 MHz, DMSO) δ 179.95 (N-<u>C</u>S-NH), 176.20 (Cq-<u>C</u>O-NH), 142.76 (<u>Cq</u>$_{Ar}$-N), 128.91 (<u>2C</u>H$_{Ar}$), 117.33 (<u>C</u>H$_{Ar}$), 113.22 (<u>2C</u>H$_{Ar}$-Cq$_{Ar}$-N), 58.61 (NH-<u>C</u>H$_2$-N), 57.73 (N-<u>Cq</u>), 54.47 (<u>C</u>H-NH-CS), 44.46 (<u>C</u>H$_2$-N-CS), 32.01 (<u>C</u>H$_2$-CH-NH), 27.14 (<u>C</u>H$_2$-Cq-CO), 25.21 (CH_2-<u>C</u>H$_2$-CH_2-CH), 25.08 (<u>C</u>H$_2$-CH_2-CH_2-CH).

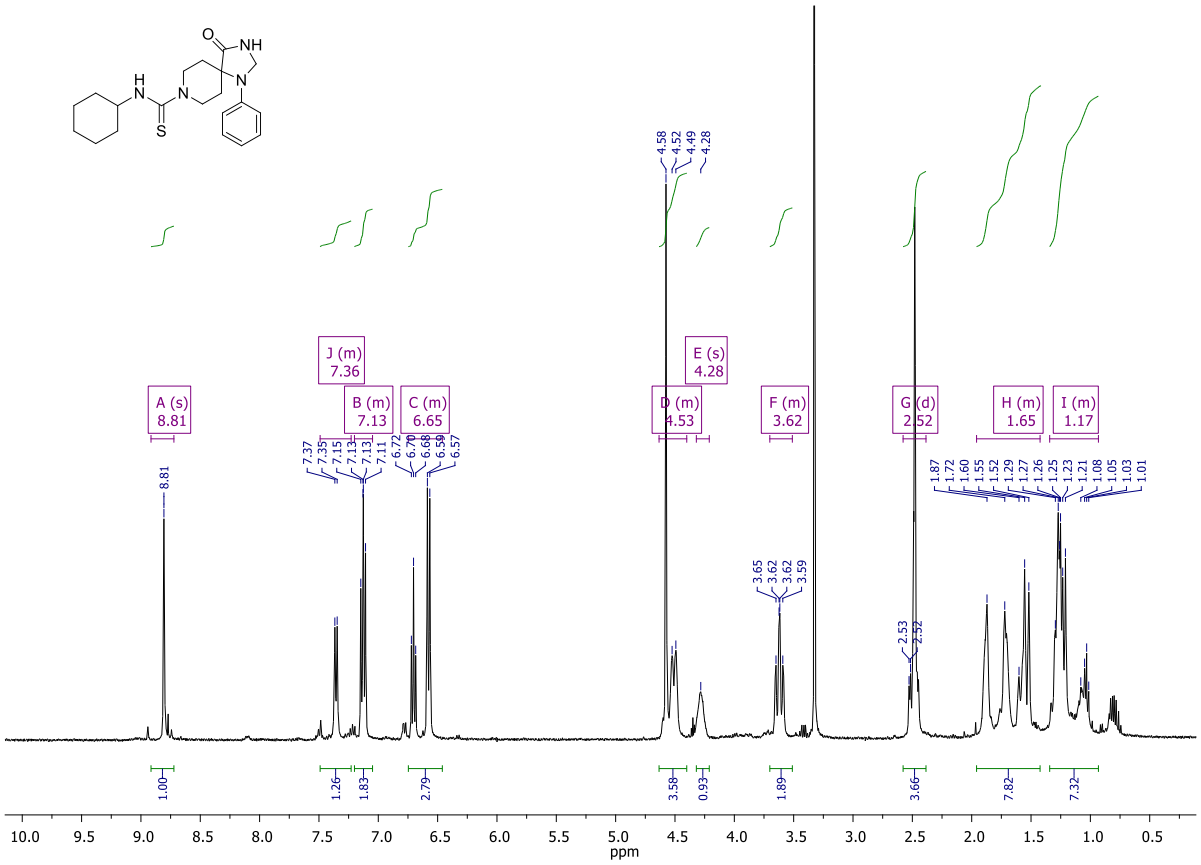
A (s) 8.81
B (m) 7.13
C (m) 6.65
D (m) 4.53
E (s) 4.28
F (m) 3.62
G (d) 2.52
H (m) 1.65
I (m) 1.17
J (m) 7.36
ppm

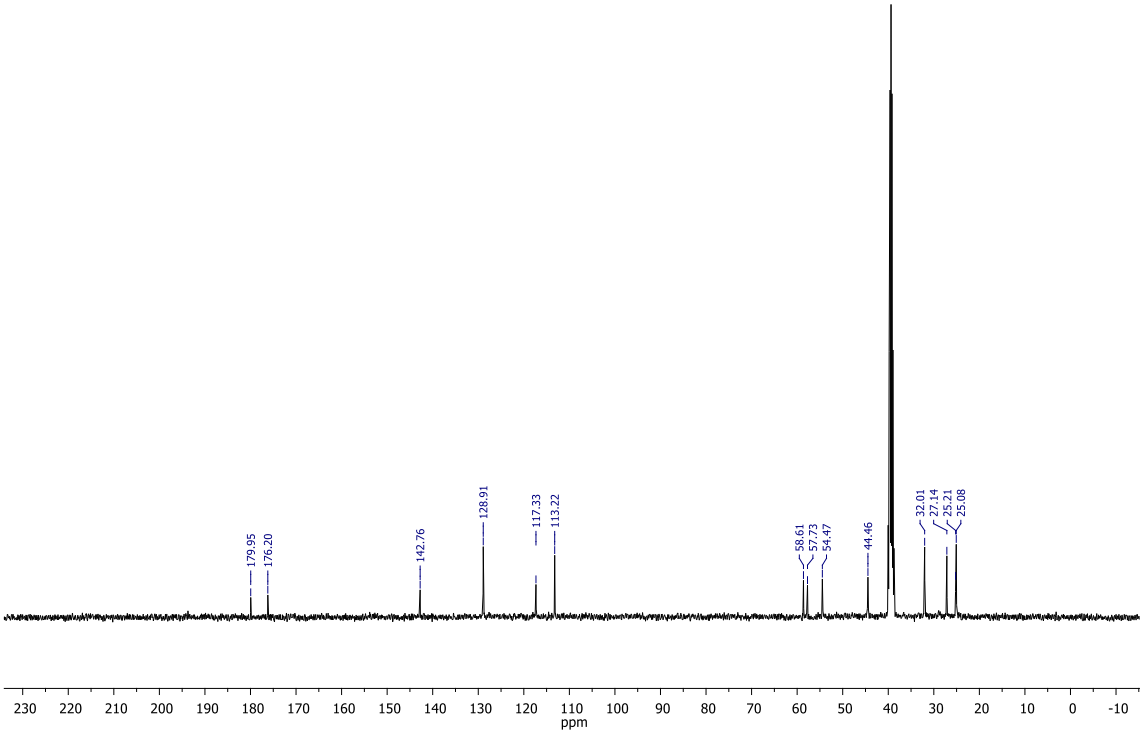
ppm

14.5 CO^{2+}-Calcein essay

Briefly, the protocol requires, first, to seed cells in order to reach a 50% confluence. When this feature is gained, cells are washed with Krebs-Ringer Buffer (KRB), in order to remove cellular debris and the medium. Then it is added a labelling solution, containing 1 μM calcein, 2 μM $CoCl_2$ and 20 μM sulfinpyrazone, as it inhibits molecular extrusion, and the system is stirred with cells at 37°C for 15 minutes. After this, it is washed carefully again with KRB, in order to remove unbound dyes, and then with a modified KRB, enriched with 1M $CaCl_2$. The system is then loaded into fluorescence microscope, where constant 37 °C temperature and low illumination are required, as respectively HeLa cells and calcein are sensitive to them. It is even important to avoid extended and intense excitation, which induce a fluorophore decay independent from Co^{2+} quenching. Selected region of interest near mitochondria and one in the background are selected to measure kinetic trends and then an imaging acquisition with a frequency of 500 msec is started. First basal acquisition is maintained for a minute, to monitor the system is in an equilibrium state. After this, 500 nM ionomycin solution is introduced into the selected region, as it facilitates Ca^{2+} into cells. So, imagine acquisition is maintain for nine more minutes and then collected and elaborated to gain measures of mPTP opening, as arbitrary fluorescence units. Starting from them, first, the background trace is removed and slope of the curve in the first minute after ionomycin stimulation are calculated. Then, the significative curve is derived from the average of the slopes, as the one closest to the average itself. Finally, converting arbitrary fluorescence units into percentage, significative curves after pre-treatment with different compounds can be compared.

Figure 94 shows results obtained from 1µM DCU derivatives **1–3** and **14-18** administration.

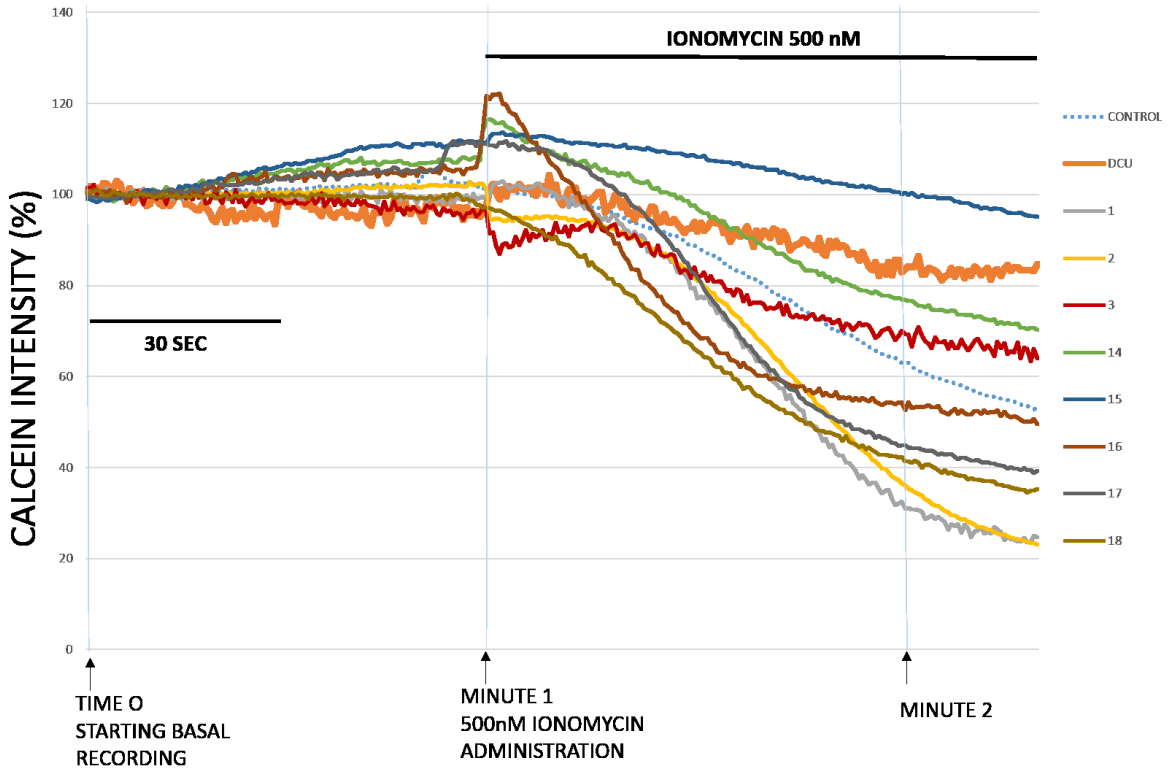

Figure 94: mPTP opening after pre-treatment with 1µM urea derivatives

As shown in figure 94, compounds with the kinetic curve above the control in the first minute after ionomycin administration (minute 2) are active as inhibitors of mPTP opening, as they prevent in this way Co^{2+} entry into mitochondria and its quenching calcein. Thus, calcein fluorescence intensity decrease is lower if compared to control. Inversely, compounds with the kinetic curve below the control behave as activators of mPTP opening. Thus given, according to preliminary results, among all the examined compounds, **3**, **14** and **15** seem to be inhibitors of mPTP opening, while compounds **1**, **2** and **16**, **17** and **18** seem to be activators.

15. Discussion and conclusions

This project was conducted with the purpose of investigating inhibitors of mPTP complex opening with potential interesting application in ischemic-reperfusion injury (IRI).
Two classes of derivatives were produced starting from DCU and 1-phenyl-1, 3, 8-triaza-spiro[4,5]decan-4-one models. DCU model was applied to produce symmetric and asymmetric ureas, thioureas and carbamates, while the 1-phenyl-1, 3, 8-triaza-spiro[4,5]decan-4-one template was used to produce *N*-8 derivatives.

Preliminary results attested 1, 3-diphenylurea **(3)**, 1, 3-dibenzylthiourea **(15)** and 1-cyclohexyl-3-phenyl-thiourea **(16)** as active inhibitor of mPTP opening. On the contrary, 1, 3-dicyclopentylurea **(1)** and 1, 3-dicyclopropylurea (**2)** seem to have no effect or low activation effect.

Considering this early preliminary results, it seems that a steric recognition plays an important role regarding DCU derivatives: the smaller the cycles attached to the urea moiety, the lower the inhibition effect. Moreover, it seems that 1, 3-dicyclopropylurea (**2)** slightly promote mPTP opening. Remarkably, carbamates (compounds **17** and **18**) demonstrate an agonist effect on mPTP opening (Figure 95).

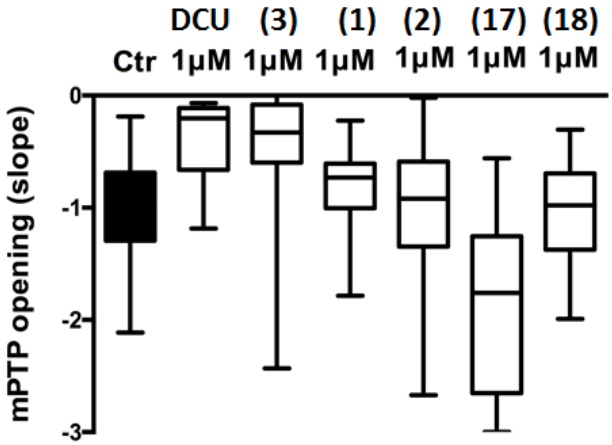

Figure 95: Preliminary results on inhibition of MPTP opening with ureas and carbamates

For the previous reasons, further investigation regarding the steric hindrance on nitrogen atoms is required and will be investigated in the nearly future.

Results with thioureas derivatives have a more complex interpretation (Figure 96).

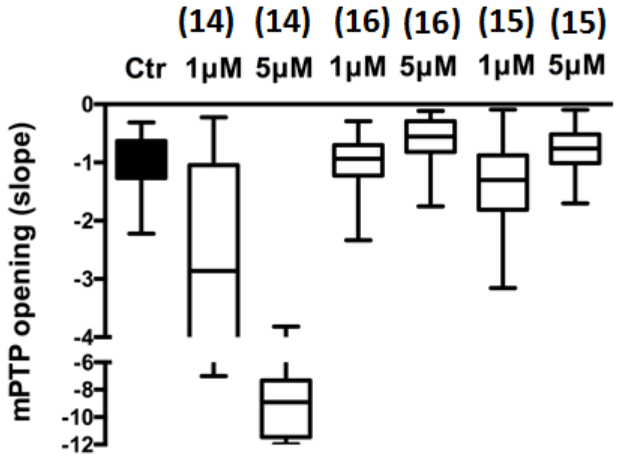

Figure 96: Preliminary results on inhibition of MPTP opening with thioureas

1-cyclohexyl-3-phenyl-thiourea **(16)** and 1, 3-dibenzylthiourea **(15)** seem to show a rather low inhibition activity at 5 µM concentration. However, it seems that compound **15** shows a low agonist activity at low concentration, suggesting that this compound could have different interactions within the mitochondria.

1, 3-dicyclohexylthiourea **(14)** demonstrates a clear agonist effect. This result is quiet peculiar, even more when confronted with 1, 3-dicyclohexylurea that, on the contrary, has a great inhibition activity on mPTP opening. This difference highly suggests the need of further studies regarding the role of carbonyl or thiocarbonyl in ureas and thioureas on mPTP opening or inhibition. Moreover, if these preliminary results would be confirmed, thioureas could be evaluated as starting points for antitumor compounds development.

Up to now *N*-8 derivatives of 1-phenyl-1, 3, 8-triaza-spiro[4,5]decan-4-one are still on biological evaluation, even if preliminary results show 1-phenyl-8-tosyl-1, 3, 8–triaza-spiro[4,5]decan-4-one **(21)** to possess a rather strong inhibition effect (even at nanomolar concentration).

Abbreviations

Ac_2O Acetic anhydride; ADP Adenosin Diphosphate; ATP Adenosin Triphosphate; CDI Carbonyldiimidazole; CsA Cyclosporin A; CH_2Cl_2 Dichloromethane, CH_3CN Acetonitrile; DCOW Decanter Centrifuge Orange Waste; DCC Dicyclohexylcarbodiimide, DCU Dicyclohexylurea, DIPEA Diisopropyl-ethyl-amine; DMSO-d_6 Dimethyl-sulfoxide, DS degree of substitution; ETC Electron transport chain, EtOH Ethanol; Et_2O Diethylether, EtOAc Ethyl Acetate, FAD Flavinic transporter, h hours, HCl hydrochloric acid H_2O water, IMS Inter-membrane space, IRI Ischemia - reperfusion injury, K_2CO_3 Potassium carbonate, KRB Krebs-Ringer Buffer, mp Melting point, MeOH methanol; mCypD Mitochondrial Cyclophilin D; MPT Mitochondrial Permeability Transition; mPTP Mitochondrial Permeability Transition Pore; NAD Nicotinammidic transporters, NaOH Sodium Hydroxide, NH_4OH Ammonium Hydroxide, mPTP Mitochondrial Permability Transition Pore, P_i inorganic phosphate, RT Room Temperature, SAR Structure - Activity Relationship, THF Tetrahydrofuran

Bibliography

1. Davies FS, Albrigo LG. *Citrus*. Oxon, UK: Cab International; 1994.

2. Chang K. The evaluation of citrus demand and supply. In: *International Citrus Congress*. 1992.

3. Hodges AW, Rahmani M, Stevens TJ *et al. Economic Impacts of the Florida Citrus Industry*. Florida; 2014.

4. FAO (Food and Agriculture Organization of the United Nations). *Citrus Fruit Statistics 2015*. Rome; 2016.

5. Ladaniya MS. Fruit Biochemistry. In: *Citrus fruits: biology, technology and evaluation*. 1st ed. San Diego, CA, USA: Academic Press Inc., 2008, pp.125–190.

6. Sandhu KS, Minhas KS, Sidhu JS. Processing of Citrus Juices. In: Sinha NK, Sidhu JS, Barta J, et al., eds. *Handbook of fruits and fruit processing*. 2nd ed. Ames, Iowa, USA: Wiley-Blackwell, 2012, pp.489–533.

7. Kimball DA. Description of Citrus Fruit. In: *Citrus Processing*. 2nd ed. Gaithersburg, Maryland, USA: Aspen Publishers, Inc., 1999, pp.7–42.

8. Topuz A, Topakci M, Canakci M *et al.* Physical and nutritional properties of four orange varieties. *J. Food Eng.* 2005; **66**: 519–523.

9. Stinco CM, Fernández-Vázquez R, Hernanz D *et al.* Industrial orange juice debittering: Impact on bioactive compounds and nutritional value. *J. Food Eng.* 2013; **116**: 155–161.

10. Park GL, Byers JL, Pritz CM *et al.* Characteristics of California Navel Orange Juice ana pulpwash. *J. Food Sci.* 1983; **48**: 627–632.

11. Le Gall G, Puaud M, Colquhoun LJ. Discrimination between orange juice and pulp wash by 1H nuclear magnetic resonance spectroscopy: Identification of marker compounds. *J. Agric. Food Chem.* 2001; **49**: 580–588.

12. Ting S V. Nutrient labeling of citrus products. In: Nagy S, Shaw PE, Veldhuise MK, eds. *Citrus Science and Technology*. Connecticut, USA: AVI Publishers, 1977, pp.401–444.

13. Trumbo P, Yates AA, Schlicker S *et al.* Dietary Reference Intakes: Vitamin A, Vitamin K, Arsenic, Boron, Chromoium, Copper, Iodine, Iron, Manganese, Molybdenum, Nickel, Silicon, Vanadium, and Zinc. *J. Am. Diet. Assoc.* 2001; **101**: 294–301.

14. Layrisse M, García-Casal MN. Strategies for the prevention of iron deficiency through foods in the household. *Nutr. Rev.* 1997; **55**: 233–239.

15. Streiff RR. Folate levels in citrus and other juices. *Am. J. Clinc. Nutr.* 1971; **24**: 1390–1392.

16. Ting SV, Newhall WF. Occurence of natural anti-oxidants in citrus fruits. *J. Food Sci.* 1965; **30**: 57–62.

17. Church CJ, A. CW. *Food values of commonly used portions of fruits and vegetables*. Philadelphia, PA, USA: Lippincot Publishing Company; 1970.

18. Leopold LF, Leopold N, Diehl H-A *et al.* Quantification of carbohydrates in fruit juices using FTIR spectroscopy and multivariate analysis. *Spectrosc. An Int. J.* 2011; **26**: 93–104.

19. Ladaniya MS. Nutritive and medicinal value of citrus fruits. In: *Citrus fruits: biology, technology and evaluation*. 1st ed. San Diego, CA, USA: Academic Press Inc., 2008, pp.501–514.

20. So F V, Guthrie N, Chambers AF *et al.* Inhibition of human breast cancer cell proliferation and delay of mammary tumorigenesis by flavonoids and citrus juices. *Nutr. Cancer* 1996; **26**: 167–181.

21. Miyagi Y, Om AS, Chee KM *et al.* Inhibition of Azoxymethane-Induced Colon Cancer by Orange Juice. *Nutr. Cancer* 2000; **36**: 224–229.

22. Bates RP, Morris JR, Crandall PG. Principles and practices of small - and medium - scale fruit juice processing. *FAO Agric. Serv. Bull.* 2001: 11–15.

23. FAO (Food and Agriculture Organization of the United Nations). *Codex Alimentarius. volume 6, Fruit Juices and related Prodcuts*. 2nd ed. Rome: Food and Agriculture Organization; 1992.

24. Lee HS, Coates GA. Vitamin C in frozen, fresh squeezed, unpasteurized, polyethylene-bottled orange juice: A

storage study. *Food Chem.* 1999; **65**: 165–168.

25. Linton M, McClements JMJ, Patterson MF. Survival of Escherichia coli O157:H7 during Storage in Pressure-Treated Orange Juice. *J. Food Prot.* 1999; **9**: 975–1096.

26. Pao S, Davis CL. Enhancing microbiological safety of fresh orange juice by fruit immersion in hot water and chemical sanitizers. *J. Food Prot.* 1999; **62**: 756–760.

27. Berk Z. Production of single-strenght citrus juice. In: *Citrus Fruit Processing*. 1st ed. London, UK: Academic Press, 2016, pp.127–185.

28. Kimball DA. Processing Methods, Equipment, and Engineering. In: *Citrus Processing*. 2nd ed. Gaithersburg, Maryland, USA: Aspen Publishers, Inc., 1999, pp.73–140.

29. JBT FoodTech. Citrus Juice Extractor. *http://www.jbtfoodtech.com/solutions/equipment/citrus-juice-extractor.* 2016: Last accessed: 05/01/2017.

30. Versteeg C, Rombouts FM, Spaansen CH *et al.* Thermostability and Orange Juice Cloud Destabilizing Properties of Multiple Pectinesterases From Orange. *J. Food Sci.* 1980; **45**: 969–971.

31. Fellers PJ, Carter RD. Effect of thermal processing and storage of chilled orange juice and flavor quality. *Fluss. Obs.* 1993; **60**: 436–441.

32. Rebeck HM. Processing of citrus juices. In: Ashurst PR, ed. *Production and Packaging of Non-Carbonated Fruit Juices and Fruit Beverages*. Glasgow, UK: Blackie Academic and Professional, 1995, pp.221–252.

33. Farnworth E., Lagacé M, Couture R *et al.* Thermal processing, storage conditions, and the composition and physical properties of orange juice. *Food Res. Int.* 2001; **34**: 25–30.

34. Lee HS, Coates GA. Effect of thermal pasteurization on Valencia orange juice color and pigments. *LWT - Food Sci. Technol.* 2003; **36**: 153–156.

35. Cinquanta L, Albanese D, Cuccurullo G *et al.* Effect on orange juice of batch pasteurization in an improved pilot-scale microwave oven. *J. Food Sci.* 2010; **75**: 46–50.

36. Yeom HW, Streaker CB, Howard Zhang Q *et al.* Effects of pulsed electric fields on the quality of orange juice and comparison with heat pasteurization. *J. Agric. Food Chem.* 2000; **48**: 4597–4605.

37. Hodgins AM, Mittal GS, Griffiths MW. Pasteurization of Fresh Orange Juice Using Low-Energy Pulsed Electrical Field. *J. Food Sci.* 2002; **67**: 2294–2299.

38. Cerdán-Calero M, Izquierdo L, Sentandreu E. Valencia Late orange juice preserved by pulp reduction and high pressure homogenization: Sensory quality and gas chromatography-mass spectrometry analysis of volatiles. *LWT - Food Sci. Technol.* 2013; **51**: 476–483.

39. Tran MTT, Farid M. Ultraviolet treatment of orange juice. *Innov. Food Sci. Emerg. Technol.* 2004; **5**: 495–502.

40. Ros-Chumillas M, Belissario Y, Iguaz A *et al.* Quality and shelf life of orange juice aseptically packaged in PET bottles. *J. Food Eng.* 2007; **79**: 234–242.

41. Crandall PG, Chen CS, Davis KC. Preparation and Storage of 72° Brix Orange Juice Concentrate. *J. Food Sci.* 1987; **52**: 381–385.

42. Berk Z. Production of citrus juice concentrates. In: *Citrus Fruit Processing*. 1st ed. London, UK: Academic Press, 2016, pp.187–218.

43. Braddock RJ, Kesterson JW. Use of Enzymes to increase yield of orange juice pulp-wash solids. *Proc. Fla. State Hort. Sot., Stat* 1974; **87**: 310–312.

44. Braddock RJ, Kesterson JW. Enzyme use to reduce viscosity and increase recovery of soluble solids from citrus pulp-washing operations. *J. Food Sci.* 1976; **41**: 82–85.

45. Sreenath HK, Crandall PG, Baker RA. Utilization of citrus by-products and wastes as beverage clouding agents. *J. Ferment. Bioeng.* 1995; **80**: 190–194.

46. Bampidis VA, Robinson PH. Citrus by-products as ruminant feeds: A review. *Anim. Feed Sci. Technol.* 2006; **128**: 175–217.

47. Abbasi H, Seidavi A, Liu W *et al.* Investigation on the effect of different levels of dried sweet orange (Citrus sinensis) pulp on performance, carcass characteristics and physiological and biochemical parameters in broiler chicken. *Saudi J. Biol. Sci.* 2015; **22**: 139–146.

48. Tripodo MM, Mondello F, Lanuzza F. Simultaneous Recovery of Dietary Fibres and Hesperidin From Industrial Lemon Waste. 2012; **2**: 731–738.

49. El Boushy ARY, van der Poel AFB. Fruit, Vegetable and Bewers' Waste. In: *Handbook of Poultry Feed From Waste: Processing and Use*. 2nd Ed. Dordrecht, NL: Springer Science Business Media B. V., 2000.

50. Braddock RJ. *Handbook of Citrus By-Products and Processing Technology*. 1st ed. New York, USA: Wiley; 1999.

51. Von Loesecke HW. Citrus Fruits Industry. *Ind. Eng. Chem.* 1952; **44**: 476–82.

52. Pavón-Silva T, Pacheco-Salazar V, Sánchez-Meza JC *et al.* Physicochemical and biological combined treatment applied to a food industry wastewater for reuse. *J. Environ. Sci. Heal. Pt. A* 2009; **44**: 108–115.

53. Amor C, Lucas MS, Pirra AJ *et al.* Treatment of concentrated fruit juice wastewater by the combination of biological and chemical processes. *J. Environ. Sci. Health. A. Tox. Hazard. Subst. Environ. Eng.* 2012; **47**: 1809–17.

54. Koppar A, Pullammanappallil P. Anaerobic digestion of peel waste and wastewater for on site energy generation in a citrus processing facility. *Energy* 2013; **60**: 62–68.

55. Xie Z, Guan W, Ji F *et al.* Production of biologically activated carbon from orange peel and landfill leachate subsequent treatment technology. *J. Chem.* 2014; **2014**.

56. Tripodo MM, Lanuzza F, Micali G *et al.* Citrus waste recovery: A new environmentally friendly procedure to obtain animal feed. *Bioresour. Technol.* 2004; **91**: 111–115.

57. Widmer WW, Montanari AM. Citrus waste streams as a source for phytochemicals. *Proc. Fla. State Hort. Soc* 1994; **107**: 284–288.

58. Maroulis ZB, Saravacos GD. *Food Plant Economy*. New York: CRC Press; 2008.

59. Dietrich WC, Van Atta GR. Valencia Orange-Seed Oil. *Oil Soap* 1944: 19–22.

60. Fong CH, Hasegawa S, Miyake M *et al.* Limonoids and their glucosides in Valencia orange seeds during fruit growth and development. *J. Agric. Food Chem.* 1993; **41**: 112–115.

61. Akpata MI, Akubor PI. Chemical composition and selected functional properties of sweet orange (Citrus sinensis) seed flour. *Plant Foods Hum. Nutr.* 1999; **54**: 353–362.

62. Jorge N, Da Silva AC, Aranha CPM. Antioxidant activity of oils extracted from orange (Citrus sinensis) seeds. *Ann. Brazilian Acad. Sci.* 2016; **88**: 951–958.

63. El-Adawy TA, Rahma EH, El-Bedawy AA *et al.* Properties of some citrus seeds. Part 3. Evaluation as a new source of protein and oil. *Mol. Nutr. Food Res.* 1999; **43**: 385–391.

64. Dhifi W, Mnif W. Valorization of Some By-Products of Maltese Orange from Tunisia: Peel Essential Oil and Seeds Oil. *Anal. Chem. Lett.* 2011; **1**: 397–401.

65. Rivas B, Torrado A, Torre P *et al.* Submerged citric acid fermentation on orange peel autohydrolysate. *J. Agric. Food Chem.* 2008; **56**: 2380–2387.

66. Aravantinos-Zafiris G, Oreopoulou V, Tzia C *et al.* Fibre Fraction from Orange Peel Residues after Pectin Extraction. *LWT - Food Sci. Technol.* 1994; **27**: 468–471.

67. Marín FR, Soler-Rivas C, Benavente-García O *et al.* By-products from different citrus processes as a source of customized functional fibres. *Food Chem.* 2007; **100**: 736–741.

68. Larrea MA, Chang YK, Martìnez Bustos F. Effect of some operational extrusion parameters on the constituents of orange pulp. *Food Chem.* 2005; **89**: 301–308.

69. AOAC. *Official methods of analysis of AOAC International*. 17th ed. Gaithersburg, Maryland, USA; 2000.

70. Mamma D, Christakopoulos P. Biotransformation of Citrus By-Products into Value Added Products. *Waste and Biomass Valorization* 2014; **5**: 529–549.

71. Sharma N, Dobhal M, Joshi Y *et al.* Flavonoids: A versatile source of anticancer drugs. *Pharmacogn. Rev.* 2011; **5**: 1.

72. Prabasari I, Pettolino F, Liao ML *et al.* Pectic polysaccharides from mature orange (Citrus sinensis) fruit albedo cell walls: Sequential extraction and chemical characterization. *Carbohydr. Polym.* 2011; **84**: 484–494.

73. Guccione C, Bergonzi MC, Piazzini V *et al.* A Simple and Rapid HPLC - PDA MS Method for the Profiling of Citrus Peels and Traditional Italian Liquors. *Planta Med* 2016; **82**: 1039–1045.

74. Mira B, Blasco M, Berna A *et al.* Supercritical CO2 extraction of essential oil from orange peel. Effect of operation conditions on the extract composition. *J. Supercrit. Fluids* 1999; **14**: 95–104.

75. Jabri Karoui I, Marzouk B. Characterization of bioactive compounds in Tunisian bitter orange (Citrus aurantium L.) peel and juice and determination of their antioxidant activities. *Biomed Res. Int.* 2013; **2013**.

76. Wang YC, Chuang YC, Hsu HW. The flavonoid, carotenoid and pectin content in peels of citrus cultivated in Taiwan. *Food Chem.* 2008; **106**: 277–284.

77. Ververidis F, Trantas E, Douglas C *et al.* Biotechnology of flavonoids and other phenylpropanoid-derived natural products. Part I: Chemical diversity, impacts on plant biology and human health. *Biotechnol. J.* 2007; **2**: 1214–1234.

78. Koutinas M, Patsalou M, Stavrinou S *et al.* High temperature alcoholic fermentation of orange peel by the newly isolated thermotolerant Pichia kudriavzevii KVMP10. *Lett. Appl. Microbiol.* 2016; **62**: 75–83.

79. Pourbafrani M, Talebnia F, Niklasson C *et al.* Protective effect of encapsulation in fermentation of limonene-contained media and orange peel hydrolyzate. *Int. J. Mol. Sci.* 2007; **8**: 777–787.

80. Miran W, Nawaz M, Jang J *et al.* Conversion of orange peel waste biomass to bioelectricity using a mediator-less microbial fuel cell. *Sci. Total Environ.* 2016; **547**: 197–205.

81. Miranda R, Bustos-Martinez D, Blanco CS *et al.* Pyrolysis of sweet orange (Citrus sinensis) dry peel. *J. Anal. Appl. Pyrolysis* 2009; **86**: 245–251.

82. Santos CM, Dweck J, Viotto RS *et al.* Application of orange peel waste in the production of solid biofuels and biosorbents. *Bioresour. Technol.* 2015; **196**: 469–479.

83. Martín MA, Siles JA, El Bari H *et al.* Orange Peel: Organic Waste or Energetic Resource? *http://www.ramiran.net/ramiran2010/docs/ Ramiran2010_0083_final.pdf* 2008: Last accessed: 05/01/2017.

84. Siles JA, Vargas F, Gutiérrez MC *et al.* Integral valorisation of waste orange peel using combustion, biomethanisation and co-composting technologies. *Bioresour. Technol.* 2016; **211**: 173–182.

85. Torrado AM, Cortés S, Salgado JM *et al.* Citric acid production from orange peel wastes by solid-state fermentation. *Brazilian J. Microbiol.* 2011; **42**: 394–409.

86. Hashemian S, Shayegan J. A comparative study of cellulose agricultural wastes (almond shell, pistachio shell, walnut shell, tea waste and orange peel) for adsorption of violet B dye from aqueous solutions. *Orient. J. Chem.* 2014; **30**: 2091–2098.

87. Dhakal RP, Ghimire KN, Inoue K. Adsorptive separation of heavy metals from an aquatic environment using orange waste. *Hydrometallurgy* 2005; **79**: 182–190.

88. Lu D, Cao Q, Li X *et al.* Kinetics and equilibrium of Cu(II) adsorption onto chemically modified orange peel cellulose biosorbents. *Hydrometallurgy* 2009; **95**: 145–152.

89. Jeyaseelan C, Gupta A. Orange Peel as Natural Adsorbent for the Removal of Chromium (VI) from Water Samples. *Indo Glob. J. Pharm. Sci.* 2014; **4**: 2249.

90. Braddock RJ, Temelli F, Cadwallader KR. Citrus essential oils - A dossier for material safety data sheet. *Food Technol.* 1986; **40**: 114–116.

91. Murdock DI, Allen WE. Germicidal Effect of Orange Peel Oil and D-Limonene in Water and Orange Juice. *Food Technol.* 1960; **14**: 441–445.

92. Dugo P, Mondello L, Cogliandro E *et al.* On the genuineness of citrus essential oils. Part XLVI. Polymethoxylated flavones of the non-volatile residue of Italian sweet orange and mandarin essential oils. *Flavour Fragr. J.* 1994; **9**: 105–111.

93. Verzera A, Trozzi A, Dugo G *et al.* Biological lemon and sweet orange essential oil composition. *Flavour Fragr. J.* 2004; **19**: 544–548.

94. Owusu-Yaw J, Matthews RF, West PF. Alcohol Deterpenation of Orange Oil. *J. Food Sci.* 1986; **51**: 1180–1182.

95. Dugo P, Mondello L, Bartle KD *et al.* Deterpenation of sweet orange and lemon essential oils with supercritical carbon dioxide using silica gel as an adsorbent. *Flavour Fragr. J.* 1995; **10**: 51–58.

96. Rezzadori K, Benedetti S, Amante ER. Proposals for the residues recovery: Orange waste as raw material for new products. *Food Bioprod. Process.* 2012; **90**: 606–614.

97. Berna A, Tárrega A, Blasco M *et al.* Supercritical CO2 extraction of essential oil from orange peel; effect of the height of the bed. *J. Supercrit. Fluids* 2000; **18**: 227–237.

98. Bauer K, Garbe D, Surburg H. Cyclic Terpenes. In: *Common Fragrance and Flavor Materials*. 4th ed. Weinheim, DE: Wiley-VCH, 2001, pp.48–74.

99. Tan Q, Day DF. Bioconversion of limonene to α-terpineol by immobilized Penicillium digitatum. *Appl. Microbiol. Biotechnol.* 1998; **49**: 96–101.

100. Adams A, Demyttenaere JCR, De Kimpe N. Biotransformation of (R)-(+)- and (S)-(-)-limonene to α-terpineol by Penicillium digitatum - Investigation of the culture conditions. *Food Chem.* 2003; **80**: 525–534.

101. Maròstica MRJ, Pastore GM. Production of R-(+)-α-terpineol by the biotransformation of limonene from orange essential oil, using cassava waste water as medium. *Food Chem.* 2006; **101**: 345–350.

102. Ferrer JL, Austin MB, Stewart C *et al.* Structure and function of enzymes involved in the biosynthesis of phenylpropanoids. *Plant Physiol. Biochem.* 2008; **46**: 356–370.

103. Falcone Ferreyra ML, Rius SP, Casati P. Flavonoids: biosynthesis, biological functions, and biotechnological applications. *Front. Plant Sci.* 2012; **3**: 1–15.

104. Shashank K, Abhay K. Review Article Chemistry and Biological Activities of Flavonoids: An Overview. *Sci. World J* 2013; **4**: 32–48.

105. Gil-Izquierdo A, Gil MI, Ferreres F. Effect of processing techniques at industrial scale on orange juice antioxidant and beneficial health compounds. *J. Agric. Food Chem.* 2002; **50**: 5107–5114.

106. Garg A, Garg S, Zaneveld LJD *et al.* Chemistry and Pharmacology of The Citrus Bioflavonoid Hesperidin. 2001; **669**: 655–669.

107. Montanari A, Chen J, Widmer W. Citrus Flavonoids: A Review of Past Biological Activity Against Disease. In: Manthey JA, Buslig BS, eds. *Flavonoids in the living system*. 1 ed. New York, USA: Springer Science Business Media B. V., 1998, pp.103–116.

108. Ortuño A, Arcas MC, Botía JM *et al.* Increasing resistance against Phytophthora citrophthora in tangelo Nova fruits by modulating polymethoxyflavones levels. *J. Agric. Food Chem.* 2002; **50**: 2836–2839.

109. Ortuño A, Gómez P, Báidez A *et al.* Citrus sp.: A Source of Flavonoids of Pharmaceutical Interest. In: Patil BS, Turner ND, Miller EG, et al., eds. *Potential Health Benefit of Citrus*. 1st ed. Washington, DC, USA: American Chemical Society, 2006, pp.175–185.

110. Montanari A, Widmer W, Nagy S. Health Promoting Phytochemicals in Citrus Fruit and Juice Products. In: Johns T, Romeo JT, eds. *Recent Advances in Phytochemistry vol. 31 - Functionality of Food Phytochemicals*. 1st Ed. New York, USA: Springer Science Business Media B. V., 1997, pp.31–52.

111. Sawalha SMS, Arráez-Román D, Segura-Carretero A *et al.* Quantification of main phenolic compounds in sweet and bitter orange peel using CE-MS/MS. *Food Chem.* 2009; **116**: 567–574.

112. Marston A, Hostettmann K. Separation and Quantification of Flavonoids. In: Andersen OM, Markham KR, eds. *Flavonoids: Chemistry, Biochemistry and Applications*. 1st Ed. Boca Raton, FL, USA: CRC Press, 2006, pp.1–36.

113. Pfaltzgraff L a, De bruyn M, Cooper EC *et al.* Food waste biomass: a resource for high-value chemicals. *Green Chem.* 2013; **15**: 307–314.

114. Lo Curto R, Tripodo MM, Leuzzi U *et al.* Flavonoids recovery and SCP production from orange peel. *Bioresour. Technol.* 1992; **42**: 83–87.

115. Di Mauro A, Fallico B, Passerini A *et al.* Recovery of hesperidin from orange peel by concentration of extracts on styrene-divinylbenzene resin. *J. Agric. Food Chem.* 1999; **47**: 4391–4397.

116. Luengo E, Álvarez I, Raso J. Improving the pressing extraction of polyphenols of orange peel by pulsed electric fields. *Innov. Food Sci. Emerg. Technol.* 2013; **17**: 79–84.

117. Manthey JA, Grohmann K. Phenols in citrus peel byproducts. Concentrations of hydroxycinnamates and polymethoxylated flavones in citrus peel molasses. *J. Agric. Food Chem.* 2001; **49**: 3268–3273.

118. Bocco A, Cuvelier M, Richard H *et al.* Antioxidant Activity and Phenolic Composition of Citrus Peel and Seed Extracts. *J. Agric. Food Chem.* 1998; **46**: 2123–2129.

119. Li S, Yu H, Ho CT. Nobiletin: Efficient and large quantity isolation from orange peel extract. *Biomed. Chromatogr.* 2006; **20**: 133–138.

120. Uckoo RM, Jayaprakasha GK, Patil BS. Rapid separation method of polymethoxyflavones from citrus using flash chromatography. *Sep. Purif. Technol.* 2011; **81**: 151–158.

121. Weber B, Hartmann B, Stöckigt D *et al.* Liquid chromatography/mass spectrometry and liquid chromatography/nuclear magnetic resonance as complementary analytical techniques for unambiguous identification of polymethoxylated flavones in residues from molecular distillation of orange peel oils (Citrus x Sinensis). *J. Agric. Food Chem.* 2006; **54**: 274–278.

122. Gaydou EM, Berahia T, Wallet J-C *et al.* Gas chromatography of some polymethoxylated flavones and their determination in orange peel oils. *J. Chromatogr. A* 1991; **549**: 440–445.

123. Li S, Lo CY, Ho CT. Hydroxylated polymethoxyflavones and methylated flavonoids in sweet orange (Citrus sinensis) peel. *J. Agric. Food Chem.* 2006; **54**: 4176–4185.

124. Manthey JA, Grohmann K. Concentrations of Hesperidin and Other Orange Peel Flavonoids in Citrus Processing Byproducts. *J. Agric. Food Chem.* 1996; **44**: 811–814.

125. Anagnostopoulou MA, Kefalas P, Kokkalou E *et al.* Analysis of antioxidant compounds in sweet orange peel by HPLC-diode array detection-electrospray ionization mass spectrometry. *Biomed. Chromatogr.* 2005; **19**: 138–148.

126. Anagnostopoulou MA, Kefalas P, Papageorgiou VP *et al.* Radical scavenging activity of various extracts and fractions of sweet orange peel (Citrus sinensis). *Food Chem.* 2006; **94**: 19–25.

127. Manthey JA. Fractionation of orange peel phenols in ultrafiltered molasses and mass balance studies of their antioxidant levels. *J. Agric. Food Chem.* 2004; **52**: 7586–7592.

128. de Rijke E, Out P, Niessen WMA *et al.* Analytical separation and detection methods for flavonoids. *J. Chromatogr. A* 2006; **1112**: 31–63.

129. Braconnot H. Investifations into a new acid spread throughout all plants. *Ann. Chim. Phys. Ser. 2* 1825; **28**: 173–178.

130. Harholt J, Suttangkakul A, Vibe Scheller H. Biosynthesis of Pectin. *Plant Physiol.* 2010; **153**: 384–395.

131. El-Nawawi SA, Shehata FR. Extraction of pectin from Egyptian orange peel. Factors affecting the extraction. *Biol. Wastes* 1987; **20**: 281–290.

132. Kar F, Arslan N. Characterization of orange peel pectin and effect of sugars, L-ascorbic acid, ammonium persulfate, salts on viscosity of orange peel pectin solutions. *Carbohydr. Polym.* 1999; **40**: 285–291.

133. Gee M, Mccomb EA, Mccready RM. A method for the characterization of pectic substances in some fruit and sugar-beet marcs. *J. Food Sci.* 1957; **23**: 72–75.

134. Kratchanova M, Pavlova E, Panchev I. The effect of microwave heating of fresh orange peels on the fruit tissue and quality of extracted pectin. *Carbohydr. Polym.* 2004; **56**: 181–185.

135. Prakash Maran J, Sivakumar V, Thirugnanasambandham K *et al.* Optimization of microwave assisted extraction of pectin from orange peel. *Carbohydr. Polym.* 2013; **97**: 703–709.

136. Aravantinos-Zafiris G, Oreopoulou V. The effect of nitric acid extraction variables on orange pectin. *J. Sci. Food Agric.* 1992; **60**: 127–129.

137. Joye DD, Luzio GA. Process for selective extraction of pectins from plant material by differential pH. *Carbohydr. Polym.* 2000; **43**: 337–342.

138. Ma E, Cervera Q, Mejía Sánchez GM. Integrated utilization of orange peel. *Bioresour. Technol.* 1993; **44**: 61–63.

139. Srivastava P, Malviya R. Extraction, Characterization and Evaluation of Orange Peel Waste Derived Pectin as a

Pharmaceutical Excipient. *Nat. Prod. J.* 2011; **1**: 65–70.

140. Pandharipande S, Makode H. Separation of oil and pectin from orange peel and study of effect of pH of extracting medium on the yield of pectin. *Eng. Res. Stud.* 2012: 6–9.

141. Liu Y, Shi J, Langrish TAG. Water-based extraction of pectin from flavedo and albedo of orange peels. *Chem. Eng. J.* 2006; **120**: 203–209.

142. Albersheim P, Neukom H, Deuel H. Splitting of pectin chain molecules in neutral solutions. *Arch. Biochem. Biophys.* 1960; **90**: 46–51.

143. Yeoh S, Zhang S, Shi J *et al.* A Comparison of Different Techniques for Water-Based Extraction of Pectin From Orange Peels. *Chem. Eng. Commun.* 2008; **195**: 511–520.

144. Boukroufa M, Boutekedjiret C, Petigny L *et al.* Bio-refinery of orange peels waste: A new concept based on integrated green and solvent free extraction processes using ultrasound and microwave techniques to obtain essential oil, polyphenols and pectin. *Ultrason. Sonochem.* 2015; **24**: 72–79.

145. Guo X, Han D, Xi H *et al.* Extraction of pectin from navel orange peel assisted by ultra-high pressure, microwave or traditional heating: A comparison. *Carbohydr. Polym.* 2012; **88**: 441–448.

146. Yang N, Jin Y, Tian Y *et al.* An experimental system for extraction of pectin from orange peel waste based on the o-core transformer structure. *Biosyst. Eng.* 2016; **148**: 48–54.

147. Ibarz A, Pagán A, Tribaldo F *et al.* Improvement in the measurement of spectrophotometric data in the m-hydroxydiphenyl pectin determination methods. *Food Control* 2006; **17**: 890–893.

148. Monsoor MA, Kalapathy U, Proctor A. Determination of pectin degree of esterification by diffuse reflectance Fourier transform infrared spectroscopy. *Food Chem.* 2000; **68**: 327–332.

149. McComb EA, McCready RM. Determination of Acetyl in Pectin and in Acetylated Carbohydrate Polymers Hydroxamic Acid Reaction. *Anal. Chem.* 1957; **29**: 819–821.

150. Wüestenberg T. Cellulose. In: *Cellulose and Cellulose Derivatives in Food Industry*. 1st Ed. Weinheim, DE: Wiley-VCH, 2014, pp.91–142.

151. Bicu I, Mustata F. Optimization of isolation of cellulose from orange peel using sodium hydroxide and chelating agents. *Carbohydr. Polym.* 2013; **98**: 341–348.

152. Grigelmo-Miguel N, Martín-Belloso O. Characterization of dietary fiber from orange juice extraction. *Food Res. Int.* 1998; **31**: 355–361.

153. Wüstenberg T. *Cellulose and Cellulose Derivatives in the Food Industry*.; 2015.

154. Hon DN-S, Shiraishi N. *Wood and Cellulosic Chemistry*. Second Ed. (Hon DN-S, Shiraishi N, eds.). CRC Press; 2013.

155. Bicu I, Mustata F. Cellulose extraction from orange peel using sulfite digestion reagents. *Bioresour. Technol.* 2011; **102**: 10013–10019.

156. Eaks IL, Sinclair WB. Cellulose, hemicellulose fractions in the alcohol-insoluble solids of Valencia orange peel. *J. Food Sci.* 1980; **45**: 985–988.

157. Brendel O, Iannetta PPM, Stewart D. A Rapid and Simple Method to Isolate Pure Alpha-Cellulose. *Phytochem. Anal.* 2000; **11**: 7–10.

158. Ejikeme PM. Investigation of the physicochemical properties of microcrystalline cellulose from agricultural wastes I: Orange mesocarp. *Cellulose* 2008; **15**: 141–147.

159. Xuan Z, Tang Y, Li X *et al.* Study on the equilibrium, kinetics and isotherm of biosorption of lead ions onto pretreated chemically modified orange peel. *Biochem. Eng. J.* 2006; **31**: 160–164.

160. Ververis C, Georghiou K, Danielidis D *et al.* Cellulose, hemicelluloses, lignin and ash content of some organic materials and their suitability for use as paper pulp supplements. *Bioresour. Technol.* 2007; **98**: 296–301.

161. Ayedun H, Oyede RT, Osinfade BG *et al.* Acetylation of Orange Waste For Possible Industrial Use. *Asian J. Chem.* 2012; **24**: 1938–1940.

162. Yaşar F, Toğrul H, Arslan N. Flow properties of cellulose and carboxymethyl cellulose from orange peel. *J. Food Eng.* 2007; **81**: 187–199.

163. Rustemeyer P. History of CA and evolution of the markets. *Macromol. Symp.* 2004; **208**: 1–6.

164. Maim CJ, Mench JW, Kendall DL *et al.* Aliphatic Acid Esters of Cellulose preparation by acid chloride-pyridine procedure. *J Ind Eng Chem* 1951; **43**: 684–688.

165. Steinmeier H. Acetate manufacturing, process and technology - chemistry of cellulose acetylation. In: Rustemeyer P, ed. *Cellulose Acetates: Properties and Applications*. Weinheim, DE: Wiley-VCH, 2004, pp.49–60.

166. Hamalainen C, Reid JD. Partial Acetylation of Cotton Cellulose by Ketene. *Ind. Eng. Chem.* 1949; **41**: 1018–1021.

167. Malm CJ, Tanghe LJ, Laird BC. Preparation of Cellulose Acetate - Action of Sulfuric Acid. *Ind. Eng. Chem.* 1946; **38**: 77–82.

168. LaNieve HL. Cellulose Acetate and Triacetate Fibers. In: Lewin M, ed. *Handbook of Fiber Chemistry*. 3rd Ed. Boca Raton, FL, USA: CRC Press - Taylor & Francis Group, 2006, pp.773–810.

169. PRWEB. Continued Growth in Cigarette Filter Tow Production Sustains Cellulose Acetate Demand, According to a New Report by Global Industry Analysts, Inc. *http://www.prweb.com/releases/cellulose_acetate_market/acetate_tows_market/prweb12598343.htm (Last accessed: 16.01.2017)* 2015.

170. Gupta BS. Manufactured Textile Fibers. In: Kent JA, ed. *Handbook of Industrial Chemistry and Biotechnology*. 12th Ed. New York, USA: Springer US, 2012, pp.419–473.

171. Steinmeier H. Chemistry of cellulose acetylation. *Macromol. Symp.* 2004; **208**: 49–60.

172. Ganster J, Fink H. Cellulose and Cellulose Acetate. In: Kabasci S, ed. *Bio-Based Plastics: Materials and Applications*. 1st Ed. West Sussex, UK: Wiley, 2014, pp.35–62.

173. Balser K, Hoppe L, Eicher T *et al.* Cellulose Esters. In: Elvers B, ed. *Ullmann's Encyclopedia of Industrial Chemistry*. 7th Ed. Wiley-VCH, 2000, pp.333–380.

174. USDA Foreign Agricultural Service. *Italy Citrus Annual 2016*. Rome; 2016.

175. Stremple P. GC/MS analysis of polymethoxyflavones in citrus oils. *HRC J. High Resolut. Chromatogr.* 1998; **21**: 587–591.

176. Li S, Pan MH, Lo CY *et al.* Chemistry and health effects of polymethoxyflavones and hydroxylated polymethoxyflavones. *J. Funct. Foods* 2009; **1**: 2–12.

177. European Parliament and Council. Directive 2009/32/EC of the European Parliament and of the Council of 23 April 2009. *Off. J. Eur. Union* 2009; **L141**: 3–11.

178. Gnanasambandam R, Proctor A. Determination of pectin degree of esterification by diffuse reflectance Fourier transform infrared spectroscopy. *Food Chem.* 2000; **68**: 327–332.

179. Mojzita D, Wiebe M, Hilditch S *et al.* Metabolie engineering of fungal strains for conversion of D-galacturonate to meso-Galactarate. *Appl. Environ. Microbiol.* 2010; **76**: 169–175.

180. Islam MR, Muslim T, Rahman MA. Investigation on Orange Peel: Derivatization of Isolated Cellulosic Material and Analysis of the Fatty Acids Composition. *Dhaka Univ. J. Sci.* 2012; **60**: 77–78.

181. Altmann R. The cellular organelles and their relations to cells. In: *The Elementary Organism*. Leipzig, DE: Veit & Co., 1890, p.125.

182. Palade GE. An electron microscope study of the mitochondrial structure. *J. Histochem. Cytochem.* 1953; **1**: 188–211.

183. Sjostrand FS. Electron Microscopy of Mitochondria and Cytoplasmic Double Membranes. *Nature* 1953; **171**: 30–31.

184. Rich PR. The molecular machinery of Keilin's respiratory chain. *Biochem. Soc. Trans.* 2003; **31**: 1095–1105.

185. Sazanov LA. A giant molecular proton pump: structure and mechanism of respiratory complex I. *Nat. Rev. Mol. Cell Biol.* 2015; **16**: 375–388.

186. Mitchell P. Chemiosmotic Coupling in Oxidative and Photosynthetic Phosphorylation. *Bio. Rev.* 1966; **41**: 445–

502.

187. Mccarty R. A Plant Biochemist's View of H+-ATPases And Atp Synthases. *J. Exp. Biol.* 1992; **172**: 431–441.

188. Walker JE, Fearnley IM, Gay NJ *et al.* Primary structure and subunit stoichiometry of F1-ATPase from bovine mitochondria. *J. Mol. Biol.* 1985; **184**: 677–701.

189. Lodish HF, Berk A, Kaiser C *et al.* Cellular Energetics. In: *Molecular Cell Biology*. 5th Ed. New York, USA: W.H. Freeman and Company, 2004, pp.301–350.

190. Hong S, Pedersen PL. ATP synthase and the actions of inhibitors utilized to study its roles in human health, disease, and other scientific areas. *Microbiol. Mol. Biol. Rev.* 2008; **72**: 590–641.

191. Jastroch M, Divakaruni AS, Mookerjee S *et al.* Mitochondrial proton and electron leaks. *Essays Biochem.* 2010; **47**: 53–67.

192. Küster U, Bohnensack R, Kunz W. Control of oxidative phosphorylation by the extramitochondrial ATP/ADP ratio. *BBA - Bioenerg.* 1976; **440**: 391–402.

193. Bonora M, Wieckowski MR, Chinopoulos C *et al.* Molecular mechanisms of cell death: central implication of ATP synthase in mitochondrial permeability transition. *Oncogene* 2014; **1**: 1–12.

194. Berridge MJ, Bootman MD, Lipp P. Calcium - a life and death signal. *Nature* 1998; **395**: 645–648.

195. Brini M, Calì T, Ottolini D *et al.* Intracellular calcium Homeostasis and Signaling. In: Banci L, ed. *Metallomics and the Cell*. Dordrecht, NL: Springer Science Business Media B. V., 2013, pp.119–168.

196. Kerr JFR, Wyllie AH, Currie AR. Apoptosis: a Basic Biological Phenomenon With Wide- Ranging Implications in Tissue Kinetics. *Br. J. Cancer* 1972; **26**: 239–257.

197. Wajant H. The Fas signaling pathway: more than a paradigm. *Science* 2002; **296**: 1635–1636.

198. Vucic D, Deshayes K, Ackerly H *et al.* SMAC negatively regulates the anti-apoptotic activity of melanoma inhibitor of apoptosis (ML-IAP). *J. Biol. Chem.* 2002; **277**: 12275–12279.

199. Imahashi K, Pott C, Goldhaber JI *et al.* Cardiac-specific ablation of the Na+-Ca2+ exchanger confers protection against ischemia/reperfusion injury. *Circ. Res.* 2005; **97**: 916–921.

200. Morciano G, Giorgi C, Bonora M *et al.* Molecular identity of the mitochondrial permeability transition pore and its role in ischemia-reperfusion injury. *J. Mol. Cell. Cardiol.* 2015; **78**: 142–153.

201. Boyman L, Williams GSB, Lederer WJ. Mitochondrial Calcium and Ischemia: Reperfusion Injury in Heart. In: Hockenbery DM, ed. *Mitochondria and Cell Death*. 1st Ed. New York, USA: Humana Press, 2016, pp.16–43.

202. Chinopoulos C, Konràd C, Kiss G *et al.* Modulation of F0F1-ATP synthase activity by cyclophilin D regulates matrix adenine nucleotide levels. *FEBS J.* 2011; **278**: 1112–1125.

203. Bonora M, Bononi A, De Marchi E *et al.* Role of the c subunit of the F O ATP synthase in mitochondrial permeability transition. *Cell Cycle* 2013; **12**: 674–683.

204. Lardy H a, Johnson D, McMurray WC. Antibiotics as tools for metabolic studies. I. A survey of toxic antibiotics in respiratory, phosphorylative and glycolytic systems. *Arch. Biochem. Biophys.* 1958; **78**: 587–597.

205. Symersky J, Osowski D, Walters DE *et al.* Oligomycin frames a common drug-binding site in the ATP synthase. *Proc. Natl. Acad. Sci. U. S. A.* 2012; **109**: 13961–5.

206. Von Ballmoos C, Dimroth P. Two distinct proton binding sites in the ATP synthase family. *Biochemistry* 2007; **46**: 11800–11809.

207. Lysenkova LN, Turchin KF, Korolev AM *et al.* Synthesis and properties of a novel brominated oligomycin A derivative. *J. Antibiot. (Tokyo).* 2012; **65**: 223–5.

208. Lysenkova LN, Turchin KF, Korolev AM *et al.* Synthesis and cytotoxicity of oligomycin A derivatives modified in the side chain. *Bioorganic Med. Chem.* 2013; **21**: 2918–2924.

209. Bonora M, Morganti C, Morciano G *et al.* Comprehensive analysis of mitochondrial permeability transition pore activity in living cells using fluorescence-imaging-based techniques. *Nat. Protoc.* 2016; **11**: 1067–80.

210. Hamann S, Kiilgaard JF, Litman T *et al.* Measurement of Cell Volume Changes by Fluorescence. *J. Fluoresc.* 2002; **12**: 139–145.